

ISSN (1230-0322)

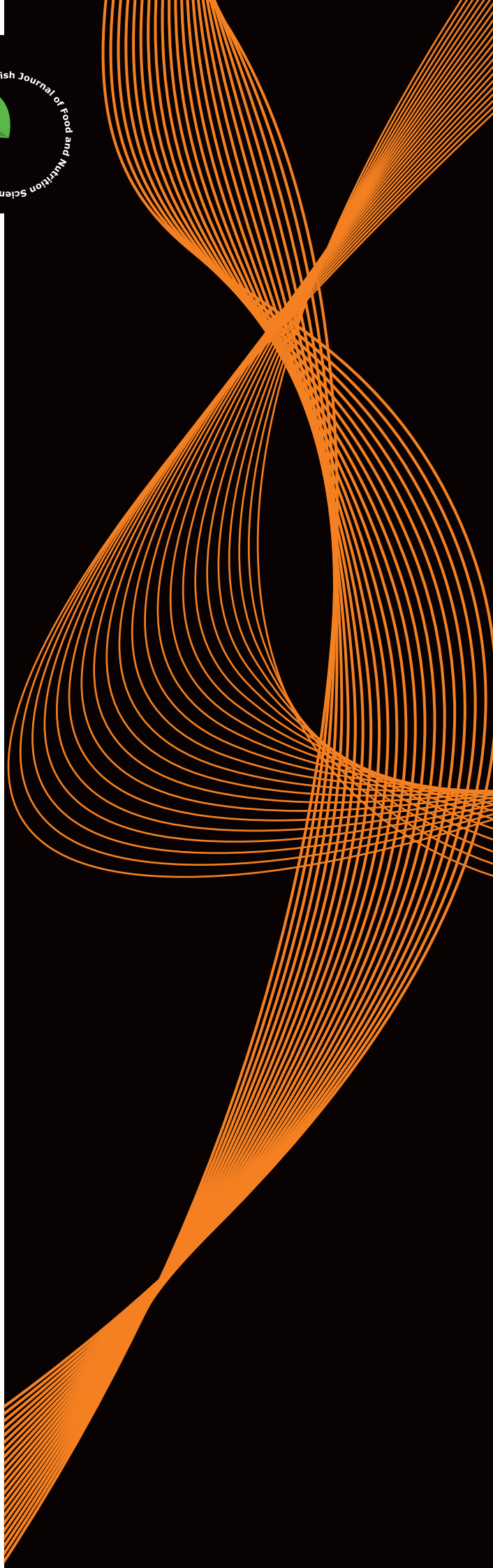
2021, Vol. 71, No. 3

Food

Published

by Institute of Animal
Reproduction and Food
Research of the Polish
Academy of Sciences,
Olsztyn

Polish Journal of Food and Nutrition Sciences
formerly Acta Alimentaria Polonica



Published since 1957 as
Roczniki Chemii i Technologii Żywności and Acta Alimentaria Polonica (1975–1991)

EDITOR-IN-CHIEF

Dr. Magdalena Karamać, Department of Chemical and Physical Properties of Food, Institute of Animal Reproduction and Food Research of the Polish Academy of Sciences, Olsztyn, Poland

SECTION EDITORS

Food Technology Section

Prof. Adriano Gomes da Cruz, Department of Food, Federal Institute of Education, Science and Technology of Rio de Janeiro (IFRJ), Rio de Janeiro, Brazil

Dr. Zeb Pietrasik, Meat, Food and Bio Processing Branch, Alberta Agriculture and Forestry, Leduc, Canada

Prof. Alberto Schiraldi, DISTAM, University of Milan, Italy

Food Chemistry Section

Prof. Ryszard Amarowicz, Department of Chemical and Physical Properties of Food, Institute of Animal Reproduction and Food Research of the Polish Academy of Sciences, Olsztyn, Poland

Dr. Agnieszka Kosińska-Cagnazzo, Independent Researcher, Sion, Switzerland

Food Quality and Functionality Section

Prof. Vural Gökmen, Department of Food Engineering, Hacettepe University, Ankara, Turkey

Prof. Piotr Minkiewicz, Department of Food Biochemistry, University of Warmia and Mazury in Olsztyn, Poland

Nutritional Research Section

Prof. Jerzy Juśkiewicz, Department of Biological Function of Food, Institute of Animal Reproduction and Food Research of the Polish Academy of Sciences, Olsztyn, Poland

Prof. Andre Mazur, INRA, Clermont, France

Dr. Luisa Pozzo, The Institute of Agricultural Biology and Biotechnology, CNR, Pisa, Italy

LANGUAGE EDITOR

Prof. Ron Pegg, University of Georgia, Athens, USA

STATISTICAL EDITOR

Dr. Magdalena Karamać, Institute of Animal Reproduction and Food Research of the Polish Academy of Sciences, Olsztyn, Poland

EXECUTIVE EDITOR, NEWS AND MISCELLANEA SECTION

Joanna Molga, Institute of Animal Reproduction and Food Research of the Polish Academy of Sciences, Olsztyn, Poland;

E-mail: pjfn@pan.olsztyn.pl

SCOPE: The Journal covers fundamental and applied research in food area and nutrition sciences with a stress on interdisciplinary studies in the areas of food, nutrition and related subjects.

POLICY: Editors select submitted manuscripts in relation to their relevance to the scope. Referees are selected from the Advisory Board and from Polish and international scientific centres. Identity of referees is kept confidential.

AUTHORSHIP FORMS referring to Authorship Responsibility, Conflict of Interest and Financial Disclosure, Copyright Transfer and Acknowledgement, and Ethical Approval of Studies are required for all authors.

FREQUENCY: Quarterly – one volume in four issues (March, June, September, December).

COVERED by Web of Science, Current Contents/Agriculture, Biology & Environmental Sciences, Journal Citation Reports and Science Citation Index Expanded, BIOSIS (Biological Abstracts), SCOPUS, FSTA (formerly: Food Science and Technology Abstracts), CAS (Chemical Abstracts), AGRICOLA, AGRO-LIBREX data base, EBSCO, FOODLINE, Leatherhead FOOD RA data base FROSTI, AGRIS and Index Copernicus data bases, Polish Scientific Journals Contents (PSJC) Life Science data base available at <http://psjc.icm.edu.pl> and any www browser; ProQuest: The Summon, Bacteriology Abstracts, Immunology Abstracts.

EDITORIAL AND BUSINESS CORRESPONDENCE: Submit contributions (see Instructions to Authors) and address all communications regarding subscriptions, changes of address, etc. to:

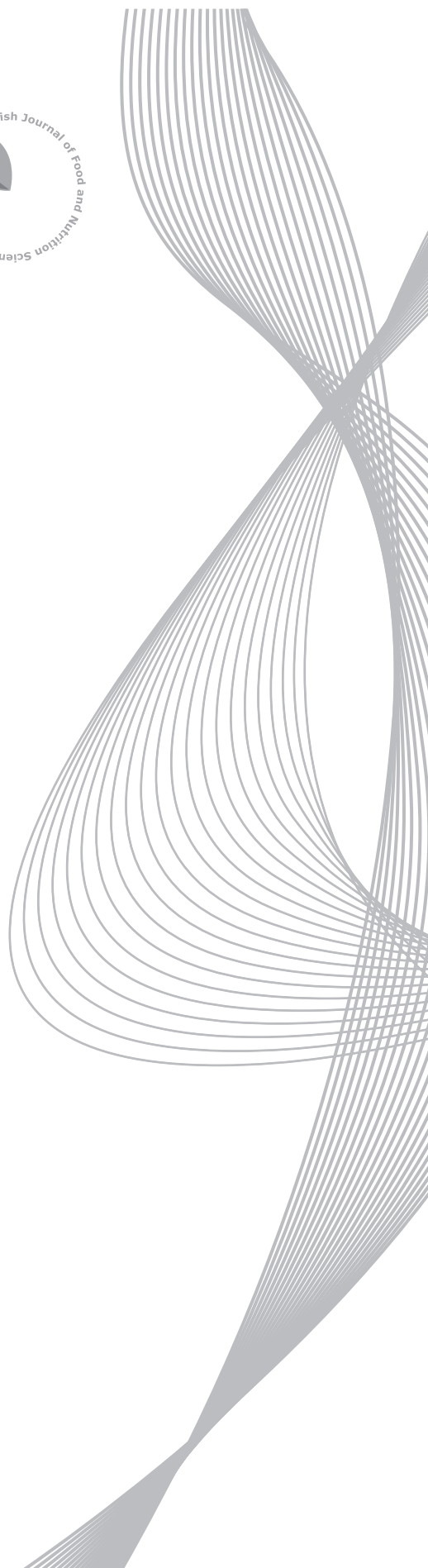
CORRESPONDENCE TO: Ms. Joanna Molga
Polish Journal of Food and Nutrition Sciences
Institute of Animal Reproduction and Food Research
of Polish Academy of Sciences
ul. Tuwima 10, 10-747 Olsztyn, Poland
e-mail: pjfn@pan.olsztyn.pl; <http://journal.pan.olsztyn.pl>

ISSN (1230-0322)
2021, Vol. 71, No. 3

Published

by Institute of Animal
Reproduction and Food
Research of the Polish
Academy of Sciences,
Olsztyn

Polish Journal of Food and Nutrition Sciences
formerly Acta Alimentaria Polonica



Advisory Board of PJFNS 2019–2022

Marek Adamczak

University of Warmia and Mazury in Olsztyn, Poland

Huda Al-Kateb

Birmingham City University, Birmingham, UK

Wilfried Andlauer

University of Applied Sciences and Arts Western Switzerland
Valais, Sion, Switzerland

Anna Brzozowska

Warsaw University of Life Sciences, Poland

Zuzana Ciesarova

VUP Food Research Institute, Bratislava, Slovak Republic

Maria Dolores Del Castillo

CSIC-UAM, Madrid, Spain

Juana Frias

Institute of Food Science, Technology and Nutrition
(ICTAN), Madrid, Spain

Liwei Gu

University of Florida, Gainesville, USA

Henryk Jeleń

Poznań University of Life Sciences, Poland

Georgios Koutsidis

Northumbria University, Newcastle-upon-Tyne, UK

Andrzej Lenart

Warsaw University of Life Sciences, Poland

John Lodge

Northumbria University, Newcastle-upon-Tyne, UK

Adolfo J. Martinez-Rodriguez

CSIC-UAM, Madrid, Spain

Francisco J. Morales

CSIC, Madrid, Spain

Zhongli Pan

University of California, Davis, USA;
World Food Center, China

Ron B. Pegg

University of Georgia, Athens, USA

Mariusz K. Piskula

Institute of Animal Reproduction and Food Research
of the Polish Academy of Sciences in Olsztyn, Poland

Da-Wen Sun

National University of Ireland, Dublin, Ireland

Lida Wądołowska

Warmia and Mazury University, Olsztyn, Poland

Zenon Zduńczyk

Institute of Animal Reproduction and Food Research
of the Polish Academy of Sciences in Olsztyn, Poland

Henryk Zieliński

Institute of Animal Reproduction and Food Research
of the Polish Academy of Sciences in Olsztyn, Poland

POLISH JOURNAL OF FOOD AND NUTRITION SCIENCES

covered by CURRENT CONTENTS/AGRICULTURE, BIOLOGY & ENVIRONMENTAL SCIENCES, JOURNAL CITATION REPORTS AND SCIENCE CITATION INDEX EXPANDED, SCOPUS, DOAJ, EBSCO, BIOSIS, IFIS Publishing and CAS abstracts, and AGRO-Librex, FROSTI, and AGRIS data bases

2021, VOL. 71, NO. 3

ORIGINAL PAPERS

Physiological and Antagonistic Properties of <i>Pichia kluyveri</i> for Curative and Preventive Treatments Against Post-Harvest Fruit Fungi.	
<i>M. Mewa-Ngongang, H.W. du Plessis, B.S. Chidi, U.F. Hutchinson, K.S.O. Ntwampe, V.I. Okudoh, N.P. Jolly</i>	245
Expression Profile of Brain Aging and Metabolic Function are Altered by Resveratrol or α-Ketoglutarate Supplementation in Rats Fed a High-Fat Diet.	
<i>P. Szczurek-Janicka, K. Ropka-Molik, M. Oczkiewicz, S. Orczewska-Dudek, M. Pietras, M. Pieszka</i>	255
Phenolic Contents and Antioxidant Activity of Extracts of Selected Fresh and Dried Herbal Materials.	
<i>M. Kozłowska, I. Ścibisz, J.L. Przybył, M. Ziarno, A. Żbikowska, E. Majewska</i>	269
Influence of a Sulphur Dioxide Active Storage System on the Quality of <i>Ribes rubrum</i> L. Berries.	
<i>L. Brondino, D. Cadario, N.R. Giuggioli</i>	279
Effect of Ohmic Heating on the Rheological Characteristics and Electrical Conductivity of Mulberry (<i>Morus nigra</i>) Puree.	
<i>G. Hardinasinta, M. Mursalim, J. Muhidong, S. Salengke</i>	289
Optimized Extraction, Microencapsulation, and Stability of Anthocyanins from <i>Ardisia compressa</i> K. Fruit.	
<i>M.V. Antonio-Gómez, Y. Salinas-Moreno, F. Hernández-Rosas, F. Martínez-Bustos, I. Andrade-González, J.A. Herrera-Corredor</i>	299
Effect of Ultrasound, Steaming, and Dipping on Bioactive Compound Contents and Antioxidant Capacity of Basil and Parsley.	
<i>M. Dadan, U. Tylewicz, S. Tappi, K. Rybak, D. Witrowa-Rajchert, M. Dalla Rosa</i>	311
Hydrolyzed Collagen from Salmon Skin Increases the Migration and Filopodia Formation of Skin Keratinocytes by Activation of FAK/Src Pathway.	
<i>W. Woonnoi, L. Chotphruethipong, S. Tanasawet, S. Benjakul, N. Sutthiwong, W. Sukketsiri</i>	323
Protective Effect of the Ethanol Extract from <i>Hericiium erinaceus</i> Against Ethanol-Induced Gastric Ulcers.	
<i>G. Lv, X. Song, Z. Zhang</i>	333
Instruction for Authors	343

© Copyright by Institute of Animal Reproduction and Food Research
of Polish Academy of Sciences, Olsztyn, Poland
www.pan.olsztyn.pl

Subscription

2021 – One volume, four issues per volume. Annual subscription rates are: Poland 150 PLN, all other countries 80 EUR.

Prices are subject to exchange rate fluctuation. Subscription payments should be made by direct bank transfer to Bank Gospodarki Żywnościowej, Olsztyn, Poland, account No 17203000451110000000452110 SWIFT code: GOPZPLWOLA with corresponding banks preferably. Subscription and advertising offices at the Institute of Animal Reproduction and Food Research of Polish Academy of Sciences, ul. J. Tuwima 10, 10-747 Olsztyn, Poland, tel./fax (48 89) 5234670, fax (48 89) 5240124, e-mail: pjfns@pan.olsztyn.pl; <http://journal.pan.olsztyn.pl>

Zamówienia prenumeraty: Joanna Molga (e-mail: pjfns@pan.olsztyn.pl)

Wersja pierwotna (referencyjna) kwartalnika PJFNS: wersja papierowa (ISSN 1230-0322)
Nakład: 70 egz.; Ark. wyd. 15; Ark. druk. 15
Skład i druk: Mercurius, www.mercurius.com.pl

Physiological and Antagonistic Properties of *Pichia kluyveri* for Curative and Preventive Treatments Against Post-Harvest Fruit Fungi

Maxwell Mewa-Ngongang^{1,2} , Heinrich Wilbur du Plessis^{1*} , Boredi Silas Chidi^{1,2} ,
Urecia Faith Hutchinson^{1,2} , Karabo Seteno Obed Ntwampe^{2,3} , Vincent Ifeanyi Okudoh² , Neil Paul Jolly¹ 

¹Post-Harvest and Agro-Processing Technologies, ARC Infruitec-Nietvoorbij

(The Fruit, Vine and Wine Institute of the Agricultural Research Council), Private Bag X5026, Stellenbosch, 7599, South Africa

²Bioresource Engineering Research Group (BioERG), Department of Biotechnology, Cape Peninsula University of Technology,
P.O. Box 652, Cape Town, 8000, South Africa

³Center of Excellence in Carbon-Based Fuels, School of Chemical and Minerals Engineering, North-West University,
Private Bag X1290, Potchefstroom 2520, South Africa

Key words: biocontrol, *Botrytis cinerea*, *Monilinia laxa*, spoilage, antagonistic yeast

Postharvest fruit loss due to spoilage is mainly attributed to fungal infections. Synthetic chemicals can be used to preserve fruits, but they are expensive and pose risks to human health. The replacement of these chemicals by safer and cost-effective biocontrol agents is now a priority. This study investigated the physiological characteristics of *Pichia kluyveri* and its potential use as a biofungicide. The antagonistic effect of *P. kluyveri* against *Botrytis cinerea* and *Monilinia laxa* was tested on yeast peptone dextrose agar, grapes, apples, and pears. Yeast growth was variably possible at different temperatures, pH, and salinity levels. Strain-dependent antagonistic responses were observed on agar plates, where *M. laxa* was the more sensitive fungus to the antagonistic yeast. *P. kluyveri* demonstrated strong physiological properties under stressful temperature, pH, and salinity conditions. Preventive applications of *P. kluyveri* to apples were 95% effective against *B. cinerea* and 100% effective against *M. laxa*. Fruit type-dependent responses were evident on pears. Similarly, preventive application on grapes was also effective against the fungal pathogens studied. In general, the antagonistic responses were both fungus- and treatment- (curative and preventive) dependent. Therefore, the preventive use of *P. kluyveri* against post-harvest fruit-fungal infections proved to be an effective method for biological control of grapes, apples, and pears against fungal spoilage organisms *Botrytis cinerea* and *Monilinia laxa*.

INTRODUCTION

Fruits are important in a balanced diet, as they are generally rich in fibre, minerals, water, and vitamins. Unfortunately, the majority of fruits are lost or their shelf life is shortened due to spoilage by fungal pathogens [Zhu, 2006]. While pre-harvest infections and spoilage is a problem [Fourie *et al.*, 2002], 25% of fruit spoilage occurs during post-harvest handling and is of major concern to the global agricultural industry [Droby, 2005; Singh & Sharma, 2007]. Prior to thermal preservation techniques, *Penicillium expansum* was responsible for complete post-harvest spoilage of apples globally [Morales *et al.*, 2007]. In table grapes, apples, and many other crop species, *Botrytis cinerea*, *Colletotrichum acutatum* and *Rhizopus stolonifer* are usually responsible for spoilage [Sharma *et al.*, 2009; Williamson *et al.*, 2007]. Additionally, brown rot and grey mould of South African stone fruits are linked to *Monilinia laxa* and *B. cinerea*, respectively [Fourie *et al.*, 2002].

Fruit-derived beverages are also subject to microbial spoilage, all which impacts negatively on the economy [Parveen *et al.*, 2016]. *Dekkera*, *Zygosaccharomyces*, *Pichia*, and *Hanseniaspora* species are the most common spoilage organisms of fruit-derived beverages [Du Toit & Pretorius, 2000; Sáez *et al.*, 2010].

The reduction of microbial spoilage in fruits is conventionally achieved by treatment with chemical fungicides. However, organisations, such as the World Health Organization and the European Economic Community highlighted major health-related concerns associated with their usage in food industries [Ciani & Fatichenti, 2001]. In addition, the resistance of some pathogens to chemical preservatives often prompts an increase in chemical preservative dosages, above acceptable limits [Benito *et al.*, 2009], which can negatively affect product quality. As a result, safer, cheaper, and cost-effective alternatives have recently been the central focus. The use of safer biological systems such as yeast is another potential

* Corresponding Author:
Tel.: +27 21 809 3063;
Email: DPlessisHe@arc.agric.za

Submitted: 4 May 2021
Accepted: 22 June 2021
Published on-line: 20 July 2021



source of biocontrol agents against fruit and fruit-derived beverages [Ciani & Faticenti, 2001; Comitini *et al.*, 2004a; Grzegorzczak *et al.*, 2017; Mehlomakulu *et al.*, 2014; Parveen *et al.*, 2016]. Thus far, several yeasts have been reported to have antagonistic properties against fruit and fruit-derived beverages spoilage pathogens [Aloui *et al.*, 2015; Cordero-Bueso *et al.*, 2017; El Ghaouth *et al.*, 2004; Mehlomakulu *et al.*, 2014; Mewa-Ngongang *et al.*, 2017, 2019a]. Yeasts are excellent biocontrol agents because their growth requirements are simple and their growth kinetics on many fruits and in beverages are competitive [Liu *et al.*, 2013; Muccilli & Restuccia, 2015]. An additional advantage of biological systems is their ability to produce extracellular compounds with antimicrobial properties against many fruit pathogens such as spoilage yeasts, bacteria, and fungi [Comitini *et al.*, 2004a,b; Grzegorzczak *et al.*, 2017; Mehlomakulu *et al.*, 2014].

Several authors have highlighted the importance of non-*Saccharomyces* yeasts in addressing food spoilage [Mewa-Ngongang *et al.*, 2017, 2019b; Oro *et al.*, 2014]. Their widespread use in the food industry, their ability to handle and grow quicker than spoilage organisms, and their ability to produce killer toxins have been widely acknowledged. The biotechnological potential of *Pichia kluyveri* has been highlighted as a producer of aromatic and growth inhibition compounds in beverages [Crafack *et al.*, 2013; Jolly *et al.*, 2014]. The aim of this study was to evaluate the physiological properties of *P. kluyveri* and to assess its potential in suppressing post-harvest fungal growth of *B. cinerea* and *M. laxa* on yeast peptone dextrose agar, apples (Golden delicious), table grapes (Regal seedless), and pears (Packham's Triumph).

MATERIALS AND METHODS

Strain selection and maintenance

Previously isolated from Marula (*Scelerocarya birrea*) juice, the yeast *P. kluyveri* Y1164 was selected after screening several yeasts from the ARC Infruitec-Nietvoorbij yeast culture collection (The Fruit, Vine and Wine Institute of the Agricultural Research Council, Stellenbosch, South Africa). *B. cinerea* and *M. laxa* were supplied by the Post-harvest Pathology Laboratory (ARC Infruitec-Nietvoorbij). Yeast cells and spores of *B. cinerea* and *M. laxa* were propagated at 25°C and maintained at 4°C on yeast peptone dextrose agar (yeast extract 10 g/L, peptone 20 g/L, dextrose 20 g/L, and 20 g/L agar) (YPDA, Biolab, Merck, Modderfontein, South Africa). The pH was 6.5 after autoclaving.

Yeast cells and fungal spore preparation

To investigate the antagonistic effects of *P. kluyveri* on fungal growth, yeast cells were cultivated in YPD broth (Biolab, Merck) at a pH of 6.5 for 24 h at 25°C, using a rotary shaker (150 rpm). Fungus spores were detached from the YPDA cultures and suspended in sterile distilled water. A microscope (SN-EU 1712504, BioBlue Lab, Euromex Microscopes, Arnhem, Holland) and a Neubauer counting chamber were used to determine the cell or spore concentrations at 400× magnification.

Characterisation of physiological properties: Salinity, pH, and temperature

The ability of *P. kluyveri* to grow under different salinity (0.05, 0.10, 0.15, and 0.20 g/mL NaCl), pH (1, 2, 3, 7, and 8), and temperature (5, 15, 30, and 40°C) conditions was investigated. A pre-inoculum was prepared by transferring a wire loopful of *P. kluyveri* cells into a test tube containing 10 mL of sterile YPD broth and incubated without agitation at 28°C for 24 h. Subsequently, test tubes containing 5 mL of pH- and saline-adjusted YPD broth (in triplicate) were inoculated at a final concentration of 10^3 cells/mL of *P. kluyveri* and incubated without agitation at 28°C for 7 days. For the determination of growth at various temperatures, test tubes containing 5 mL of YPD broth were inoculated as mentioned above, but incubated at different temperatures for 7 days. After incubation, cell concentrations were determined microscopically using a Neubauer counting chamber. Based on the initial inoculum of 10^3 cells/mL, low, medium, and high growth was defined as those concentrations ranging from 10^3 to 10^4 , 10^4 to 10^5 , and 10^5 to 10^6 cells/mL, respectively.

Antagonistic effect of *P. kluyveri* on fungal growth: Plate assay

This assay was adapted from Medina-Córdova *et al.* [2016]. YPDA plates were prepared and a mycelial culture disc (5 mm) of either *B. cinerea* or *M. laxa* was placed 2.5 cm away from the plate edges. A volume of 15 µL yeast cells suspension (10^8 cells/mL) was deposited 3 cm from the disc and the plates were sealed with laboratory film (Parafilm®). After incubation at 28°C for 7 days, the diameter of the fungal growth zones was measured. Negative controls were prepared by seeding a mycelial disc at the centre of the YPDA plate under analogous incubation conditions. The antagonistic effect of the yeast was measured in terms of the comparative reduction in fungal growth (diameter) between treatments and negative controls (average of three replicates).

Preventive and curative treatments: Apple, grape, and pear bioassays

Golden Delicious apples (*Malus domestica*) and Packham's Triumph pears (*Pyrus communis* 'Bosc') were obtained from a local producer, Two-A-Day Group Ltd (Grabouw, South Africa). Regal Seedless table grapes (*Vitis vinifera*) were obtained from the Cultivar Development Division of ARC Infruitec-Nietvoorbij. Apples and pears (10 replicates consisting of three pears/apples per replicate) were washed, dried, and sprayed with 70% ethanol and uniformly wounded with a sterile cork borer (approximately 5 mm diameter and 3 mm deep). The ethanol was allowed to dry prior to the next step. After wound infliction, fruits were allowed to dry before undergoing preventive or curative treatments. For preventive treatments, wounded fruits were inoculated with 20 µL (10^6 cells/mL) of *P. kluyveri* cell suspension using a micropipette and incubated overnight at room temperature. Subsequently, the yeast cells were allowed to colonise the fruits for 24 h before inoculation with 20 µL (10^5 cells/mL) of *B. cinerea* or *M. laxa* suspension. For curative treatments, the wounded fruits were inoculated with 20 µL (10^5 fungal spores/mL) of *B. cinerea* or *M. laxa*, incubated for 24 h and then inoculated

with 20 μL (10^6 cells/mL) of *P. kluyveri* suspension. Treated fruit was maintained at -0.5°C for 4 weeks, and then stored at room temperature ($\pm 20^\circ\text{C}$) for 7 days, to simulate shipping conditions and shelf life in a commercial setting. Positive results were characterised by the absence of fungal development on the fruit surfaces. For preventive and curative treatments/bioassays, negative controls were prepared by inoculating fruits with 20 μL (10^5 fungal spores/mL) of *B. cinerea* or *M. laxa* suspensions under similar maintenance and storage conditions. During the incubation period for all the treatments, there was an 80% relative humidity. Comparative analysis of the differences in lesion diameters/growth inhibition between the negative controls and inoculated fruits was done to determine if the yeast is a successful biocontrol agent against *B. cinerea* and *M. laxa*. For both treatments, the percentage inhibition was obtained, considering that the negative control was 100% of the lesion diameter. Table grapes (20 replicates consisting of 10 grape berries per replicate) were uniformly wounded with a sterile needle (2 mm diameter, 1 wound per berry) and allowed to dry prior to preventive and curative treatments. For preventive treatments, wounded grapes (10 grapes per replicate) were sprayed with 10 mL (10^6 cells/mL) of *P. kluyveri* cell suspension, incubated overnight at room temperature and sprayed with 10 mL (10^5 cells/mL) of *B. cinerea* or *M. laxa* suspension. For curative treatments, the wounded grapes were sprayed with 10 mL (10^5 fungal spores/mL) of *B. cinerea* or *M. laxa*, incubated for 24 h, and then sprayed with 10 mL (10^6 cells/mL) of *P. kluyveri* suspension. The negative controls (10 berries each) were prepared by spraying the fungal spores on the wounded berries without yeast treatment. All grape treatments were also maintained at -0.5°C for 4 weeks, and then stored at room temperature ($\pm 20^\circ\text{C}$) for 7 days. The antagonistic properties of *P. kluyveri* were analysed visually by assessing the grape colour changes and fungal development on treated grapes.

Statistical analysis

The experiment was randomised and the data for each experiment was analysed separately. To determine whether there were significant differences within the physiological parameters (pH, temperature, and salinity), analysis of variance was performed using general linear means procedure of SAS version 9.4 (SAS Institute Inc, Cary, NC, USA). Fisher's least significant difference (LSD) values were calculated at the 5% probability level ($p=0.05$) to facilitate comparison between treatment means.

RESULTS AND DISCUSSION

Physiological properties of *P. kluyveri*

The results in Table 1 show growth characteristics of *P. kluyveri* under different pH, saline, and temperature conditions in YPD. One of the required properties of biocontrol agents (e.g., yeast) is the ability to tolerate a broad spectrum of the aforementioned conditions. These conditions are fruit type-dependent and critical during postharvest because they affect the growth of both antagonistic yeasts and fruit fungal pathogens. Prior to postharvest control treatments, it was important to establish whether yeast growth was

possible under a very wide spectrum of conditions. Relatively low yeast count was observed at 5°C (1.55×10^3 cells/mL) and 40°C (1.58×10^3 cells/mL), at pH 1 (1.64×10^3 cells/mL), and 0.15 g/mL (1.37×10^3 cells/mL) and 0.20 g/mL (1.07×10^3 cells/mL) salinity. A moderate count was observed at 0.10 g/mL salinity (1.41×10^4 cells/mL). The highest cell counts were obtained at 15°C (3.75×10^5 cells/mL) and 30°C (3.17×10^5 cells/mL), at pH 2 (1.86×10^5 cells/mL), pH 3 (1.74×10^5 cells/mL), pH 7 (5.50×10^5 cells/mL), pH 8 (4.55×10^5 cells/mL), and 0.05 g/mL salinity (4.72×10^5 cells/mL). The optimal growth temperature range of *P. kluyveri* corresponds to the South African mean annual temperatures between $17\text{--}22^\circ\text{C}$ ["CapeFarmMapper," n.d.]. Meaning that yeast growth and antagonistic properties can be stimulated under most agricultural and postharvest conditions of South Africa.

The ideal pH and saline conditions for *P. kluyveri* also relate to the intrinsic properties of most fruits, i.e. pH 3.2–4.5 and <0.1 g/mL salt, respectively [Kessels, 2003]. These findings were also comparable to the findings of Psani & Kotzekidou [2006] where the large majority of *Debaryomyces hansenii* (15 strains) and *Torulaspora delbrueckii* (32 strains) were able to grow optimally at 15°C , pH 2.5, and 0.1 g/mL NaCl. Previously, both yeast growth and the killer properties of yeast were associated with changes in environmental conditions such as temperature, salinity, and pH [Tipper & Bostian, 1984]. As in the current study, Çelik et al. [2017] also reported insignificant growth rates of most yeast strains (*P. kluyveri*, *Candida zemplinina*, *P. occidentalis*, and *Saccharomyces cerevisiae*) when the temperature was below 15°C under grape-must fermentation conditions (pH 3.18). Although this study is the first to report on some antagonistic

TABLE 1. Cell count of *Pichia kluyveri* Y1164 grown for 7 days at different temperatures, pH, and salinity levels.

Parameter	Value	Cell count (cells/mL)
Temperature ($^\circ\text{C}$)	5	$1.55 \times 10^3 \pm 2.59 \times 10^{2c}$
	15	$3.75 \times 10^5 \pm 2.69 \times 10^{4a}$
	30	$3.17 \times 10^5 \pm 1.44 \times 10^{4b}$
	40	$1.58 \times 10^3 \pm 3.77 \times 10^{2c}$
pH	1	$1.64 \times 10^3 \pm 1.56 \times 10^{2d}$
	2	$1.86 \times 10^5 \pm 0.91 \times 10^{4c}$
	3	$1.74 \times 10^5 \pm 0.83 \times 10^{4c}$
	7	$5.50 \times 10^5 \pm 3.67 \times 10^{4a}$
Salinity (NaCl concentration, g/mL)	8	$4.55 \times 10^5 \pm 0.97 \times 10^{4b}$
	0.05	$4.72 \times 10^5 \pm 1.90 \times 10^{4a}$
	0.10	$1.41 \times 10^4 \pm 3.13 \times 10^{3b}$
	0.15	$1.37 \times 10^3 \pm 1.44 \times 10^{2b}$
	0.20	$1.07 \times 10^3 \pm 3.17 \times 10^{3b}$

The values and standard deviation in the table are means of three repeats. Different letters in a column represent statistically significant differences ($p < 0.05$) for temperature, pH or salinity, respectively.

properties of *P. kluyveri*, our findings on the physiological properties of *P. kluyveri* were not surprising, since another *Pichia* species (*P. anomala* J121) was previously considered efficient biocontrol yeasts because of their ability to grow under harsh conditions, *i.e.* temperature (3–37°C), pH (2.0–12.4), and water activity of 0.92 (NaCl) and 0.85 (glycerol) [Fredlund *et al.*, 2004].

Antagonistic effect of *P. kluyveri* against fungal growth

Figure 1 and Figure 2 show the antagonistic effect of *P. kluyveri* against two fruit fungal pathogens, *B. cinerea* and *M. laxa*. The mean growth diameter on the negative control was 45.58 and 63.42 mm for *M. laxa* and *B. cinerea*, respectively (Figure 1). The most sensitive fungus to the antagonistic yeast was *M. laxa*, which showed a growth inhibition of 54.6% after 7 days of incubation (Figure 2). Compared

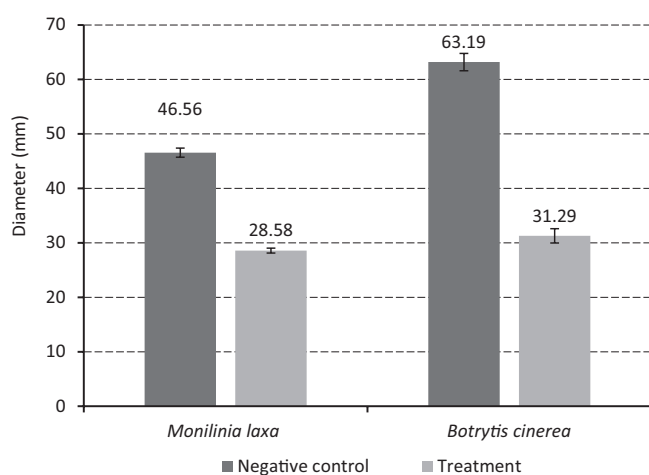


FIGURE 1. Diameters of *Botrytis cinerea* and *Monilinia laxa* growth zones (negative control) and growth of these fungi in the presence of *Pichia kluyveri* Y1164 (treatment) on yeast peptone dextrose agar plates.

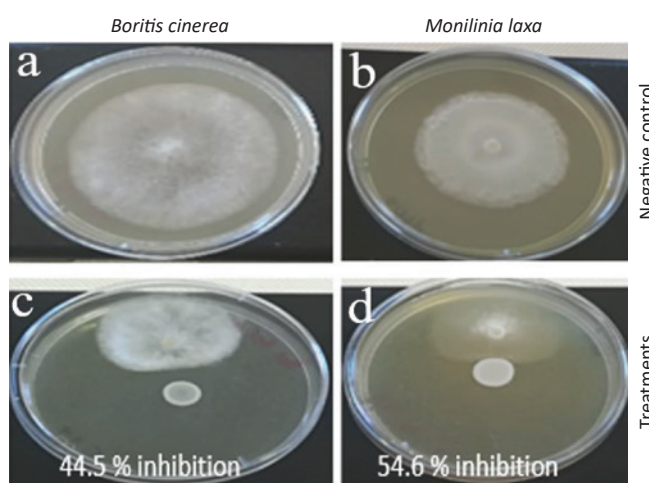


FIGURE 2. Photograph of the inhibition assay on yeast peptone dextrose agar plates showing the inhibition potential of *Pichia kluyveri* Y1164 on *Botrytis cinerea* and *Monilinia laxa*. Growth inhibition is given as the percentage difference between fungal growth diameter of *Botrytis cinerea* (a) and *Monilinia laxa* (b) controls as well as *Botrytis cinerea* (c) and *Monilinia laxa* (d) treatments. Each plate is a representative example of three replicates.

to the negative control ($p < 0.05$), 44.5% growth inhibition was observed against *B. cinerea*. Although *B. cinerea* (negative control) grew faster than *M. laxa* on YPDA, the antagonistic effect of *P. kluyveri* was still maintained and seemed independent of fungal growth kinetics. Additionally, species-dependent antagonistic responses were evident on solidified medium assays. Previously, the screening and the identification of antimicrobial producing yeasts such as *Candida intermedia* [Huang *et al.*, 2011] and *Sporidiobolus pararoseus* [Huang *et al.*, 2012] was achieved on solid medium. A similar study by Mewa-Ngongang *et al.* [2019b] also demonstrated the broad antagonistic effect of *P. kluyveri* on solidified plate assays, therefore supporting the findings of this research. Although the pre-screening of biocontrol agents on agar media is common, more rapid and cost-effective methods still need to be developed.

Preventive and curative treatments: Apple bioassay

As shown in Figure 3 and Figure 4, *P. kluyveri* applied preventively, was effective in suppressing fungal growth to 95.12% (Lesion diameter, LD=3.29 mm) and 100% (LD=0.0 mm) for *B. cinerea* and *M. laxa*, respectively. The curative treatments were not as effective, since growth suppression of *B. cinerea* was only 51.32% (LD=32.77 mm) and 45.68% (LD=26.49 mm) for *M. laxa*, compared to the negative controls. As shown in Figure 3 and Figure 4 preventive/curative biocontrol treatments against both fungal pathogens (*B. cinerea* and *M. laxa*) followed similar trends where smaller lesions were observed for *M. laxa*. Gril *et al.* [2008] also categorised *M. laxa* as a pathogen of apple fruits, but not its principal or preferred host. Sansone *et al.* [2018] proved that the biocontrol of *B. cinerea* BNM 0527 was more effective under preventive rather than curative treatments on apples. These authors also showed a 75% and 48% spoilage reduction by *Rhodosporidium fluviale* as preventive and curative treatments, respectively. These results confirm the old notion that says, 'prevention is better than cure'.

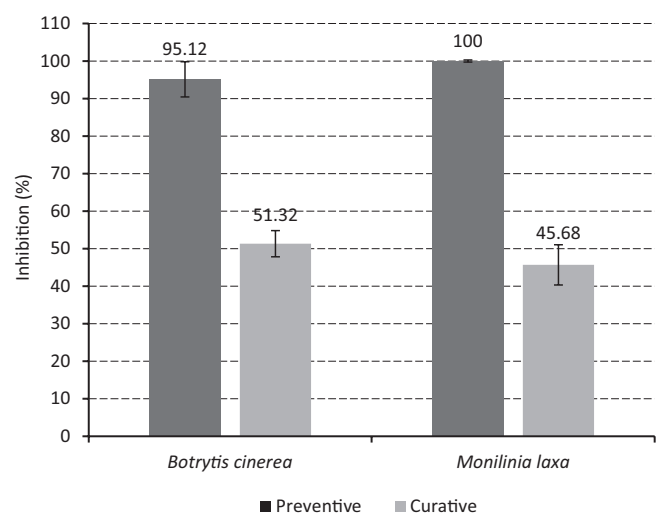


FIGURE 3. Growth inhibition of *Botrytis cinerea* and *Monilinia laxa* on apples with the associated level of biological control by *Pichia kluyveri* Y1164 used as preventive and curative treatments. Values are the average of 10 replicates consisting of three apples per replicate \pm standard deviation ($n=30$). The lesion diameters, from which the percentage inhibition was obtained, are shown in Figure 4.

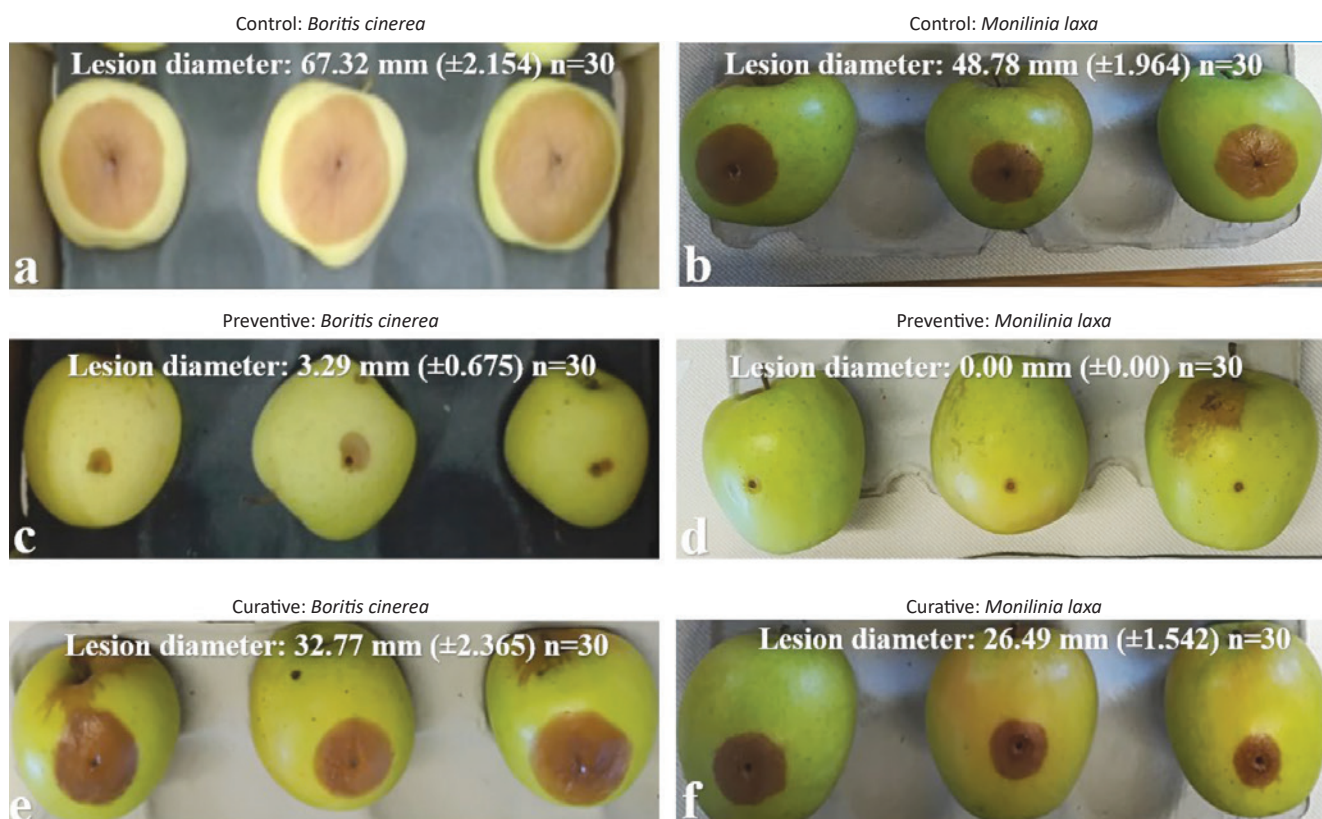


FIGURE 4. Photograph of apples showing lesion diameters because of spoilage caused by *Botrytis cinerea* (a) and *Monilinia laxa* (b) with the associated level of biological control by *Pichia kluyveri* Y1164 against preventive *Botrytis cinerea* (c) and *Monilinia laxa* (d) treatments as well as curative *Botrytis cinerea* (e) and *Monilinia laxa* (f) treatments. Values are the average of 10 replicates consisting of three apples per replicate \pm standard deviation ($n=30$). Each set (consisting of three apples) is a representative example after 4 weeks at -0.5°C and then at room temperature ($\pm 20^{\circ}\text{C}$) for 7 days.

Preventive and curative treatments: Table grape bioassay

The antagonistic effect of *P. kluyveri* applied as preventive and curative grape treatments on the growth of *B. cinerea* and *M. laxa* are shown in Figure 5. A 100% growth inhibition was observed, which was demonstrated by the absence of spoilage for the preventive treatments. Translating to effective control of both *B. cinerea* and *M. laxa* infections, compared to the controls. Slightly different observation was made on the curative treatments where it would be important to mention that the result interpretation in this part was also based on visual observations whereby, a jar was considered as a mini bunch of grape berries that was inspected for decay not as single fruit like in the case of apples and pears. One out of 20 jars infected with *B. cinerea* in the curative treatment showed signs of spoiled berries (95% inhibition), while a 100% inhibition was observed for the curative treatments of *M. laxa*. This result is comparable to the 100% suppression of *Aspergillus carbonarius*, *Colletotrichum acutatum*, and *Rhizopus stolonifer* growth on grapes by *Candida zemplinina*, *Candida pyralidae*, *Saccharomyces cerevisiae*, and *P. kluyveri* [Fiori et al., 2014; Mewa-Ngongang et al., 2019b; Zhu et al., 2015]. Although preventive results were notable, curative biocontrol applications resulted in substandard grape colour and texture, although spoilage was vastly minimised. It is also plausible that, apart from antagonistic properties of *P. kluyveri*, volatile compounds [Fiori et al., 2014; Lutz et al., 2013], hydrolytic

enzymes [Hernández et al., 2008], mycotoxins [Thompson et al., 2013] or proteases [Buzzini & Martini, 2002] may have affected fungal growth. The results from this study also showed the effectiveness of *P. kluyveri* against *B. cinerea* and *M. laxa* growth and the advantage of preventive treatments during fruit processing.

Preventive and curative treatments: Pear bioassay

The bioassay with pear fruits confirmed the antagonistic effect of *P. kluyveri* on *B. cinerea* and *M. laxa*, with a significant ($p < 0.05$) reduction in lesion diameter when applied as preventive treatments (Figure 6 and Figure 7). As a preventive treatment, *P. kluyveri* exhibited a 73.16% (LD=9.21 mm) and 78.65% (LD=7.07 mm) inhibition against *B. cinerea* and *M. laxa*, respectively. Curative treatments showed a 58.59% (LD=14.21 mm) and 52.08% (LD=15.45 mm) inhibition against *B. cinerea* and *M. laxa*, respectively. Enhanced control for preventive treatments could be due to the ability of the yeasts to quickly colonise the wound, release antimicrobial substances, and successfully outgrow fungal pathogens. Therefore, the use of *P. kluyveri* as a preventive treatment can provide an effective strategy to reduce post-harvest decay of pears. Results suggest that the yeast competes with the fungal pathogens for space and nutrients. However, it is also possible that *P. kluyveri* produced secondary metabolites (e.g. diffusible compounds) with antifungal properties [Andrade et al., 2014; Nally et al., 2015; Núñez et al., 2015].

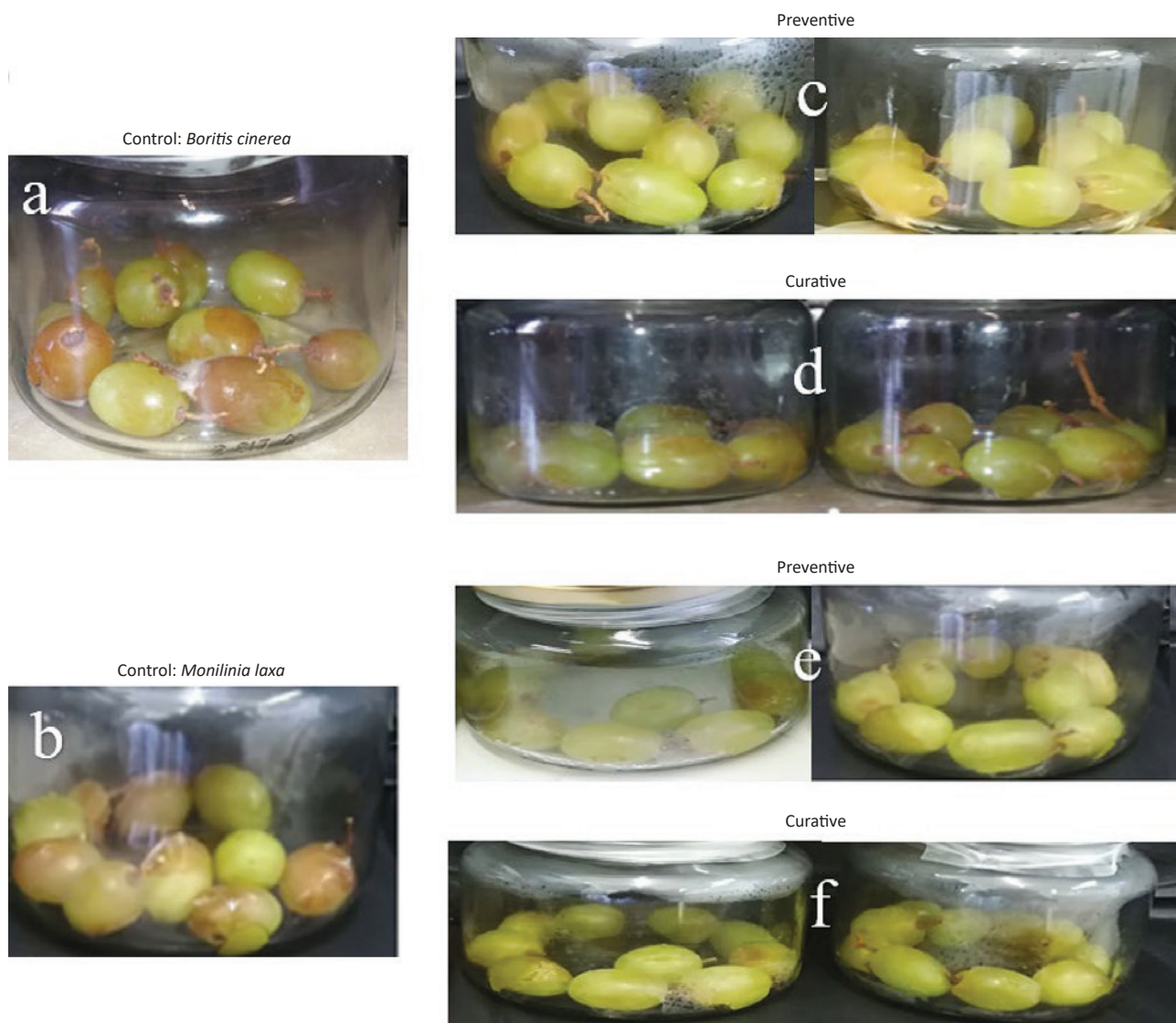


FIGURE 5. Photograph of the jars showing table grapes spoilage caused by *Botrytis cinerea* and *Monilinia laxa* and the associated biological control of *Pichia kluyveri* Y1164 against *Botrytis cinerea* (c) and *Monilinia laxa* (e) preventive treatments as well as *Botrytis cinerea* (d) and *Monilinia laxa* (f) curative treatments. Twenty replicates consisting of 10 grape berries per replicate were tested against both *Botrytis cinerea* (a) and *Monilinia laxa* (b) controls. Each set displayed in this figure is a representative example after 4 weeks at -0.5°C and then at room temperature ($\pm 20^{\circ}\text{C}$) for 7 days.

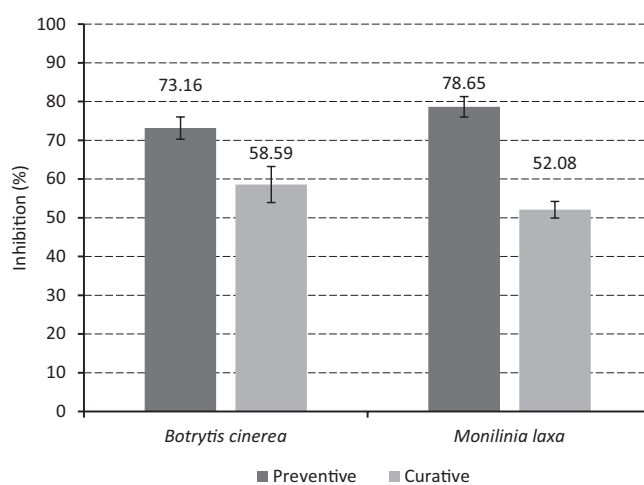


FIGURE 6. Growth inhibition of *Botrytis cinerea* and *Monilinia laxa* on pears with the associated level of biological control by *Pichia kluyveri* Y1164 used as preventive and curative treatments. Values are the average of 10 replicates consisting of three pears per replicate \pm standard deviation ($n=30$). The lesion diameters, from which the percentage inhibition was obtained, are shown in Figure 7.

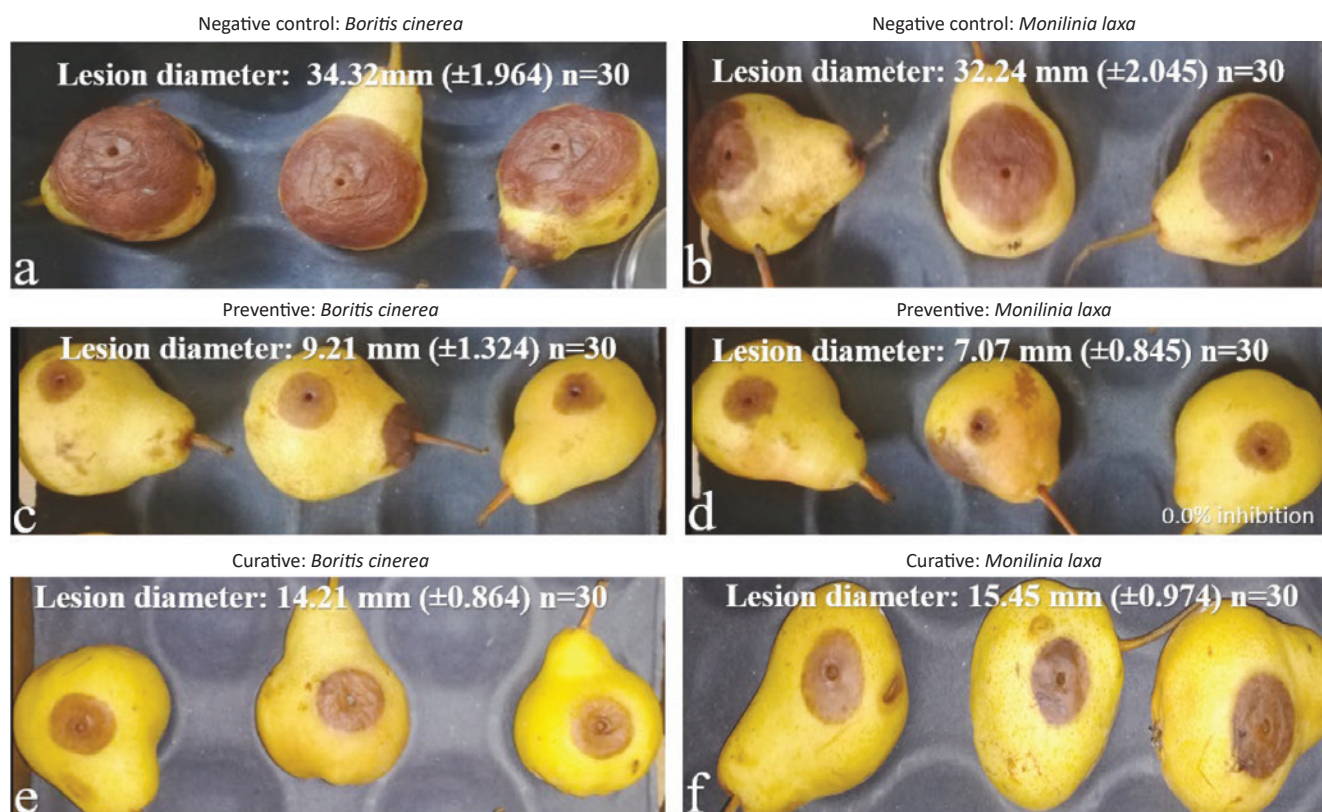


FIGURE 7. Photograph of pears showing lesion diameters because of spoilage caused by *Botrytis cinerea* (a) and *Monilinia laxa* (b) with the associated level of biological control by *Pichia kluyveri* Y1164 against preventive *Botrytis cinerea* (c) and *Monilinia laxa* (d) treatments as well as curative *Botrytis cinerea* (e) and *Monilinia laxa* (f) treatments. Values are the average of 10 replicates consisting of three pears per replicate \pm standard deviation ($n=30$). Each set (consisting of three pears) is a representative example after 4 weeks at -0.5°C and then at room temperature ($\pm 20^{\circ}\text{C}$) for 7 days.

CONCLUSIONS

The biocontrol yeast *P. kluyveri* Y1164 inhibited *B. cinerea* and *M. laxa* growth on apples, pears, and table grapes when applied preventively. However, *P. kluyveri* Y1164 was not as effective when applied as a curative treatment. Biological control can be considered as a preventive strategy to reduce postharvest fungal spoilage of fruits. Exploring pre-harvest efficacy of the biocontrol yeast *P. kluyveri* Y1164, as well as its efficacy against other fruit fungal pathogens can be investigated in future studies.

RESEARCH FUNDING

This work was supported by the Agricultural Research Council (ARC) and National Research Foundation (NRF) of South Africa (Grant Numbers: SFP160505164079 and 117833). The opinions, findings and conclusions or recommendations expressed in this publication is that of the authors alone, and the NRF accepts no liability whatsoever in this regard. The authors thank the students, interns, technicians and research assistants who contributed.

CONFLICT OF INTERESTS

Authors declare no conflict of interests.

ORCID IDs

B.S. Chidi <https://orcid.org/0000-0001-8497-7596>
 H.W. du Plessis <https://orcid.org/0000-0001-8092-6492>
 U.F. Hutchinson <https://orcid.org/0000-0002-5219-6223>
 N.P. Jolly <https://orcid.org/0000-0001-7278-6442>
 M. Mewa-Ngongang <https://orcid.org/0000-0003-2588-3973>
 S.K.O. Ntwampe <https://orcid.org/0000-0001-7516-6249>
 V.I. Okudoh <https://orcid.org/0000-0002-8468-1338>

REFERENCES

- Aloui, H., Licciardello, F., Khwaldia, K., Hamdi, M., Restuccia, C. (2015). Physical properties and antifungal activity of bioactive films containing *Wickerhamomyces anomalus* killer yeast and their application for preservation of oranges and control of post-harvest green mold caused by *Penicillium digitatum*. *International Journal of Food Microbiology*, 200, 22–30. <https://doi.org/10.1016/j.ijfoodmicro.2015.01.015>
- Andrade, M.J., Thorsen, L., Rodríguez, A., Córdoba, J.J., Jespersen, L. (2014). Inhibition of ochratoxigenic moulds by *Debaryomyces hansenii* strains for biopreservation of dry-cured meat products. *International Journal of Food Microbiology*, 170, 70–77. <https://doi.org/10.1016/j.ijfoodmicro.2013.11.004>
- Benito, S., Palomero, F., Morata, A., Uthurry, C., Suárez-Lepe, J.A. (2009). Minimization of ethylphenol precursors in red wines

- via the formation of pyranoanthocyanins by selected yeasts. *International Journal of Food Microbiology*, 132(2–3), 145–152.
<https://doi.org/10.1016/j.ijfoodmicro.2009.04.015>
4. Buzzini, P., Martini, A. (2002). Extracellular enzymatic activity profiles in yeast and yeast-like strains isolated from tropical environments. *Journal of Applied Microbiology*, 93(2), 1020–1025.
<https://doi.org/10.1046/j.1365-2672.2002.01783.x>
 5. Cape Farm Mapper. [http://gis.elsenburg.com/apps/cfm] (accessed: 6 June 2018).
 6. Çelik, Z.D., Erten, H., Darici, M., Cabaroğlu, T. (2017). Molecular characterization and technological properties of wine yeasts isolated during spontaneous fermentation of *Vitis vinifera* L. cv. Narince grape must grown in ancient wine making area Tokat, Anatolia. *BIO Web of Conference*, 9, art. no. 02017.
<https://doi.org/10.1051/bioconf/20170902017>
 7. Ciani, M., Fatichenti, F. (2001). Killer toxin of *Kluyveromyces phaffii* DBVPG 6076 as a biopreservative agent to control apiculate wine yeasts. *Applied Environmental Microbiology*, 67(7), 3058–3063.
<https://doi.org/10.1128/AEM.67.7.3058-3063.2001>
 8. Comitini, F., De, J.I., Pepe, L., Mannazzu, I., Ciani, M. (2004a). *Pichia anomala* and *Kluyveromyces wickerhamii* killer toxins as new tools against *Dekkera/Brettanomyces* spoilage yeasts. *FEMS Microbiology Letters*, 238(1), 235–240.
<https://doi.org/10.1111/j.1574-6968.2004.tb09761.x>
 9. Comitini, F., Di Pietro, N., Zacchi, L., Mannazzu, I., Ciani, M. (2004b). *Kluyveromyces phaffii* killer toxin active against wine spoilage yeasts: purification and characterization. *Microbiology*, 150(8), 2535–2541.
<https://doi.org/10.1099/mic.0.27145-0>
 10. Cordero-Bueso, G., Mangieri, N., Maghradze, D., Foschino, R., Valdetara, F., Cantoral, J.M., Vigentini, I. (2017). Wild grape-associated yeasts as promising biocontrol agents against *Vitis vinifera* fungal pathogens. *Frontiers in Microbiology*, 8, art. no. 2025.
<https://doi.org/10.3389/fmicb.2017.02025>
 11. Crafac, M., Mikkelsen, M.B., Saerens, S., Knudsen, M., Blennow, A., Lowor, S., Takrama, J., Swiegers, J.H., Petersen, G.B., Heimdal, H. (2013). Influencing cocoa flavour using *Pichia kluyveri* and *Kluyveromyces marxianus* in a defined mixed starter culture for cocoa fermentation. *International Journal of Food Microbiology*, 167(1), 103–116.
<https://doi.org/10.1016/j.ijfoodmicro.2013.06.024>
 12. Droby, S. (2005). Improving quality and safety of fresh fruits and vegetables after harvest by the use of biocontrol agents and natural materials. *Acta Horticulturae*, 709, 45–52.
<https://doi.org/10.17660/ActaHortic.2006.709.5>
 13. Du Toit, M., Pretorius, I.S. (2000). Microbial spoilage and preservation of wine: using weapons from nature's own arsenal – a review. *South African Journal of Enology and Viticulture*, 21(1), 74–96.
<https://doi.org/10.21548/21-1-3559>
 14. El-Ghaouth, A., Wilson, C., Wisniewski, M. (2004). Biologically-based alternatives to synthetic fungicides for the control of post-harvest diseases of fruit and vegetables. In: Naqvi, S.A.M.H. (Eds.), *Diseases of Fruits and Vegetables*. Volume II. Springer, Dordrecht, pp. 511–535.
https://doi.org/10.1007/1-4020-2607-2_14
 15. Fiori, S., Urgeghe, P.P., Hammami, W., Razzu, S., Jaoua, S., Migheli, Q. (2014). Biocontrol activity of four non-and low-fermenting yeast strains against *Aspergillus carbonarius* and their ability to remove ochratoxin A from grape juice. *International Journal of Food Microbiology*, 189, 45–50.
<https://doi.org/10.1016/j.ijfoodmicro.2014.07.020>
 16. Fourie, P.H., Holz, G., Calitz, F.J. (2002). Occurrence of *Botrytis cinerea* and *Monilinia laxa* on nectarine and plum in Western Cape orchards, South Africa. *Australasian Plant Pathology*, 31, 197–204.
<https://doi.org/10.1071/AP02007>
 17. Fredlund, E., Blank, L.M., Schnürer, J., Sauer, U., Passoth, V. (2004). Oxygen- and glucose-dependent regulation of central carbon metabolism in *Pichia anomala*. *Journal of Applied Environmental Microbiology*, 70(10), 5905–5911.
<https://doi.org/10.1128/AEM.70.10.5905-5911.2004>
 18. Gril, T., Celar, F., Munda, A., Javornik, B., Jakse, J. (2008). AFLP analysis of intraspecific variation between *Monilinia laxa* isolates from different hosts. *Plant Disease*, 92(12), 1616–1624.
<https://doi.org/10.1094/PDIS-92-12-1616>
 19. Grzegorzczak, M., Żarowska, B., Restuccia, C., Cirvilleri, G. (2017). Post-harvest biocontrol ability of killer yeasts against *Monilinia fructigena* and *Monilinia fructicola* on stone fruit. *Food Microbiology*, 61, 93–101.
<https://doi.org/10.1016/j.fm.2016.09.005>
 20. Hernández, A., Martín, A., Córdoba, M.G., Benito, M.J., Aranda, E., Pérez-Nevado, F. (2008). Determination of killer activity in yeasts isolated from the elaboration of seasoned green table olives. *International Journal of Food Microbiology*, 121(2), 178–188.
<https://doi.org/10.1016/j.ijfoodmicro.2007.11.044>
 21. Huang, R., Che, H.J., Zhang, J., Yang, L., Jiang, D.H., Li, G.Q. (2012). Evaluation of *Sporidiobolus pararoseus* strain YCXT3 as biocontrol agent of *Botrytis cinerea* on post-harvest strawberry fruits. *Biological Control*, 62(1), 53–63.
<https://doi.org/10.1016/j.biocontrol.2012.02.010>
 22. Huang, R., Li, G.Q., Zhang, J., Yang, L., Che, H.J., Jiang, D.H., Huang, H.C. (2011). Control of post-harvest *Botrytis* fruit rot of strawberry by volatile organic compounds of *Candida intermedia*. *Phytopathology*, 101(7), 859–869.
<https://doi.org/10.1094/PHYTO-09-10-0255>
 23. Jolly, N.P., Varela, C., Pretorius, I.S. (2014). Not your ordinary yeast: non-*Saccharomyces* yeasts in wine production uncovered. *FEMS Yeast Research*, 14(2), 215–237.
<https://doi.org/10.1111/1567-1364.12111>
 24. Liu, J., Sui, Y., Wisniewski, M., Droby, S., Liu, Y. (2013). Review: utilization of antagonistic yeasts to manage post-harvest fungal diseases of fruit. *International Journal of Food Microbiology*, 167(2), 153–160.
<https://doi.org/10.1016/j.ijfoodmicro.2013.09.004>
 25. Lutz, M.C., Lopes, C.A., Rodriguez, M.E., Sosa, M.C., Sangorín, M.P. (2013). Efficacy and putative mode of action of native and commercial antagonistic yeasts against post-harvest pathogens of pear. *International Journal of Food Microbiology*, 164(2–3), 166–172.
<https://doi.org/10.1016/j.ijfoodmicro.2013.04.005>
 26. Medina-Córdova, N., López-Aguilar, R., Ascencio, F., Castellanos, T., Campa-Córdova, A.I., Angulo, C. (2016). Biocontrol activity of the marine yeast *Debaryomyces hansenii* against phytopathogenic fungi and its ability to inhibit mycotoxins production in maize grain (*Zea mays* L.). *Biological Control*, 97, 70–79.
<https://doi.org/10.1016/j.biocontrol.2016.03.006>

27. Mehlomakulu, N.N., Setati, M.E., Divol, B. (2014). Characterization of novel killer toxins secreted by wine-related non-*Saccharomyces* yeasts and their action on *Brettanomyces* spp. *International Journal of Food Microbiology*, 188, 83–91. <https://doi.org/10.1016/j.ijfoodmicro.2014.07.015>
28. Mewa-Ngongang, M., du Plessis, H.W., Hutchinson, U.F., Mekuto, L., Ntwampe, S.K. (2017). Kinetic modelling and optimisation of antimicrobial compound production by *Candida pyralidae* KU736785 for control of *Candida guilliermondii*. *Food Science and Technology International*, 23(4), 358–370. <https://doi.org/10.1177/1082013217694288>
29. Mewa-Ngongang, M., du Plessis, H.W., Ntwampe, S.K., Chidi, B.S., Hutchinson, U.F., Mekuto, L., Jolly, N.P. (2019a). Grape pomace extracts as fermentation medium for the production of potential biopreservation compounds. *Foods*, 8(2), art. no. 51. <https://doi.org/10.3390/foods8020051>
30. Mewa-Ngongang, M., du Plessis, H.W., Ntwampe, S.K.O., Chidi, B.S., Hutchinson, U.F., Mekuto, L., Jolly, N.P. (2019b). The use of *Candida pyralidae* and *Pichia kluyveri* to control spoilage microorganisms of raw fruits used for beverage production. *Foods* 8(10), art. no. 454. <https://doi.org/10.3390/foods8100454>
31. Morales, H., Marín, S., Rovira, A., Ramos, A.J., Sanchis, V. (2007). Patulin accumulation in apples by *Penicillium expansum* during postharvest stages. *Letters in Applied Microbiology*, 44(1), 30–35. <https://doi.org/10.1111/j.1472-765X.2006.02035.x>
32. Muccilli, S., Restuccia, C. (2015). Bioprotective role of yeasts. *Microorganisms*, 3(4), 588–611. <https://doi.org/10.3390/microorganisms3040588>
33. Nally, M.C., Pesce, V.M., Maturano, Y.P., Rodriguez-Assaf, L.A., Toro, M.E., Castellanos de Figueroa, L.I., Vazquez, F. (2015). Antifungal modes of action of *Saccharomyces* and other biocontrol yeasts against fungi isolated from sour and grey rots. *International Journal of Food Microbiology*, 204, 91–100. <https://doi.org/10.1016/j.ijfoodmicro.2015.03.024>
34. Núñez, F., Lara, M.S., Peromingo, B., Delgado, J., Sánchez-Montero, L., Andrade, M.J. (2015). Selection and evaluation of *Debaryomyces hansenii* isolates as potential bioprotective agents against toxigenic *penicillia* in dry-fermented sausages. *Food Microbiology*, 46, 114–120. <https://doi.org/10.1016/j.fm.2014.07.019>
35. Oro, L., Ciani, M., Comitini, F. (2014). Antimicrobial activity of *Metschnikowia pulcherrima* on wine yeasts. *Journal of Applied Microbiology*, 116(5), 1209–1217. <https://doi.org/10.1111/jam.12446>
36. Parveen, S., Wani, A.H., Bhat, M.Y., Koka, J.A., Wani, F.A. (2016). Management of post-harvest fungal rot of peach (*Prunus persica*) caused by *Rhizopus stolonifer* in Kashmir Valley, India. *Plant Pathology & Quarantine*, 6(1), 19–29. <https://doi.org/10.5943/ppq/6/1/4>
37. Psani, M., Kotzekidou, P. (2006). Technological characteristics of yeast strains and their potential as starter adjuncts in Greek-style black olive fermentation. *World Journal of Microbiology and Biotechnology*, 22, 1329–1336. <https://doi.org/10.1007/s11274-006-9180-y>
38. Sáez, J.S., Lopes, C.A., Kirs, V.C., Sangorrín, M.P. (2010). Enhanced volatile phenols in wine fermented with *Saccharomyces cerevisiae* and spoiled with *Pichia guilliermondii* and *Dekkera bruxellensis*. *Letters in Applied Microbiology*, 51(2), 170–176. <https://doi.org/10.1111/j.1472-765X.2010.02878.x>
39. Sansone, G.Y., Lambrese, V., Calvente, G., Fernández, D., Benuzzi, M., Sanz Ferramola, M. (2018). Evaluation of *Rhodospodium fluviale* as biocontrol agent against *Botrytis cinerea* on apple fruit. *Letters in Applied Microbiology*, 66(5), 455–461. <https://doi.org/10.1111/lam.12872>
40. Sharma, R.R., Singh, D., Singh, R. (2009). Biological control of post-harvest diseases of fruits and vegetables by microbial antagonists: A review. *Biological Control*, 50(3), 205–221. <https://doi.org/10.1016/j.biocontrol.2009.05.001>
41. Singh, D., Sharma, R.R. (2007). *Post-Harvest Diseases Of Fruit, Vegetables, And Their Management*, first ed. Daya Publishing House, New Delhi, India.
42. Thompson, R.S., Aveling, T.A.S., Blanco, P.R. (2013). A new semi-selective medium for *Fusarium graminearum*, *F. proliferatum*, *F. subglutinans* and *F. verticillioides* in maize seed. *South African Journal of Botany*, 84, 94–101. <https://doi.org/10.1016/j.sajb.2012.10.003>
43. Tipper, D.J., Bostian, K.A. (1984). Double-stranded ribonucleic acid killer systems in yeasts. *Microbiological Reviews*, 48(2), 125–156. <https://doi.org/10.1128/mr.48.2.125-156.1984>
44. Williamson, B., Tudzynski, B., Tudzynski, P., Van Kan, J.A. (2007). *Botrytis cinerea*: the cause of grey mould disease. *Molecular Plant Pathology*, 8(5), 561–580. <https://doi.org/10.1111/j.1364-3703.2007.00417.x>
45. Zhu, C., Shi, J., Jiang, C., Liu, Y. (2015). Inhibition of the growth and ochratoxin A production by *Aspergillus carbonarius* and *Aspergillus ochraceus* in vitro and in vivo through antagonistic yeasts. *Food Control*, 50, 125–132. <https://doi.org/10.1016/j.foodcont.2014.08.042>
46. Zhu, S.J. (2006). Non-chemical approaches to decay control in post-harvest fruit. In *Advances in Postharvest Technologies for Horticultural Crops*. Research Signpost, Trivandrum, India, ISBN, 8130801108, pp. 297–313.

Expression Profile of Brain Aging and Metabolic Function are Altered by Resveratrol or α -Ketoglutarate Supplementation in Rats Fed a High-Fat Diet

Paulina Szczurek-Janicka^{1,*} , Katarzyna Ropka-Molik² , Maria Oczkowicz² ,
Sylwia Orczewska-Dudek¹ , Mariusz Pietras¹ , Marek Pieszka¹ 

¹Department of Animal Nutrition and Feed Sciences, National Research Institute of Animal Production, Krakowska Str. 1, 32–083 Balice, Poland

²Department of Animal Molecular Biology, National Research Institute of Animal Production, Krakowska Str. 1, 32–083 Balice, Poland

Key words: α -ketoglutarate, brain aging, gene expression profiling, high-fat diet, resveratrol, rats

The aim of this study was to examine the impact of different dietary interventions started at middle age on the metabolic phenotype and gene expression profiling in the hypothalamus. One-year old rats were fed either a control diet, high-fat diet (HFD), HFD supplemented with resveratrol (HFD+RESV), or HFD supplemented with α -ketoglutarate (HFD+AKG). A 6-week HFD feeding led to significant changes in concentrations of plasma glucose, insulin, lipids, and thyroid hormones. Moreover, 32% of the 84 analyzed genes correlated with aging were differentially expressed compared to the control group, with the largest functional class being related to inflammatory response. Dietary RESV ameliorated the changes in plasma glucose, total cholesterol, and triiodothyronine concentrations induced by HFD feeding and significantly downregulated 60% of the surveyed genes compared to the control group, resulting in a major molecular shift compared to HFD alone. In contrast, AKG supplementation did not affect the metabolic phenotype, but prevented the gene expression pattern caused by HFD consumption, mimicking the effects observed in the control group. HFD feeding induces metabolic dysfunction and age-related genetic alterations in the hypothalamus of middle-aged rats, while dietary RESV or AKG may partially retard these effects, even though these compounds act in a different and specific manner.

ABBREVIATIONS

AKG – α -ketoglutarate, AUC – area under the curve, BW – body weight, HDL – high-density lipoproteins, HFD – high-fat diet, LDL – low-density lipoproteins, NPY – neuropeptide Y, RESV – resveratrol, rT3 – reverse triiodothyronine, SD – standard deviation, T3 – triiodothyronine, T4 – thyroxine, TG – triacylglycerols.

INTRODUCTION

Aging is a complex and still poorly understood process, even in the light of its great importance and ubiquity. Studies in diverse species showed that both environmental, genetic, as well as dietary alterations might have profound effects on aging, while the most effective way to extend lifespan and delay the onset of age-associated phenotypes is caloric restriction (CR) [Baur *et al.*, 2006; Dacks *et al.*, 2013]. Efforts have been made to identify natural or synthetic compounds that mimic its action but without dietary sacrifice.

One of the most popular CR mimetics is resveratrol (RESV), a natural polyphenol known for its anti-inflammatory, anticancer, cardioprotective, neuroprotective, and antioxidant properties [Baur *et al.*, 2006; Testa *et al.*, 2014]. Although its effect on lifespan varies among species, it has been demonstrated to protect against certain age-related pathologies, including metabolic deficits and cognitive decline [Barger *et al.*, 2008; Testa *et al.*, 2014]. Unfortunately, in humans and other mammals, RESV features a relatively low bioavailability [Walle *et al.*, 2004].

α -Ketoglutarate (AKG), a key intermediate of the Krebs cycle and a keto acid providing carbon backbone for glutamate and glutamine, seems to be another interesting anti-aging compound. It has been shown that AKG may prolong the lifespan of model organisms and delay the onset of multiple hallmarks of aging [Chin *et al.*, 2014; Radzki *et al.*, 2009]. The AKG-induced longevity effect is mediated by the regulation of cellular energy metabolism involving ATP synthase and mTOR kinase [Chin *et al.*, 2014]. Indeed, elevated concentration of AKG has been also reported during

* Corresponding Author:

E-mail: paulina.szczurek@iz.edu.pl (P. Szczurek-Janicka)

Submitted: 8 April 2021

Accepted: 17 June 2021

Published on-line: 20 July 2021



fasting and CR [Chin *et al.*, 2014]. Moreover, AKG inhibits the production of oxygen radicals and thus may prevent neurons from oxidative stress and lipid peroxidation [Niemiec *et al.*, 2011; Thomas *et al.*, 2015]. There are also indications that intermediates of the Krebs cycle, including AKG, may affect the rate of aging at the epigenetic level through DNA methylation and histone modification [Salminen *et al.*, 2014]. The major site of catabolism of orally administrated AKG is the small intestine, with the AKG half-life being usually short due to the rapid metabolism in enterocytes and the liver [Dąbek *et al.*, 2005].

On the other hand, increasing evidence demonstrates a direct link between high-fat diet (HFD) consumption and metabolic dysfunction, which favors pathological brain aging and cognitive decline [Uranga *et al.*, 2010]. Perturbation in metabolism, such as high fasting glucose, insulin resistance, hypertension, elevated adiposity or lipolysis rate, may exacerbate oxidative stress and inflammation in the brain, and thus modulate hippocampal synaptic plasticity and impair learning and memory functions [Uranga *et al.*, 2010]. Systemic metabolic complications caused by HFD feeding lead to a pre-diabetic phenotype and obesity, current threats of public health, and furthermore, obesity has been correlated with more severe brain atrophy [Lizarbe *et al.*, 2019; Uranga *et al.*, 2010]. Taking into account the growing number of older people, understanding the possible link between dietary factors, metabolic response, and the rate of aging is of particular importance.

During aging, the brain undergoes numerous changes at the molecular, cellular, and structural levels. Even though the causes of brain aging remain mostly unknown, it seems that temporal patterns of gene expression might serve as biomarkers of aging. Moreover, hormonal shifts induced by changes in nutrient availability might have a profound effect on age-related transcriptional profiles [Anderson & Weindruch, 2010]. As metabolism is largely regulated by the hypothalamus, understanding the effects of aging on its physiology may provide valuable information on aging itself. Importantly, the hypothalamic gene expression appears to be required for some protective responses to CR [Barger *et al.*, 2008].

Because gene expression profiling can be used to determine the biological age of a tissue, and because many nutrients with anti-ageing potential act in a tissue-specific manner, we hypothesized that dietary supplementation with RESV or AKG would cause a beneficial shift in the metabolism and gene expression pattern of animals fed HFD towards control animals. Thus, the present study aimed to examine the effect of different dietary interventions started at middle age on metabolic phenotype and gene expression profiling associated with aging in rat hypothalamus. The interventions included HFD, HFD supplemented with RESV, HFD supplemented with AKG, and a standard chow diet as a control. Additionally, RESV was encapsulated within a triacylglycerol matrix to increase its bioavailability in the gastrointestinal tract. A rat model has been used repeatedly to study the effects of HFD consumption or CR on human aging [Andersen *et al.*, 2011; Franco *et al.*, 2016].

MATERIALS AND METHODS

Animals and diet

All experimental procedures were approved by the second Local Ethical Review Committee for Animal Experiments in Cracow, Poland (approval no 1162/2015) and were performed according to the approved guidelines.

Adult 1-year old male Wistar rats ($n=24$), weighing 479 ± 39.5 g at a study beginning, were purchased from the Medical University of Silesia, Katowice, Poland. Rats were housed 6 per cage and maintained under standard laboratory conditions on 12-h/12-h light/dark cycle and a temperature of $22\pm 3^\circ\text{C}$. All animals had access to food and water available *ad libitum*. After a 14-day adaptation period, when all rats were fed a standard chow diet [NRC, 1995], animals were randomly assigned to one of the four intervention groups ($n=6$): Control group, fed a standard chow diet; HFD group, fed a high-fat diet; HFD+RESV group, fed the same high-fat diet but supplemented with resveratrol; or HFD+AKG group, fed the same high-fat diet but supplemented with α -ketoglutarate. A high-fat diet was composed of 40% energy from lard. The composition and nutritional value of the control and high-fat diets analyzed by AOAC methods [AOAC, 2000] are presented in Table 1. The dose of *trans*-resveratrol (Great Forest Biomedical Ltd., Hangzhou, China) in the form of microcapsules was 660 mg/kg of feed, while the dose of AKG (Gramineer Int. AB, Lund, Sweden) was 12.8 g/kg of feed. Animals' body weight was measured weekly. At the end of a 6-week experiment, rats were anesthetized with CO_2 and euthanized by decapitation.

Resveratrol encapsulation

Resveratrol was encapsulated using a mixture of C12-C22 fatty acids in the form of triacylglycerols (TG) (Berg+Schmidt, Hamburg, Germany) and calcium sulfate (Chempur, Piekary Śląskie, Poland) [Müller *et al.*, 2002]. The TG were dissolved in a ceramic pot in a water bath at 80°C , and a mixture of calcium sulfate and resveratrol was added so the final volume concentration was 4%, and mixed thoroughly. Resveratrol accounted for 76% of the mixture volume. After obtaining a homogeneous mixture, the solution was stirred with a ceramic stirrer until it solidified at room temperature. The pot with the mixture was then placed in a refrigerator at -20°C for 60 min. Finally, the mixture was ground on a laboratory mill with a 1.5×1.5 mm mesh diameter. The encapsulated RESV was prepared once before the start of the experiment and each batch of feed containing RESV was prepared every 10 days. Before being added to the feed, RESV was stored in a refrigerator at 4°C , protected from light.

Blood biochemical analysis

Blood samples (about 10 mL) were collected during slaughter by heart puncture, transferred to tubes with lithium heparin (Equimed, Kraków, Poland), and immediately placed on ice. Plasma samples were collected after centrifugation ($3000\times g$ for 10 min at 4°C) and stored at -20°C before further handling. Concentrations of plasma glucose, TG, total cholesterol, as well as low and high density lipoprotein cholesterol

TABLE 1. Composition and nutritional value of standard chow (Control) and high-fat diet (HFD).

Component (g/100 g)	Control	HFD
Oatmeal	18.0	–
Barley meal	20.0	–
Wheat meal	23.0	–
Wheat bran	20.0	–
Rapeseed oil	3.0	–
Milk powdered	10.0	48.0
Yeast	5.0	–
Premix	1.0	1.0
Lard	–	40.0
Corn starch	–	11.0
Nutritional value per 1 kg of dry weight		
Metabolic energy (MJ/kg)	11.4	20.6
Total protein (g)	157	157
Raw fat (g)	55.1	404
Raw fiber (g)	44.9	–
Raw ash (g)	34.2	–
Starch (g)	414	92.5
Magnesium (g)	0.07	0.07
Phosphorus (g)	3.12	4.22
Sodium (g)	1.14	2.80
Iron (mg)	126	63.8
Copper (mg)	9.69	8.57
Manganese (mg)	50.9	25.0
Zinc (mg)	61.2	107
Cobalt (mcg)	123	53.3
Iodine (mcg)	104	0.30
Selenium (mcg)	0.36	0.03
Vitamin A (IU)	5727	5192
Vitamin D3 (IU)	500	500
Vitamin E (mg)	9.67	11.0
Vitamin B1 (mg)	6.74	2.32
Vitamin B2 (mg)	7.78	11.0
Vitamin B6 (mg)	6.21	2.75
Vitamin B12 (mcg)	6.21	18.2
Vitamin C (mg)	1.29	–
Vitamin K3 (mg)	0.67	0.66
Folic acid (mg)	1.29	0.48
Nicotinic acid (mg)	97.9	12.7
Pantothenic acid (mg)	23.9	19.7
Choline (mg)	1199	652
Biotin (mg)	0.21	0.16

fractions (LDL/HDL) were determined with the colorimetric method using commercial kits (Cormay, Łomianki, Poland) and a Beckman DU-640 spectrophotometer (Fullerton, CA, USA), according to the manufacturer's instructions. Radio-immunological quantitation of ghrelin and leptin as well as insulin, neuropeptide Y (NPY), and thyroid hormones (T3, T4, rT4) was performed with commercial kits (Phoenix Pharmaceuticals, Burlingame, CA, USA or Merck Millipore, Burlington, MA, USA, respectively) in a gamma counter (LKB Wallac MiniGamma 1275, Mt Waverley, Australia). Additionally, the glucose level was measured weekly in a blood drop from the tail vein using a glucometer and test strips (Roche Accu-Chek Active, Basel, Switzerland).

Gene expression analysis

The hypothalamic transcriptional level of 84 genes correlated with aging was analyzed using RT² Profiler™ PCR Array Rat Aging system (Qiagen, Hilden, Germany, Table 2). Hypothalamus was rapidly dissected and immediately placed in an RNAlater solution (Ambion, Austin, TX, USA), incubated at 4°C for 24 h, and stored at -20°C until further handling. Total RNA was isolated using PureLink RNA Mini Kit (Thermo

TABLE 2. A list of genes analyzed with microarray.

Biological process	Gene symbol
Genomic instability	<i>BUB1B, MRPL43, POLRMT, TFAM, TFB1M, TFB2M, ZMPSTE24</i>
Telomere attrition	<i>POT1, RAPIA, TERF1, TERF2, TINF2, TPP1</i>
Mitochondrial dysfunction	<i>MRPL43, NDUFB11, POLRMT, SIRT3, SIRT6, TFAM, TFB1M, TFB2M</i>
Proteostasis	<i>ARL6IP6, BUB1B, FOXO1, HSF1 (TCF5), JAKMIP3, RNFI44B, TXNIP, VPS13C</i>
Laminopathies	<i>LMNA, LMNB1, LMNB2, ZMPSTE24</i>
Neurodegeneration & synaptic transmission	<i>CALB1, GFAP, MBP, SCN2B, SNAP23</i>
Epigenetic alterations	<i>ARID1A, SIRT3, SIRT6</i>
DNA binding	<i>ARID1A, ELP3, EP300, FBXL16, LOC100362548, ZBTB10, ZFR, ZFP9</i>
RNA binding	<i>ELAVL1, LSM5, ZFR</i>
Inflammatory response	<i>ANGEL2, ANXA3, ANXA5, C1QA, C1QB, C1QC, C1S, C3, C3AR1, C4A, C4B, C5AR1 (GPR77), CCR1, CD14, CD163, CFH, CFHR1, CX3CL1, CXCL16, FCER1G, FCGBP, FCGR1A, FCGR2A, FCGR2B, GFA, LYZL1, LTF, MBP, PANX1, S100A8, S100A9, TLR2, TLR4, TMEM135, TMEM33, TOLLIP</i>
Apoptosis	<i>CASP1 (ICE), CLU, EP300, PDCD6, TOLLIP</i>
Cellular senescence	<i>CDKN1C (P57KIP2), RGD1564788, VWA5A</i>
Cell cycle	<i>BUB1B, CDKN1C (P57KIP2)</i>
Cytoskeleton regulators	<i>COL1A1, EML1</i>
Oxidative stress	<i>EP300</i>
Transcriptional regulation	<i>ARID1A, EP300, FOXO1, HSF1 (TCF5), PHF3, SMAD2 (MADH2)</i>

Fisher Scientific, Waltham, MA, USA) following the manufacturer's protocol. RNA concentration and integrity were assessed using TapeStation 2200 and RNA ScreenTape 2200 (Agilent, Santa Clara, CA, USA). The RNA Integrity Number for all samples was >7.5 . The RNA samples were stored at -80°C before further handling. The 1000 ng of extracted RNA was reverse-transcribed using a cDNA conversion kit (RT² First Strand Kit, Qiagen, Hilden, Germany) according to manufacturer's recommendations. The cDNA was used in the RT² Profiler™ PCR Array Rat Aging system (Qiagen, Hilden, Germany, Cat. no. PARN-178Z) in combination with RT² SYBR® Green qPCR Mastermix (Qiagen, Hilden, Germany, Cat. no. 330529). The plate contained primers for all analyzed genes designed by Qiagen company, as well as appropriate RNA sequences that were used as housekeeping assays and quality controls. Gene expression was determined by real-time PCR using an ABI-7500 thermocycler (Applied Biosystems, Thermo Fisher Scientific, Waltham, MA, USA) according to the manufacturer's instructions. C_T values were analyzed by the data analysis web portal at <http://www.qiagen.com/geneglobe> with the C_T cut-off set to 35, normalized using reference genes, and ΔC_T method was used to express transcript level. Changes in gene expression were illustrated as a fold increase/decrease. The cut-off fold-change for differential expression was set as 1.5.

Statistical analysis

Statistical significance for plasma and growth parameters was assessed using one-way ANOVA with Tukey's correction for multiple comparisons or Kruskal-Wallis test with Dunn's correction for non-Gaussian data distribution using GraphPad Prism v7 (GraphPad Software, San Diego, CA, USA). Data were expressed as mean \pm standard deviation (SD). The real-time PCR array data were statistically analyzed by the data analysis web portal at <http://www.qiagen.com/geneglobe>. In all statistical analyses, differences were considered significant at $p \leq 0.05$.

RESULTS AND DISCUSSION

Metabolic phenotype of rats after different dietary interventions

Increasing evidence implicates that nutrition, and especially Western-type diet with high saturated fat content, and simultaneously low in fiber, polyphenols, vitamins, and minerals, might act like a pro-aging stimulus for many biochemical and physiological aspects of brain aging [Morrison *et al.*, 2010; Nuthikattu *et al.*, 2019; Uranga *et al.*, 2010]. On the contrary, CR and its mimetics are reported to maintain metabolic function, guarantee successful brain aging, and increase lifespan in most organisms studied [Anderson & Weindruch, 2010; Zhou *et al.*, 2012]. However, the specific effects of different dietary interventions, regarding particularly brain aging, remain poorly understood. We used middle-aged rats to assess aging phenotypes under various dietary conditions implemented in the period before the increase in mortality. High-quality foods consumed in middle age appear to be strongly associated with better health of individuals

surviving to older ages, which is critical to maintaining well-being in aging societies.

Here, as expected, a 6-week consumption of HFD composed of 40% lard (high in saturated fatty acids) resulted in alterations in carbohydrate and lipid metabolism (Figure 1). Glucose concentration was significantly ($p \leq 0.05$) higher in HFD and HFD+AKG groups compared to the control group. Followed the increase in plasma glucose level at the end of a 6-week study, a significantly ($p \leq 0.05$) elevated blood glucose concentration measured weekly and expressed as area under the curve (AUC) was noted in all groups treated with HFD compared to the control rats (Figure 1). Total cholesterol level was significantly ($p \leq 0.05$) higher in HFD and HFD+AKG groups compared to the control group. The concentrations of HDL and LDL cholesterol fractions were significantly ($p \leq 0.05$) higher in all groups receiving HFD compared to the control group. A strong correlation between HFD and such conditions as insulin resistance, hyperglycemia, hyperinsulinemia, and hyperlipidemia, is widely known and has been repeatedly reported [Baur *et al.*, 2006; Cho *et al.*, 2012; Mohamed *et al.*, 2010; Morrison *et al.*, 2010; Nuthikattu *et al.*, 2019; Uranga *et al.*, 2010].

No differences were observed in the metabolic phenotype after HFD supplementation with AKG (Figure 1), which is in contrast to Radzki *et al.* [2009] and Tian *et al.* [2020], who demonstrated an improved plasma lipid profile in hypercholesterolemic rats or improved glucose tolerance in HFD-fed mice, respectively. On the contrary, HFD supplementation with RESV ameliorated the increase in plasma glucose and total cholesterol levels (Figure 1); however, the differences were not statistically significant. The antidiabetic effect of CR and RESV has been well described in the literature [Barger *et al.*, 2008; Baur *et al.*, 2006; Lagouge *et al.*, 2006]. A parallel lack of RESV effect on plasma insulin (Figure 1) might suggest improved insulin sensitivity, which indeed has been demonstrated by other authors [Andersen *et al.*, 2011; Baur *et al.*, 2006]. Similarly, the hypocholesterolemic effect of RESV is also in the agreement with other rodent studies [Cho *et al.*, 2012; Miura *et al.*, 2003]. There are suggestions that RESV might inhibit hepatic 3-hydroxy-3-methylglutaryl reductase activity, a rate-limiting enzyme for cholesterol synthesis, or increase fecal bile acids excretion [Cho *et al.*, 2012]. It should be emphasized that in our study RESV was encapsulated within a triglyceride matrix to increase its digestive stability and bioavailability after oral administration. As previously shown, RESV features low bioaccessibility and only its trace amounts reach the circulation [Walle *et al.*, 2004].

The results of the present study also support the finding that HFD consumption results in a high circulation leptin level [Kandhare *et al.*, 2018; Mohamed *et al.*, 2010], although in our study a statistically significant ($p \leq 0.05$) difference was noted only in HFD+AKG group compared to the control group (Figure 1). A high leptin concentration may indicate leptin resistance due to a lack of leptin receptor in the hypothalamus or abnormalities in postreceptor signaling [Jimoh *et al.*, 2018; Mohamed *et al.*, 2010]. A significant increase in leptin level only in the HFD+AKG group is challenging to explain and needs further investigation. Perhaps a more long-term study would reveal differences in all groups fed HFD.

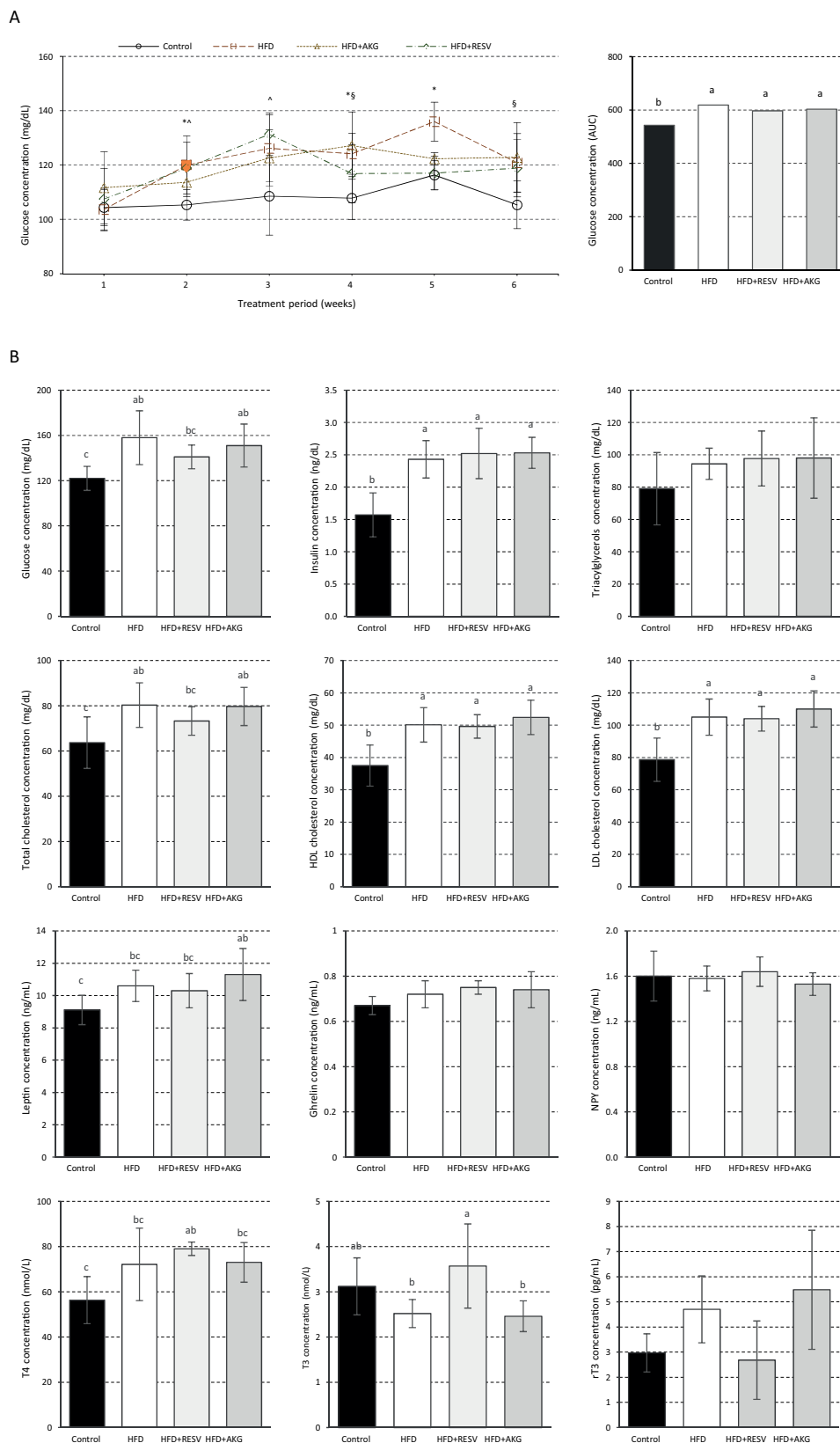


FIGURE 1. Biochemical parameters of blood plasma in rats. Middle-aged rats fed for 6 weeks with high-fat diet (HFD), HFD supplemented with resveratrol (HFD+RESV), HFD supplemented with α -ketoglutarate (HFD+AKG) or standard feed (control group – Control).

* – indicates a significant difference between Control and HFD at $p \leq 0.05$; ^ – indicates a significant difference between Control and HFD+RESV at $p \leq 0.05$; § – indicates a significant difference between Control and HFD+AKG at $p \leq 0.05$; ° – indicates a significant difference between HFD and HFD+RESV at $p \leq 0.05$. ^{a,b} – values with different superscripts differ significantly at $p \leq 0.05$.

(A) Changes in plasma glucose level during the 6-week treatment period. (B) Plasma biochemistry on the last day of the study. HDL, high density lipoproteins; LDL, low density lipoproteins; NPY, neuropeptide Y; T4, thyroxine; T3, triiodothyronine; rT3, reverse triiodothyronine. ^{a,b,c} – values with different superscripts differ significantly at $p \leq 0.05$.

On the other hand, RESV is suggested to reverse hyperleptinemia and improve central leptin action [Franco *et al.*, 2016; Jimoh *et al.*, 2018]; however, our study failed to confirm such a correlation.

The present study also implicates minimal participation of ghrelin and NPY in the modulation of metabolic response to HFD under the current settings, as no significant differences were detected in their plasma concentrations (Figure 1). Nevertheless, both ghrelin and NPY are essential regulators of energy expenditure and have been previously reported to be affected by HFD [Briggs *et al.*, 2013; Mohamed *et al.*, 2010].

In the case of thyroid hormones, T4 was significantly ($p \leq 0.05$) higher in the HFD+RESV group compared to the control group, while the concentration of T3 was significantly ($p \leq 0.05$) higher only in the HFD+RESV group when compared to HFD and HFD+AKG groups (Figure 1). In contrast, there were no statistically significant differences in the concentration of rT3. It is known that euthyroidism is extremely important to control the rate and direction of metabolism. Our results indicate hypothyroidism and the conversion of T3 and/or rT3 to T4 in the animals fed HFD. A similar pattern of thyroid hormones followed HFD was noted by Mohamed *et al.* [2010], as well as Cheserek *et al.* [2016]. In the same study [Cheserek *et al.*, 2016], HFD supplementation with RESV elevated plasma T3 to a similar level as in the group fed a low-fat diet. The observed restoration of the T3 level may lead to a reduction

in oxidative stress since T3 might act as a free radical scavenger [Cheserek *et al.*, 2016].

As it was predicted, the HFD-induced shift in metabolism had a profound effect on rats' BW gain, which was significantly ($p \leq 0.05$) higher in HFD and HFD+RESV groups compared to the control group (Figure 2). Similarly, the final BW was higher in all groups fed HFD; however, it differed significantly only between HFD and control groups ($p \leq 0.05$), while average water intake was significantly ($p \leq 0.05$) lower in HFD and HFD+AKG groups compared to the control group. The obtained results are in line with other studies [Cho *et al.*, 2012; Morrison *et al.*, 2010]. The consumption of HFD is usually associated with an increased caloric intake and simultaneously increase in total body adiposity [Morrison *et al.*, 2010]. Although feed intake was significantly ($p \leq 0.05$) lower in all groups fed HFD compared to the control group, and we did not measure direct calorie intake, the energy content of a standard rat diet was substantially lower compared to HFD (Table 1). Unlike in other studies [Cho *et al.*, 2012; Lagouge *et al.*, 2006; Miura *et al.*, 2003], we have not however observed the protective effect of RESV against diet-induced obesity (Figure 2). In contrast, dietary AKG suppressed HFD-induced BW gain in rats (Figure 2). Similar results after dietary AKG intake were observed in rodents fed HFD [Radzki *et al.*, 2009; Tian *et al.*, 2020], as well as in mice fed a basal diet [Chen *et al.*, 2017]. It is suggested that AKG might reduce deposition of the adipose tissue, improve lipolysis and fatty

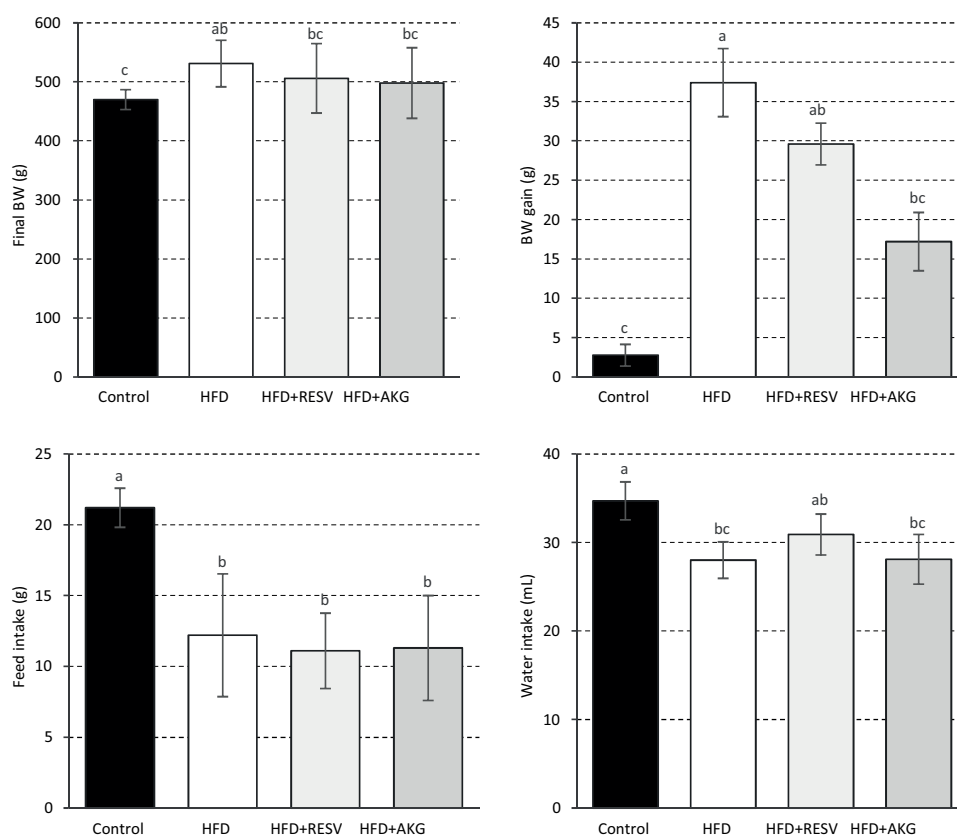


FIGURE 2. Final body weight (BW), BW gain, average daily feed intake, and water intake of rats. Middle-aged rats fed for 6 weeks with high-fat diet (HFD), HFD supplemented with resveratrol (HFD+RESV), HFD supplemented with α -ketoglutarate (HFD+AKG) or standard feed (control group – Control). ^{a,b,c} – values with different superscripts differ significantly at $p \leq 0.05$.

acid oxidation or modify the composition of gastrointestinal microbiota [Chen *et al.*, 2017]. It should also be noted that the HFD+AKG group was the only group with significantly elevated plasma leptin level, while leptin serves as an essential obesity indicator [Kandhare *et al.*, 2018].

Gene expression profiling

Furthermore, to compare the age-associated gene expression profile under the different dietary interventions, the hypothalamic transcriptome of middle-aged rats was measured using the real-time PCR microarray technology. Mounting evidence indicates that alterations in the gene expression levels might have a severe impact on brain function, both at the cellular and behavioral level [Berchtold *et al.*, 2008]. The genes involved in lifespan regulation are often associated with the metabolic signaling pathways [Fraser *et al.*, 2005], and HFD-induced alterations in levels of energy substrates and hormones might be potent modulators of brain aging [Morrison *et al.*, 2010]. Increased oxidative stress, and in particular protein oxidation, is suspected to mediate the effects of HFD on brain pathogenesis and cognitive decline in the elderly [Morrison *et al.*, 2010]. Moreover, age-related cognitive disturbances are often promoted by insulin resistance, diabetes, and alterations in adipose tissue deposition [Morrison *et al.*, 2010]. It remains unclear, however, whether dietary stressors and the resulting metabolic dysfunction accelerate the normal brain aging or initiate completely new pathological

processes. Metabolic decline within the brain itself and general decreased catabolic and anabolic capacity with aging has been also reported in both human imaging studies and microarray studies with rodents [Berchtold *et al.*, 2008].

In our study, however, HFD feeding for 6 weeks caused a moderate change in the genetic pattern of the rat hypothalamus. The significant ($p \leq 0.05$) changes in gene expression with the fold regulation threshold of 1.5 in the rat hypothalamus are presented in Table 3 and Table 4. Of the 84 analyzed genes associated with the aging process, one gene (*CFH*) was overexpressed, whereas expression levels of 26 (31%) decreased in the HFD group compared to the control group. Of the downregulated genes, 35% (9/26) might be assigned to inflammatory response, 19% (5/26) to transcriptional regulation, 19% (5/26) to proteostasis, 12% (3/26) to DNA binding, 12% (3/26) to neurodegeneration and synaptic transmission, and 12% (3/26) to laminopathies. Additionally, four genes were downregulated by more than 2-fold (*FCGBP*, *GFAP*, *LMNB2*, *SCN2B*) with *FCGBP* being the top gene (Table 3). A non-supervised hierarchical clustering of the entire dataset to display a heat map with dendrograms indicating co-regulated genes is presented in Figure 3. The results show that group 3 (HFD + AKG) is the closest to the control group. This suggests that the AKG supplementation has the potential to counteract the effects of HFD on gene expression.

Interestingly, an extensive analysis of 16 different mouse tissues showed that most of the age-related changes in gene

TABLE 3. The hypothalamic gene expression profile associated with aging – part A.

Gene symbol	Gene name	Fold change ¹		
		Control vs HFD	Control vs HFD+RESV	Control vs HFD+AKG
<i>CFH</i>	Complement factor H	1.69 ($p=0.0479$)	–	–
<i>ANGEL2</i>	Angel homolog 2 (Drosophila)	–	–2.02 ($p=0.0063$)	–
<i>ANXA5</i>	Annexin A5	–	–1.60 ($p=0.0028$)	–
<i>C1QA</i>	Complement component 1, q subcomponent, A chain	–	–3.50 ($p=0.0008$)	–
<i>C1QC</i>	Complement component 1, q subcomponent, C chain	–	–2.77 ($p=0.0062$)	–
<i>C1S</i>	Complement component 1, s subcomponent	–1.76 ($p=0.0422$)	–2.75 ($p=0.0102$)	–
<i>C3</i>	Complement component 3	–	–2.24 ($p=0.0085$)	–
<i>C4A</i>	Complement component 4A (Rodgers blood group)	–	–4.50 ($p=0.0001$)	–
<i>C4B</i>	Complement component 4B (Chido blood group)	–	–2.63 ($p=0.0016$)	–
<i>C5A1</i>	Complement component 5a receptor 1	–	–1.80 ($p=0.0295$)	–
<i>CD14</i>	CD14 molecule	–	–3.22 ($p=0.0039$)	–
<i>CX3CL1</i>	Chemokine (C-X3-C motif) ligand 1	–	–4.88 ($p=0.0006$)	–
<i>CXCL16</i>	Chemokine (C-X-C motif) ligand 16	–	–1.83 ($p=0.0049$)	–
<i>FCGBP</i>	Fc fragment of IgG binding protein	–3.65 ($p<0.0001$)	–3.00 ($p=0.0003$)	–1.97 ($p=0.0008$)
<i>FCGR1A</i>	Fc fragment of IgG, high affinity Ia, receptor (CD64)	–	–1.95 ($p=0.0271$)	–
<i>LTF</i>	Lactotransferrin	–1.67 ($p=0.0240$)	–	–
<i>PANX1</i>	Pannexin 1	–	–2.63 ($p=0.0003$)	–

TABLE 3 – continued.

Gene symbol	Gene name	Fold change ¹		
		Control vs HFD	Control vs HFD+RESV	Control vs HFD+AKG
<i>TLR2</i>	Toll-like receptor 2	–	–1.97 ($p=0.0107$)	–
<i>TLR4</i>	Toll-like receptor 4	–1.59 ($p=0.0184$)	–1.93 ($p=0.0005$)	–
<i>TMEM135</i>	Transmembrane protein 135	–1.65 ($p=0.0003$)	–2.16 ($p=0.0049$)	–
<i>TMEM33</i>	Transmembrane protein 33	–1.61 ($p=0.0005$)	–2.22 ($p=0.0039$)	–
<i>TOLLIP</i>	Toll interacting protein	–1.84 ($p=0.0033$)	–3.20 ($p=0.0020$)	–
<i>MBP</i>	Myelin basic protein	–1.74 ($p=0.0127$)	–1.97 ($p=0.0076$)	–
<i>GFAP</i>	Glial fibrillary acidic protein	–2.93 ($p<0.0001$)	–3.87 ($p<0.0001$)	–
<i>SCN2B</i>	Sodium channel, voltage-gated, type II, beta	–2.24 ($p=0.0006$)	–4.10 ($p<0.0001$)	–
<i>PHF3</i>	PHD finger protein 3	–1.63 ($p=0.0010$)	–1.96 ($p=0.0066$)	–
<i>SMAD2</i>	SMAD family member 2	–	–2.06 ($p=0.0005$)	–
<i>ARID1A</i>	AT rich interactive domain 1A (SWI-like)	–1.79 ($p=0.0025$)	–2.37 ($p=0.0077$)	–
<i>EP300</i>	E1A binding protein p300	–1.74 ($p=0.0104$)	–2.21 ($p=0.0210$)	–
<i>FOXO1</i>	Forkhead box O1	–1.60 ($p=0.0004$)	–2.01 ($p=0.0105$)	–
<i>HSF1</i>	Heat shock transcription factor 1	–1.54 ($p=0.0042$)	–1.82 ($p=0.0287$)	–
<i>ARL6IP6</i>	ADP-ribosylation-like factor 6 interacting protein 6	–1.62 ($p=0.0019$)	–2.81 ($p=0.0014$)	–
<i>JAKMIP3</i>	Janus kinase and microtubule interacting protein 3	–1.65 ($p=0.0055$)	–1.91 ($p=0.0144$)	–
<i>RNF144B</i>	Ring finger protein 144B	–	–2.47 ($p=0.0071$)	–
<i>TXNIP</i>	Thioredoxin interacting protein	–1.50 ($p=0.0444$)	–3.22 ($p=0.0003$)	–
<i>ELP3</i>	RCG52086-like	–	–2.33 ($p=0.0030$)	–
<i>FBXL16</i>	F-box and leucine-rich repeat protein 16	–	–3.00 ($p=0.0009$)	–
<i>ZBTB10</i>	Zinc finger and BTB domain containing 10	–	–1.76 ($p=0.0086$)	–
<i>ZFP9</i>	Zinc finger protein 9	–1.56 ($p=0.0116$)	–1.80 ($p=0.0246$)	–
<i>SIRT6</i>	Sirtuin (silent mating type information regulation 2 homolog) 6	–1.96 ($p=0.0036$)	–3.03 ($p=0.0009$)	–
<i>MRPL43</i>	Mitochondrial ribosomal protein L43	–1.54 ($p<0.0001$)	–1.59 ($p=0.0058$)	–
<i>TFAM</i>	Transcription factor A, mitochondrial	–	–1.50 ($p=0.0067$)	–
<i>ZMPSTE24</i>	Zinc metalloproteinase, STE24 homolog (<i>S. cerevisiae</i>)	–	–1.67 ($p=0.0227$)	–
<i>LMNA</i>	Lamin A	–1.53 ($p=0.0005$)	–1.99 ($p<0.0001$)	–
<i>LMNB1</i>	Lamin B1	–1.97 ($p=0.0023$)	–2.02 ($p=0.0124$)	–
<i>LMNB2</i>	Lamin B2	–2.14 ($p=0.0013$)	–2.87 ($p=0.0019$)	–
<i>POT1</i>	Protection of telomeres 1A	–	–1.59 ($p=0.0285$)	–
<i>TERF2</i>	Telomeric repeat binding factor 2	–1.78 ($p=0.0005$)	–2.45 ($p=0.0027$)	–
<i>TPPI</i>	Tripeptidyl peptidase I	–	–1.76 ($p=0.0086$)	–
<i>COL1A1</i>	Collagen, type I, alpha 1	–	–2.54 ($p=0.0396$)	–
<i>EML1</i>	Echinoderm microtubule associated protein like 1	–1.86 ($p=0.0006$)	–2.50 ($p=0.0012$)	–
<i>CDKN1C</i>	Cyclin-dependent kinase inhibitor 1C	–	–3.83 ($p=0.0010$)	–

¹Only genes whose expression differed significantly ($p\leq 0.05$) with the fold regulation threshold of 1.5 are shown. Middle-aged rat fed for 6 weeks with high-fat diet (HFD), HFD supplemented with resveratrol (HFD+RESV), HFD supplemented with α -ketoglutarate (HFD+AKG) or standard feed (control group – Control).

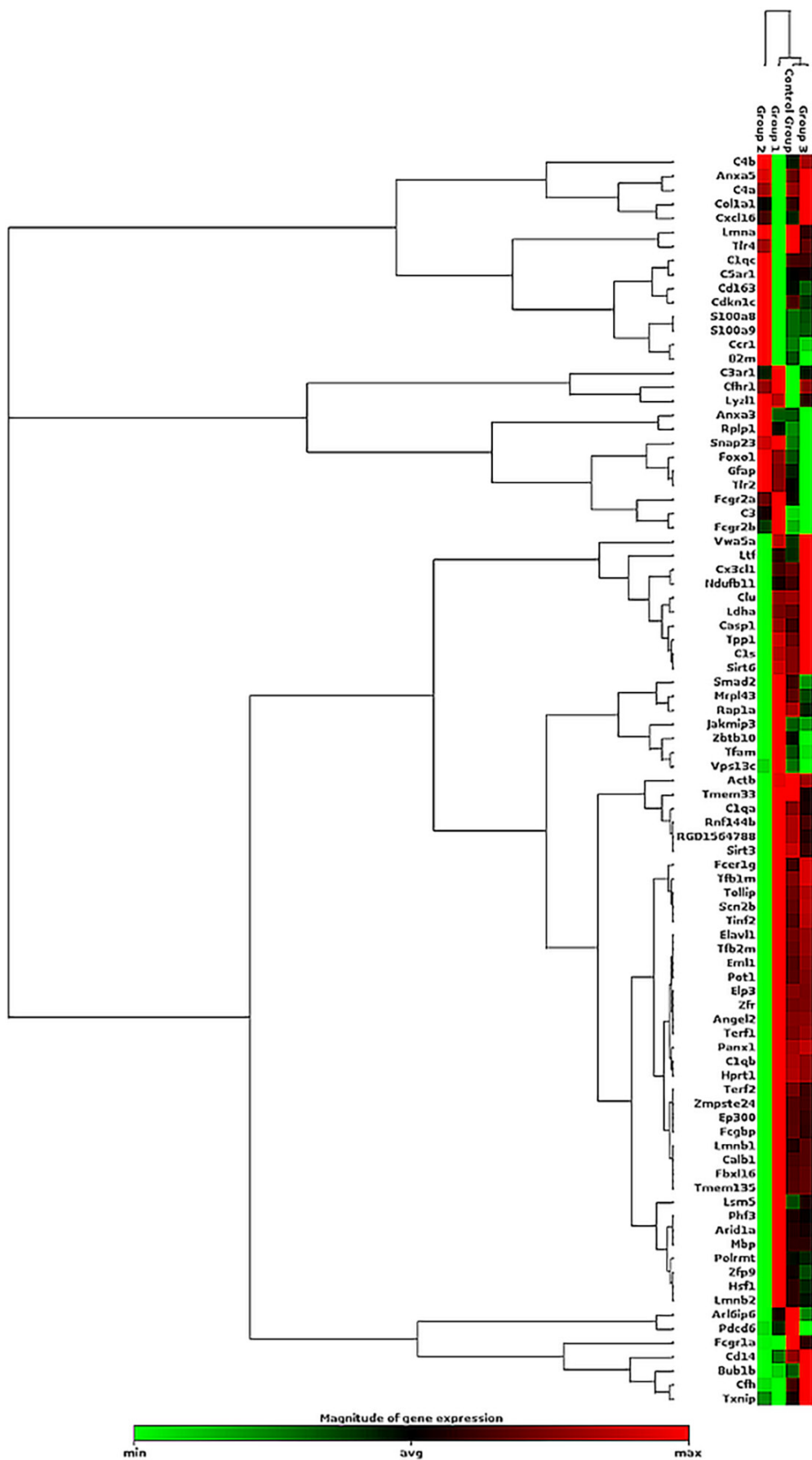


FIGURE 3. Clustergram displaying a heat map with dendrograms indicating co-regulated genes across groups. Gene expression analyzed in the hypothalamus of middle-aged rats fed for 6 weeks with high-fat diet (HFD – Group 1), HFD supplemented with resveratrol (HFD+RESV – Group 2), HFD supplemented with α -ketoglutarate (HFD+AKG – Group 3) or standard feed (Control – control Group).

expression are relatively small in magnitude (less than 2-fold) [Zahn *et al.*, 2007]. This coincides with our results because only 4 genes displayed the fold change higher than 2. Nevertheless, perhaps a more extended period of HFD exposure would induce more pronounced neuropathological changes in middle-aged rats. In addition, the gene expression pattern may vary depending on animal species, sex, specific tissue or even cell type, and thus individual areas of the brain undergo different patterns of age-related gene expression [Berchtold *et al.*, 2008; Fraser *et al.*, 2005; Ximerakis *et al.*, 2019]. So far, most of the available data on genetic markers of brain aging comes from studies on cortex, cerebellum or hippocampus [Fraser *et al.*, 2005; González-Velasco *et al.*, 2020; Mohan *et al.*, 2016; Weindruch *et al.*, 2002]. In our study, the age-related genetic profile was evaluated in the hypothalamus because hypothalamic neurons are known to regulate neuroendocrine and autonomic nervous system control of energy balance, and mediate many responses to the nutritional deficit including CR [Dacks *et al.*, 2013; Lizarbe *et al.*, 2017]. Moreover, Lizarbe *et al.* [2017] have reported that HFD intake affects hypothalamic energy metabolism and leads to localized inflammatory state, astrocytosis, and microgliosis.

Previous studies have identified hundreds of genes differently expressed as organism ages, with those involved in stress response, inflammation, mitochondrial dysfunction or oxidative stress being consistently increased, and those related to tissue-specific functions being decreased [González-Velasco *et al.*, 2020; Mohan *et al.*, 2016; Zhou *et al.*, 2012]. This is in line with our study as one of the major pathways differently expressed in HFD group was the inflammatory response (Table 3). It is well known that the brain undergoes numerous perturbations in inflammatory signaling during aging, and although it might be neuroprotective under some circumstances, generally it has been linked to the development of neuropathology and neuronal dysfunction [Berchtold *et al.*, 2008; De Magalhães *et al.*, 2009; Uranga *et al.*, 2010]. The top downregulated gene in the HFD group was *FCGBP* which encodes the Fc fragment of the IgG-binding protein (Table 3). In this group, there was also the only significantly up-regulated gene – *CFH*, acting as a negative regulator of the alternative pathway of the complement system [Noris & Remuzzi, 2013]. The upregulation of *CFH* was also noted in the liver of rats fed HFD [Xie *et al.*, 2010].

The other two top genes, *GFAP* and *SCN2B*, belong to the functional class of genes involved in neurodegeneration and synaptic transmission, while age-related abnormalities in synaptic functions are hypothesized to be a key event mediating cognitive decline [Mohan *et al.*, 2016]. Moreover, neuronal *GFAP* gene expression, coding intermediate filament structural proteins and being a specific marker for mature astrocytes, is reported to show the highest correlation with the biological age [González-Velasco *et al.*, 2020]. However, most of the studies reported increased expression of both *GFAP* and *SCN2B* in rodents' brain during aging [Boisvert *et al.*, 2018; XiYang *et al.*, 2016]. Therefore, the results obtained might suggest a specific molecular pathway of synaptic modification after HFD treatment.

Interestingly, the addition of RESV into HFD resulted in a major molecular shift in the rat hypothalamus (Table 3).

In the HFD+RESV group, a total of 50 genes (60%) were identified as significantly underexpressed, and no gene overexpressed, when compared to the control group (Table 3). Among them, 42% (21/50) belong to inflammatory response pathways, while 12% each (6/50) are involved in transcriptional regulation, proteostasis or DNA binding, 8% (4/50) in laminopathies, and 6% each (3/50) in neurodegeneration and synaptic transmission, mitochondrial dysfunction, genomic instability or telomere attrition. A large group of genes was significantly downregulated by more than 2-fold (32 genes) with *CIQA*, *C4A*, *CDKN1C*, *CX3CL1*, *GFAP*, and *SCN2B* displaying a >3.5-fold decrease in expression levels and *CX3CL1* being the top gene. Of the 50 genes significantly differentially expressed in the HFD+RESV group, 25 (50%) exhibited expression changes in the same direction as in the HFD group (Table 3). Moreover, when compared to the HFD group, dietary supplementation with RESV caused a significant up-regulation of two genes associated with inflammatory response (*CFHR1*, *LYZL1*), and down-regulation of five genes, three of which could be assigned to inflammatory response, 1 to proteostasis, and 1 to cytoskeleton regulation (Table 4).

Barger *et al.* [2008] showed that RESV supplementation, similar to CR, opposed most of the age-related transcriptional alterations in the aging heart of 30-month old mice. On the other hand, lesser effects on aging inhibition were obtained in skeletal muscle and neocortex. In our study, most of the down-regulated genes in the HFD+RESV group were identified to be critical for the activation of immune response and the induction of the complement components (*CIQA*, *CIQC*, *c1S*, *C3*, *C4A*, *C4B*, *C5AR1*). The overexpression of the complement system cascade is a common signature of aging and a trigger for the production of proinflammatory peptide fragments leading to neuronal damage [De Magalhães *et al.*, 2009; Noris & Remuzzi, 2013; Weindruch *et al.*, 2002]. Therefore, decreased expression of complement cascade genes suggests that RESV, even when given with HFD, may beneficially influence markers of brain aging.

It is speculated that the neuroprotective action of RESV results mainly from the reduction of oxidative stress and neuroinflammation. Even though our data fit in part with this trend, it should be noted that RESV has pleiotropic properties and the ability to activate multiple signaling pathways [Baur *et al.*, 2006; Lagouge *et al.*, 2006]. Furthermore, it seems that the effects induced by RESV supplementation did not consist in inhibiting the negative effect of HFD, but on the contrary, elicited a completely different molecular response in the rat hypothalamus. This is confirmed by the fact that only 8% of the genes analyzed were significantly differentially expressed between HFD and HFD+RESV groups (Table 4), and yet significant differences were noted compared to the control group (Table 3). Another clue is that these minor changes in the metabolic response induced by the addition of RESV were sufficient to elicit an entirely different molecular response. Indeed, glucose or cholesterol metabolism (both parameters decreased in the HFD+RESV group) has been associated with brain aging and lifespan modulation [Dacks *et al.*, 2013; Nuthikattu *et al.*, 2019].

On the contrary, HFD supplementation with AKG remarkably attenuated aging-related changes in the hypothalamic

TABLE 4. The hypothalamic gene expression profile associated with aging – part B.

Gene symbol	Gene name	Fold change ¹		
		HFD vs HFD+RESV	HFD vs HFD+AKG	HFD+RESV vs HFD+AKG
<i>CFHR1</i>	Complement component factor h-like 1	2.91 ($p=0.0108$)	–	–
<i>LYZL1</i>	Lysozyme-like 1	2.16 ($p=0.0108$)	–	–
<i>FCGBP</i>	Fc fragment of IgG binding protein	–	1.86 ($p=0.0214$)	–
<i>ANXA5</i>	Annexin A5	–1.51 ($p=0.0176$)	–	–
<i>C1QC</i>	Complement component 1, q subcomponent, C chain	–	–	–2.26 ($p=0.0434$)
<i>C1S</i>	Complement component 1, s subcomponent	–	–	–2.27 ($p=0.0313$)
<i>C3</i>	Complement component 3	–	–	–1.91 ($p=0.0421$)
<i>C4A</i>	Complement component 4A (Rodgers blood group)	–	–	–3.06 ($p=0.0240$)
<i>C4B</i>	Complement component 4B (Chido blood group)	–	–	–2.08 ($p=0.0366$)
<i>CXCL16</i>	Chemokine (C-X-C motif) ligand 16	–1.81 ($p=0.0297$)	–	–1.62 ($p=0.0334$)
<i>PANX1</i>	Pannexin 1	–1.83 ($p=0.0236$)	–	–1.83 ($p=0.0493$)
<i>TOLLIP</i>	Toll interacting protein	–	–	–2.35 ($p=0.0437$)
<i>MBP</i>	Myelin basic protein	–	–	–1.71 ($p=0.0325$)
<i>GFAP</i>	Glial fibrillary acidic protein	–	1.94 ($p=0.0397$)	–2.56 ($p=0.0180$)
<i>SCN2B</i>	Sodium channel, voltage-gated, type II, beta	–	–	–2.99 ($p=0.0182$)
<i>PHF3</i>	PHD finger protein 3	–	–	–1.70 ($p=0.0348$)
<i>SMAD2</i>	SMAD family member 2	–	–	–1.77 ($p=0.0109$)
<i>ARID1A</i>	AT rich interactive domain 1A (SWI-like)	–	–	–1.92 ($p=0.0495$)
<i>ELP3</i>	RCG52086-like	–	–	–1.98 ($p=0.0269$)
<i>FBXL16</i>	F-box and leucine-rich repeat protein 16	–	–	–2.52 ($p=0.0221$)
<i>ARL6IP6</i>	ADP-ribosylation-like factor 6 interacting protein 6	–	–	–2.23 ($p=0.0244$)
<i>JAKMIP3</i>	Janus kinase and microtubule interacting protein 3	–	1.59 ($p=0.0202$)	–1.84 ($p=0.0332$)
<i>RNF144B</i>	Ring finger protein 144B	–	–	–2.33 ($p=0.0147$)
<i>TXNIP</i>	Thioredoxin interacting protein	–2.08 ($p=0.0231$)	–	–2.14 ($p=0.0400$)
<i>LMNA</i>	Lamin A	–	–	–1.75 ($p=0.0207$)
<i>LMNB1</i>	Lamin B1	–	1.63 ($p=0.0224$)	–
<i>LMNB2</i>	Lamin B2	–	1.67 ($p=0.0496$)	–2.23 ($p=0.0382$)
<i>COL1A1</i>	Collagen, type I, alpha 1	–2.97 ($p=0.0132$)	–	–
<i>EML1</i>	Echinoderm microtubule associated protein like 1	–	1.57 ($p=0.0223$)	–2.12 ($p=0.0176$)
<i>CDKN1C</i>	Cyclin-dependent kinase inhibitor 1C	–	–	–3.17 ($p=0.0448$)

¹Only genes whose expression differed significantly ($p\leq 0.05$) with the fold regulation threshold of 1.5 are shown. Middle-aged rat fed for 6 weeks with high-fat diet (HFD), HFD supplemented with resveratrol (HFD+RESV), HFD supplemented with α -ketoglutarate (HFD+AKG) or standard feed (control group – Control).

gene expression profile caused by HFD feeding, leading to a molecular response almost identical as in the control group (Table 3). In the HFD+AKG group, only one of the 84 genes surveyed – *FCGBP* – regulating neurodegeneration and synaptic transmission, was significantly downregulated compared to the control group, although a fold change tended

to be lower compared with other groups (Table 3). When the gene expression profile was compared to the HFD group, AKG supplementation induced the significant over-expression of six genes (assigned to inflammatory response, neurodegeneration and synaptic transmission, proteostasis, laminopathies or cytoskeleton regulation) which represented

7% of the genes surveyed (Table 4). A large variation was also recorded between HFD+RESV and HFD+AKG groups (24 genes with significantly different expression levels) (Table 4).

Although the effect of AKG on brain aging is yet to be unraveled, it has been demonstrated that AKG has strong antioxidant activity and may prevent mitochondrial dysfunction and dyslipidemia in the brain [Thomas *et al.*, 2015]. It is believed that by reducing oxidative stress and stimulating the production of cellular ATP, AKG may have a beneficial effect on brain performance and cognitive function; however, this effect has been described in terms of alleviating the symptoms of Alzheimer's disease, not normal brain aging [Thomas *et al.*, 2015]. Additionally, Niemiec *et al.* [2011] have demonstrated that in older mice, AKG improves serum redox homeostasis to the level observed in young animals. Interestingly, the effect differed depending on AKG chemical structure, as its calcium salts reduced lipid peroxidation and enhanced total antioxidant capacity, while sodium salts modulated the activity of antioxidant enzymes [Niemiec *et al.*, 2011]. Therefore, one can speculate that the ability of AKG to suppress the genetic effect of HFD feeding is due to its antioxidative properties. On the other hand, Chin *et al.* [2014] proved that AKG supplementation in the adult stage was sufficient for lifespan extension and delaying age-related phenotypes through the regulation of cellular energy metabolism and inhibition of ATP synthase and TOR function, suggesting a similar model to CR.

CONCLUSION

Despite enormous efforts, our understanding of the ability of different dietary regimes to prevent or accelerate various aspects of brain aging is still relatively poor. Based on our study results, it is difficult to determine the exact relationship between plasma metabolic indicators and the molecular markers of brain aging. However, we proved that metabolic alterations induced by HFD consumption, such as high circulating glucose, insulin and lipids levels, might profoundly affect age-related markers in the middle-aged rats' hypothalamus, with the largest functional class being related to inflammatory response. Secondly, we showed that dietary RESV may ameliorate the metabolic changes induced by HFD feeding and cause a major molecular shift compared to HFD alone. In contrast, AKG supplementation did not affect the metabolic phenotype, but prevented the gene expression pattern caused by HFD consumption, mimicking the effects observed in the control group. Therefore, it seems that HFD-induced metabolic and genetic disturbances might be at least partially compensated with RESV or AKG supplementation, even though these compounds act in a different and specific manner. To sum up, our study demonstrated that nutritional intervention is a powerful approach to modulate molecular markers of brain aging, which in turn, may represent new diagnostic or therapeutic targets for optimizing the health span. Furthermore, in future studies, it could be interesting to look how different dietary conditions started at midlife would affect the metabolic and molecular responses in the individuals living in old age.

RESEARCH FUNDING

The authors received no specific funding for the study.

CONFLICT OF INTERESTS

The authors declare that there is no conflict of interest.

ORCID IDs

M. Oczkowicz <https://orcid.org/0000-0001-8975-0200>
 S. Orczewska-Dudek <https://orcid.org/0000-0001-6726-923X>
 M. Pieszka <https://orcid.org/0000-0002-4342-2719>
 M. Pietras <https://orcid.org/0000-0003-4683-9840>
 K. Ropka-Molik <https://orcid.org/0000-0002-8555-0495>
 P. Szczurek-Janicka <https://orcid.org/0000-0001-9008-3505>

REFERENCES

- Andersen, G., Burkon, A., Sulzmaier, F.J., Walker, J.M., Leckband, G., Fuhst, R., Erbersdobler, H.F., Somoza, V. (2011). High dose of dietary resveratrol enhances insulin sensitivity in healthy rats but does not lead to metabolite concentrations effective for SIRT1 expression. *Molecular Nutrition & Food Research*, 55(8), 1197–1206. <https://doi.org/10.1002/mnfr.201100292>
- Anderson, R.M., Weindruch, R. (2010). Metabolic reprogramming, caloric restriction and aging. *Trends in Endocrinology & Metabolism*, 21(3), 134–141. <https://doi.org/10.1016/j.tem.2009.11.005>
- AOAC International. (2000). Official Methods of Analysis of the Association of Official Analytical Chemists. 17th ed. Gaithersburg, MD, USA.
- Barger, J.L., Kayo, T., Vann, J.M., Arias, E.B., Wang, J., Hacker, T.A., Wang, Y., Raederstorff, D., Morrow, J.D., Leewenburgh, C., Allison, D.B., Saupe, K.W., Cartee, G.D., Weindruch, R., Prolla, T.A. (2008). A low dose of dietary resveratrol partially mimics caloric restriction and retards aging parameters in mice. *PLoS One*, 3(6), art. no. e2264. <https://doi.org/10.1371/annotation/c54ef754-1962-4125-bf19-76d3ec6f19e5>
- Baur, J.A., Pearson, K.J., Price, N.L., Jamieson, H.A., Lerin, C., Kalra, A., Prabhu, V.V., Allard, J.S., Lopez-Lluch, G., Lewis, K., Pistell, P.J., Poosala, S., Becker, K.G., Boss, O., Gwinn, D., Wang, M., Ramaswamy, S., Fishbein, K.W., Spencer, R.G., Lakatta, W.G., Le Couteur, D., Shaw, R.J., Navas, P., Puigserver, P., Ingram, D.K., de Cabo, R., Sinclair, D.A. (2006). Resveratrol improves health and survival of mice on a high-calorie diet. *Nature*, 444, 337–342. <https://doi.org/10.1038/nature05354>
- Berchtold, N.C., Cribbs, D.H., Coleman, P.D., Rogers, J., Head, E., Kim, R., Beach, T., Miller, C., Troncoso, J., Trojanowski, J.Q., Zielke, R.H., Cotman, C.W. (2008). Gene expression changes in the course of normal brain aging are sexually dimorphic. *Proceedings of National Academy of Sciences*, 105(40), 15605–15610. <https://doi.org/10.1073/pnas.0806883105>
- Boisvert, M.M., Erikson, G.A., Shokhirev, M.N., Allen, N.J. (2018). The aging astrocyte transcriptome from multiple regions of the mouse brain. *Cell Reports*, 22(1), 269–285. <https://doi.org/10.1016/j.celrep.2017.12.039>

8. Briggs, D.I., Lockie, S.H., Wu, Q., Lemus, M.B., Stark, R., Andrews, Z.B. (2013). Calorie-restricted weight loss reverses high-fat diet-induced ghrelin resistance, which contributes to rebound weight gain in a ghrelin-dependent manner. *Endocrinology*, 154(2), 709–717.
<https://doi.org/10.1210/en.2012-1421>
9. Chen, S., Bin, P., Ren, W., Gao, W., Liu, G., Yin, J., Duan, J., Li, Y., Yao, K., Huang, R., Tan, B., Yin, Y. (2017). Alpha-ketoglutarate (AKG) lowers body weight and affects intestinal innate immunity through influencing intestinal microbiota. *Oncotarget*, 8(24), art. no. 38184.
<https://doi.org/10.18632/oncotarget.17132>
10. Cheserek, M.J., Wu, G., Li, L., Li, L., Karangwa, E., Shi, Y., Le, G. (2016). Cardioprotective effects of lipoic acid, quercetin and resveratrol on oxidative stress related to thyroid hormone alterations in long-term obesity. *Journal of Nutritional Biochemistry*, 33, 36–44.
<https://doi.org/10.1016/j.jnutbio.2016.02.008>
11. Chin, R.M., Fu, X., Pai, M.Y., Vergnes, L., Hwang, H., Deng, G., Diep, S., Lomenick, B., Meli, V.S., Monsalve, G.C., Hu, E., Whelan, S.A., Wang, J.X., Jung, G., Solis, G.M., Fazlollahi, F., Kaweteerawat, C., Quach, A., Nili, M., Krall, A.S., Godwin, H.A., Chang, H.R., Faull, K.F., Guo, F., Jiang, M., Trauger, S.A., Saghatelian, A., Braas, D., Christofk, H.R., Clarke, C.F., Teitell, M.A., Petrascheck, M., Reue, K., Jung, M.E., Frand, A.R., Huang, J. (2014). The metabolite α -ketoglutarate extends lifespan by inhibiting ATP synthase and TOR. *Nature*, 510(7505), 397–401.
<https://doi.org/10.1038/nature13264>
12. Cho, S.J., Jung, U.J., Choi, M.S. (2012). Differential effects of low-dose resveratrol on adiposity and hepatic steatosis in diet-induced obese mice. *British Journal of Nutrition*, 108(12), 2166–2175.
<https://doi.org/10.1017/S0007114512000347>
13. Dacks, P.A., Moreno, C.L., Kim, E.S., Marcellino, B.K., Mobbs, C.V. (2013). Role of the hypothalamus in mediating protective effects of dietary restriction during aging. *Frontiers in Neuroendocrinology*, 34(2), 95–106.
<https://doi.org/10.1016/j.yfrne.2012.12.001>
14. Dąbek, M., Kruszewska, D., Filip, R., Hotowy, A., Pierzynowski, Ł., Wojtasz-Pająk, A., Szymanczyk, S., Valverde-Piedra, J.L., Werpachowska, E., Pierzynowski, S.G. (2005). α -Ketoglutarate (AKG) absorption from pig intestine and plasma pharmacokinetics. *Journal of animal physiology and animal nutrition*, 89(11–12), 419–426.
<https://doi.org/10.1111/j.1439-0396.2005.00566.x>
15. De Magalhães, J.P., Curado, J., Church, G.M. (2009). Meta-analysis of age-related gene expression profiles identifies common signatures of aging. *Bioinformatics*, 25(7), 875–881.
<https://doi.org/10.1093/bioinformatics/btp073>
16. Franco, J.G., Dias-Rocha, C.P., Fernandes, T.P., Maia, L.A., Lisboa, P.C., Moura, E.G., Pazos-Moura, C.C., Trevenzoli, I.H. (2016). Resveratrol treatment rescues hyperleptinemia and improves hypothalamic leptin signaling programmed by maternal high-fat diet in rats. *European Journal of Nutrition*, 55(2), 601–610.
<https://doi.org/10.1007/s00394-015-0880-7>
17. Fraser, H.B., Khaitovich, P., Plotkin, J.B., Pääbo, S., Eisen, M.B. (2005). Aging and gene expression in the primate brain. *PLoS Biology*, 3(9), art. no. e274.
<https://doi.org/10.1371/journal.pbio.0030274>
18. González-Velasco, O., Papy-García, D., Le Douaron, G., Sánchez-Santos, J.M., De Las Rivas, J. (2020). Transcriptomic landscape, gene signatures and regulatory profile of aging in the human brain. *Biochimica et Biophysica Acta – Gene Regulatory Mechanisms*, 1863(6), art no. 194491.
<https://doi.org/10.1016/j.bbagr.2020.194491>
19. Jimoh, A., Tanko, Y., Ayo, J.O., Ahmed, A., Mohammed, A. (2018). Resveratrol increases serum adiponectin level and decreases leptin and insulin level in an experimental model of hypercholesterolemia. *Pathophysiology*, 25(4), 411–417.
<https://doi.org/10.1016/j.pathophys.2018.08.005>
20. Kandhare, A.D., Bandyopadhyay, D., Thakurdesai, P.A. (2018). Low molecular weight galactomannans-based standardized fenugreek seed extract ameliorates high-fat diet-induced obesity in mice via modulation of FASn, IL-6, leptin, and TRIP-Br2. *RSC Advances*, 8(57), 32401–32416.
<https://doi.org/10.1039/C8RA05204B>
21. Lagouge, M., Argmann, C., Gerhart-Hines, Z., Meziane, H., Lerin, C., Daussin, F., Messadeq, N., Milne, J., Lambert, P., Elliott, P., Geny, B., Laakso, M., Puigserver, P., Auwex, J. (2006). Resveratrol improves mitochondrial function and protects against metabolic disease by activating SIRT1 and PGC-1 α . *Cell*, 127, 1109–1122.
<https://doi.org/10.1016/j.cell.2006.11.013>
22. Lizarbe, B., Cherix, A., Duarte, J.M., Cardinaux, J.R., Gruetter, R. (2019). High-fat diet consumption alters energy metabolism in the mouse hypothalamus. *International Journal of Obesity*, 43(6), 1295–1304.
<https://doi.org/10.1038/s41366-018-0224-9>
23. Miura, D., Miura, Y., Yagasaki, K. (2003). Hypolipidemic action of dietary resveratrol, a phytoalexin in grapes and red wine, in hepatoma-bearing rats. *Life Science*, 73(11), 1393–1400.
[https://doi.org/10.1016/S0024-3205\(03\)00469-7](https://doi.org/10.1016/S0024-3205(03)00469-7)
24. Mohamed, I.A., Zaki, N.A., Walaa, A.M. (2010). Alterations in insulin, leptin, orexin-A and neuropeptide-Y levels in the high-fat diet fed rats. *Australian Journal of Basic and Applied Sciences*, 4(6), 1473–1481.
25. Mohan, A., Mather, K.A., Thalamuthu, A., Baune, B.T., Sachdev, P.S. (2016). Gene expression in the aging human brain: an overview. *Current Opinion in Psychiatry*, 29(2), 159–167.
<https://doi.org/10.1097/YCO.0000000000000238>
26. Morrison, C.D., Pistell, P.J., Ingram, D.K., Johnson, W.D., Liu, Y., Fernandez-Kim, S.O., White, C.L., Purpera, M.N., Uranga, R.M., Bruce-Keller, A.J., Keller, J.N. (2010). High fat diet increases hippocampal oxidative stress and cognitive impairment in aged mice: implications for decreased Nrf2 signaling. *Journal of Neurochemistry*, 114(6), 1581–1589.
<https://doi.org/10.1111/j.1471-4159.2010.06865.x>
27. Müller, R.H., Radtke, M., Wissing, S.A. (2002). Nanostructured lipid matrices for improved microencapsulation of drugs. *International Journal of Pharmaceutics*, 242(1–2), 121–128.
[https://doi.org/10.1016/S0378-5173\(02\)00180-1](https://doi.org/10.1016/S0378-5173(02)00180-1)
28. Niemiec, T., Sikorska, J., Harrison, A., Szmidi, M., Sawosz, E., Wirth-Dzieciolowska, E., Wilczak, J., Pierzynowski, S. (2011). Alpha-ketoglutarate stabilizes redox homeostasis and improves arterial elasticity in aged mice. *Journal of Physiology and Pharmacology*, 62(1), art. no. 37.
29. Noris, M., Remuzzi, G. (2013). Overview of complement activation and regulation. *Seminars in Nephrology*, 33(6), 479–492.
<https://doi.org/10.1016/j.semnephrol.2013.08.001>

30. NRC. (1995). Nutrient requirement of laboratory animals. In: National Research Council (US) Subcommittee on Laboratory Animal Nutrition. National Academies Press (US), Washington (DC), USA.
31. Nuthikattu, S., Milenkovic, D., Rutledge, J., Villablanca, A. (2019). The western diet regulates hippocampal microvascular gene expression: an integrated genomic analyses in female mice. *Scientific Reports*, 9(1), art. no. 19058. <https://doi.org/10.1038/s41598-019-55533-9>
32. Radzki, R.P., Bienko, M., Pierzynowski, S.G. (2009). Effect of dietary alpha-ketoglutarate on blood lipid profile during hypercholesterolaemia in rats. *Scandinavian Journal of Clinical and Laboratory Investigation*, 69(2), 175–180. <https://doi.org/10.1080/00365510802464633>
33. Salminen, A., Kaarniranta, K., Hiltunen, M., Kauppinen, A. (2014). Krebs cycle dysfunction shapes epigenetic landscape of chromatin: Novel insights into mitochondrial regulation of aging process. *Cell Signal*, 26(7), 1598–1603. <https://doi.org/10.1016/j.cellsig.2014.03.030>
34. Testa, G., Biasi, F., Poli, G., Chiarpotto, E. (2014). Calorie restriction and dietary restriction mimetics: a strategy for improving healthy aging and longevity. *Current Pharmaceutical Design*, 20(18), 2950–2977. <https://doi.org/10.2174/13816128113196660699>
35. Tian, Q., Zhao, J., Yang, Q., Wang, B., Deavila, J.M., Zhu, M.J., Du, M. (2020). Dietary alpha-ketoglutarate promotes beige adipogenesis and prevents obesity in middle-aged mice. *Aging Cell*, 19(1), art. no. e13059. <https://doi.org/10.1111/acer.13059>
36. Thomas, S.C., Alhasawi, A., Appanna, V.P., Auger, C., Appanna, V.D. (2015). Brain metabolism and Alzheimer's disease: The prospect of a metabolite-based therapy. *Journal of Nutrition, Health and Aging*, 19(1), 58–63. <https://doi.org/10.1007/s12603-014-0511-7>
37. Uranga, R.M., Bruce-Keller, A.J., Morrison, C.D., Fernandez-Kim, S.O., Ebenezer, P.J., Zhang, L., Dasuri, K., Keller, J.N. (2010). Intersection between metabolic dysfunction, high fat diet consumption, and brain aging. *Journal of Neurochemistry*, 114, 344–361. <https://doi.org/10.1111/j.1471-4159.2010.06803.x>
38. Walle, T., Hsieh, F., DeLegge, M.H., Oatis, J.E., Walle, U.K. (2004). High absorption but very low bioavailability of oral resveratrol in humans. *Drug Metabolism & Disposition*, 32(12), 1377–1382. <https://doi.org/10.1124/dmd.104.000885>
39. Weindruch, R., Kayo, T., Lee, C.K., Prolla, T.A. (2002). Gene expression profiling of aging using DNA microarrays. *Mechanisms of Ageing and Development*, 123(2–3), 177–193. [https://doi.org/10.1016/S0047-6374\(01\)00344-X](https://doi.org/10.1016/S0047-6374(01)00344-X)
40. Xie, Z., Li, H., Wang, K., Lin, J., Wang, Q., Zhao, G., Jia, W., Zhang, Q. (2010). Analysis of transcriptome and metabolome profiles alterations in fatty liver induced by high-fat diet in rat. *Metabolism*, 59(4), 554–560. <https://doi.org/10.1016/j.metabol.2009.08.022>
41. Ximerakis, M., Lipnick, S.L., Innes, B.T., Simmons, S.K., Adiconis, X., Dionne, D.Mayweather, B.A., Nguyen, L., Niziolek, Z., Ozek, C., Butty, V.L., Isserlin, R., Buchanan, S.M., Levine, S.S., Regev, A., Bader, G.D., Levin, J.Z., Rubin, L.L. (2019). Single-cell transcriptomic profiling of the aging mouse brain. *Nature Neuroscience*, 22(10), 1696–1708. <https://doi.org/10.1038/s41593-019-0491-3>
42. XiYang, Y.B., Wang, Y.C., Zhao, Y., Ru, J., Lu, B.T., Zhang, Y.N., Wang, N.C., Hu, W.Y., Liu, J., Yang, J.W., Wang, Z.J., Hao, C.G., Feng, Z.T., Xiao, Z.C., Dong, W., Quan, X.Z., Zhang, L.F., Wang, T.H. (2016). Sodium channel voltage-gated beta 2 plays a vital role in brain aging associated with synaptic plasticity and expression of COX5A and FGF-2. *Molecular Neurobiology*, 53(2), 955–967. <https://doi.org/10.1007/s12035-014-9048-3>
43. Zahn, J.M., Poosala, S., Owen, A.B., Ingram, D.K., Lustig, A., Carter, A., Weeraratna, A.T., Taub, D.D., Gorospe, M., Mazan-Mamczarz, K., Lakatta, E.G., Boheler, K.R., Xu, X., Mattson, M.P., Falco, G., Ko, M.S., Schlessinger, D., Firman, J., Kummerfeld, S.K., Wood, W.H., Zonderman, A.B., Kim, S.K., Becker, K.G. (2007). AGEMAP: a gene expression database for aging in mice. *PLoS Genetics*, 3(11), art. no. e201. <https://doi.org/10.1371/journal.pgen.0030201>
44. Zhou, B., Yang, L., Li, S., Huang, J., Chen, H., Hou, L., Wang, J., Green, C.D., Yan, Z., Huang, X., Kaeberein, M., Zhu, L., Xiao, H., Liu, Y., Han, J.D. (2012). Midlife gene expressions identify modulators of aging through dietary interventions. *Proceedings of the National Academy of Sciences USA*, 109(19), E1201–E1209. <https://doi.org/10.1073/pnas.1119304109>

Phenolic Contents and Antioxidant Activity of Extracts of Selected Fresh and Dried Herbal Materials

Mariola Kozłowska^{1*} , Iwona Ścibisz² , Jarosław L. Przybył³ , Małgorzata Ziarno² ,
Anna Żbikowska² , Ewa Majewska¹ 

¹Department of Chemistry Institute of Food Science, Warsaw University of Life Sciences-SGGW,
Nowoursynowska 159C Str., 02–776 Warsaw, Poland

²Department of Food Technology and Assessment, Institute of Food Science, Warsaw University of Life Sciences-SGGW,
Nowoursynowska 159C Str., 02–776 Warsaw, Poland

³Department of Vegetable and Medicinal Plants, Institute of Horticulture Sciences, Warsaw University of Life Sciences-SGGW,
Nowoursynowska 159 Str., 02–776 Warsaw, Poland

Key words: coriander, lovage, tarragon, Indian borage, total phenolics, phenolic acids, flavonoids

Total phenolic content (TPC) and phenolic profiles of extracts of the aerial parts of coriander (*Coriandrum sativum* L.), lovage (*Levisticum officinale* Koch.), and tarragon (*Artemisia dracunculus* L.), and leaves of Indian borage (*Plectranthus amboinicus*) have been investigated. The extracts were prepared using 70% (v/v) ethanol and fresh or air-dried herbal material. Besides phenolic composition, DPPH[•] and ABTS^{•+} scavenging activity, and ferric-reducing antioxidant power (FRAP) were determined. The extracts from dried herbal materials exhibited higher TPC and more potent antioxidant activity than those from fresh counterparts. The highest TPC (146.77 g GAE/kg extract) and antioxidant activity (0.491, 0.643, and 0.396 mol TE/kg extract in DPPH, ABTS, and FRAP assays, respectively) were detected for the extract from dried leaves of Indian borage, while the lowest values were determined for the extract from fresh aerial parts of coriander. Five phenolic acids (rosmarinic, chlorogenic, caffeic, ferulic, and neochlorogenic acids) and four flavonoids ((+)-catechin, rutin, hyperoside, and astragalgin) were identified in the samples. Only caffeic acid was present in all extracts. Its content in the extracts of dried tarragon and Indian borage was lower than in those of the fresh material. A significant correlation was found between antioxidant activity and the content of phenolic acids. Rutin was found to be the major flavonoid in most extracts. Based on the present study results, the possibility of using the extracts obtained from both fresh and air-dried herbs as potential components for functional food formulation can be considered in the future.

ABBREVIATIONS

TPC: total phenolic content; FRAP: ferric-reducing antioxidant power; GAE: gallic acid equivalents; TE: Trolox equivalents.

INTRODUCTION

Plant materials, especially spices and herbs, have been used as food sources since the dawn of time, and their healing properties have been discovered with time as well. Nowadays, special attention is paid to a healthy lifestyle, diet as well as food products from organic farming where no chemicals are used. Due to this fact, a growing interest can be observed in plant material potency in the treatment and prevention of certain diseases. Spices and aromatic herbs are generally recognized by consumers as being safer for use in food manufacturing and processing, especially

in dairy, meat, and bakery products, than synthetic food additives [Słowianek & Leszczyńska, 2016; Ulewicz-Magulska & Wesolowski, 2019]. Both fresh and dried herbal materials are excellent additives to a variety of dishes, improving their appearance and enhancing their taste and aroma. Less desirable ingredients, such as salt, sugar or fat, can sometimes be partially replaced by such herbal materials [Tapsell *et al.*, 2006]. Spices and herbs are cultivated in the open-field systems, quite often in home gardens as well as in pots or boxes on balconies and terraces. In this way, it is easy to obtain the raw herbal material of one's own without unnecessary expenditures. However, the quality of the raw herbal material is significantly influenced not only by the method of its cultivation, climatic and genetic factors, but also by the method of drying and storage, especially with regard to the biologically active compounds it contains, including *e.g.* phenolic compounds [Calín-Sánchez *et al.*, 2020; Złotek *et al.*, 2019]. Their presence in such a material may affect its antioxidant

* Corresponding Author:

Tel.: +48 22 593 7614; Fax: +48 22 593 76 35;

E-mail: mariola_kozlowska@sggw.edu.pl (M. Kozłowska)

Submitted: 15 February 2021

Accepted: 14 June 2021

Published on-line: 20 July 2021



properties, thus making it a viable ingredient for functional food formulations aimed to retard the process of lipid oxidation [Kozłowska *et al.*, 2014, 2019].

Herbal plants are an extremely vast group of medicinal, spicy, and melliferous plants, and those rich in essential oils. They are used in food and pharmaceutical industries because of their strong antioxidant properties caused by the presence of phenolic compounds [Pabón-Baquero *et al.*, 2018; Shahidi & Ambigaipalan, 2015], which are accumulated in various plant parts, including fruits, leaves, seeds, and rhizomes, and can be classified into flavonoids, phenolic acids, stilbenes, lignans, and tannins. Plant phenolics positively influence human health, by inhibiting the oxidation of low density lipoproteins and the growth of bacteria, viruses, fungi, and by stimulating the growth of beneficial bacteria and activating or inhibiting enzymes that bind a specific receptor [Papuc *et al.*, 2017; Shahidi & Ambigaipalan, 2015]. Spices and herbs, but also beverages, fruits, and cereal products are important sources of plant phenolics in the human diet. The average phenolic intake in an adult population was estimated at approximately one gram of polyphenol per day [Zujko *et al.*, 2012]. This may be important in reducing free radicals generation in a human body.

Drying fresh spices and herbs reduces their water content, and thus contributes to their shelf life extension by slowing or inhibiting the growth of microorganisms and affects the intensity of the ongoing biochemical and chemical reactions [Bourdoux *et al.*, 2018; Calín-Sánchez *et al.*, 2020; Roshanak *et al.*, 2016]. This process can also lead to changes in the appearance and aroma of herbs due to the loss of volatiles or the formation of new ones as a result of oxidation and esterification reactions [Calín-Sánchez *et al.*, 2020]. Some changes in the composition of bioactive components of plant material, such as phenolic compounds, ascorbic acid, and pigments, are also likely [Hossain *et al.*, 2010; Roshanak *et al.*, 2016]. Drying herbal material often requires finding the optimal conditions for a particular plant species, so as not to cause significant loss of color and taste, and to protect sensitive active ingredients [Calín-Sánchez *et al.*, 2020]. In the case of mass production, the use of technical drying methods, such as convection oven, microwave, and freeze drying, is necessary. The selection of an appropriate drying method depends on the efficiency and the frequency of its use to attain optimal benefits without increasing costs and to assure the high quality of the dried material. However, the simplest, low-cost, and feasible for use at home method is natural drying in the shade, in a ventilated area or in the sunlight. Manually collected plants are dried by spreading them out in thin layers on trays or tying in bunches and hanging them with the leaves down [Hossain *et al.*, 2010]. This type of drying, without auxiliary energy, either in the open-field or in special places is usually preferred for drying small quantities of plant material. Naturally air dried food products are also preferable by consumers who search for commodities made of natural substances or by natural processes. The naturally dried form is usually obtained from the whole aerial part of the fresh plant material, irrespective of the particular organs such as leaves, seeds or stems.

In the presented research, such herbs as coriander, tarragon, lovage, and Indian borage, were subjected to natural air drying, and the phenolic contents and antioxidant activity of extracts of the dried material and the fresh herbal material were compared. Although the content of phenolic compounds and their composition in these herb species had already been the topic of other publications [Al-Juhaimi & Ghafoor, 2011; Bhatt *et al.*, 2013; Spréa *et al.*, 2020; Tajner-Czopek *et al.*, 2020], they were often determined for individual organs of herbs, not for the whole aerial part, either fresh or naturally dried. Therefore, the aim of this study was to determine the antioxidant properties and the phenolic compound profile of the extracts of aerial parts of fresh herbal materials and material air-dried without sun exposure.

MATERIALS AND METHODS

Reagents

The Folin-Ciocalteu's phenol reagent, 2,2-diphenyl-1-picrylhydrazyl (DPPH) radical, gallic acid, 6-hydroxy-2,5,7,8-tetramethylchroman-2-carboxylic acid (Trolox), 2,2'-azino-bis-(3-ethylbenzothiazoline-6-sulfonic acid) diammonium salt (ABTS), and 2,4,6-tri(2-pyridyl)-s-triazine (TPTZ) were purchased from Sigma-Aldrich (Poznań, Poland). High performance liquid chromatography (HPLC) standards were bought from Merck (Darmstadt, Germany) and Chroma-Dex® (Irvine, CA, USA). Other chemicals and solvents were obtained from Avantor Performance Materials (Gliwice, Poland). All of them were of analytical grade and were used as received, without further purification.

Plant material

The tested herbs included coriander (*Coriandrum sativum* L., family Apiaceae), lovage (*Levisticum officinale* Koch., family Apiaceae), tarragon (*Artemisia dracunculus* L., family Asteraceae), and Indian borage (*Plectranthus amboinicus* (Lour) Spreng; synonym: *Coleus amboinicus*, *Coleus aromaticus*, family Lamiaceae). All of them were purchased in pots at the beginning of July 2016 at the local market of Warsaw, Poland. Coriander, lovage, and tarragon came from a family business located in the heart of Kujawy, near Włocławek, Poland. The fresh aerial parts of these herbs, reaching approximately 25 cm in length, were cut off and divided into two batches. One (fresh) was cut into 1 cm long pieces and immediately used for extraction. The other batch of the fresh plant material was dried. For this purpose, several bunches of the tested herbs (approximately 1 cm in diameter) were prepared, which were subsequently hung upside down in a dry place without the sun exposure. The appropriate air flow and the average temperature of 25°C remained constant throughout the drying process. In the case of Indian borage, only fresh leaves and leaves dried without the sun exposure in appropriate air flow at the average temperature of 25°C, on trays covered with cotton sheets, were used for extraction. The leaves on the trays were occasionally tossed. When herbs began to crumple easily between the fingers, they were crushed using mortar and pestle (particles passing through a 3 mm screen), packed, and stored in airtight containers until further use. The average moisture content of all dried herbal material was around 9.3 ± 0.2 g/100 g.

Extract preparation

The extraction of the fresh and dried herbal material was performed with 70% (v/v) ethanol based on the procedure reported by Kozłowska *et al.* [2015] with some modifications. Briefly, 20 g of each herbal material was transferred into the flasks containing 250 mL of aqueous ethanol. Then, the mixtures were stirred in a water bath for 10 h at 45°C. The plant residues were filtered off through Whatman No. 1 paper filter, and ethanol was evaporated under vacuum on a rotary evaporator at 40°C (Rotavapor R-200, Büchi Labortechnik, Flail, Switzerland). Next, the resultant extracts were freeze-dried (Alpha 1–4 LSC-plus, Osterode am Harz, Germany) and stored frozen until further use (-20°C). The same extraction procedure was repeated for the new batch of the fresh and dried herbal material (20 g) using 70% (v/v) aqueous ethanol (250 mL). The extraction yield was evaluated based on the mass balance.

Total phenolic content (TPC)

The content of total phenolics in freeze-dried herbal extracts was measured using a method given by Singleton & Rossi [1965] with slight modification. A stock solution of the herbal extract was obtained by dissolving 1 mg of each extract in 2 mL of 70% (v/v) ethanol. Then, 1 mL of such prepared solution was diluted with distilled water (9 mL) and mixed with the Folin-Ciocalteu's phenol reagent (0.5 mL). After 3 min, 5 mL of saturated Na₂CO₃ solution was added. The mixture was made up to 50 mL with distilled water and stirred for about 1 min. The sample was stored for 1 h at room temperature in the dark. Then the absorbance was recorded at 765 nm on a Shimadzu UV-1650 PC spectrophotometer (Kyoto, Japan) and used to calculate the TPC using gallic acid as a standard (0.2–5 mg/L). The results were expressed in g of gallic acid equivalents (GAE) per kg of extract.

HPLC analysis

The HPLC-DAD analysis of the phenolic compounds of the herbal extracts was performed using a Shimadzu Prominence chromatograph equipped with a SIL-20AC HT

autosampler, an SPD-M20A photodiode array detector, and LCsolution 1.21 SP1 chromatography software (Shimadzu, Kyoto, Japan). Separation was performed using a C-18 column with a solid core and a porous outer layer (Kinetex™, 100Å, 2.6 μm, 100×4.60 mm i.d., Phenomenex, Torrance, CA, USA) and binary gradient of acetonitrile (ACN) and deionized water, acidified to pH 2 with phosphoric acid (0 min – 12.5% ACN; 4.0 min – 23% ACN; 6.0 min – 50% ACN; 6.01 min – 12.5% ACN; 10 min – stop) at flow rate 1.5 mL/min and temperature 40°C. Herbal extracts (2 mg/mL), before injection (1 μL), were dissolved in 70% (v/v) ethanol and filtered with 0.20 μm pore size PTFE Iso-Disc™ filters (Supelco Analytical™, Bellefonte, PA, USA). Commercially available standards were prepared according to the ChromaDex's Tech Tip 0003: Reference Standard Recovery and Dilution [ChromaDex, 2016]. Six-point calibration curves were plotted according to the external standard method by correlating concentrations of the solutions with the obtained peak area. Parameters of method validation, such as linearity range (mg/mL), precision (expressed as coefficient of variation – CV, %), limit of detection (LOD, μg/L), limit of quantitation (LOQ, μg/L), and recovery (%) were calculated according to International Conference on Harmonization ICH Q2 (R1) guidelines [2005] and their values are shown in Table 1. The signal-to-noise ratio approach was used to determine LOD (S/N of 3:1) and LOQ (S/N of 10:1). The compounds present in the extracts were identified by comparing their retention times and UV-VIS spectra (190–450 nm) with those of the standards, and quantified from the peak area according to the calibration curve equation of a respective standard.

DPPH radical scavenging activity

The antiradical activity of the herbal extracts was measured using the DPPH method according to Gow-Chin & Hui-Yin [1995] with a slight modification. The herbal extract solutions were prepared by dissolving 3 mg of each freeze-dried extract in 2 mL of 70% (v/v) ethanol. A 1 mL aliquot of freshly prepared DPPH• methanolic solution (0.3 mM) was

TABLE 1. Parameters of the HPLC method validation.

Standard	Calibration equation	R ² (n=6)	Linear range (mg/mL)	LOD (μg/L)	LOQ (μg/L)
Neochlorogenic acid (5- <i>O</i> -caffeoylquinic acid)	y=1809.0x+1539.8	0.9996	0.39–392.00	0.02	0.06
(+)-Catechin	y=8216.4x-6069.3	0.9998	0.95–950.00	0.01	0.36
Chlorogenic acid (3- <i>O</i> -caffeoylquinic acid)	y=6517.4x-12016.6	0.9997	0.40–39.46	0.21	0.70
Caffeic acid (3,4-dihydroxycinnamic acid)	y=2592.9x+379.6	0.9996	1.00–998.40	0.03	0.08
Ferulic acid (4-hydroxy-3-methoxycinnamic acid)	y=2424.6x-1856.9	0.9995	0.40–99.68	0.11	0.35
Rutin (quercetin 3- <i>O</i> -rutinoside)	y=1434.0x-5093.0	0.9999	0.91–90.67	0.07	0.25
Hyperoside (quercetin 3- <i>O</i> -galactoside)	y=3435.5x-6882.2	0.9999	0.38–38.40	0.04	0.12
Astragalin (kaempferol 3- <i>O</i> -glucoside)	y=2104.5x-2426.3	0.9999	0.41–81.91	0.33	1.10
Rosmarinic acid	y=2017.9x+1100.4	0.9999	0.43–434.02	0.03	0.09

added to 3.8 mL of methanol and 0.2 mL of particular herbal extract. The samples were vortexed and incubated for 10 min at room temperature in the dark. Then, the absorbance was recorded using a Shimadzu UV-1650 PC spectrophotometer at 517 nm. The results were expressed as mol Trolox equivalents (TE) per kg of extract. Trolox was used as a reference standard (linear range 8–40 μM).

ABTS radical cation scavenging activity

The radical scavenging activity of extracts was also analyzed using ABTS^{•+} according to the method proposed by Re *et al.* [1999]. First, the ABTS radical cations were produced by mixing 5 mL of 14 mM ABTS solution with 5 mL of 4.9 mM potassium persulfate. Next, the mixture was allowed to stand for 12–16 h in the dark at room temperature before use. For the analysis, the obtained solution was diluted with water to the final absorbance of 0.70 ± 0.02 at 734 nm. Then, 4 mL of the ABTS^{•+} working solution was mixed with 40 μL of the herbal extract prepared by dissolving (3 mg) in 70% (v/v) ethanol (2 mL). The mixture was vortexed and left to stand at room temperature in the dark. After 6 min, the absorbance of the samples was measured at 734 nm using a Shimadzu UV-1650 PC spectrophotometer. Trolox was used as a reference standard (linear range 0–20 μM). Results were expressed as mol Trolox equivalents (TE) per kg of extract.

Ferric-reducing antioxidant power (FRAP)

The ferric-reducing antioxidant power assay was performed according to Benzie & Strain procedure [1996] with a minor modification. The FRAP reagent consisted of 10 mM TPTZ solution in 40 mM HCl, 300 mM acetate buffer (pH 3.6), and 20 mM FeCl₃ solution in proportions of 1:10:1 (v/v/v). The FRAP solution (3 mL) was used in the reaction with the herbal extract of an appropriate concentration (1.5 mg/mL). The reaction was carried out for 10 min at room temperature. Then, the absorbance of the samples was measured at 593 nm using a Shimadzu UV-1650 PC spectrophotometer. Results were reported as mol Trolox equivalents (TE) per kg of extract. A standard curve was prepared using Trolox in the concentration ranging from 80 to 500 $\mu\text{mol/L}$.

Statistical analysis

All the analyses were performed at least in triplicate and the data were expressed as mean \pm standard deviation. The results were analyzed using the analysis of variance (ANOVA) with post-hoc Tukey's HSD test at the confidence level $p < 0.05$ (Statistica 13, Statsoft, Tulsa, OK, USA). The Pearson's test was used to find the correlation between the total phenolic content, antioxidant activity determined by DPPH, ABTS, and FRAP assays, and sums of phenolic acids and flavonoids from the HPLC analysis of the herbal extracts.

RESULTS AND DISCUSSION

Extraction yield and total phenolic content

The results presented in Table 2 show that the yield of the extraction process of the herbal material ranged from 1.69% to 31.89%, with the lowest value found for the extracts obtained from the fresh leaves of Indian borage (*P.amboinicus*) and the highest one for dried aerial parts of tarragon and coriander. Generally, 7–15 times higher yields were observed for the extracts obtained from air-drying than from fresh herbal materials. However, Indian borage leaves, not only the fresh but also the dried ones, gave the aqueous ethanolic extracts with the lowest yield. Among the freeze-dried aqueous ethanolic extracts prepared from the fresh herbal material, the highest yield showed the one from coriander. The differences in yields of the extraction processes may stem from the water content in the initial material or from how the material was crushed or chopped.

The TPC of freeze-dried aqueous ethanolic extracts of the herbal material determined using the Folin-Ciocalteu method is presented in Table 2. The TPC of the extracts obtained from air-dried material was 1–1.8 times higher than that of the fresh herbal extracts. Among extracts made of both dried on air and fresh herbal materials, the extracts of Indian borage leaves had the highest TPC reaching 146.77 and 84.67 g GAE/kg, respectively. In turn, the lowest TPC was determined for the coriander extracts obtained from fresh material. In the case of dried herbal materials, the tarragon extract had the lowest TPC. The total phenolic contents of tarragon and lovage 80% methanolic extracts

TABLE 2. Extraction yield and total phenolic contents (TPC) of the herbal extracts.

Herbal material	Latin name	Extraction yield (%)	TPC (g GAE/kg extract)	
Fresh	Coriander	<i>Coriandrum sativum</i> L.	3.35 ± 0.39^c	28.07 ± 0.85^f
	Tarragon	<i>Artemisia dracunculus</i> L.	2.06 ± 0.25^d	32.91 ± 0.68^e
	Lovage	<i>Levisticum officinale</i> Koch.	2.83 ± 0.31^d	51.04 ± 0.72^c
	Indian borage	<i>Plectranthus amboinicus</i> (Lour) Spreng	1.69 ± 0.49^e	84.67 ± 0.45^b
Dried	Coriander	<i>Coriandrum sativum</i> L.	30.19 ± 0.98^a	50.57 ± 1.59^c
	Tarragon	<i>Artemisia dracunculus</i> L.	31.89 ± 1.21^a	42.53 ± 0.93^d
	Lovage	<i>Levisticum officinale</i> Koch.	22.28 ± 0.95^b	52.01 ± 0.77^c
	Indian borage	<i>Plectranthus amboinicus</i> (Lour) Spreng	21.97 ± 1.05^b	146.77 ± 2.05^a

GAE, gallic acid equivalents. Means with different letters in the column are statistically different according to Tukey' test at $p < 0.05$.

prepared using dried spices were determined by Słowianek & Leszczyńska [2016]. The reported values, 41.2 and 17.8 mg GAE/g, respectively, were related to those in our study for dried tarragon but lower for lovage extracts. Differences may be due to the use of a different type of solvent and, first of all, a different part of the herbal material in the extraction process. Ethanol, methanol, ethyl acetate, and acetone are commonly used for the extraction of phenolics from herbal materials [Sepahpour *et al.*, 2018; Swamy *et al.*, 2017]. The high polarity of these solvents can promote solubility of phenolic compounds and thus boost their extraction yield. According to Sepahpour *et al.* [2018], 80% acetone was considered to be the best solvent for extracting TPC from turmeric, torch ginger, and lemon grass, whereas 80% ethanol was the most appropriate solvent for extracting phenolic compounds from curry leaf. In the case of herbs analyzed in our study, that aqueous ethanol was twice as effective as hot water in extracting total phenolic compounds from lovage [Spréa *et al.*, 2020]. Similarly, Tajner-Czopek *et al.* [2020] noted a higher content of caffeic acid derivatives in aqueous ethanolic extracts of several herbs, including lovage and tarragon, compared to the water extracts. Furthermore, Swamy *et al.* [2017] reported that the TPC of a methanolic extract of Indian borage leaves was higher than that of the acetone and hexane extracts. However, Wangenstein *et al.* [2004] reported that ethyl acetate was a more preferred than diethyl ether and *n*-butanol solvent for phenolic extraction from coriander leaves and, also that this extract had higher TPC and better antioxidant properties than the extract from seeds. In turn, Al-Juhaimi & Ghafoor [2011] showed that stems and leaves of coriander, parsley, and mint were good materials to produce extracts rich in phenolic compounds and effectively scavenging free radicals. They also reported that extracts of leaves from these herbs featured a higher TPC and higher antioxidant activity than the extracts from stems. In our study, the TPC of the aqueous ethanolic extracts obtained from dried coriander leaves and stems was higher compared to fresh coriander material extracts (Table 2) but lower to those reported by Harsha & Anilakumar [2014]. The 70% ethanol extract of the *Coriandrum sativum* prepared from leaves dried for three days in the shade containing 7% of water, evaluated by these authors, resulted in total phenolics at 133.74 μg GAE/mg extract.

Changes in the content of biologically active constituents in herbs may be caused by the technological processes applied, such as drying and freezing. Herb drying inhibits microbial growth [Bourdoux *et al.*, 2018] and leads to a stable, easily moveable product that is available throughout the year, but it may also change the content of phenolics [Hossain *et al.*, 2010; Roshanak *et al.*, 2016]. In our research, an increase was noticed in the TPC of extracts obtained from the dried materials compared to their fresh counterparts except from lovage (Table 2). In the case of this spice, drying did not cause statistically significant changes ($p \geq 0.05$) in the content of these biologically active compounds. Contrary to the presented results, Tomsone & Kruma [2014] revealed that fresh lovage leaves and stems had higher TPC than dried samples. Also Slimestad *et al.* [2020] reported that commercially available fresh herbs had a higher content of total phenolics compared to dried herbs offered as a ground product by local

groceries. They explained that a lower TPC in dried material of the studied species might be a result of a long-term storage of dried products *versus* fresh herbs. In our study, the lower TPC of extracts of fresh plant material compared to air-dried samples may indicate that the enzymes present in fresh samples may have caused the degradation of these compounds. On the other hand, due to the low water activity in the dried samples, enzymes were inactivated, and high amounts of phenolic compounds remained in the extract. Moreover, during the drying process of herbs, the loss of moisture may be perceived as stress, which the plant responds to by activating the defense mechanism, including the production of phenolic compounds [Isah, 2019]. Similarly to the presented research, air-dried herbs from the Lamiaceae family had higher total phenolics and rosmarinic acid contents than fresh, freeze-dried and vacuum oven-dried their counterparts [Hossain *et al.*, 2010]. Roshanak *et al.* [2016] also reported that dried green tea showed higher total phenolic and flavonoid contents than fresh material.

HPLC analysis

Five phenolic acids and four flavonoids were identified by HPLC in the extracts of herbal materials (Table 3). Caffeic acid was the phenolic acid present in all the tested extracts. Its content in the extracts obtained from the fresh herbal material, was higher than in the dried material with the exception of the coriander and lovage extracts. The coriander extract from the dried material had a higher content of caffeic acid than its counterpart obtained from the fresh material. The highest and the lowest contents of caffeic acid were determined in the aqueous ethanolic extracts of Indian borage and lovage, respectively, which is consistent with the literature data [Bhatt *et al.*, 2013; Zlotek *et al.*, 2019]. In turn, Melo *et al.* [2005] found caffeic acid as the essential phenolic component of aqueous coriander extract fractions. Apart from caffeic acid, rosmarinic and chlorogenic acids were present in six out of the eight extracts tested. Ferulic acid was identified in five studied extracts and neochlorogenic acid only in two extracts obtained both from fresh and dried lovage. The highest content of rosmarinic acid was determined in the aqueous ethanolic extracts of Indian borage, while the extract from the fresh lovage showed the lowest content. The dried leaf extract of Indian borage was richer in rosmarinic acid and poorer in caffeic acid than its fresh counterparts. The rosmarinic acid is a widespread phenolic acid found as dominant in many herbs of the Lamiaceae family [Slimestad *et al.*, 2020; Yashin *et al.*, 2017], which includes Indian borage [Bhatt *et al.*, 2013]. In our study, drying the aerial part of tarragon and lovage, resulted in 23 and 2 times higher rosmarinic acid content respectively compared to the non-dried material. In turn, lovage drying caused the content of chlorogenic acid in the obtained extract to be almost 1.2 fold lower than its content in the extract from the fresh lovage. Chlorogenic acid was also the most predominant phenolic acid in the coriander extracts, especially, when dried material was used in the extraction process. The dried coriander herb also contained less caffeic acid (0.714 g/kg of extract) and ferulic acid (0.006 g/kg of extract). Previously, chlorogenic acid was determined as the major phenolic acid in lovage extracted with

TABLE 3. Content of phenolic compounds (g/kg extract) of the herbal extracts.

Herbal material	Phenolic acids					Flavonoids				
	Chlorogenic acid	Ferulic acid	Caffeic acid	Rosmarinic acid	Neochlorogenic acid	(+)-Catechin	Rutin	Hyperoside	Astragalgin	
Fresh	Coriander	2.693±0.07 ^e	nd	0.114±0.003 ^f	nd	nd	18.414±0.41 ^d	4.661±0.72 ^e	0.035±0.002 ^f	
	Tarragon	2.044±0.26 ^d	1.045±0.04 ^b	1.326±0.004 ^e	0.562±0.001 ^d	nd	22.464±0.65 ^e	4.415±0.50 ^d	nd	
	Lovage	0.902±0.10 ^e	0.711±0.07 ^c	0.029±0.003 ^e	0.163±0.015 ^f	0.538±0.061 ^a	0.417±0.049 ^f	nd	0.084±0.008 ^g	
	Indian borage	nd	nd	20.088±1.50 ^b	46.530±1.2 ^b	nd	12.888±0.370 ^b	nd	0.288±0.04 ^b	
Dried	Coriander	6.848±0.17 ^a	0.006±0.0002 ^e	0.714±0.006 ^d	nd	nd	31.779±0.96 ^b	6.109±0.68 ^b	0.070±0.001 ^e	
	Tarragon	3.645±0.03 ^b	0.637±0.02 ^d	0.330±0.02 ^e	12.930±0.13 ^c	nd	14.115±0.66 ^e	8.437±0.82 ^a	nd	
	Lovage	0.770±0.07 ^f	0.777±0.03 ^b	0.017±0.002 ^e	0.399±0.043 ^e	0.358±0.023 ^b	0.924±0.037 ^d	46.442±0.58 ^a	nd	0.126±0.012 ^c
	Indian borage	nd	nd	8.520±0.18 ^b	112.98±3.37 ^a	nd	18.120±0.42 ^b	nd	nd	0.320±0.09 ^a

“nd” – not detected. Means with different letters in the column are statistically different according to Tukey's test at $p < 0.05$.

various solvents (aqueous ethanol, water, methanol) [Spréa *et al.*, 2020; Tajner-Czopek *et al.*, 2020; Złotek *et al.*, 2019] as well as commercially available fresh and dried coriander and tarragon [Slimestad *et al.*, 2020]. In Rajeshwari & Andullu [2011] studies, methanolic extracts of coriander seeds showed a higher content of chlorogenic and caffeic acids than their ethanolic counterparts. Phenolic acids tentatively identified in coriander leaves by high-performance liquid chromatography coupled to mass spectrometric were caffeic acid derivatives, including 5-feruloylquinic and 5-*p*-coumaroylquinic acids [Kaiser *et al.*, 2013]. The mono- and dicaffeoyl quinic acid isomers as well as derivatives of sinapic, ferulic, and *p*-coumaric acids were also detected in lovage and tarragon [Spréa *et al.*, 2020; Tajner-Czopek *et al.*, 2020; Tvrdá *et al.*, 2019; Złotek *et al.*, 2019].

Four flavonoids, including astragalgin (kaempferol 3-*O*-glucoside), hyperoside (quercetin 3-*O*-galactoside), rutin (quercetin 3-*O*-rutinoside), and (+)-catechin were identified in the extracts (Table 3). Astragalgin was detected in small amounts in the coriander extracts from both fresh and dried material and in a slightly higher level in the lovage and Indian borage extracts. It is a natural flavonoid present in different medicinal plants, known for its various pharmacological properties such as anti-inflammatory, antioxidant, antidiabetic, and anticancer activities [Riaz *et al.*, 2018]. Rutin was identified in the lovage, tarragon, and coriander extracts (Table 3). Among phenolic compounds, it was the predominant chemical compound detected in the lovage extracts prepared from both fresh and dried material. In this case, no significant differences ($p \geq 0.05$) were found for the rutin content in both types of lovage extracts. The presence of rutin as the major flavonoid of the methanol lovage extracts was also confirmed by Tvrdá *et al.* [2019] and Złotek *et al.* [2019]. These authors also found other flavonoids, such as quercetin, cynarosid, apigenin, kaempferol, and/or their glycosides. TLC qualitative study indicated that 70% (v/v) ethanolic extract from tarragon contained rutin among flavonoids [Pirvu *et al.*, 2014]. The presence of rutin in tarragon and coriander extracts was also reported by Slimestad *et al.* [2020].

The aqueous ethanolic extracts obtained from fresh and air-dried lovage, and dried coriander were richer in flavonoids than in phenolic acids (Figure 1). In turn, phenolic acids were the major compounds of the extracts from the fresh and air-dried leaves of Indian borage and from the air-dried aerial part of tarragon. It was also observed that the extracts from dried coriander and Indian borage contained more flavonoids and phenolic acids than those obtained from their fresh counterparts. On the other hand, extracts from the fresh tarragon had a slightly higher content of flavonoids compared to the extracts prepared from dried material. In turn, the content of phenolic acids in the extracts from air-dried tarragon was over 3 times higher than the one determined in the extracts from fresh raw material. However, a similar amount of flavonoids and phenolic acids was observed in the lovage extracts obtained from both dried and fresh herbal material. Among the fifteen herbs analyzed by HPLC and mass spectrometry, the highest contents of flavonoids, measured as aglycones after acid hydrolysis, were found in lovage, mint, dill, and parsley [Justesen & Knuthsen, 2001]. However, it should

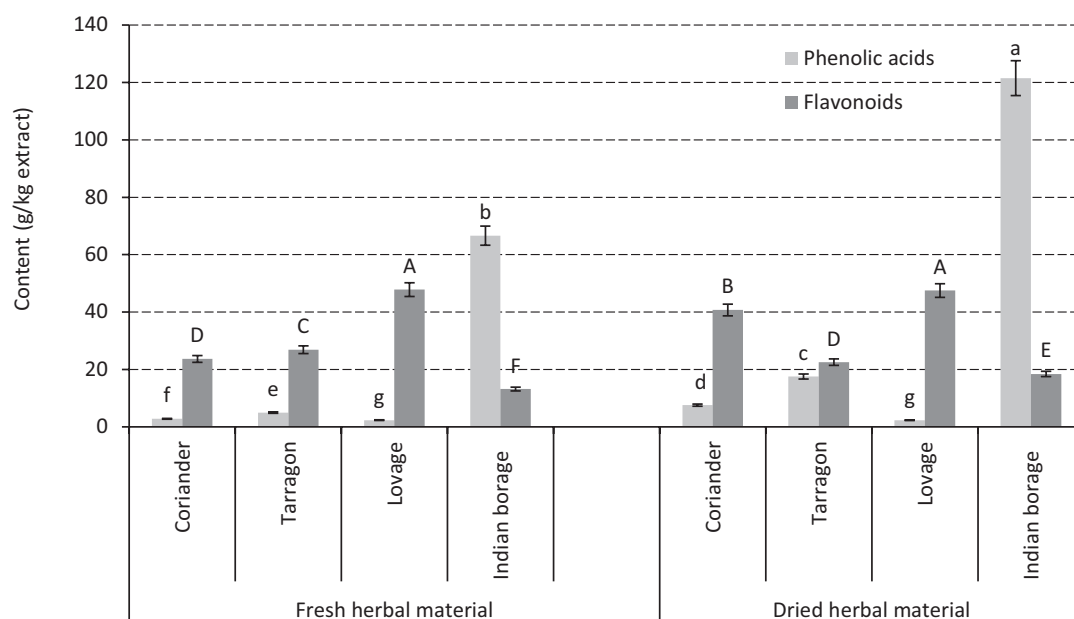


FIGURE 1. Phenolic acid and flavonoid contents of the herbal extracts. Significantly different values are marked with different letters above the bars (separately A-F and a-g) at $p < 0.05$.

be mentioned that the contents of both flavonoids and phenolic acids in herbal material may depend on plant cultivation conditions, harvest time as well as on genetic and ontogenetic factors. As an example, Karamać *et al.* [2020] found that the content ratio of flavonoids to phenolic acids in aerial parts of *Camelina sativa* changed significantly across the plant growth cycle. In turn, flavonoid content was lower in tarragon herb harvested at the beginning of September compared to the tarragon harvested at the beginning of July [Zawiślak & Nurzyńska-Wierdak, 2014].

Antioxidant activity

The antioxidant properties of the herbal extracts are shown in Table 4. They were determined by DPPH, ABTS, and FRAP assays. All herbal extracts showed the ability to scavenge the $ABTS^{•+}$ and $DPPH^{•}$, and to reduce $Fe(III)$. The results of antiradical activity determination indicated that the extracts from air-dried herbal material had significantly ($p < 0.05$) higher both $DPPH^{•}$ and $ABTS^{•+}$ scavenging activities than those made of the fresh raw material. In the case of FRAP, only the dried tarragon aerial parts and Indian borage leaves yielded extracts with higher antioxidant activity than the fresh plants. FRAP of other dried herbal material extracts did not differ significantly ($p \geq 0.05$) from the corresponding extracts of fresh plants. The type of herb was also a factor differentiating antioxidant activity. The highest $DPPH^{•}$ and $ABTS^{•+}$ radical scavenging activity and FRAP was reported for the Indian borage leaf extracts. The antioxidant activity of other extracts obtained from fresh material decreased in the following order: Indian borage > lovage > coriander > tarragon, regardless of the assay used for its determination. In the case of extracts obtained from air-dried plants, the order of their antioxidant activity changed as follows: Indian borage > lovage > tarragon > coriander in the ABTS assay, Indian borage > lovage > tarragon =

coriander in the DPPH assay, and Indian borage > lovage = tarragon > coriander in the FRAP assay.

The high antioxidant activity of Indian borage extracts compared to that of the other extracts examined may be due to the high content of rosmarinic acid in this herbal material (Table 3 and 4), which is a strong antioxidant and, among hydroxycinnamic acids, exhibited high scavenging activity due to the fact that its molecule contains four hydroxyl groups in structure [Chen & Ho, 1997]. Our results are consistent with the earlier report showing that rosmarinic acid was predominantly responsible for the radical scavenging activity of Indian borage [Bhatt *et al.*, 2013]. This acid significantly contributes to the antioxidant activity of many other plants of the Lamiaceae family, like sage,

TABLE 4. Antioxidant activity of the herbal extracts (mol TE/kg extract).

Herbal material	DPPH [•] scavenging activity	ABTS ^{•+} scavenging activity	FRAP	
Fresh	Coriander	0.092 ± 0.003 ^f	0.097 ± 0.005 ^f	0.067 ± 0.005 ^d
	Tarragon	0.037 ± 0.002 ^g	0.051 ± 0.005 ^g	0.042 ± 0.010 ^e
	Lovage	0.159 ± 0.001 ^d	0.204 ± 0.004 ^d	0.109 ± 0.003 ^c
	Indian borage	0.288 ± 0.006 ^b	0.435 ± 0.009 ^b	0.205 ± 0.007 ^b
Dried	Coriander	0.129 ± 0.005 ^e	0.137 ± 0.004 ^e	0.059 ± 0.006 ^d
	Tarragon	0.156 ± 0.003 ^d	0.151 ± 0.003 ^e	0.092 ± 0.005 ^c
	Lovage	0.191 ± 0.004 ^c	0.227 ± 0.004 ^c	0.103 ± 0.004 ^c
	Indian borage	0.491 ± 0.009 ^a	0.643 ± 0.006 ^a	0.396 ± 0.014 ^a

TE, Trolox equivalents; FRAP, ferric-reducing antioxidant power. Means with different letters in the column are statistically different according to Tukey's test at $p < 0.05$.

TABLE 5. Coefficients of Pearson correlations between total phenolic content (TPC), antioxidant activity determined by DPPH, ABTS and FRAP assays, and sums of phenolic acids and flavonoids from HPLC analysis.

	TPC	DPPH	ABTS	FRAP	Phenolic acids	Flavonoids
DPPH	0.978*					
ABTS	0.976*	0.988*				
FRAP	0.983*	0.982*	0.979*			
Phenolic acids	0.962*	0.939*	0.949*	0.968*		
Flavonoids	-0.387	-0.375	-0.415	-0.454	-0.623	

*Significant correlation at $p < 0.05$. FRAP, ferric-reducing antioxidant power.

thyme, oregano, basil, and marjoram [Yashin *et al.*, 2017]. Studies on the antioxidant activity of Indian borage also showed that the extract from the stem was a more effective DPPH[•] scavenger than the leaf extract [Bhatt *et al.*, 2013; Kumaran & Karunakaran, 2006]. In our study, also lovage extracts showed significant antioxidant activity, which corresponds to the report by Spréa *et al.* [2020] who demonstrated better results regarding antioxidant properties of aqueous ethanolic extracts obtained from the edible aerial parts of *L. officinale* (leaves and stems) in comparison with decoction extracts. It may be related to a higher concentration of phenolic compounds in hydroethanolic extracts than in decoction extracts. In turn, phenolic acids, especially caffeic acid, were considered as principal components responsible for the antioxidant activity of the aqueous coriander extract [Melo *et al.*, 2005]. The antioxidant activity of caffeic acid is attributed to its chemical structure, including *inter alia* the presence of hydroxyl groups *ortho*-substituted in a benzene ring, and the existence of an unsaturated aliphatic chain, which increases the stability of the phenoxy radical by resonance [Chen & Ho, 1997]. The total antioxidant capacity of herbal material may depend not only on the content of the phenolic compounds and their activity, but also on the presence of other antioxidants, such as vitamin C, and possible synergistic or antagonistic interaction between phenolic antioxidants [Shahidi & Ambigaipalan, 2015; Yashin *et al.*, 2017]. Drying methods are also among the factors that may affect the changes in the content of biologically active compounds in plants, thus influencing their antioxidant potential [Calín-Sánchez *et al.*, 2020].

The coefficients of Person correlation between antioxidant activity and the phenolic contents in the tested herbal extracts are shown in Table 5. A strong correlation was found between DPPH[•] scavenging activity ($r=0.978$), ABTS^{•+} scavenging activity ($r=0.976$), FRAP ($r=0.983$), and TPC. A positive correlation was also found between results of all antioxidant activity assays and the content of phenolic acids. On the other hand, negative correlations were determined between the antioxidant activities of extracts and their flavonoid contents. In turn, the results of all antioxidant activity assays correlated significantly with each other ($r=0.976-0.983$).

An excellent correlation between the total phenolics content and the % inhibition of DPPH[•] was previously shown for the coriander leaf-supplemented bread samples [Das *et al.*, 2012]. Positive correlations between TPC of the seed and leaf coriander extracts obtained using different solvents and antiradical activity against DPPH[•] were also reported by Wangenstein *et al.* [2004]. A high linear correlation was also achieved between the results of the ABTS and DPPH assays for the ethanolic extracts from 23 different dried herbs and spices commercialized in Brazil [Mariutti *et al.*, 2008]. This indicates that the average reactivity of the compounds present in different extracts towards both radicals could be considered similar. A strong correlation was observed by Kozłowska *et al.* [2016] between TPC and radical scavenging activity of seed oil samples from anise, coriander, caraway, white mustard, and nutmeg, and the methanolic extracts derived from these oils.

CONCLUSIONS

The presented research demonstrated the high total phenolic contents and potent antioxidant activity, measured as DPPH[•] and ABTS^{•+} scavenging activity and FRAP of aqueous ethanolic extracts of coriander, lovage, and tarragon aerial parts, and Indian borage leaves. Generally, the higher total content of phenolic compounds and better antioxidant activity were found for the extracts prepared from air-dried herbal materials compared to those from fresh plants. Phenolic acid content in the herbal extracts significantly correlated with antioxidant activity. Caffeic acid was present in all extracts but its content was higher in the extracts from fresh than dried material for most plants. In turn, rosmarinic acid was the predominant phenolic acid in dried material in comparison to fresh counterparts. In brief, the drying of leaves and the aerial parts of herbal material did not cause any loss of phenolic compounds and did not reduce the antioxidant activity of their extracts. Therefore, extracts of both fresh and air-dried herbs can serve as potential components of functional food formulations.

RESEARCH FUNDING

This research did not receive any specific grant from funding agencies in the public, commercial, or not-for-profit sectors.

CONFLICT OF INTEREST

The authors declare no conflict of interest.

ORCID IDs

M. Kozłowska <https://orcid.org/0000-0002-9252-3268>
 E. Majewska <https://orcid.org/0000-0002-5910-1119>
 J.L. Przybył <https://orcid.org/0000-0003-0959-184X>
 I. Ścibisz <https://orcid.org/0000-0003-1291-8962>
 M. Ziarno <https://orcid.org/0000-0001-7445-6375>
 A. Żbikowska <https://orcid.org/0000-0001-7013-4520>

REFERENCES

- Al-Juhaimi, F., Ghafoor, K. (2011). Total phenols and antioxidant activities of leaf and stem extracts from coriander, mint and parsley grown in Saudi Arabia. *Pakistan Journal of Botany*, 43(4), 2235–2237.
- Benzie, I.F.F., Strain, J.J. (1996). The ferric reducing ability of plasma (FRAP) as a measure of “Antioxidant Power”. The FRAP assay. *Analytical Biochemistry*, 239(1), 70–76. <https://doi.org/10.1006/abio.1996.0292>
- Bhatt, P., Joseph, G.S., Negi, P.S., Varadaraj, M.C. (2013). Chemical composition and nutraceutical potential of Indian borage (*Plectranthus amboinicus*) stem extract. *Journal of Chemistry*, 2013, art. no. 320329. <https://doi.org/10.1155/2013/320329>
- Bourdoux, S., Rajkovic, A., De Sutter, S., Vermeulen, A., Spilimbergo, S., Zambon, A., Hofland, G., Uyttendaele, M., Devlieghere, F. (2018). Inactivation of *Salmonella*, *Listeria monocytogenes* and *Escherichia coli* O157:H7 inoculated on coriander by freeze-drying and supercritical CO₂ drying. *Innovative Food Science and Emerging Technologies*, 47, 180–186. <https://doi.org/10.1016/j.ifset.2018.02.007>
- Calín-Sánchez, Á., Lipan, L., Cano-Lamadrid, M., Kharaghani, A., Masztalerz, K., Carbonell-Barrachina, Á.A., Figiel, A. (2020). Comparison of traditional and novel drying techniques and its effect on quality of fruits, vegetables and aromatic herbs. *Foods*, 9(9) art. no. 1261. <https://doi.org/10.3390/foods9091261>
- Chen, J.H., Ho, Ch-T. (1997). Antioxidant activities of caffeic acid and its related hydroxycinnamic acid compounds. *Journal of Agricultural and Food Chemistry*, 45(7), 2374–2378. <https://doi.org/10.1021/jf970055t>
- ChromaDex, Standards, Tech Tips 0003: Reference Standard Recovery and Dilution. (2016). [https://standards.chromadex.com/Documents/Tech%20Tips/techtip0003-recoverydilutionprocedures_nl_pw.pdf] (accessed: 1 February 2016).
- Das, L., Raychaudhuri, U., Chakraborty, R. (2012). Supplementation of common white bread by coriander leaf powder. *Food Science and Biotechnology*, 21(2), 425–433. <https://doi.org/10.1007/s10068-012-0054-9>
- Gow-Chin, Y., Hui-Yin, C. (1995). Antioxidant activity of various tea extracts in relation to their antimutagenicity. *Journal of Agricultural and Food Chemistry*, 43(1) 27–32. <https://doi.org/10.1021/jf00049a007>
- Harsha, S.N., Anilakumar, K.R. (2014). *In vitro* free radical scavenging and DNA damage protective property of *Coriandrum sativum* L. leaves extract. *Journal of Food Science and Technology*, 51(8), 1533–1539. <https://doi.org/10.1007/s13197-012-0648-5>
- Hossain, M.B., Barry-Ryan, C., Martin-Diana, A.B., Brunton, N.P. (2010). Effect of drying method on the antioxidant capacity of six Lamiaceae herbs. *Food Chemistry*, 123, 85–91. <https://doi.org/10.1016/j.foodchem.2010.04.003>
- International Conference on Harmonization ICHQ2 (R1) Guidelines. (2005). [https://database.ich.org/sites/default/files/Q2_R1_Guideline.pdf] (accessed: 1 February 2016).
- Isah, T. (2019). Stress and defense responses in plant secondary metabolites production. *Biological Research*, 52, art. no. 39. <https://doi.org/10.1186/s40659-019-0246-3>
- Justesen, U., Knuthsen, P. (2001). Composition of flavonoids in fresh herbs and calculation of flavonoid intake by use of herbs in traditional Danish dishes. *Food Chemistry*, 73(2), 245–250. [https://doi.org/10.1016/S0308-8146\(01\)00114-5](https://doi.org/10.1016/S0308-8146(01)00114-5)
- Kaiser, A., Kammerer, D.R., Carle, R. (2013). Impact of blanching on polyphenol stability and antioxidant capacity of innovative coriander (*Coriandrum sativum* L.) pastes. *Food Chemistry*, 140(1–2), 332–339. <https://doi.org/10.1016/j.foodchem.2013.02.077>
- Karamać, M., Gai, F., Peiretti, P.G. (2020). Effect of the growth stage of false flax (*Camelina sativa* L.) on the phenolic compound content and antioxidant potential of the aerial part of the plant. *Polish Journal of Food and Nutrition Sciences*, 70(2), 189–198. <https://doi.org/10.31883/pjfn/119719>
- Kozłowska, M., Zbikowska, M., Marciniak-Lukasiak, K., Kowalska, M. (2019). Herbal extracts incorporated into shortbread cookies: impact on color and fat quality of the cookies. *Biomolecules*, 9(12), art. no. 858. <https://doi.org/10.3390/biom9120858>
- Kozłowska, M., Żbikowska, A., Gruczyńska, E., Żontala, K., Półtorak, A. (2014). Effects of spice extracts on lipid fraction oxidative stability of cookies investigated by DSC. *Journal of Thermal Analysis and Calorimetry*, 118, 1697–1705. <https://doi.org/10.1007/s10973-014-4058-y>
- Kozłowska, M., Laudy, A.E., Przybył, J., Ziarno, M., Majewska, E. (2015). Chemical composition and antibacterial activity of some medicinal plants from Lamiaceae family. *Acta Poloniae Pharmaceutica – Drug Research*, 72(4), 757–767.
- Kozłowska, M., Gruczyńska, E., Ścibisz, I., Rudzińska, M. (2016). Fatty acids and sterols composition, and antioxidant activity of oils extracted from plant seeds. *Food Chemistry*, 213, 450–456. <https://doi.org/10.1016/j.foodchem.2016.06.102>
- Kumaran, A., Karunakaran, R.J. (2006). Antioxidant and free radical scavenging activity of an aqueous extract of *Coleus aromaticus*. *Food Chemistry*, 97(1), 109–114. <https://doi.org/10.1016/j.foodchem.2005.03.032>
- Mariutti, L.R.B., Barreto, G.P.M., Bragagnolo, N., Mercadante, A.Z. (2008). Free radical scavenging activity of ethanolic extracts from herbs and spices commercialized in Brazil. *Brazilian Archives of Biology and Technology*, 51(6), 1225–1232. <https://doi.org/10.1590/S1516-89132008000600018>
- Melo, E.A., Filho, J.M., Guerra, N.B. (2005). Characterization of antioxidant compounds in aqueous coriander extract (*Coriandrum sativum* L.). *LWT – Food Science and Technology*, 38(1), 15–19. <https://doi.org/10.1016/j.lwt.2004.03.011>
- Pabón-Baquero, L.C., Otálvaro-Álvarez, Á.M., Fernández, M.R.R., Chaparro-González, M.P. (2018). Plant extracts as antioxidant additives for food industry. In E. Shalaby (Editor). *Antioxidants in Foods and Its Applications*. IntechOpen, London, UK, pp. 87–115. <https://doi.org/10.5772/intechopen.75444>
- Papuc, C., Goran, G.V., Predescu, C.N., Nicorescu, V., Stefan, G. (2017). Plant polyphenols as antioxidant and antibacterial agents for shelf-life extension of meat and meat products: classification, structures, sources, and action mechanisms. *Comprehensive Reviews in Food Science and Food Safety*, 16(6), 1243–1268. <https://doi.org/10.1111/1541-4337.12298>

26. Pirvu, L., Hlevca, C., Nicu, I., Bubueanu, C. (2014). Comparative studies on analytical, antioxidant, and antimicrobial activities of a series of vegetal extracts prepared from eight plant species growing in Romania. *Journal of Planar Chromatography*, 27(5), 346–356.
<https://doi.org/10.1556/JPC.27.2014.5.4>
27. Rajeshwari, C.U., Andullu, B. (2011). Isolation and simultaneous detection of flavonoids in the methanolic and ethanolic extracts of *Coriandrum sativum* L. seeds by RP-HPLC. *Pakistan Journal of Food Science*, 21(1–4), 13–21.
28. Re, R., Pellegrini, N., Proteggente, A., Pannala, A., Yang, M., Rice-Evans, C. (1999). Antioxidant activity applying an improved ABTS radical cation decolorization assay. *Free Radical Biology and Medicine*, 26(9–10), 1231–1237.
[https://doi.org/10.1016/S0891-5849\(98\)00315-3](https://doi.org/10.1016/S0891-5849(98)00315-3)
29. Riaz, A., Rasul, A., Hussain, G., Zahoor, M.K., Jabeen, F., Subhani, Z., Younis, T., Ali, M., Sarfraz, I., Selamoglu, Z. (2018). Astragalins: a bioactive phytochemical with potential therapeutic activities. *Advances in Pharmacological Sciences*, 2018, art. no. 9794625.
<https://doi.org/10.1155/2018/9794625>
30. Roshanak, S., Rahimmalek, M., Goli, S.A.H. (2016). Evaluation of seven different drying treatments in respect to total flavonoid, phenolic, vitamin C content, chlorophyll, antioxidant activity and color of green tea (*Camellia sinensis* or *C. assamica*) leaves. *Journal of Food Science and Technology*, 53(1), 721–729.
<https://doi.org/10.1007/s13197-015-2030-x>
31. Sepahpour, S., Selamat, J., Manap, M.Y.A., Khatib, A., Razis, A.F.A. (2018). Comparative analysis of chemical composition, antioxidant activity and quantitative characterization of some phenolic compounds in selected herbs and spices in different solvent extraction systems. *Molecules*, 23(2), art. no. 402.
<https://doi.org/10.3390/molecules23020402>
32. Shahidi, F., Ambigaipalan, P. (2015). Phenolics and polyphenolics in foods, beverages and spices: Antioxidant activity and health effects – A review. *Journal of Functional Foods*, 18(Part B), 820–897.
<https://doi.org/10.1016/j.jff.2015.06.018>
33. Singleton, V.L., Rossi, J.A. (1965). Colorimetry of total phenolics with phosphomolybdic–phosphotungstic acid reagents. *American Journal of Enology and Viticulture*, 16, 144–158.
34. Slimestad, R., Fossen, T., Brede, C. (2020). Flavonoids and other phenolics in herbs commonly used in Norwegian commercial kitchens. *Food Chemistry*, 309, art. no. 125678.
<https://doi.org/10.1016/j.foodchem.2019.125678>
35. Słowianek, M., Leszczyńska, J. (2016). Antioxidant properties of selected culinary spices. *Herba Polonica*, 62(1), 29–41.
<https://doi.org/10.1515/hepo-2016-0003>
36. Spréa, R.M., Fernandes, Â., Calhelha, R.C., Pereira, C., Pires, T.C.S.P., Alves, M.J., Canan, C., Barros, L., Amaral, J.S., Ferreira, I.C.F.R. (2020). Chemical and bioactive characterization of the aromatic plant *Levisticum officinale* W.D.J. Koch: a comprehensive study. *Food & Function*, 11(2), 1292–1303.
<https://doi.org/10.1039/C9FO02841B>
37. Swamy, M.K., Arumugam, G., Kaur, R., Ghasemzadeh, A., Yusoff, M.M., Sinniah, U.R. (2017). GC-MS based metabolite profiling, antioxidant and antimicrobial properties of different solvent extracts of Malaysian *Plectranthus amboinicus* leaves. *Evidence-Based Complementary and Alternative Medicine*, 2017, art. no. 10.
<https://doi.org/10.1155/2017/1517683>
38. Tajner-Czopek, A., Gertchen, M., Rytel, E., Kita, A., Kucharska, A.Z., Sokół-Łętowska, A. (2020). Study of antioxidant activity of some medicinal plants having high content of caffeic acid derivatives. *Antioxidants*, 9(5) art. no. 412.
<https://doi.org/10.3390/antiox9050412>
39. Tapsell, L.C., Hemphill, I., Cobiac, L., Patch, C.S., Sullivan, D.R., Fenech, M., Roodenrys, S., Keogh, J.B., Clifton, P.M., Williams, P.G., Fazio, V.A., Inge, K.E. (2006). Health benefits of herbs and spices: the past, the present, the future. *The Medical Journal of Australia*, 185(S4), S1–S24.
<https://doi.org/10.5694/j.1326-5377.2006.tb00548.x>
40. Tomson, L., Kruma, Z. (2014). Influence of freezing and drying on the phenol content and antioxidant activity of horseradish and lovage. Conference Proceedings – Baltic Conference on Food Science and Technology “FOODBALT 2014”, eISSN 2255–9817, pp. 192–197.
41. Tvrdá, E., Varga, A., Slávik, M., Árvay, J. (2019). *Levisticum officinale* and its effects on bovine spermatozoa activity. *Journal of Microbiology, Biotechnology and Food Sciences*, 8(5), 1212–1216.
<https://doi.org/10.15414/jmbfs.2019.8.5.1212-1216>
42. Ulewicz-Magulska, B., Wesolowski, M. (2019). Total phenolic contents and antioxidant potential of herbs used for medical and culinary purposes. *Plant Foods for Human Nutrition*, 74, 61–67.
<https://doi.org/10.1007/s11130-018-0699-5>
43. Wangensteen, H., Samuelsen, A.B., Malterud, K.E. (2004). Antioxidant activity in extracts from coriander. *Food Chemistry*, 88(2), 293–297. <https://doi.org/10.1016/j.foodchem.2004.01.047>
44. Yashin, A., Yashin, Y., Xia, X., Nemzer, B. (2017). Antioxidant activity of spices and their impact on human health: a review. *Antioxidants*, 6(3), art. no. 70.
<https://doi.org/10.3390/antiox6030070>
45. Zawisłak, G., Nurzyńska-Wierdak, R. (2014). Evaluation of the yield and biological value of tarragon (*Artemisia dracunculoides* L.) in the bunch harvest cultivation. *Acta Scientiarum Polonorum, Hortorum Cultus*, 13(4), 185–198.
46. Złotek, U., Szymanowska, U., Pecio, Ł., Kozachok, S., Jakubczyk, A. (2019). Antioxidative and potentially anti-inflammatory activity of phenolics from lovage leaves *Levisticum officinale* Koch elicited with jasmonic acid and yeast extract. *Molecules*, 24(7), art. no. 1441.
<https://doi.org/10.3390/molecules24071441>
47. Zujko, M.E., Witkowska, A.M., Waśkiewicz, A., Sygnowska, E. (2012). Estimation of dietary intake and patterns of polyphenol consumption in Polish adult population. *Advances in Medical Sciences*, 57(2), 375–384.
<https://doi.org/10.2478/v10039-012-0026-6>

Influence of a Sulphur Dioxide Active Storage System on the Quality of *Ribes rubrum* L. Berries

Luca Brondino , Davide Cadario , Nicole Roberta Giuggioli* 

Department of Agricultural Forest and Food Sciences (DISAFA), University of Turin,
Largo Paolo Braccini 2 – Grugliasco 10095 Torino, Italy

Key words: red currant, storage, modified atmosphere packaging, SO₂, taste

The aim of this study was to evaluate the post-harvest changes in the quality of red currants (*Ribes rubrum* L.) cv. 'Rovada' after 60 days of storage under modified atmosphere packaging (MAP) conditions. The storage unit was a pallet, and two treatments were performed. The CO₂-MAP treatment was used as a control, while the SO₂-MAP treatment was CO₂-MAP plus SO₂. The initial gas composition was 15.0 kPa O₂ and 10.0 kPa CO₂ inside all MAPs, while SO₂-generating active sheets were added to pellets in SO₂-MAP treatment. Weight loss, total soluble solid content, titratable acidity, total phenolic and anthocyanin contents, antioxidant activity, microbial count, and visual and sensorial appearance were monitored after 30 and 60 days. The results showed that berries stored with SO₂ maintained the quality parameters for up to 60 days. Exposure to SO₂ was effective in controlling yeast evolution, reducing the population both at 30 and 60 days at one and two orders of magnitude, respectively. Red currants stored under SO₂ MAP obtained better visual quality score compared to CO₂ MAP-treated berries throughout storage.

Active emitters of SO₂, such as those proposed in this study, can be promising solutions to improve the post-harvest storage of red currants and the berries marketability.

INTRODUCTION

Red currants, belonging to the *Ribes* genus of the Saxifragaceae family, are minor crops among berries. They are berry-bearing deciduous shrubs mainly consumed as processed in juices, jams, jellies, syrups, marinades, and wines [Kampuss & Pedersen, 2003; Stępniewska *et al.*, 2016]. Consumption of fresh red currants is largely related to visual appearance, and raceme and stalk freshness are the main quality indices of shelf life. 'Jonkheer van Tets', 'Rondom', 'Rovada', 'Rosetta', 'Rotet', 'Jonifer', 'Laxton no. 1', 'Red Lake', 'Stanza', and 'Laxton's Perfection Red Dutch' are the most common red currant cultivars grown in Europe, where Poland is the most important producer [www.freshplaza.com]. Similar to other berries, red currants (*Ribes rubrum* L.) are important species for the human diet, especially due to the highest capacity to scavenge free radicals [Laczkó-Zöld *et al.*, 2018; Orsavová *et al.*, 2019]. Vitamin C (ascorbic acid) is well known to be the most important free radical scavenger, with average content in fresh berries reported at 41 mg/100 g [Talcott, 2007]. Red currants are also an important source of macro- and microelements (349.90 mg P; 1,876.94 mg K; 8.25 mg Na; 281.08 mg Ca; 1.18 mg Mn; 94.43 mg Mg; 3.73 mg Fe; and 2.41 mg Zn per 100 g of dry weight) [Plessi *et al.*, 1998].

Due to limited fresh market volumes compared to other soft berries, no larger studies on post-harvest techniques have been carried out on *R. rubrum*. Storage temperatures in the range of 0–1°C combined with high values of relative humidity (95%) have been suggested as optimum conditions in a normal atmosphere (NA) to maintain fresh berries for up to 3 weeks, but the evolution of biochemical properties is mainly associated with ripeness at harvest time and the cultivar. Management of the surrounding storage atmosphere (18 to 20% CO₂ + 2% O₂) can extend the storage time [Agar *et al.*, 1997; Roelofs & Waart, 1993], but in some cultivars, high CO₂ concentrations can result in physiological disorders, affecting berry colour and the internal breakdown [Roelofs & Waart, 1993; Thompson, 1998]. Furthermore, some physiological disorders generally manifested by flesh browning and breakdown appear in berries stored with CO₂ above 20%. The modified atmosphere pallet system has been evaluated in the post-harvest storage of berries and other fruits as an alternative preserving technique [Giuggioli *et al.*, 2019; Macnish *et al.*, 2012; Peano *et al.*, 2017] and is commercially available as a logistic solution to reduce fruit loss and optimise space in the warehouses of different fruit companies. The employment of active gas controlled-release pads or ethylene absorbers (C₂H₄) can be positively associated with this technology to improve the success of storage management for different products. Red currants are not ethylene

* Corresponding Author:

Tel.: +39 011 670 8646; Fax: +39 011 670 8658;

E-mail: nicole.giuggioli@unito.it (N.R. Giuggioli)

Submitted: 24 February 2021

Accepted: 6 July 2021

Published on-line: 22 July 2021



producers and are not susceptible to C_2H_4 , but sulphur dioxide (SO_2) release pads could be positively associated with a modified atmosphere strategy to control the decrement of the overall quality and limit the microbial growth in berries [Ahmed *et al.*, 2018; Saito *et al.*, 2020]. Similarly to other berries, red currants are not washed during the supply chain process (harvesting, packing, and transportation); therefore, approved sanitisers, such as chlorine or sodium hypochlorite, cannot be added to control possible microbial contamination. The SO_2 -generating pads have largely been used in the post-harvest process of different fruits, such as table grapes [Ahmed *et al.*, 2018; Carter *et al.*, 2015; Ozkaya *et al.*, 2008; Sortino *et al.*, 2017; Zutahy *et al.*, 2008], blueberries [Rodriguez & Zoffoli, 2016; Saito *et al.*, 2020], fragola [Hakimi *et al.*, 2017], figs [Cantín *et al.*, 2011], raspberries [Spayd *et al.*, 1984], and lemons [Smilanic *et al.*, 1995]. The amount of SO_2 required to be effective is a function of the storage temperature and the time of release of SO_2 of the emmitter used [Rivera *et al.*, 2013]. A critical point that needs to be considered in SO_2 treatment is the maximum absorption by the human body; the daily intake value permitted by the Joint FAO/WHO Expert Committee on Food Additives [JECFA, 2019] is 0–0.7 mg per kg of human body weight.

To improve the knowledge about post-harvest storage of red currants, which has so far been underreported

in literature, the aim of this study was to evaluate the influence of an SO_2 active storage system on the quality of *R. rubrum* berries stored for up to 60 days.

MATERIALS AND METHODS

Fruit source and sample preparation

Red currants (*R. rubrum* cv. Rovada) were harvested in an orchard located at Peveragno (Cuneo, Piedmont, Italy) at the harvesting maturity stage and were free of decay or mechanical or insect injury. The currants were transported directly within 30 min to the Agrifrutta Cooperative warehouse (Peveragno, Cuneo, Piedmont, Italy) for sample preparation and storage. Selected fruits were packed in rigid ventilated polyethylene terephthalate (PET) open baskets containing 0.150 kg of fruit each. Ten PET baskets were placed in a cardboard flat. Eight flats were assembled in a single layer on a 100×120 cm wood pallet base. A total of 20 layers of eight flats each were stacked onto a pallet commercial storage unit (Figure 1).

Pallet treatments and storage conditions

The red currants were sampled in two groups. The first group was palletised in an active modified atmosphere (CO_2 -MAP treatment) and used as a control. The second group was palletised

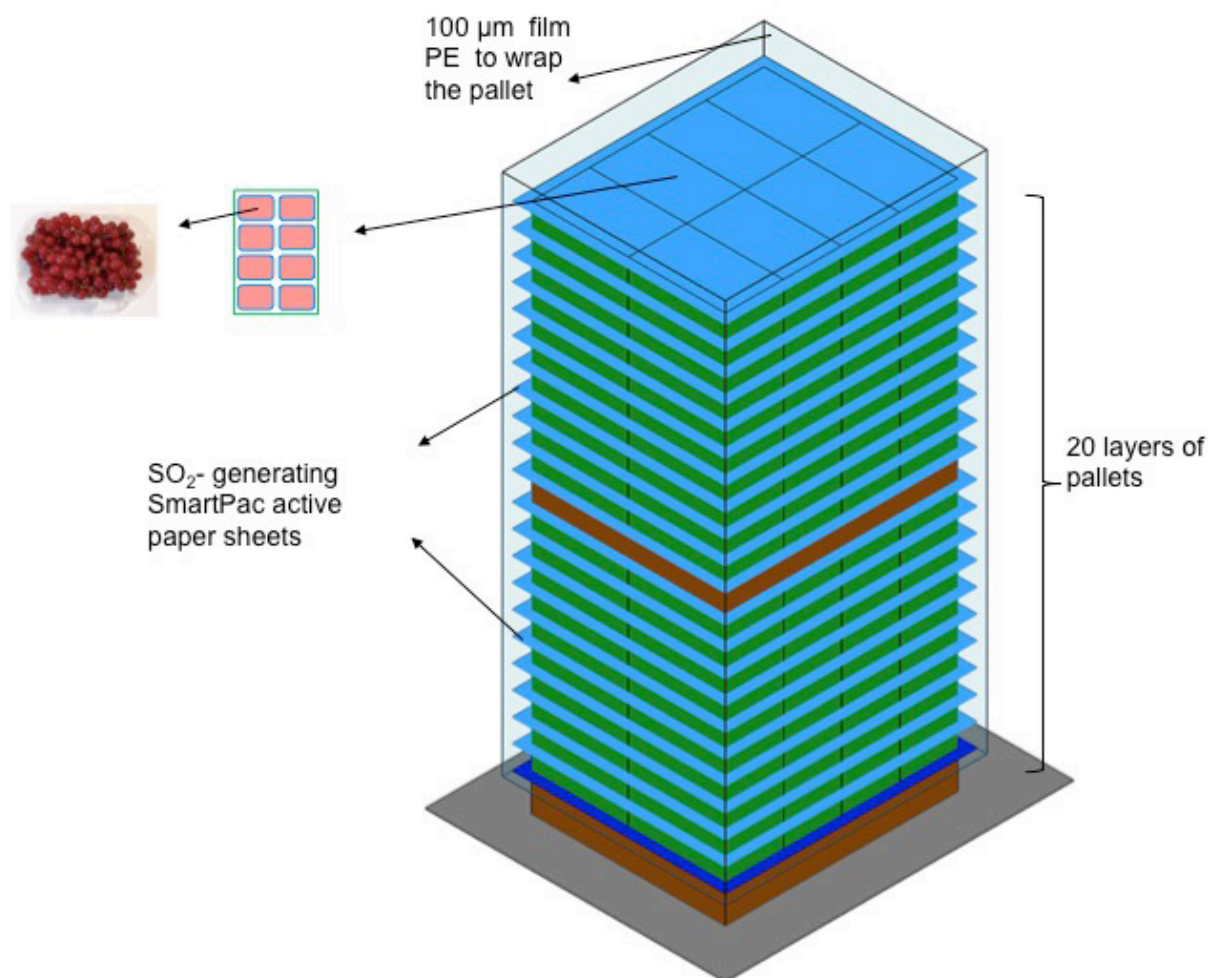


FIGURE 1. Design of the pallet unit used for storage of red currants in SO_2 modified conditions.

with CO₂ + SO₂ (SO₂-MAP treatment). Each pallet was wrapped with a 100 µm thick polyethylene film (PE) (thermally sealed at the base) with values of O₂ (O₂TR) and CO₂ (CO₂TR) transmission rates of 1572 cm³/m²/d/bar and 6111 cm³/m²/d/bar, respectively, measured at 23°C and at 50% relative humidity (RH) with a MultiPerm oxygen and carbon dioxide analyser (Extra Solution s.r.l., Pisa, Italy) according to ASTM F 2622–08 and ASTM F 2476–05 standard guidelines [Briano *et al.*, 2015].

The injection system for CO₂-MAP treatment was operated as reported by Peano *et al.* [2017] to have initial gas values of 15.0 kPa O₂ and 10.0 kPa CO₂. These values were based on previous experimental storage studies on red currants (data not published). The SO₂-generating SmartPac active paper sheets (Serroplast, Bari, Italy) were applied directly to cover each of the total 20 layers stacked onto the storage unit pallet. All samples were stored for 60 days in a cold and dark room at 1 ± 1°C and 90–95% RH. Data were collected at 0 (at the beginning of storage treatment), 30 (middle of the total storage time), and 60 days (long-term storage). For each treatment and storage time, three pallets were considered, sampling 30 random baskets in total. Figure 1 shows the experimental design of the pallet commercial unit.

Pallet atmosphere and SO₂ evaluation

A gas analyser (CheckPoint II, PBI Dansensor, Milan, Italy) was used to measure the relative changes in the carbon dioxide and oxygen concentrations. The gas composition values were measured every 10 days over the trial period and were expressed in kPa. The SO₂ concentration was measured in ppm with dosimeter tubes (Gastec 5DH, Gastec Corporation, Ayase-City, Japan). The results were expressed as an average of three replicates.

Weight loss and quality parameters

Baskets were coded before the treatments. Weight loss (%) was determined using an electronic balance (model SE622, VWR Science Education, Radnor, PA, USA), with a 10⁻² g accuracy. Weight was monitored during the entire storage period and was calculated as the difference between initial (W₀) and final (W_f) basket weights.

$$\text{Weight loss (\%)} = \frac{W_0 - W_f}{W_n} \times 100 \quad (1)$$

The results were expressed as an average of 30 replicates.

After sample blending, the total soluble solids (TSS) were evaluated with a digital refractometer Atago® Pal-1 (Atago Co. Ltd., Tokyo, Japan) and expressed as °Brix. For each quality control, the instrument was calibrated with distilled water. The titratable acidity (TA) was measured using an automatic titrator (Titrino 702, Methrom, Herisav, Switzerland), and determined potentiometrically using 0.1 N NaOH to the end point of 7.0; it was expressed as g of malic acid equivalents per 100 g of berries [Djordjević *et al.*, 2010].

Total anthocyanin content, total phenolic content, and antioxidant capacity

Twenty-five mL of an extraction solvent (500 mL methanol, 23.8 mL deionised water, and 1.4 mL 37% hydrochloric acid)

were added to 10 g of fruit. After 1 h storage in the dark at room temperature, the samples were thoroughly homogenised for 1 min with an Ultra-Turrax homogeniser (IKA, Staufen, Germany) and then centrifuged at 3,000 × g for 15 min. The supernatant obtained by centrifugation was collected, transferred into glass test tubes, and stored at -20°C until analysis. The total phenolic content (TPC) was determined by visible spectrophotometry using the Folin–Ciocalteu reagent according to the method described by Slinkard & Singleton [1977]. Gallic acid was used as a standard and absorbance of reaction mixtures was measured at 765 nm. The results were expressed as mg of gallic acid equivalents per 100 g of fruit fresh weight (mg GAE/100 g fw). The total anthocyanin content (TAC) was quantified according to the pH differential method described by Cheng & Breen [1991]. Anthocyanins were estimated by their absorbance (A) difference at 510 and 700 nm in buffers at pH 1.0 and pH 4.5, where A_{tot} = (A₅₁₅ - A₇₀₀) pH 1.0 - (A₅₁₅ - A₇₀₀) pH 4.5. The results were expressed as mg of cyanidin 3-O-glucoside (C3G) equivalents per 100 g of fruit fw. Antioxidant activity was determined as the ferric reducing antioxidant power (FRAP) following the methods of Pellegrini *et al.* [2003], with some modifications. The absorbance was read at 595 nm 4 min after the addition of appropriately diluted extracts or standard to the FRAP reagent. The results were expressed as mmol Fe²⁺ per 1 kg of fw of red currants. These analyses were performed with a UV-Vis spectrophotometer 1600 (PC VWR International, Milan, Italy).

Microbial count determination

Microbial evaluation was performed considering the count of total yeast, mould, and bacteria. Total yeasts and mould were examined according to the methods reported by the Compendium of Methods for the Microbiological Examination of Foods [Vanderzant & Splittstoesser, 1992]. The same equipment used in a previous work on strawberry was applied [Chiabrando *et al.*, 2018]. All plates were incubated at 30°C for 5 days. Three replicates were analysed, and the microbial counts were expressed as colony-forming units (CFU) per g of berry sample. Total aerobic bacteria (TAB) counts were determined according to ISO 4833–2 [2013]. Three replicates were analysed, and the microbial counts were expressed as colony-forming units (CFU) per g of berry sample.

Sensorial evaluation

Evaluation of the red currant fruits was also determined by means of sensory analysis, involving 10 panellists (five men and five women, 25–60 years old) who were previously trained using commercial berry samples. They received 15 bunches from each sample and provided sample descriptions based on consistency and taste (including sweet, acid, herbaceous, and astringent taste), and total aroma. All attributes were evaluated using a 9-point scale (ranging from ‘very intense’ as ‘9’ to ‘none’ as ‘1’). The taste test was performed 1 h after red currants were taken out of the stored pallet at room temperature (20 ± 1°C).

Visual evaluation

Visual evaluation was performed considering raceme and pedicel desiccation, healthy bunches, and visual quality.

The same panellists as for sensory analysis were recruited. Healthy bunches were defined as the percentage of not damaged fruit. All attributes of freshness of the rachis and pedicels and the visual quality were scored using a 5-point scale. Desiccation scores were 1 = as green as at harvest; 2 = slight browning; 3 = browning but no shrivelling; 4 = browning and some shrivelling; and 5 = dry and brown. Visual quality scores were 5 = excellent, no defects; 4 = very good, minor defects; 3 = fair, moderate defects; 2 = poor, major defects; and 1 = unusable. Scores above 3 were considered unmarketable [Sortino *et al.*, 2017].

Statistical analyses

All pooled data were analysed using SPSS Statistics 24 (2017, IBM, Milan, Italy) for MAC. Analysis of variance (ANOVA) was performed, followed by Tukey's post-hoc test ($p \leq 0.05$), when the differences were significant.

RESULTS AND DISCUSSION

Pallet atmosphere and SO₂ evaluation

MAP technology is well known to be applied as the most easy and convenient tool to extend shelf life and protect berries from external contaminants. The fruit respiration rate, storage temperature, and selectivity of the wrapping film to gas are key factors that contribute to maintaining the required gas composition. Changes in the storage atmosphere composition in the range of 18 to 20% CO₂ and 2% O₂ could be successful in extending the shelf life of *R. rubrum* up to 14 weeks [Thompson, 1998]. As reported in Figure 2, the initial gas composition in the different units of storage was 15.0 kPa O₂ and 10.0 kPa CO₂. A different trend was observed between the two MAP treatments. Considering O₂, a general decrease was observed for each pallet system, even if it was more evident for the berries stored with only CO₂. After 40 days of storage, the O₂ content was under 5.0 kPa, achieving values of 1.5 kPa at the end of storage. Berries stored with SO₂ instead maintained values of 5.6 kPa at the end of storage. The different concentrations of O₂ could be explained by the increase of microbial counts (moulds and bacteria) in red currants stored with the MAP-CO₂ treatments. As a consequence, different levels of CO₂ were recorded among treatments. Up to 30 days, a similar evolution was monitored, then an increase of up to 15.0 kPa (60 days) was achieved for the MAP-CO₂ treatment stored pallets. In blueberries, Smilanick & Henson [1992] reported concentration of SO₂ in 100 ppm at 0°C to control decay diseases. The success of SO₂ treatments is a function of the time of exposure to gas multiplied by the concentration. SO₂-generating SmartPac active sheets were active throughout the entire storage time; furthermore, the gas was recorded for up to 60 days (Figure 3). The highest concentration (20 ppm) was observed after 10 days of storage. Subsequent measurements recorded lower SO₂ concentrations, achieving 0.8 ppm at the end of storage, indicating effective adsorption from the surface of red currants.

Weight loss and quality parameters

The loss of marketable berries along the entire supply chain is registered at around 45% [Temocico *et al.*, 2014].

Weight loss is affected by water loss, which is the major cause of post-harvest deterioration and compromises the visual appearance, chemical content, and flavour of the product [Lufu *et al.*, 2020]. Berry turgidity and raceme and stalk freshness are the main visual quality criteria for the final consumer, and their status is a function of the hydration of fruit tissues. As reported in Figure 4, both MAP treatments were able to limit the weight loss of red currants up to 60 days, and no statistically significant ($p > 0.05$) differences were observed among the different treatments. Both CO₂ and SO₂ gas controlled weight loss to under 5%, which can be considered the limit value for soft berries' marketability [Giuggioli *et al.*, 2019]. Weight loss of the samples analysed in our study was in the range of 0.67–0.73% and 1.00–1.15% after 30 and 60 days of storage, respectively. The maintenance of high humidity around the stored berries thanks to MAP action limited the transpiration activity of red currants, and this is probably due to the proper water transmission rates of the PE film.

The total soluble solid (TSS) contents of fresh and stored red currants are shown in Table 1. The TSS content of fresh berries was in line with data reported by Djordjević *et al.* [2010]. Moreover, similarly to the results reported by Temocico *et al.* [2014], the change in atmospheric composition during storage did not affect the soluble solid content in all samples (Table 1). Storage for up to 60 days caused no significant ($p > 0.05$) decrease in the TSS content, moving from 10.9 °Brix to 10.1 °Brix and 9.7 °Brix for CO₂ and SO₂ MAP treatments, respectively. No significant differences were observed

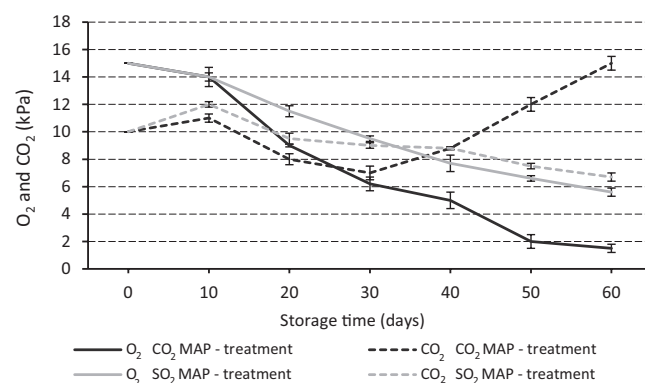


FIGURE 2. Gas evolution (O₂ and CO₂) during red currants 60 days storage.

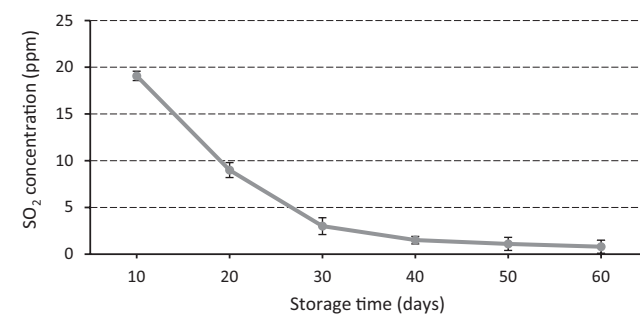


FIGURE 3. SO₂ concentration during red currants 60 days storage under modified atmosphere packaging (MAP) conditions.

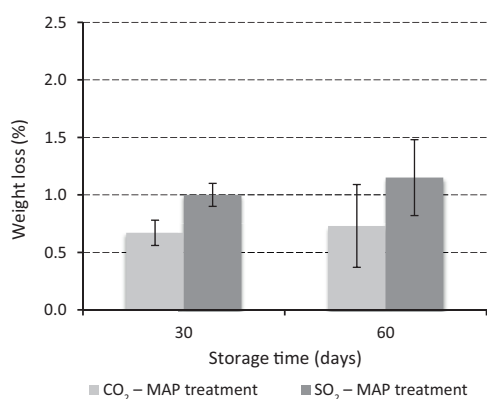


FIGURE 4. Weight loss of red currants during storage under modified atmosphere packaging (MAP) conditions.

among red currant samples exposed to SO₂ and CO₂ at the time, while differences ($p \leq 0.05$) were determined among MAP treatments only after 30 days of storage. Generally, SO₂ and CO₂ treatments, as observed on other fruits, did not affect the total soluble solid content during storage [Cantín *et al.*, 2011, 2012]. The titratable acidity (TA) of red currants ranged from 1.2 to 1.0 g/100 g fw at 60 days of storage, but TA changes during storage and differences between MAP treatments were not significant ($p \leq 0.05$) (Table 1). Generally, losses of total acidity were reported to be accelerated by storage in elevated CO₂ atmospheres [Harb & Streif 2004]; in this case, the concentration of CO₂ achieved in the stored pallet was appropriate for the maintenance of titratable acidity levels to values similar to those at harvest.

Total anthocyanin content, total phenolic content, and antioxidant capacity

The contents of phenolic compounds of fresh and stored red currants are reported in Table 2. The total anthocyanin content (TAC) of fresh fruits of cultivar Rovada was 22.1 mg C3G/100 g fw. This value was in the range of 18–34 mg/100 g fw as suggested by Benvenuti *et al.* [2004] for red currants grown in Italy and was lower than that recorded for cultivars grown in Finland (26.5–104 mg/100 g fw) [Mattila *et al.*, 2016]. Among anthocyanins, red currants are rich in cyanidin glycosides including cyanidin 3-*O*-glucoside, cyanidin 3-*O*-sambusoside, cyanidin 3-*O*-rutinose, cyanidin 3-sophoroside, cyanidin 3-glucosylrutinoside, and cyanidin-3-xylosylrutinoside [Jara-Palacios *et al.*, 2019; Mattila *et al.*, 2016]. No statistically significant ($p > 0.05$) differences were observed over time for each MAP treatment, and between treatments (Table 2). The total phenolic content (TPC) of red currant before storage was 233 mg GAE/100 g fw, which is consistent with values reported in the literature [Laczkó-Zöld *et al.*, 2018]. Similarly to anthocyanins, TPC showed the same evolution among samples over time, and statistically insignificantly lower content was determined in red currants under SO₂ MAP storage. Storage atmospheres enriched in CO₂ could prevent the increase in total antioxidant activity; however, the mechanism of control is still not clear, as no available data have been reported on the effect of SO₂ on evolution of total antioxidant activity in red currants. The initial antioxidant capacity of fresh

TABLE 1. Total soluble solids (TSS) content and titratable acidity (TA) of red currants stored under modified atmosphere packaging (MAP) conditions.

Parameter	Treatment	Storage time (days)		
		0	30	60
TSS (°Brix)	CO ₂ -MAP	10.9 ± 0.5 ^{aA*}	9.5 ± 0.1 ^{aB}	10.1 ± 0.3 ^{aA}
	SO ₂ -MAP	10.9 ± 0.5 ^{aA}	10.8 ± 0.4 ^{aA}	9.7 ± 0.6 ^{aA}
TA (g/100 g)	CO ₂ -MAP	1.2 ± 0.1 ^{aA}	1.0 ± 0.2 ^{aA}	1.0 ± 0.1 ^{aA}
	SO ₂ -MAP	1.2 ± 0.1 ^{aA}	1.1 ± 0.2 ^{aA}	1.0 ± 0.1 ^{aA}

*Mean values with different lowercase letters within a row and capital letters within a column for each parameter measured are significantly different ($p \leq 0.05$).

TABLE 2. Total anthocyanin content (TAC), total phenolic content (TPC), and ferric reducing antioxidant power (FRAP) of red currants stored under modified atmosphere packaging (MAP) conditions.

	Treatment	Storage time (days)		
		0	30	60
TAC (mg C3G/100 g fw)	CO ₂ -MAP	22.1 ± 6.1 ^{a*}	20.5 ± 9.2 ^a	27.4 ± 11 ^a
	SO ₂ -MAP	22.1 ± 6.1 ^a	19.7 ± 1.6 ^a	17.2 ± 4.3 ^a
TPC (mg GAE/100 g fw)	CO ₂ -MAP	233 ± 11 ^a	267 ± 20 ^a	203 ± 21 ^a
	SO ₂ -MAP	233 ± 11 ^a	70 ± 18 ^a	197 ± 20 ^a
FRAP (mmol Fe ²⁺ /kg fw)	CO ₂ -MAP	44.5 ± 1.7 ^a	37.1 ± 0.9 ^b	36.9 ± 1.1 ^b
	SO ₂ -MAP	44.5 ± 1.7 ^a	35.8 ± 1.1 ^b	34.6 ± 1.2 ^b

*Mean values in the row with different letters are significantly different ($p \leq 0.05$); GAE – gallic acid equivalents; C3G – cyanidin 3-*O*-glucoside equivalents; fw – fresh weight.

red currants was 44.5 mmol Fe²⁺/kg fw. It is well known that the total anthocyanin and phenolic contents influence the antioxidant capacity in fruit [Orsavová *et al.*, 2019]. Significant ($p \leq 0.05$) differences were observed for FRAP of stored red currants when compared with fresh berries.

Microbial hazard evaluation

The microbial population is an important factor that influences the quality and safety of fresh fruit [Mostafidi *et al.*, 2020], and can be affected by different pre- and post-harvest sources. Clean pallets and sanitised containers during storage should be available for freshly harvested berries. The maintenance of the high humidity level required in storage makes red currants more susceptible to decay; therefore, sanitisation tools are necessary. MAP is generally considered a good technique to preserve fruits, and CO₂ or other gasses, such as O₃ and SO₂, can minimise contamination due to the sanitiser effect of their molecules [Daeschel & Udombijitkul, 2007]. Berries at picking (0 days) showed a microbial count of 13,000, 15,000, and 3,100 CFU/g for yeast, mould, and bacteria, respectively (Table 3). After that time, the two storage treatments showed different effects in terms of controlling

TABLE 3. Microbial counts of red currants stored under modified atmosphere packaging (MAP) conditions.

Microorganism	Treatment	Storage time (days)		
		0	30	60
Yeast (CFU/g)	CO ₂ -MAP	13,000±465 ^{a*}	22,000±1,200 ^a	6,000±115 ^b
	SO ₂ -MAP	13,000±465 ^a	2,800±150 ^b	100±14 ^c
Mould (CFU/g)	CO ₂ -MAP	15,000±330 ^b	17,000±930 ^b	100,000±980 ^a
	SO ₂ -MAP	15,000±330 ^b	400±72 ^c	19,000±1,100 ^a
Bacteria (CFU/g)	CO ₂ -MAP	3,100±124 ^b	2,800±100 ^b	250,000±1,500 ^a
	SO ₂ -MAP	3,100±124 ^a	100±25 ^c	1,500±88 ^b

*Mean values in the row with different letters are significantly different ($p \leq 0.05$).

microbial evolution. SO₂ was effective in controlling yeast evolution, reducing the population both at 30 and 60 days at one and two orders of magnitude, respectively. Less of an effect was observed for the CO₂ treatment but only at 60 days. When berries were exposed to SO₂, its dissolution into a water solution developed three molecular species, namely SO₂ (SO₂×H₂O), bisulphite (HSO₃⁻), and sulphite (SO₃²⁻) [Divol *et al.*, 2012]. The toxic effect against yeast is mainly ascribed to SO₂ because it has no charge; consequently, it should easily pass through the microbial cell membranes. Moreover, the high acidity and the low pH of red currants would be unfavourable to yeast intracellular processes [Divol *et al.*, 2012]. Considering mould, no treatments successfully inhibited them for 60 days when compared to their presence at harvest (0 days). SO₂ samples had 19,000 CFU/g, and CO₂-treated samples had 100,000 CFU/g. The increase in the mould content in the control samples (CO₂ MAP treatment) was probably due to the high humidity in the pallet system because it could not be adsorbed by the SO₂-generating SmartPac active paper sheets. For the same reason, bacterial proliferation was also very high at 60 days of storage for the sample stored

in CO₂-MAP. Exposure to SO₂ deeply reduced the initial bacterial microbial count (3,100 CFU/g); 97% after 30 days and 52% after 60 days.

Sensorial evaluation

Sensorial quality was expressed by the personal preferences of the panellists, and the results are reported in Figure 5. Sensory studies on fresh red currants about the hedonistic overall quality are scarce in the literature, but it is well known that one of the most distinctive attributes of *R. rubrum* is the astringency of fruits, which is mainly affected by flavonol glycosides, derivatives of hydroxycinnamic acids, and various nitrous compounds [Schwarz & Hofmann, 2007a,b]. At harvest (0 days) (Figure 5), red currants ranked a high score in terms of consistency attribute, astringent and acid taste, and total aroma, while the herbaceous and sweet taste were of moderate intensity. A similar profile in terms of sensorial properties among treatments was reported both at 30 (Figure 5A) and 60 days (Figure 5B), indicating that the gas (CO₂ and SO₂) inside the MAP does not differentiate the taste of berries. In fact, after 30 and 60 days the same number

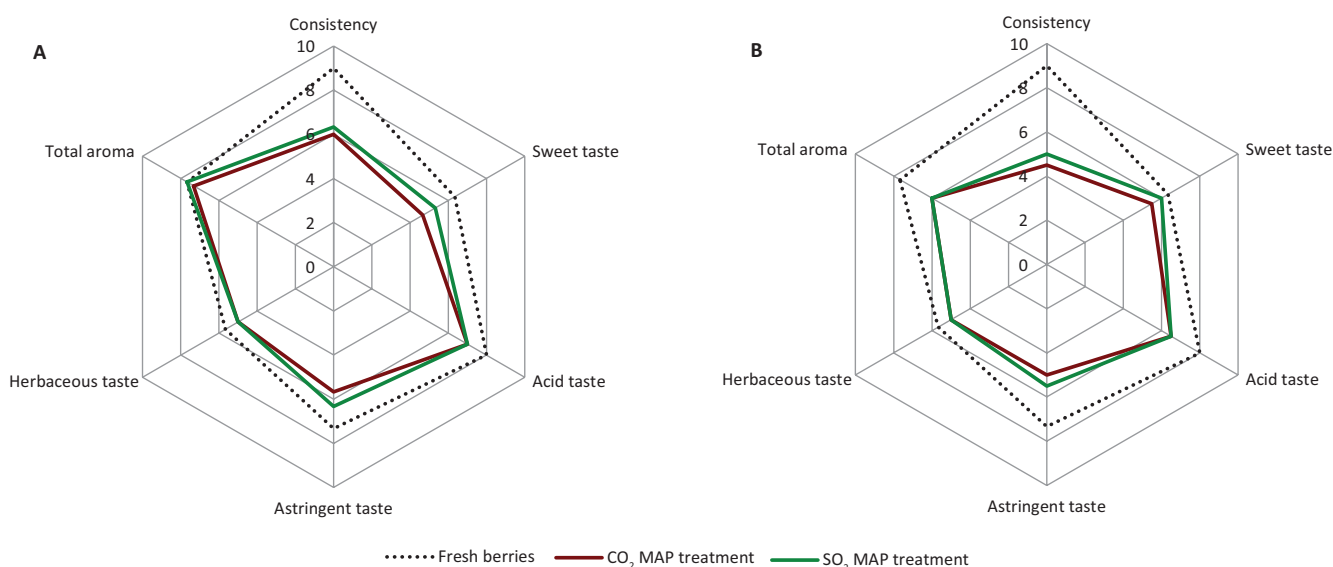


FIGURE 5. Sensory attributes of red currants after 30 days (A) and 60 days (B) of storage under modified atmosphere packaging (MAP) conditions.

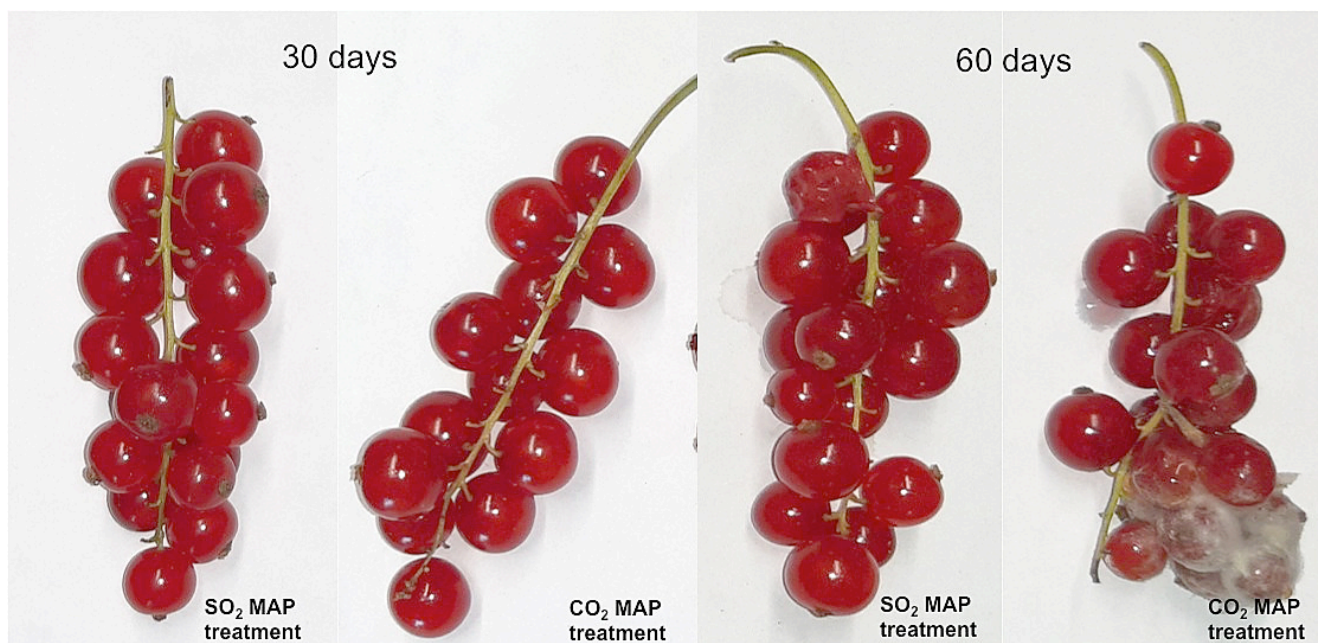


FIGURE 6. Red currants during the storage under modified atmosphere packaging (MAP) conditions.

of points were scored for acid (7.0 and 6.5) and herbaceous notes (5 both after 30 and 60 days), while for the others attributes no more than 0.5 of differences (no significant differences, $p > 0.05$) were scored. After 30 days, berries maintained the highest properties in terms of overall total aroma and acid taste. The perception by panel test decreased at 60 days, while the consistency had already changed (decreasing the score) during the short storage time (30 days). By observing the sensorial profile at the end of storage (60 days), it was possible to determine that astringent and acid notes of taste were the principal hedonistic indicators that influenced the overall acceptability of red currant cv. Rovada samples when stored. Sulphite residues are generally responsible for the decline in the flavour of fruit and affect consumers' willingness to fruit consumption [Shoaei *et al.*, 2019]. However, in this study, there seemed to be no aversion to the red currants; in fact, a similar profile was observed between samples stored in CO_2 and SO_2 MAP.

Visual evaluation

The acceptance of fresh fruits in terms of marketability of the product was preliminary linked to an ideal visual appearance, which is expressed in terms of the absence of defects concerning external and internal parts of fruits, colour, and shape development. In red currants, a high number of berries per raceme, large and uniform fruits throughout the cluster, their complete red coloration, and the maintenance of a green raceme and pedicel are important visual quality criteria for the fresh market. Results of the visual evaluation of berries stored in CO_2 and SO_2 MAP treatments were expressed as raceme and pedicel desiccation, percentage of healthy bunches, and an overall visual quality (Table 4). Generally, the visual evaluation decreased over time, but red currants stored under SO_2 MAP obtained better visual quality score compared to CO_2 MAP treatment berries throughout storage. Figure 6 provides the images of red currants over storage.

TABLE 4. Parameters of visual evaluation of red currants stored under modified atmosphere packaging (MAP) conditions.

Treatment	Storage time (days)	Raceme and pedicel desiccation ¹	Healthy bunches (%)	Visual quality ²
Fresh berries	0	5.0±0.0 ^{a*}	100±0.0 ^a	5.0±0.0 ^a
CO_2 -MAP	30	4.3±0.2 ^b	85±12 ^a	4.0±0.3 ^b
SO_2 -MAP	30	4.5±0.1 ^b	95±5.0 ^a	4.8±0.2 ^a
CO_2 -MAP	60	3.0±0.3 ^c	68±10 ^c	2.0±0.1 ^d
SO_2 -MAP	60	3.3±0.4 ^c	75±8.0 ^b	3.5±0.4 ^c

*Means values in the column with different letters are significantly different ($p \leq 0.05$). ¹Expressed in desiccation scores, were 1 = as green as at harvest; 2 = slight browning; 3 = browning but no shrivelling; 4 = browning and some shrivelling; and 5 = dry and brown. ²Expressed in visual quality scores, were 5 = excellent, no defects; 4 = very good, minor defects; 3 = fair, moderate defects; 2 = poor, major defects; and 1 = unusable.

CONCLUSION

Red currants are an interesting fruit belonging to the berries with a high potential in terms of health properties. The extent of the fresh market, which is still limited compared to those of other soft berries, such as blueberries or raspberries, needs to be supported by advances in post-harvest research. In this study, *R. rubrum* berries were stored at low temperatures under different MAP treatments, and external appearance traits, as well as internal quality properties, were examined for up to 60 days. Exposure to SO_2 gas controlled microbial decay, resulting in a good visual appearance and promising maintenance of the most important sensorial attributes. Active emitters of SO_2 , such as those proposed, can be useful for the storage of red currants in extended storage after harvesting.

Moreover, this technique could also be promising in the transport of red currants. Regardless of the bioactive compounds, future advances will be necessary regarding detailed phenolic composition to analyse and enhance this application.

ACKNOWLEDGEMENTS

We would like to thank the professionals, colleagues, and collaborators who actively participated in this research project.

RESEARCH FUNDING

Research developed by the program ALTA FORMAZIONE IN APPRENDISTATO 2019–2022. Regione Piemonte (Art. 45–D. Lgs. N. 81/2015).

ORCID IDs

L. Brondino <https://orcid.org/0000-0001-6476-9298>
D. Cadario <https://orcid.org/0000-0002-3473-3275>
N.R. Giuggioli <https://orcid.org/0000-0002-7532-5729>

REFERENCES

- Agar, I.T., Streif, J., Bangerth, F. (1997). Effect of high CO₂ and controlled atmosphere (CA) on the ascorbic and dehydroascorbic acid content of some berry fruits. *Postharvest Biology and Biotechnology*, 11(1), 47–55.
[https://doi.org/10.1016/S0925-5214\(97\)01414-2](https://doi.org/10.1016/S0925-5214(97)01414-2)
- Ahmed, S., Roberto, S.R., Domingues, A.R., Shahab, M., Chavez, Junior, O.J., Sumida, C.H., de Souza, R.T. (2018). Effects of different sulfur dioxide pads on Botrytis Mold in 'Italia' table grapes under cold storage. *Horticulturae*, 4(4), art. no. 29.
<https://doi.org/10.3390/horticulturae4040029>
- Benvenuti, S., Pellati, F., Melegari, M., Bertelli, D. (2004). Polyphenols, anthocyanins, ascorbic acid, and radical scavenging activity of *Rubus*, *Ribes*, and *Aronia*. *Journal of Food Science*, 69(3), FCT164–FCT169.
<https://doi.org/10.1111/j.1365-2621.2004.tb13352.x>
- Briano, R., Giuggioli, N.R., Girenti, V., Peano, C. (2015). Biodegradable and compostable film and modified atmosphere packaging in postharvest supply chain of raspberry fruits (cv. Grandeur). *Journal of Food Processing and Preservation*, 39(6), 2061–2073.
<https://doi.org/10.1111/jfpp.12449>
- Cantín, C.M., Minas, I.S., Goulas, V., Jiménez, M., Mangano, G.A., Michailides, T.J., Crisosto, C.H. (2012). Sulfur dioxide fumigation alone or in combination with CO₂-enriched atmosphere extends the market life of highbush blueberry fruit. *Postharvest Biology and Technology*, 67, 84–91.
<https://doi.org/10.1016/j.postharvbio.2011.12.006>
- Cantín, C.M., Palou, L., Bremer, V., Michailides, T.J., Crisosto, C.H. (2011). Evaluation of the use of sulfur dioxide to reduce postharvest losses on dark and green figs. *Postharvest Biology and Technology*, 59(2), 150–158.
<https://doi.org/10.1016/j.postharvbio.2010.09.016>
- Carter, M.Q., Chapman, M.H., Gabler, F., Brandl, M.T. (2015). Effect of sulfur dioxide fumigation on survival of foodborne pathogens on table grapes under standard storage temperature. *Food Microbiology*, 49, 189–196.
<https://doi.org/10.1016/j.fm.2015.02.002>
- Cheng, G.W., Breen, P.J. (1991). Activity of phenylalanine ammonia-lyase (PAL) and concentrations of anthocyanins and phenolics in developing strawberry fruit. *Journal of the American Society of Horticultural Science*, 116(5), 865–869.
<https://doi.org/10.21273/JASHS.116.5.865>
- Chiabrando, V., Giuggioli, N., Maghenzani, M., Peano, C., Giacalone, G. (2018). Improving storability of strawberries with gaseous chlorine dioxide in perforated clamshell packaging. *Polish Journal of Food and Nutrition Sciences*, 68(2), 141–148.
<https://doi.org/10.1515/pjfn-2017-0024>
- Daeschel, M.A., Udombijitkul, P. (2007). Microbial safety concerns of berry fruit. In Y. Zhao (Ed.) *Berry Fruits Value Added Products for Health Promotion*. Chapter 8, Taylor & Francis Group, New York, USA, pp. 229–259.
<https://doi.org/10.1201/9781420006148.ch8>
- Divol, B., du Toit, M., Duckitt, E. (2012). Surviving in the presence of sulphur dioxide: Strategies developed by wine yeasts. *Applied Microbiology and Biotechnology*, 95, 601–613.
<https://doi.org/10.1007/s00253-012-4186-x>
- Djordjević, B., Šavikin, K., Zdunić, G., Janković T., Vulić, T., Oparnica, C., Radivojević, D. (2010). Biochemical properties of red currant varieties in relation to storage. *Plant Foods for Human Nutrition*, 65, 326–332.
<https://doi.org/10.1007/s11130-010-0195-z>
- Fresh plaza: Poland the largest producer of currants in EU and second global. Available on-line: [www.freshplaza.com] (accessed: 15 November 2020).
- Giuggioli, N.R., Briano, R., Baudino, C., Peano, C. (2019). Postharvest warehouse management of *Actinidia arguta* fruits. *Polish Journal of Food and Nutrition Sciences*, 69(1), 63–70.
<https://doi.org/10.31883/pjfn-2019-0006>
- Harb, J., Streif, J. (2014). Controlled atmosphere storage of highbush blueberries cv. 'Duke'. *European Journal of Horticultural Science*, 69(2), S. 66–72.
- Hakimi, S.S., Sreenivas, K.N., Shankarappa, T.H., Krishna, H.C., Sadananda, G.K. (2017). Effect of sulphur dioxide pads on enhancement of shelf life of strawberry (*Fragaria ananassa*) under ambient condition. *International Journal of Current Microbiology and Applied Sciences*, 6(7), 2371–2377.
<https://doi.org/10.20546/ijcmas.2017.607.339>
- ISO 4833–2. (2003). Microbiology of food and animal feeding stuffs – Horizontal method for the enumeration of microorganisms. Colony-count technique at 30°C.
- Jara-Palacios, M.J., Santisteban, A., Gordillo, B., Hernanz, D., Heredia, F.J., Escudero-Gilete, M.L. (2019). Comparative study of red berry pomaces (blueberry, red raspberry, red currant and blackberry) as source of antioxidants and pigments. *European Food Research Technology*, 245, 1–9.
<https://doi.org/10.1007/s00217-018-3135-z>
- JECFA, Joint FAO/WHO Expert Committee on Food Additives (2019). 87th Meeting, Rome, Italy, World Health Organization & Food and Agriculture Organization of the United Nations.
- Laczko-Zöld, E., Komlósi, A., Ülkei, T., Fogarasi, E., Croitoru, M., Fülöp, I., Domokos, E., Ștefănescu, R., Varga, E. (2018). Extractability of polyphenols from black currant, red currant and goose-

- berry and their antioxidant activity. *Acta Biologica Hungarica*, 69(2), 156–169.
<https://doi.org/10.1556/018.69.2018.2.5>
21. Lufu, R., Ambaw, A., Opara, U.L. (2020). Water loss of fresh fruit: influencing pre-harvest, harvest and postharvest factors. *Scientia Horticulturae*, 272, art. no. 109519.
<https://doi.org/10.1016/j.scienta.2020.109519>
 22. Kampuss K., Pedersen, H.L. (2003). A review of red and white currant (*Ribes rubrum* L.). *Small Fruits Review*, 2(3), 23–46.
https://doi.org/10.1300/J301v02n03_03
 23. Macnish, A.J., Padda, M.S., Pupin, F., Tsouvaltzis, P.I., Deltsidis, A.I., Sims, C.A., Brecht, J.K., Mitcham, E.J. (2012). Comparison of pallet cover systems to maintain strawberry fruit quality during transport. *HortTechnology*, 22(4), 493–501.
<https://doi.org/10.21273/HORTTECH.22.4.493>
 24. Mattila, P.H., Hellström, J., Karhu, S., Pihlava, J.M., Veteläinen, M. (2016). High variability in flavonoid contents and composition between different North-European currant (*Ribes* spp.) varieties. *Food Chemistry*, 204, 14–20.
<https://doi.org/10.1016/j.foodchem.2016.02.056>
 25. Mostafidi, M., Sanjabi, M.R., Shir Khan, F., Zahedi, M.T. (2020). A review of recent trends in the development of the microbial safety fruits and vegetables. *Trends in Food Science and Technology*, 103, 321–332.
<https://doi.org/10.1016/j.tifs.2020.07.009>
 26. Orsavová, J., Hlaváčová, I., Mlček, J., Snopek, L., Mišurcová, L. (2019). Contribution of phenolic compounds, ascorbic acid and vitamin E to antioxidant activity of currant (*Ribes* L.) and gooseberry (*Ribes uva-crispa* L.) fruits. *Food Chemistry*, 284, 323–333.
<https://doi.org/10.1016/j.foodchem.2019.01.072>
 27. Ozkaya, O., Dundar, O., Ozdemir, A.E. (2008). Evaluation of ethanol and sulfur dioxide pad effects on quality parameters of stored table grapes. *Asian Journal of Chemistry*, 20(2), 1544–1550.
 28. Peano, C., Giuggioli, N.R., Girgenti, V., Palma, A., D'Aquino, S., Sottile, F. (2017). Effect of palletized MAP storage on the quality and nutritional compounds of the Japanese Plum cv. Angeleno (*Prunus salicina* Lindl.) *Journal of Food Processing and Preservation*, 41(2), art. no. e12786.
<https://doi.org/10.1111/jfpp.12786>
 29. Pellegrini, N., Serafini, M., Colombi, B., Del Rio, D., Salvatore, S., Bianchi, M., Brighenti, F. (2003). Total antioxidant capacity of plant foods, beverages and oils consumed in Italy by three different *in vitro* assays. *The Journal of Nutrition*, 133(9), 2812–2819.
<https://doi.org/10.1093/jn/133.9.2812>
 30. Plessi, M., Bertelli, D., Rastelli, G., Albasini, A., Monzani, A. (1998). Fruits of *Ribes*, *Rubus*, *Vaccinium* and *Prunus* genus. Metal contents and genome. *Fresenius' Journal of Analytical Chemistry*, 361, 353–354.
<https://doi.org/10.1007/s002160050902>
 31. Rivera, S.A., Zoffoli, J.P., Latorre, B.A. (2013). Determination of optimal sulfur dioxide time and concentration product for postharvest control of gray mold of blueberry fruit. *Postharvest Biology and Technology*, 83, 40–46.
<https://doi.org/10.1016/j.postharvbio.2013.03.007>
 32. Rodriguez, J., Zoffoli, J.P. (2016). Effect of sulfur dioxide and modified atmosphere packaging on blueberry postharvest quality. *Postharvest Biology and Technology*, 117, 230–238.
<https://doi.org/10.1016/j.postharvbio.2016.03.008>
 33. Roelofs, F.P.M.M., Waart, A.J.P. (1993). Long-term storage of red currants under controlled atmosphere conditions. *Acta Horticulturae*, 352, 217–222.
<https://doi.org/10.17660/ActaHortic.1993.352.31>
 34. Saito, S., Obenland, D., Xiao, C.L. (2020). Influence of sulfur dioxide-emitting polyethylene packaging on blueberry decay and quality during extended storage. *Postharvest Biology and Technology*, 160, art. no. 111045.
<https://doi.org/10.1016/j.postharvbio.2019.111045>
 35. Schwarz, B., Hofmann, T. (2007a). Sensory guided decomposition of red currant juice (*Ribes rubrum*) and structure determination of key astringent compounds. *Journal of Agricultural and Food Chemistry*, 55(4), 1394–1404.
<https://doi.org/10.1021/jf0629078>
 36. Schwarz, B., Hofmann, T. (2007b). Isolation, structure determination, and sensory activity of mouth drying and astringent nitrogen containing phytochemicals isolated from red currants (*Ribes rubrum*). *Journal of Agricultural and Food Chemistry*, 55(4), 1405–1410.
<https://doi.org/10.1021/jf0632076>
 37. Shoaie, F., Heshmati, A., Khorshidi, M. (2019). The risk assessment of sulphite intake through dried fruit consumption in Hamadan, Iran. *Journal of Food Quality and Hazards Control*, 6(3), 121–127.
<https://doi.org/10.18502/jfqhc.6.3.1386>
 38. Slinkard, K., Singleton, V.L. (1977). Total phenol analysis: automation and comparison with manual methods. *American Journal of Enology and Viticulture*, 28(1), 49–55.
 39. Smilanick, J.L., Henson, D.J. (1992). Minimum gaseous sulfur dioxide concentrations and exposure periods to control *Botrytis cinerea*. *Crop Protection*, 11(6), 535–540.
[https://doi.org/10.1016/0261-2194\(92\)90171-Z](https://doi.org/10.1016/0261-2194(92)90171-Z)
 40. Smilanick, J.L., Margosan, D.A., Henson, D.J. (1995). Evaluation of heated solutions of sulfur dioxide, ethanol, and hydrogen peroxide to control postharvest green mold of lemons. *Plant Disease*, 79, 742–747.
<https://doi.org/10.1094/PD-79-0742>
 41. Sortino, G., Allegra, A., Passafiume, R., Gianguzzi, G., Gullo, G., Gallotta, A. (2017). Postharvest application of sulphur dioxide fumigation to improve quality and storage ability of “Red Globe” grape cultivar during long cold storage. *Chemical Engineering Transaction*, 58, 404–408.
<https://doi.org/10.3303/CET1758068>
 42. Spayd, S.E., Norton, R.A., Hayrynen, L.D. (1984). Influence of sulfur dioxide generators on red raspberry quality during postharvest storage. *Journal of Food Science*, 49(4), 1067–1069.
<https://doi.org/10.1111/j.1365-2621.1984.tb10393.x>
 43. Stepniowska, A., Czech, A., Malik, A., Chalabis-Mazurek, A., Ognik, K. (2016). The influence of winemaking on the content of natural antioxidants and mineral elements in wines made from berry fruits. *Journal of Elementology*, 21(3), 871–880.
<https://doi.org/10.5601/jelem.2015.20.4.1020>
 44. Talcott, S.T. (2007). Chemical components of berry fruits. In Y. Zhao (Ed.) *Berry Fruit Value Added Products for Health Promotion*. Chapter 2, Taylor & Francis Group, New York, USA, pp. 51–72.
<https://doi.org/10.1201/9781420006148>
 45. Thompson, A.K. (1998). *Controlled Atmosphere Storage of Fruits and Vegetables*. CAB Intl., Wallingford, UK.

46. Temocico, G., Stoian, E., Ion, V., Tudor, V. (2014). Results regarding behaviour of some small fruits under controlled atmosphere conditions. *Romanian Biotechnological Letters*, 19(2), 9162–9169.
47. Vanderzant, C., Splittstoesser, D.F. (1992). *Compendium of Methods for the Microbiological Examination of Foods*. 3rd edition. American Public Health Association (APHA), Washington, USA.
48. Zutahy, Y., Lichter, A., Kaplunov, T., Lurie, S. (2008). Extended storage of 'Redglobe' grapes in modified SO₂ generating pads. *Postharvest Biology and Technology*, 50(1), 12–17. <https://doi.org/10.1016/j.postharvbio.2008.03.006>

Effect of Ohmic Heating on the Rheological Characteristics and Electrical Conductivity of Mulberry (*Morus nigra*) Puree

Gemala Hardinasinta¹, Mursalim Mursalim, Junaedi Muhidong, Salengke Salengke*¹

Department of Agricultural Engineering, Hasanuddin University, Makassar, 90245, Indonesia

Key words: ohmic heating, mulberry puree, rheological characteristics, pseudo activation energy, electrical conductivity

The effect of temperatures (30–90°C) and concentrations (50% and 100%) on rheological parameters of mulberry puree processed with ohmic heating (OH) were evaluated. The electrical conductivities of mulberry puree ranged from 0.022 to 0.102 S/m for 50% puree and 0.052 to 0.185 S/m for 100% puree. The best model for rheological parameters of mulberry puree was the power law model ($R^2 > 0.90$). The effects of OH treatment and temperature of puree on the flow behavior index (n) were insignificant ($p \geq 0.05$). However, a significant difference ($p < 0.05$) between consistency coefficient (K) of OH-treated and control sample was observed in 100% puree. The pseudo activation energy (E_a) of ohmic-treated puree was 9.67 kJ/mol for 50% puree and 3.69 kJ/mol for 100% puree, both of these values were significantly lower than that of the unprocessed 100% puree (16.07 kJ/mol). The obtained E_a indicates that after undergoing ohmic heating pretreatment, consistency coefficient of mulberry puree became less sensitive to temperature.

INTRODUCTION

Mulberry (*Morus nigra*) is a fruit-bearing plant that can grow in a wide range of climates, geographical, and soil conditions which allows widespread cultivation of this plant [Rodrigues *et al.*, 2019]. Mulberry fruit is an exotic fruit characterized by a dark-purplish color with a diameter of 10–12 mm. This fruit is known for its sweet and acidic flavor and has been used as an ingredient in folk medicines [Polat & Satil, 2012; Rodrigues *et al.*, 2019]. In addition, mulberry fruit is rich in bioactive compounds such as anthocyanins and phenolic acids, as well as nutrients such as fatty acids, amino acids, and vitamins [Jiang & Nie, 2015]. Increasing customers' demand for functional food and beverages, and the versatility of mulberry plant makes the mulberry fruit a good raw material for the production of the fruit-based functional foods and beverages.

Diversification of fruit-based products has led to the increase in the utilization of fruit puree both for direct consumption and for the manufacture of semi-finished products. For direct consumption, fruit purees are mostly valued for their pleasant sensory and health-promoting properties provided by bioactive compounds which are naturally present in the fruits. These compounds are well known for their antioxidant activity [Marangoni Júnior *et al.*, 2020; Mohammadi-Moghaddam *et al.*, 2020]. Processing fruits into purees is intended to prolong the usability and availability of fruits

beyond their producing regions and harvest season. Fruit purees can be re-processed into various products such as juices, smoothies, baby foods, rehydrated drinks, and sports drinks [Bakke *et al.*, 2020; Tirloni *et al.*, 2020]. One of the important properties that need to be considered in the processing of fruit purees and their end products is rheological properties. Many authors [Bozkurt & Icier, 2009; de Castilhos *et al.*, 2018; Deshmukh *et al.*, 2015] have indicated that rheological properties can be used as a basis for operating design, processing optimization, and quality evaluation. Rheological characteristics of fruit puree are affected by temperature, concentration, ripening stage of fruit, product formulation, and processing method [Gomathy *et al.*, 2015; Lemus-Mondaca *et al.*, 2016]. The use of heat treatment combined with the continual stirring and pumping may result in undesirable effects on the product such as structural breakdown, which in turn can affect sensory quality and consistency coefficient of the product [Gomathy *et al.*, 2015].

Processing fruit purees and their derivative products involves pasteurization or sterilization process which can be conducted by conventional thermal processing, non-thermal processing such as high hydrostatic pressure (HHP), and novel thermal processing such as ohmic heating. The non-thermal and novel thermal processing, such as ohmic and microwave heating, have been rigorously evaluated for processing various types of products and these technologies have been reported to provide comparable or better nutrient and sensory

* Corresponding Author:

E-mail: ssalengke@yahoo.co.id (S. Salengke)

Submitted: 24 May 2021

Accepted: 9 July 2021

Published on-line: 20 August 2021



profiles compared to the conventional heating [Darvishi *et al.*, 2020; Mannozi *et al.*, 2019; Rinaldi *et al.*, 2020].

Ohmic heating technology is considered as a novel thermal processing for inactivation of microbial contaminants in food products. With this technology, the heat is generated internally due to the passage of electric current through the processed product, which in turn brings about the movement of ions contained in the product. The passage of electric current generates heat due to the electrical resistance of the product. Therefore, the effectiveness of this technology is greatly dependent on the electrical conductivity of the product. Electrical conductivity is affected by product composition and characteristics, such as pH and acidity, salt and sugar content, and solid content [Castro *et al.*, 2003; Icier & Ilicali, 2005; Poojitha & Athmaselvi, 2018; Varghese *et al.*, 2014]. Ohmic heating is generally considered as a fast and uniform heating process. This phenomenon has been reported by numerous researchers [Fadavi *et al.*, 2018; Salengke & Sastry, 2007; Sarkis *et al.*, 2013]. The effectiveness of ohmic heating in inactivation of microorganism has also been reported [Hashemi & Roohi, 2019; Hashemi *et al.*, 2019; Park & Kang, 2013]. Therefore, it is important to evaluate the electrical conductivity of individual products under ohmic heating prior to implementing it to the real processing steps in order to achieve the desirable heating effects.

The implementation of ohmic heating in various processes has been reported in numerous studies. These processes include pasteurization and sterilization [Cappato *et al.*, 2018; Hardinasinta *et al.*, 2021], evaporation [Sabanci & Icier, 2020], blanching and pre-treatment [Mannozi *et al.*, 2019], extraction [Hasizah *et al.*, 2018], thawing [Fattahi & Zamindar, 2020], and fermentation [Salengke *et al.*, 2019]. Studies evaluating the application of ohmic heating for food processing mainly focused on the change in electrical conductivity, bioactive compound profile, antioxidant activity, color, and enzymatic inactivation in correlation to the product composition. Currently, there is limited information that can be found regarding the effect of ohmic heating on rheological characteristics of fruit-based products. Only papaya pulp [Gomathy *et al.*, 2015], quince nectar [Bozkurt & Icier, 2009], sour cherry juice concentrate [Sabanci & Icier, 2020], and peach cubes in syrup [Rinaldi *et al.*, 2020] have been studied in this respect. To the best of the author's knowledge, no studies were found regarding the effect of ohmic pretreatment on rheological characteristics of mulberry puree. Therefore, it is important to determine the influence of ohmic pretreatment on rheological characteristics of mulberry puree. This study is an important step in the early-stage development of ohmic heating for processing mulberry fruit product.

This study was aimed at determining the effect of ohmic heating and puree concentration on rheological characteristics and electrical conductivity of mulberry puree.

MATERIALS AND METHOD

Sample preparation

Mulberry puree was processed from frozen mulberry fruit purchased from a local market. Prior to processing, 10 kg

TABLE 1. Characteristics of mulberry puree at different concentrations.

Puree concentration	Total soluble solid (°Bx)	Moisture content (g/100 g)	pH
50%	3.17±0.06 ^b	95±0.103 ^a	3.55±0.01 ^a
100%	6.73±0.06 ^a	88±0.454 ^b	3.50±0.13 ^a

Data are expressed in mean ± standard deviation of 2 replicates. ^{a-b}Different letters indicate a significant difference between samples ($p < 0.05$).

of mulberry fruits were thawed with running water and then washed to remove foreign materials. The fruits were then separated based on maturity level and ripe fruits displaying a dark-purplish color were selected. Two concentrations (50% and 100% puree) of mulberry puree were used in this experiment. The 100% puree was made by crushing the whole fruit using a commercial blender without the addition of water. The obtained puree was collected in a bucket and blended again to obtain homogenous consistency. The 50% puree was processed by mixing the 100% puree and distilled water with the ratio of 1:1 (*w/w*). Samples were stored in 500 mL polytetrafluoroethylene (PTFE) bottles and kept in a freezer at -18°C until used. The characteristics of the material used in the experiment, such as pH, total soluble solid, and moisture content, are listed in Table 1.

Ohmic heating treatment

The ohmic heating system used in this experiment consisted of a static ohmic heating chamber, a power supply equipped with a temperature control and a data acquisition system. The heating chamber was made from PTFE with internal diameter of 4 cm, outer diameter of 8.89 cm, and length of 16 cm. The maximum volume of the heating chamber was 150 mL. The ohmic heating chamber was fitted with two stainless steel electrodes (custom-made of SS304 rod) at both ends of the chamber. The temperature of the sample during heating was measured using a thermocouple which was installed at the center of the chamber. The applied voltage, electric current, and temperature were recorded every 2 s using a data acquisition system. The schematic diagram of ohmic heating system is illustrated in Figure 1.

Ohmic heating treatment was carried out at 110°C with a 30 s holding time. This temperature is in the range of the sterilization temperature generally used for fruit juices [Petruzzi *et al.*, 2017; Renard & Maingonnat, 2012]. The average voltage gradient applied to the product was 18.5 V/cm.

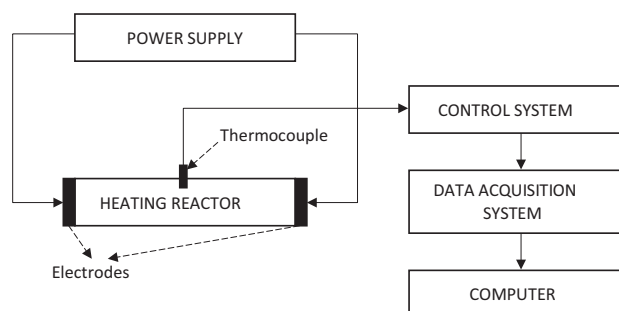


FIGURE 1. Schematic diagram of ohmic heating system.

Rheological measurement

The rheological behavior of ohmic-heated puree and unprocessed puree (control) at the concentration of 50 and 100% was measured using a concentric cylinder type viscometer (LVDV-I Prime, Brookfield Engineering, Middleborough, MA, USA). The viscometer was operated using rotational speed of 0–100 rpm and 10–100% torque using a specific spindle from the low viscosity (LV) and regular viscosity (RV) spindle set. The viscosity (cP) and % torque (T) values were collected at each rotational speed. The experiment was conducted at four temperatures of 30, 50, 70, and 90°C and each experiment was repeated in duplicate.

The torque and rotational speed obtained from the measurement were converted into shear stress and shear rate value using two different methods depending on the type of spindle used during measurement. Mitschka method [Mitschka, 1982] was used for the RV spindle set which was a disk-type spindle, while the method described in the Brookfield AM-ETEK guidelines was used for the LV cylindrical-type spindle [Brookfield, 2017].

In order to determine the rheological parameters of mulberry puree, several rheological models were applied. The rheological models were power law (Equation 1), and Herschel-Bulkley (Equation 2) [Bozkurt & Icier, 2009].

$$\sigma = K\dot{\gamma}^n \quad (1)$$

$$\sigma = \sigma_0 + K\dot{\gamma}^n \quad (2)$$

where: σ is shear stress (Pa), $\dot{\gamma}$ is shear rate (1/s), K is consistency coefficient ($\text{Pa} \times \text{s}^n$), n is flow behavior index, and σ_0 is yield stress (Pa).

The effect of temperature on the viscosity of mulberry puree was determined using the consistency coefficient value with the pseudo Arrhenius equation below [Kobus *et al.*, 2019]:

$$K = K_0 \exp \frac{E_a}{RT} \quad (3)$$

where: K_0 is consistency coefficient, E_a is pseudo activation energy, R is universal gas constant (0.008314 kJ/mol \times K), and T is absolute temperature.

Statistical analysis

Statistical analysis was conducted to determine the best-fitted rheological model for mulberry puree. The residual standard error (RSE) and coefficient of determination (R^2) were calculated by using a linear regression model. The model that provided the best fit was determined based on statistical criteria such as highest R^2 and lowest RSE. The effect of temperature and concentration treatment on the rheological parameters of mulberry puree were analyzed using one-way ANOVA followed by the Tukey contrast multiple comparison test with a 95% confidence level. A paired t-test was also conducted to analyze the effect of ohmic heating on the rheological parameters. All statistical analyses were conducted by using RStudio software (RStudio, PBC, Boston, MA, USA).

RESULTS AND DISCUSSIONS

The electrical conductivity of mulberry puree

The heating characteristics of mulberry puree at different concentrations are shown in Figure 2. A linear increase in electrical conductivity was observed following the temperature elevation during ohmic heating. The result obtained in this study was consistent with the previous studies which demonstrated that electrical conductivity of tomato concentrate increased linearly with the heating temperature as a result of reduced drag force of ionic compounds inside the product [Fadavi & Salari, 2019]. Electrical conductivity is affected by the ionic compounds of the product. Applying electric current on a product initiates the movement of the ionic compounds inside it towards the opposite direction of its charge and increases its temperature. The temperature elevation decreases the viscosity of the aqueous phase and consequently reduces the drag force of the ions and increases the product's electrical conductivity [Srivastav & Roy, 2014].

The electrical conductivities of mulberry puree at 30–110°C were in the range of 0.022–0.102 S/m for 50% puree and 0.052–0.185 S/m for 100% puree (Figure 2). Statistical analysis conducted for electrical conductivity of 50% and 100% puree at 30, 50, 70, 90, and 110°C indicated that at these treatment conditions the electrical conductivities were significantly ($p < 0.05$) different (Table 2). Mulberry puree at the concentration of 100% exhibited higher electrical conductivity compared to that of 50% puree. Moreover, the electrical conductivity of mulberry puree found in this study was lower than the electrical conductivity of mulberry juice treated by ohmic heating (0.1–0.4 S/m) [Darvishi *et al.*, 2020]. In a study reported by Icier & Ilicali [2005], the electrical conductivity of orange juice concentrates decreased as the solid concentration increased. Since the mass fraction of pure juice was lower than that of puree, higher electrical conductivity value was expected in the pure juice product. Meanwhile, the difference in electrical conductivity between 100% and 50% purees (Figure 2, Table 2) could be due to the decreasing content of ions per volume of the product. Fruits have been reported to contain anions and cations, *i.e.* F^- , NO_3^- , NO_2^- , Br^- and PO_4^{3-} ; as well as NH_4^+ , Ca^+ , and Mg^+ , respectively [Hajar *et al.*, 2010]. These ions provided a specific level of electrical conductivity of the fruit juices, depending on

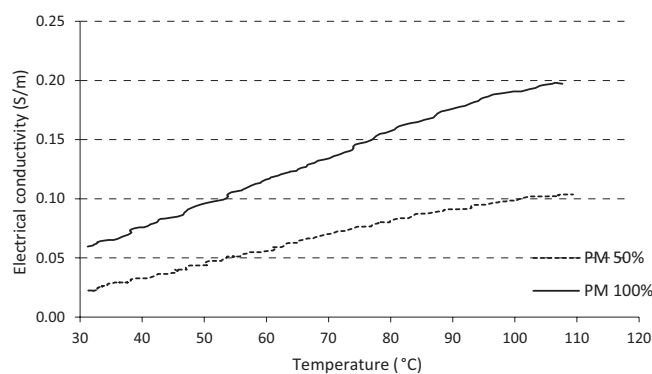


FIGURE 2. The electrical conductivity of mulberry puree (MP) during ohmic heating.

TABLE 2. Electrical conductivity (S/m) of mulberry puree at different concentrations and temperatures.

Puree concentration	Temperature				
	30°C	50°C	70°C	90°C	110°C
50%	0.022±0.000 ^e	0.042±0.003 ^g	0.068±0.004 ^{def}	0.089±0.003 ^{ce}	0.102±0.002 ^{cd}
100%	0.052±0.008 ^{eg}	0.087±0.015 ^{ce}	0.125±0.014 ^{bc}	0.163±0.018 ^{ab}	0.185±0.013 ^a

Data are expressed as mean ± standard deviation of 2 replicates. ^{a-g}Different letters indicate a significant difference between samples (p<0.05).

the types of ions and their concentration [Almeida & Huber, 1999; Hajar *et al.*, 2010]. In our study, dilution of puree during the sample preparation step decreased the ion concentration and simultaneously decreased the electrical conductivity of 50% puree. Another effect of the dilution was the decrease in the total soluble solid content (Table 1).

Rheological behavior of mulberry puree

Generally, both power law and Herschel-Bulkley models displayed a satisfactory R² value of over 0.95 for all treatment conditions. However, the power law model showed lower RSE values (RSE<0.038) compared to the Herschel-Bulkley model (RSE<0.267), which implies that statistically, this model is more applicable for mulberry puree at all conditions. In the Herschel-Bulkley model, the yield stress value significantly affected the model accuracy and applicability. Several studies have neglected the yield stress value measured during experiment if the value is considered to be low or statistically not different with 0 [Lemus-Mondaca *et al.*, 2016; Payne & Reyes-de-Corcuera, 2021]. The rheological study conducted

for murtilla berries (*Ugni molinae* Turcz) showed that the yield stress ranging from 6.31×10^{-12} to 3.47×10^2 Pa was considered low. Similarly, the yield stress values obtained in this study fell in the same range as that of murtilla berries (1.9 Pa to 9.0×10^1 Pa) and therefore they can be neglected. Therefore, the power law model can be chosen as the best-fitted model for describing the rheological characteristics of mulberry puree. Several studies have reported that the power law model was the best-fitted model for rheological behaviors of cloudy apple juice [Kobus *et al.*, 2019], malbec grape juice concentrates [Evangelista *et al.*, 2020], and orange pulp [Payne & Reyes-de-Corcuera, 2021].

The power law model was fitted by plotting the logarithms of shear stress and shear rate. The slope and y-intercept obtained from the graph described the flow behavior index (n) and consistency coefficient (K) of the puree, respectively. The flow curves (Figure 3 and Figure 4) roughly illustrated that the application of ohmic heating affected the temperature dependence of mulberry puree's rheological characteristic. It can be explained by how the flow curve of control sample at 30°C was lower than those at the other temperature levels, while the flow curve of ohmic-heated sample at

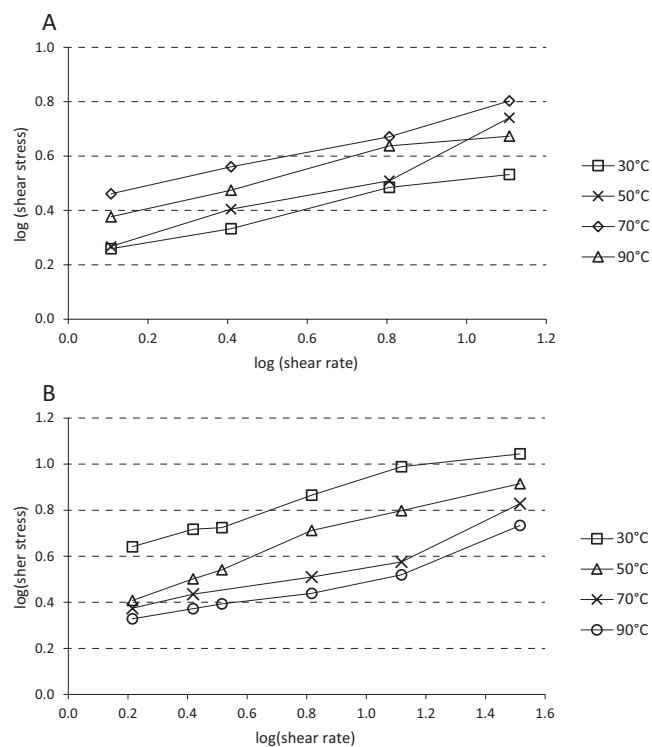


FIGURE 3. Flow curves of 50% mulberry puree; (A) control and (B) ohmic heating.

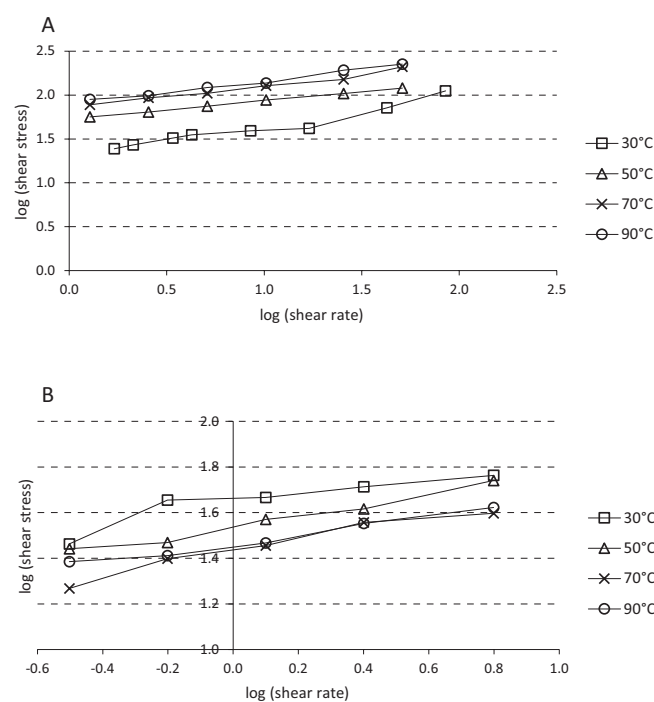


FIGURE 4. Flow curves of 100% mulberry puree; (A) control and (B) ohmic heating.

TABLE 3. Rheological parameters of ohmic-heated and unprocessed (control) mulberry puree.

Puree concentration	Temperature (°C)	Control		Ohmic heating	
		Flow behavior index, n	Consistency coefficient, K (Pa×s ⁿ)	Flow behavior index, n	Consistency coefficient, K (Pa×s ⁿ)
50%	30	0.24±0.07 ^a	2.14±0.63 ^a	0.37±0.10 ^a	3.01±1.52 ^a
	50	0.27±0.24 ^a	2.98±1.91 ^a	0.33±0.01 ^a	2.36±0.21 ^a
	70	0.25±0.09 ^a	2.99±0.19 ^a	0.30±0.00 ^a	1.75±0.01 ^a
	90	0.22±0.13 ^a	3.04±1.11 ^a	0.25±0.02 ^a	1.65±0.31 ^a
100%	30	0.25±0.14 ^a	44.53±34.71 ^a	0.20±0.00 ^a	42.48±0.01 ^a
	50	0.13±0.09 ^a	107.36±73.54 ^a	0.17±0.09 ^a	39.35±6.97 ^a
	70	0.16±0.12 ^a	122.95±71.49 ^a	0.13±0.00 ^a	35.24±0.01 ^a
	90	0.14±0.12 ^a	133.32±65.45 ^a	0.17±0.05 ^a	33.71±5.50 ^a

Data are expressed as mean ± standard deviation of 2 replicates. ^aThe same letter in the same group indicates an insignificant difference between samples ($p \geq 0.05$).

30°C was higher. However, ohmic heating did not cause any change in the flow behavior of mulberry puree since both control and ohmic-treated products followed the same rheological model. Studies on various processing methods for fruit juice and puree, such as ultrasound [Rojas *et al.*, 2016], vacuum evaporation [Sabanci & Icier, 2020], and high hydrostatic pressure [Lemus-Mondaca *et al.*, 2016], have reported that processing methods did not cause an overall change in the flow behavior. However, distinct changes were observed in the rheological characteristics, such as consistency coefficient, flow behavior index, and yield stress.

The effect of processing conditions and temperature on rheological characteristics of mulberry puree

The flow behavior index (n) and consistency coefficient (K) at different temperatures and concentrations of mulberry puree were listed in Table 3. Based on the flow behavior index obtained, $0 < n < 1$, the mulberry puree was classified as a non-Newtonian pseudoplastic fluid. The pseudoplastic fluid is distinguished by the decreasing value of apparent viscosity following the increase in shear stress. Fruit juice and puree, in general, are heterogeneous solutions containing a significant amount of solid particles that are dispersed in the liquid phase rich in soluble compounds. Therefore, when subjected to shear stress, it creates a momentum transfer among particles which affects the apparent viscosity of the product. The apparent viscosity of mulberry puree decreased following the increase of shear stress. The viscosity reduction is a result of structural damage of the molecular chain by hydrodynamic forces, causing the molecular constituent alignment parallel to the current lines and reducing the flow resistance of a fluid [Evangelista *et al.*, 2020; Ribeiro *et al.*, 2018].

The effect of temperature and ohmic heating treatment on flow behavior index was statistically not significant ($p \geq 0.05$) (Table 3 and Table 4), indicating that the pseudoplastic behavior was independent of temperature and the non-thermal effect of electricity can be neglected particularly at the voltage gradient of 18.5 V/cm. Nevertheless, there was a decreasing tendency of flow behavior index as the temperature increased

with the most noticeable effect in the fresh puree. The independence of flow behavior index on temperature was also shown for guava juice concentrates [Abdullah *et al.*, 2018], grape juice [de Castilhos *et al.*, 2018], and cloudy apple juice [Kobus *et al.*, 2019]. Findings from studies reporting the effect of ohmic heating on rheological behaviors of fruit products varied. Bozkurt & Icier [2009] reported that no significant difference in flow behavior index value was observed between ohmic and conventional heating of quince nectar. In addition, evaluation of ohmic heating for sweet whey processing under different electric fields showed that the flow behavior index was similar for all treatments applied [Costa *et al.*, 2018]. However, ohmic heating of papaya pulp did result in a higher flow behavior index compared to the fresh papaya pulp [Gomathy *et al.*, 2015].

The consistency coefficients (K) of mulberry puree at different temperatures and concentrations are shown in Table 3. One-way ANOVA results indicated an insignificant effect of temperature treatment on K-value [$F(3, 4) = 1.587$, $p = 0.325$] (Table 3). Nevertheless, reverse tendencies for this relationship were noticeable between control and ohmic-heated sample. With the control samples, an increase in consistency coefficient was observed as temperature was increased. On the other hand, the K-value of puree undergoing ohmic heating decreased as the temperature increased, implying that the product becomes less viscous at higher temperature. Most studies reported that temperature

TABLE 4. The pseudo activation energy (E_a) of ohmic-heated and unprocessed (control) mulberry puree at different concentrations.

Puree concentration	Parameter	Control	Ohmic heating
50%	E_a (kJ/mol)	5.03	9.67
	R^2	0.70	0.96
100%	E_a (kJ/mol)	16.07	3.69
	R^2	0.80	0.98

R^2 – coefficient of determination.

elevation significantly decreased the consistency coefficient and the overall viscosity of fruit juice and puree [de Castilhos *et al.*, 2018; Deshmukh *et al.*, 2015; Evangelista *et al.*, 2020; Kobus *et al.*, 2019; Ribeiro *et al.*, 2018]. Temperature elevation in fluid enhances the thermal energy of molecules, which results in a higher degree of molecular agitation and reduction of the intermolecular force, hence decreasing the fluid viscosity [Abdullah *et al.*, 2018; Deshmukh *et al.*, 2015; Evangelista *et al.*, 2020; Kobus *et al.*, 2019]. The tendency of increasing K-value which was observed in the control sample (Table 3) can be explained by the larger amount of insoluble solid and particle size found in unprocessed puree which tends to form clumps. A study conducted by Lukhmana *et al.* [2018] described that cherry puree consisted of smaller micronized particles exhibiting a lower viscosity compared to the puree sample which did not undergo any micronization. This study further explained that the non-uniformity of cell cluster surface led to the agglomeration of cells into larger clusters and therefore increased the viscosity of puree. The heat applied during ohmic processing could lead to the membrane destruction inside the cells and cause structural changes of the sample [Castro *et al.*, 2004; Hardinasinta *et al.*, 2021].

The structural changes that happened during heating are the main reason for the different trend shown by the K-value of the control sample and the ohmic-treated sample (Table 3). As the temperature increased, the mulberry puree processed with ohmic heating exhibited a lower consistency coefficient compared to the fresh puree. Similarly, in comparison to the fresh pulp, a lower consistency coefficient was obtained in ohmic-heated papaya pulp as the result of heat treatment [Gomathy *et al.*, 2015]. Several studies have been conducted to compare the effect of ohmic heating and conventional processing method on the consistency coefficient and the results varied depending on the applied treatment. There was no significant difference between the processing methods used in quince nectar [Bozkurt & Icier, 2009] and sour cherry juice concentrate [Sabanci & Icier, 2020]. However, the application of ohmic heating in processing a syrup containing peach cubes resulted in a lower consistency coefficient compared to the conventional heating. It was reported that the significant decrease in viscosity was caused by the degradation of β -eliminative and rapid hydrolysis of water-soluble pectin at low pH [Rinaldi *et al.*, 2020].

In addition, the non-thermal effect of ohmic heating has also been evaluated for sweet whey processing. Costa *et al.* [2018] reported that a significant difference of K-value was obtained in sweet whey samples processed at the highest voltage gradient (9 V/cm) and no significant difference with the conventional heating was observed when ohmic heating was done at lower voltage gradients (2–7 V/cm). Other alternative processing methods, such as pulsed electric field (PEF) and HHP, also evoked inconsistent effects on the product viscosity and consistency coefficient. For instance, the HHP processing assisted with ohmic pre-treatment did not affect the viscosity of the product significantly [Rinaldi *et al.*, 2020]. However, another study conducted with murtilla berries reported that a notable increase of consistency coefficient was obtained after HHP treatment at 500 MPa due to increasing pectin particles interaction [Lemus-Mondaca *et al.*, 2016]. Meanwhile, PEF treatment of almond milk decreased its consistency index at 7–21 kV/cm, but increased it at the highest voltage gradient of 28 kV/cm [Manzoor *et al.*, 2019].

The high pseudo activation energy (E_a) was found for K in the control sample at 100% concentration (Table 4). Higher E_a indicates higher sensitivity of the K-value towards temperature [Bozkurt & Icier, 2009; Evangelista *et al.*, 2020; Kobus *et al.*, 2019]. The significant difference between E_a of the control samples at 50% and 100% (Table 4) implies that at higher concentration, the K-value of unprocessed mulberry puree exhibited higher sensitivity over temperature. It can be explained by the combination effect provided by the temperature and concentration treatment which enhance the effect of temperature at higher concentration. Paired t-test also showed that the difference between rheological parameters (n and K value) of the control and ohmic-heated sample was significant only for the K-value of 100% puree (Table 5).

An opposite trend was observed for the ohmic-heated sample, where the E_a decreased as the concentration increased (Table 4), indicating that the influence of temperature in the viscosity reduction of mulberry puree is highly noticeable at lower solid concentrations. A similar declining trend of E_a vs. concentration was obtained in merlot and malbec grape juice [de Castilhos *et al.*, 2018; Evangelista *et al.*, 2020], while other studies reported a positive correlation between E_a and concentration [Bozdogan *et al.*, 2020; Deshmukh *et al.*, 2015]. Comparable E_a values were reported in sapotapa

TABLE 5. Paired t-test result for the effect of ohmic heating on rheological parameters of mulberry puree.

	Puree concentration	Mean \pm SD		n	95% confidence interval for mean difference		t	df
		Control	Ohmic heating					
(Pa \times s ⁿ)								
Consistency coefficient (K)	50%	2.78 \pm 0.95	2.19 \pm 0.83	8	-0.08	0.27	1.27	7
	100%	102.03 \pm 60.37	37.83 \pm 4.96	8	0.07	0.62	2.94*	7
(-)								
Flow behavior index (n)	50%	0.24 \pm 0.11	0.31 \pm 0.06	8	-0.16	0.03	-1.58	7
	100%	0.17 \pm 0.10	0.16 \pm 0.04	8	-0.06	0.07	0.14	7

SD – standard deviation, n – total number of data, t – t-test statistic value, df – degree of freedom; *p < 0.05.

juice at 10.2–38.9°Bx [Deshmukh *et al.*, 2015] and gongura leave puree [Meher *et al.*, 2019], except for the ohmic-treated puree at 100% concentration which had a significantly higher E_a value. For this specific condition, a similar E_a value was acquired from sumac extract at 45.65% total solids [Bozdogan *et al.*, 2020], sapotapa juice at 49.4°Bx [Deshmukh *et al.*, 2015], and merlot juice at 45°Bx [de Castilhos *et al.*, 2018].

CONCLUSIONS

The electrical conductivity of mulberry puree increased with temperature and concentration. The higher electrical conductivity obtained at a lower concentration was the result of dilution process during samples' preparation, which lowered the content of ionic compounds in the sample. Mulberry puree can be categorized as a pseudoplastic fluid with a shear-thinning behavior and its rheological properties can be modeled using the power law model. Flow behavior index displayed an independent tendency towards temperature and processing method, implying that both thermal and non-thermal effect was insignificant for the pseudoplastic behavior of mulberry puree. Coefficient of consistency, on the other hand, exhibited a correlation with the processing method, where opposite trends were observed between the K -value of ohmic-heated and control samples. The obtained E_a further explains that the effect of temperature was more visible for the unprocessed mulberry puree and that ohmic heating process could be used to maintain the consistency of mulberry puree especially at high concentration.

RESEARCH FUNDING

This study was financially supported by the Directorate General of Higher Education, Ministry of Education and Culture, Republic of Indonesia under the 2018–2020 PMDSU research grant.

CONFLICT OF INTEREST

Authors declare no conflict of interest.

ORCID IDs

G. Hardinasinta <https://orcid.org/0000-0002-5777-6454>
S. Salengke <https://orcid.org/0000-0001-7777-2971>

REFERENCES

- Abdullah, N., Chin, N.L., Yusof, Y.A., Talib, R.A. (2018). Modeling the rheological behavior of thermosonic extracted guava, pomelo, and soursop juice concentrates at different concentration and temperature using a new combination model. *Journal of Food Processing and Preservation*, 42(2), art. no. e13517. <https://doi.org/10.1111/jfpp.13517>
- Almeida, D.P.F., Huber, D.J. (1999). Apoplastic pH and inorganic ion levels in tomato fruit: A potential means for regulation of cell wall metabolism during ripening. *Physiologia Plantarum*, 105(3), 506–512. <https://doi.org/10.1034/j.1399-3054.1999.105316.x>
- Bakke, A.J., Carney, E.M., Higgins, M.J., Moding, K., Johnson, S.L., Hayes, J.E. (2020). Blending dark green vegetables with fruits in commercially available infant foods makes them taste like fruit. *Appetite*, 150, art. no. 104652. <https://doi.org/10.1016/j.appet.2020.104652>
- Bozdogan, A., Yasar, K., Soyler, M., Ozalp, C. (2020). Rheological behavior of sumac (*Rhus coriaria* L.) extract as affected by temperature and concentration and investigation of flow behavior with CFD. *Biointerface Research in Applied Chemistry*, 10(6), 7120–7134. <https://doi.org/10.33263/BRIAC106.71207134>
- Bozkurt, H., Icier, F. (2009). Rheological characteristics of quince nectar during ohmic heating. *International Journal of Food Properties*, 12(4), 844–859. <https://doi.org/10.1080/10942910802102962>
- Brookfield, A. (2017). *More Solutions to Sticky Problems*. Ametec Brookfield. <https://doi.org/10.16309/j.cnki.issn.1007-1776.2003.03.004>
- Cappato, L.P., Ferreira, M.V.S., Moraes, J., Pires, R.P.S., Rocha, R.S., Silva, R., Neto, R.P.C., Tavares, M.I.B., Freitas, M.Q., Rodrigues, F.N., Calado, V.M.A., Raices, R.S.L., Silva, M.C., Cruz, A.G. (2018). Whey acerola-flavoured drink submitted Ohmic Heating: Bioactive compounds, antioxidant capacity, thermal behavior, water mobility, fatty acid profile and volatile compounds. *Food Chemistry*, 263, 81–88. <https://doi.org/10.1016/j.foodchem.2018.04.115>
- Castro, I., Teixeira, J.A., Salengke, S., Sastry, S.K., Vicente, A.A. (2003). The influence of field strength, sugar, and solid content on electrical conductivity of strawberry products. *Journal of Food Process Engineering*, 26(1), 17–29. <https://doi.org/10.1111/j.1745-4530.2003.tb00587.x>
- Castro, I., Teixeira, J.A., Salengke, S., Sastry, S.K., Vicente, A.A. (2004). Ohmic heating of strawberry products: Electrical conductivity measurements and ascorbic acid degradation kinetics. *Innovative Food Science and Emerging Technologies*, 5(1), 27–36. <https://doi.org/10.1016/j.ifset.2003.11.001>
- Costa, N.R., Cappato, L.P., Ferreira, M.V.S., Pires, R.P.S., Moraes, J., Esmerino, E.A., Silva, R., Neto, R.P.C., Tavares, M.I.B., Freitas, M.Q., Silveira Júnior, R.N., Rodrigues, F.N., Bisaggio, R.C., Cavalcanti, R.N., Raices, R.S.L., Silva, M.C., Cruz, A.G. (2018). Ohmic Heating: A potential technology for sweet whey processing. *Food Research International*, 106, 771–779. <https://doi.org/10.1016/j.foodres.2018.01.046>
- Darvishi, H., Salami, P., Fadavi, A., Saba, M.K. (2020). Processing kinetics, quality and thermodynamic evaluation of mulberry juice concentration process using ohmic heating. *Food and Bio-products Processing*, 123, 102–110. <https://doi.org/10.1016/j.fbp.2020.06.003>
- de Castilhos, B.M., Betiol, L.F.L., de Carvalho, G.R., Telis-Romero, J. (2018). Experimental study of physical and rheological properties of grape juice using different temperatures and concentrations. Part II: Merlot. *Food Research International*, 105, 905–912. <https://doi.org/10.1016/j.foodres.2017.12.026>
- Deshmukh, P.S., Manjunatha, S.S., Raju, P.S. (2015). Rheological behaviour of enzyme clarified sapota (*Achras sapota* L.) juice at different concentration and temperatures. *Journal of Food Science and Technology*, 52, 1896–1910. <https://doi.org/10.1007/s13197-013-1222-5>

14. Evangelista, R.R., Sanches, M.A.R., de Castilhos, B.M.M., Cantu-Lozano, D., Telis-Romero, J. (2020). Determination of the rheological behavior and thermophysical properties of malbec grape juice concentrates (*Vitis vinifera*). *Food Research International*, 137, art. no. 109431.
<https://doi.org/10.1016/j.foodres.2020.109431>
15. Fadavi, A., Salari, S. (2019). Ohmic heating of lemon and grapefruit juices under vacuum pressure – Comparison of electrical conductivity and heating rate. *Journal of Food Science*, 84(10), 2868–2875.
<https://doi.org/10.1111/1750-3841.14802>
16. Fadavi, A., Yousefi, S., Darvishi, H., Mirsaedghazi, H. (2018). Comparative study of ohmic vacuum, ohmic, and conventional-vacuum heating methods on the quality of tomato concentrate. *Innovative Food Science and Emerging Technologies*, 47, 225–230.
<https://doi.org/10.1016/j.ifset.2018.03.004>
17. Fattahi, S., Zamindar, N. (2020). Effect of immersion ohmic heating on thawing rate and properties of frozen tuna fish. *Food Science and Technology International*, 26(5), 453–461.
<https://doi.org/10.1177/1082013219895884>
18. Gomathy, K., Thangavel, K., Balakrishnan, M., Kasthuri, R. (2015). Effect of ohmic heating on the electrical conductivity, biochemical and rheological properties of papaya pulp. *Journal of Food Process Engineering*, 38(4), 405–413.
<https://doi.org/10.1111/jfpe.12172>
19. Hajar, N., Asiah, M.N., Abdullah, S., Rusop, M. (2010). Anion and cation ionic conductivity of dragon fruit. *AIP Conference Proceedings*, 1250(1), 548–551.
<https://doi.org/10.1063/1.3469732>
20. Hardinasinta, G., Salengke, S., Mursalim, M., Muhidong, J. (2021). Evaluation of ohmic heating for sterilization of berry-like fruit juice of mulberry (*Morus nigra*), bignay (*Antidesma bunius*), and jambolana (*Syzygium cumini*). *IOP Conference Series: Materials Science and Engineering*, 1034, art. no. 012050.
<https://doi.org/10.1088/1757-899X/1034/1/012050>
21. Hashemi, S.M.B., Roohi, R. (2019). Ohmic heating of blended citrus juice: Numerical modeling of process and bacterial inactivation kinetics. *Innovative Food Science and Emerging Technologies*, 52, 313–324.
<https://doi.org/10.1016/j.ifset.2019.01.012>
22. Hashemi, S.M.B., Ghalamhosseinpour, A., Niakousari, M. (2019). Application of microwave and ohmic heating for pasteurization of cantaloupe juice: microbial inactivation and chemical properties. *Journal of the Science of Food and Agriculture*, 99, 4276–4286.
<https://doi.org/10.1002/jsfa.9660>
23. Hasizah, A., Mahendradatta, M., Laga, A., Metusalach, M., Supratomo, Waris, A., Salengke, S. (2018). A novel ohmic-based technology for seaweed processing. *International Food Research Journal*, 25(4), 1341–1348.
24. Icier, F., Ilicali, C. (2005). The effects of concentration on electrical conductivity of orange juice concentrates during ohmic heating. *European Food Research and Technology*, 220, 406–414.
<https://doi.org/10.1007/s00217-004-1043-x>
25. Jiang, Y., Nie, W.J. (2015). Chemical properties in fruits of mulberry species from the Xinjiang province of China. *Food Chemistry*, 174, 460–466.
<https://doi.org/10.1016/j.foodchem.2014.11.083>
26. Kobus, Z., Nadulski, R., Wilczyński, K., Starek, A., Zawisłak, K., Rydzak, L., Andrejko, D. (2019). Modeling of rheological properties of cloudy apple juice using master curve. *CyTA – Journal of Food*, 17(1), 648–655.
<https://doi.org/10.1080/19476337.2019.1630484>
27. Lemus-Mondaca, R., Ah-Hen, K., Vega-Galvez, A., Zura-Bravo, L. (2016). Effect of high hydrostatic pressure on rheological and thermophysical properties of murtilla (*Ugni molinae* Turcz) berries. *Journal of Food Science and Technology*, 53, 2725–2732.
<https://doi.org/10.1007/s13197-016-2244-6>
28. Lukhmana, N., Kong, F., Kerr, W.L., Singh, R.K. (2018). Rheological and structural properties of tart cherry puree as affected by particle size reduction. *LWT – Food Science and Technology*, 90, 650–657.
<https://doi.org/10.1016/j.lwt.2017.11.032>
29. Mannozi, C., Rompoonpol, K., Fauster, T., Tylewicz, U., Romani, S., Rosa, M.D., Jaeger, H. (2019). Influence of pulsed electric field and ohmic heating pretreatments on enzyme and antioxidant activity of fruit and vegetable juices. *Foods*, 8(7), art.no. 247.
<https://doi.org/10.3390/foods8070247>
30. Manzoor, M.F., Ahmad, N., Aadil, R.M., Rahaman, A., Ahmed, Z., Rehman, A., Siddeeg, A., Zeng, X.A., Manzoor, A. (2019). Impact of pulsed electric field on rheological, structural, and physicochemical properties of almond milk. *Journal of Food Process Engineering*, 42(8) art. no. e13299.
<https://doi.org/10.1111/jfpe.13299>
31. Marangoni Júnior, L., De Bastiani, G., Vieira, R.P., Anjos, C.A.R. (2020). Thermal degradation kinetics of total anthocyanins in açai pulp and transient processing simulations. *SN Applied Sciences*, 2, art. no. 523.
<https://doi.org/10.1007/s42452-020-2340-0>
32. Meher, J.M., Keshav, A., Mazumdar, B. (2019). Density, steady and dynamic state shear rheological properties of gongura (*Hibiscus sabdariffa*) leave puree as a function of temperature & TSS. *Carpathian Journal of Food Science and Technology*, 11(4), 81–95.
<https://doi.org/10.34302/2019.11.4.7>
33. Mitschka, P. (1982). Simple conversion of Brookfield R.V.T. readings into viscosity functions. *Rheologica Acta*, 21, 207–209.
<https://doi.org/10.1007/BF01736420>
34. Mohammadi-Moghaddam, T., Firoozzare, A., Parak, Z., MohammadaNia, M. (2020). Physicochemical properties, sensory attributes, and antioxidant activity of black plum peel sharbat as affected by pectin and puree concentrations. *International Journal of Food Properties*, 23(1), 665–676.
<https://doi.org/10.1080/10942912.2020.1754235>
35. Park, I.K., Kang, D.H. (2013). Effect of electroporation by ohmic heating for inactivation of *Escherichia coli* O157: H7, *Salmonella enterica* serovar typhimurium, and *Listeria monocytogenes* in buffered peptone water and apple juice. *Applied and Environmental Microbiology*, 79(23), 7122–7129.
<https://doi.org/10.1128/AEM.01818-13>
36. Payne, E.M., Reyes-De-Corcuera, J.I. (2021). Combined rotational and capillary rheometry to determine slip coefficients and other rheological properties of orange pulp. *Journal of Food Science*, 86(1), 86–94.
<https://doi.org/10.1111/1750-3841.15554>

37. Petruzzi, L., Campaniello, D., Speranza, B., Corbo, M.R., Sinigaglia, M., Bevilacqua, A. (2017). Thermal treatments for fruit and vegetable juices and beverages: A literature overview. *Comprehensive Reviews in Food Science and Food Safety*, 16(4), 668–691. <https://doi.org/10.1111/1541-4337.12270>
38. Polat, R., Satil, F. (2012). An ethnobotanical survey of medicinal plants in Edremit Gulf (Balıkesir – Turkey). *Journal of Ethnopharmacology*, 139(2), 626–641. <https://doi.org/10.1016/j.jep.2011.12.004>
39. Poojitha, P., Athmaselvi, K.A. (2018). Influence of sucrose concentration on electric conductivity of banana pulp during ohmic heating. *Food Science and Technology International*, 24(8), 664–672. <https://doi.org/10.1177/1082013218787069>
40. Renard, C., Maingonnat, J.F. (2012). Thermal processing of fruits and fruit juices. In D.W. Sun (Ed.) *Thermal Food Processing: New Technologies and Quality Issues*, Second Edition, Chapter 16, CRC Press, pp. 413–438. <https://doi.org/10.1201/b12112-19>
41. Ribeiro, L.D.O., Almeida, A.C.S., Carvalho, P.De C.W., Borguini, R.G., Ferreira, C.J.S., Freitas, S.P., da Metta, V.M. (2018). Effect of processing on bioactive compounds, physicochemical and rheological characteristics of juçara, banana and strawberry smoothie. *Plant Foods for Human Nutrition*, 73, 222–227. <https://doi.org/10.1007/s11130-018-0681-2>
42. Rinaldi, M., Littardi, P., Paciulli, M., Ganino, T., Cocconi, E., Barbanti, D., Rodolfi, M., Aldini, A., Chiavaro, E. (2020). Impact of ohmic heating and high pressure processing on qualitative attributes of ohmic treated peach cubes in syrup. *Foods*, 9(8), art no. 1093. <https://doi.org/10.3390/foods9081093>
43. Rodrigues, E.L., Marcelino, G., Silva, G.T., Figueiredo, P.S., Garcez, W.S., Corsino, J., Guimarães, R.de C.A., Freitas, K. de C. (2019). Nutraceutical and medicinal potential of the *Morus* species in metabolic dysfunctions. *International Journal of Molecular Sciences*, 20(2), art. no. 301. <https://doi.org/10.3390/ijms20020301>
44. Rojas, M.L., Leite, T.S., Cristianini, M., Alvim, I.D., Augusto, P.E.D. (2016). Peach juice processed by the ultrasound technology: Changes in its microstructure improve its physical properties and stability. *Food Research International*, 82, 22–33. <https://doi.org/10.1016/j.foodres.2016.01.011>
45. Sabanci, S., Icier, F. (2020). Rheological behavior of sour cherry juices concentrated by ohmic and conventional evaporation processes under vacuum. *Journal of Food Processing and Preservation*, 44(10), art no. e14832. <https://doi.org/10.1111/jfpp.14832>
46. Salengke, S., Hasizah, A., Reta, Mochtar, A.A. (2019). Technology innovation for production of specialty coffee. *IOP Conference Series: Earth and Environmental Science*, 355, art. no. 012105. <https://doi.org/10.1088/1755-1315/355/1/012105>
47. Salengke, S., Sastry, S.K. (2007). Models for ohmic heating of solid-liquid mixtures under worst-case heating scenarios. *Journal of Food Engineering*, 83(3), 337–355. <https://doi.org/10.1016/j.jfoodeng.2007.03.026>
48. Sarkis, J.R., Mercali, G.D., Tessaro, I.C., Marczak, L.D.F. (2013). Evaluation of key parameters during construction and operation of an ohmic heating apparatus. *Innovative Food Science and Emerging Technologies*, 18, 145–154. <https://doi.org/10.1016/j.ifset.2013.02.001>
49. Srivastav, S., Roy, S. (2014). Changes in electrical conductivity of liquid foods during ohmic heating. *International Journal of Agricultural and Biological Engineering*, 7(5), 133–138. <https://doi.org/10.3965/j.ijabe.20140705.015>
50. Tirloni, E., Vasconi, M., Cattaneo, P., Moretti, V., Bellagamba, F., Bernardi, C., Stella, S. (2020). A possible solution to minimise scotta as a food waste: A sports beverage. *International Journal of Dairy Technology*, 73(2), 421–428. <https://doi.org/10.1111/1471-0307.12647>
51. Varghese, K.S., Pandey, M.C., Radhakrishna, K., Bawa, A.S. (2014). Technology, applications and modelling of ohmic heating: A review. *Journal of Food Science and Technology*, 51, 2304–2317. <https://doi.org/10.1007/s13197-012-0710-3>

Optimized Extraction, Microencapsulation, and Stability of Anthocyanins from *Ardisia compressa* K. Fruit

María Vianey Antonio-Gómez¹, Yolanda Salinas-Moreno^{2*} , Francisco Hernández-Rosas¹ , Fernando Martínez-Bustos³ , Isaac Andrade-González⁴ , José Andrés Herrera-Corredor¹ 

¹Postgraduate College, Campus Cordoba. Postgraduate in Sustainable Agrifood Innovation, Km 348 carretera Córdoba-Veracruz, 94946, Amatlán de los Reyes, Veracruz, Mexico

²National Institute of Forestry, Agriculture and Livestock Research, Experimental Field Centro Altos de Jalisco, Km 8 carretera Tepatitlán-Lagos de Moreno, Tepatitlán de Morelos, CP 47600 Jalisco, Mexico

³Center for Research and Advanced Studies of the National Polytechnic Institute, Campus Querétaro, Libramiento Norponiente No. 2000, Fraccionamiento Real de Juriquilla, CP 76230 Santiago de Querétaro, Querétaro, Mexico

⁴Technological Institute of Tlajomulco, Jalisco, Agri-Food processes pilot plant,

Km 10 carr. A San Miguel, Cuyutlán, Tlajomulco de Zúñiga, CP 45640 Jalisco, Mexico

Key words: *Ardisia compressa* K., tropical fruit, microcapsules, anthocyanins, spray drying

The fruit of *Ardisia compressa* K. is called chagalapoli and has a high anthocyanin content, with a profile dominated by malvidin derivatives. The aims of this study were: a) to determine optimal conditions (ethanol concentration, pH, and sonication time) for anthocyanin extraction from chagalapoli fruit (CF) using response surface methodology, b) to perform spray-drying microencapsulation of the anthocyanins using mixtures of polysaccharides (maltodextrin – M and Capsul® – C) as wall materials, and c) to evaluate the stability of microcapsules during storage. Of the variables examined to optimize anthocyanin extraction from CF, only ethanol concentration and pH were significant in the model. The optimal extraction conditions were: 63.5% (v/v) ethanol, pH of 2.0, and sonication time of 30 min, which led to an anthocyanin content of 1545 mg malvidin 3-*O*-galactoside equivalents/100 g of fresh fruit. The proportion of M/C as the wall materials for microcapsule (MC) preparation did not affect the encapsulation efficiency and anthocyanin retention, but high hygroscopicity was observed in the MC with a high proportion of M. The half-life of the MC ranged from 423 to 519 days, and no effect of wall materials was observed. The color stability of the MC was enhanced by increasing C proportion in wall materials. The high stability of microencapsulated anthocyanins of chagalapoli fruit makes it a suitable option as a food colorant.

INTRODUCTION

Nowadays, the food industry has an increasing demand for natural pigments prompted by the banning of most synthetic colorants commonly used in food products [Luzardo-Ocampo *et al.*, 2021], and by consumer preferences for products without artificial colorants. Anthocyanins are vegetal pigments related with shades of pink, red, blue, and purple colors, that are easily incorporated in food matrices due to their water solubility [Giusti & Wrolstad, 2003]. They also represent an alternative to synthetic dyes. Besides being pigments, anthocyanins possess several biological activities such as antioxidative, antimutagenic, and anti-inflammatory ones [Bendokas *et al.*, 2020].

In the process of incorporating a new vegetal source of pigments, it is necessary to determine the most suitable combinations of factors relating to anthocyanin recovery, as these

factors affect the performance and profitability of the extraction, and also the type of phenolics extracted [Najafabadi *et al.*, 2020] and their stability [Pedro *et al.*, 2016]. Among the factors most studied in anthocyanin extraction are: solid to solvent ratio [Pedro *et al.*, 2016], solvent type, and temperature [Ghafoor *et al.*, 2011], extraction time [Najafabadi *et al.*, 2020], and pH [Rodrigues *et al.*, 2015]. The effect of the extraction conditions on the anthocyanin yield and composition of the extract depends on the matrix [Najafabadi *et al.*, 2020]; therefore, it is recommended to adjust the conditions for each particular material.

The instability of anthocyanins to several factors commonly present during food processing, such as changes in pH, heating, exposure to light and oxygen, presence of metal ions, and enzymes [Tarone *et al.*, 2020], has limited their use as food colorants. The instability has been overcome with encapsulation technology, which permits to obtain microspheres.

* Corresponding Author:

Tel.: +52 01 800 088 2222, ext:84501

E-mail: salinas.yolanda@inifap.gob.mx (Y. Salinas-Moreno)

Submitted: 14 January 2021

Accepted: 20 July 2021

Published on-line: 20 August 2021



The microspheres or microcapsules have a wall that protects the active compound from external factors. In the case of anthocyanins, different encapsulation wall materials, *i.e.* gums, polysaccharides, and lipids or proteins, have been tested [Tarone *et al.*, 2020], on their own or in combination of two or more wall materials, to achieve the required properties that ensure satisfactory microencapsulation [Turchiuli *et al.*, 2005]. The selection of suitable wall materials is an important step in the microencapsulation process because of its effect on the microcapsule surface and stability.

Spray-drying is one of the most popular and economical techniques used in the industry to microencapsulate food ingredients [Tarone *et al.*, 2020]. For its application, it is necessary that the wall materials have emulsifying properties, with high solubility and low hygroscopicity [Loksuwan, 2007]. Carbohydrates of low molecular weight compounds have these properties. Maltodextrin is one of the most commonly used materials due to its high solubility and low viscosity [Tonon *et al.*, 2010]. Furthermore, Capsul[®], a starch that has been chemically modified through the incorporation of a lipophilic component (octenylsuccinate), has excellent stability and emulsifying properties [Rocha *et al.*, 2012].

The stability of microcapsules is determined by such features as shape, integrity, porosity, and moisture sorption characteristics. The right combinations of these features make it possible that microcapsules retain the compounds they protect for a reasonable time, when they are stored under room conditions.

Several tropical fruits have been identified as potential sources of anthocyanins [de Brito *et al.*, 2007]. One of these is the fruit of *Ardisia compressa* K. (ACK), known as chagalapoli, which has a high anthocyanin content (natural pigment) [Joaquín-Cruz *et al.*, 2015]. Recently, anthocyanins from chagalapoli fruit (CF) were used to prepare nanoparticles with succinated starch as a wall material [Escobar-Puentes *et al.*, 2020]. However, limited information is available about the optimal conditions for extracting the anthocyanins from CF, nor on the most suitable combination of wall materials for microencapsulating the anthocyanins from this fruit. In this context, the aims of this study were: a) to optimize the extraction of anthocyanins from CF, b) to microencapsulate the anthocyanins using maltodextrin and Capsul[®] mixtures as wall materials, and c) to evaluate the stability of the microcapsules.

MATERIALS AND METHODS

Reagents and plant material

The chemicals included analytical grade ethanol, hydrochloric acid, formic acid, and methanol (J.T. Baker, Phillipsburg, NJ, USA). HPLC-grade water and methanol (J.T. Baker, Phillipsburg, NJ, USA) were used for the analysis of anthocyanins as part of the mobile phases used. Commercial standards of delphinidin 3-*O*-galactoside (Dp 3-Gal) and malvidin 3-*O*-galactoside (Mv 3-Gal) were used (Extrasynthese, Genay, France) for running standard curves. The wall materials were 10 DE maltodextrin (IMSA, SA de CV, Guadalajara, Mexico), and Capsul[®] (Ingredion, Guadalajara, Mexico).

The plant material consisted of 3 kg of ripe fruits of chagalapoli (*A. compressa*) obtained from the regional market

TABLE 1. Ranges and levels of independent process variables considered in the Box-Behnken design.

Independent variable	Factors	Coded levels		
		-1	0	1
Solvent pH	A	2	2.5	3
Ethanol concentration (%)	B	50	75	100
Sonication time (min)	C	10	20	30

of San Andres Tuxtla, Veracruz, Mexico. The seed was removed, and the fruit pulp was homogenized using an Ultra Turrax homogenizer (T-10 Basic, IKA, Wilmington, NC, USA) for one min at a speed of 20,450 rpm.

Optimization of anthocyanin extraction

Response surface methodology (RSM) was used to optimize the extraction conditions of anthocyanins from CF. According to the preliminary tests, the optimal proportion of fruit pulp/solvent was established as 1:5 (*w/v*). The experimental design was based on a Box-Behnken design with three factors – pH (A), ethanol concentration (B), and sonication time (C) – with three replicates each. The response variable was the total anthocyanin content (TAC). The experimental design resulted in 15 treatments (T1 to T15) with the details of the factors and levels provided in Table 1.

Two grams of the homogenized fruit pulp and 10 mL of a solvent (aqueous ethanol) were used for each treatment. After sonication, the sample of each treatment was stirred for 30 min in a horizontal shaker at room temperature under dark conditions. Extracts were recovered by centrifugation (Centrifuge Universal Model 32. Hettich[®], Tuttlingen, Germany) of the sample at 2558×*g* for 10 min, and the total anthocyanin content (TAC) was determined with the methodology described by Moreno *et al.* [2005]. Briefly, the absorbance of the extract was measured at 530 nm using a spectrophotometer (Lambda 25 UV/Vis, Perkin Elmer, Waltham, MA, USA). A standard curve of malvidin 3-*O*-galactoside was obtained to express the results as mg Mv 3-Gal equivalents/100 g fresh weight (FW).

A second-order polynomial model was constructed to estimate the response of TAC to the different extraction treatments (Equation 1). In the equation, “*y*” is the estimated response (dependent variable); β_0 is a constant in the model; β_i is the linear effect coefficient; β_{ii} is the quadratic effect coefficient; β_{ij} is the coefficient of the interaction between two factors; x_i and x_j are the independent variables; *k* is the number of variables considered, and *i* and *j* are the factors coded into the system [Swamy *et al.*, 2014].

$$y = \beta_0 + \sum_{i=1}^k \beta_i \times x_i + \sum_{i=1}^k \beta_{ii} \times x_i^2 + \sum_{i=1}^{k-1} \sum_{j>1}^k \beta_{ij} \times x_i \times x_j \quad (1)$$

HPLC analysis of the anthocyanin extract

A Perkin-Elmer[®] Series 200 instrument, operated with Total-Chrome software and consisting of a photodiode array detector, a quaternary pump, and an autosampler with one thermostatted

column compartment was used (PerkinElmer® Instruments LLC, Shelton, CT, USA). A C18 ODS Hypersil (200 × 4.6 mm) column with a particle size of 5 μm (Thermo Fisher Scientific®, Carlsbad, CA, USA) was employed for the separation of chagapoli anthocyanins obtained under the optimized extraction conditions. The extract was filtered through a 0.20 μm Millex-LG® membrane filter (Millex PTFE, 4 mm, Sigma-Aldrich, Toluca, Mexico) prior to injection. The analysis was performed according to the method of Fossen *et al.* [2001], with the adjustments described by Moreno *et al.* [2005] in a system of gradients. Two solvents were used: A (1:9, v/v) (formic acid/water) and B (1:4:5, v/v/v) (formic acid/water/methanol). The gradient was linear from 10% B to 100% B for 17 min, isocratic elution for the next 4 min (100% B), followed by a linear gradient from 100% B to 10% B for 1 min, with an equilibrium time of 4 min, before the next injection. The flow rate was 1.2 mL/min with an injection volume of 10 μL and a column temperature of 30°C. Anthocyanins were identified by the use of commercial standards, and by comparison with the information reported by Joaquín-Cruz *et al.* [2015].

Spray-drying microencapsulation of anthocyanins

The anthocyanin extract obtained under the optimized extraction conditions was used for analyses. It was concentrated in a rotary evaporator system to remove ethanol. The carbohydrates used as wall materials were maltodextrin 10 DE (M) and Capsul® (C). Five treatments of different proportions of each carbohydrate in a weight ratio were prepared including 100% M (100M) and 100% C (100C) and combinations of M and C: 75% M and 25% C (75M25C), 50% M and 50% C (50M50C), and 25% M and 75% C (25M75C).

A suspension of extract and wall materials was prepared at a final concentration of 20% (w/v). Fifty grams of wall material were dissolved in 200 mL of distilled water and homogenized in a blender (Waring® brand) for 1 min at a low speed. Thereafter, 50 mL of concentrated extract was added and homogenized with an Ultra Turrax homogenizer (Wilmington, NC, USA) at 18,000 rpm for 5 min. Encapsulation was performed in a spray dryer (SD-Basic Lab-Plant, Huddersfield, UK) under the following conditions: inlet air temperature of 160 ± 1°C, outlet air temperature of 95 ± 5°C, pressure of 241.3 KPa, nozzle diameter of 0.5 mm, and a feed stream of 10 mL/min. These conditions were selected based on preliminary experiments by the authors. The microcapsules (MC) were collected in plastic bags, weighed, and stored in a desiccator, under darkness, at room temperature.

Efficiency of microencapsulation process and characterization of the microcapsules

The encapsulation efficiency (EE) was determined according to the methodology used by García-Tejeda *et al.* [2015]. The experimental content of total anthocyanins (TAC_e) was determined with the method of differential pH [Giusti & Wrolstad, 2001], and the results were expressed as mg Mv 3-Gal equivalents/g of microcapsules using a molar extinction coefficient of 28,000 L/(mol · cm) and a molecular weight of 463.3 g/mol.

Extraction of superficial anthocyanins was determined according to the modified method of Robert *et al.* [2010], in which 500 mg of microcapsules were treated with 10 mL

of isopropanol and dispersed by vortexing at room temperature for one min and then filtered (Millipore 0.45 μ filter). The EE was calculated using Equation (2):

$$EE = 1 - \frac{SAC}{TAC_e} \times 100 \quad (2)$$

where: TAC_e is the experimental content of total anthocyanins and SAC is the content of superficial anthocyanins; all values are expressed as mg/g of MC.

Moisture content and water activity

The moisture content (MT) of the MC was determined according to AACC Method 44–19 [AACC, 1995]. The water activity (a_w) was measured with an Aqualab® device (Model Series 3TE, Decagon Devices, Pullman, WA, USA).

Hygroscopicity and solubility

The hygroscopicity (H) of the MC was determined according to Tonnon *et al.* [2009]. Briefly, 1 g of MC was placed in a jar with an NaCl saturated solution (76% relative humidity) at 25°C. After one week, the samples were weighed, and the hygroscopicity was expressed as g of absorbed moisture per 100 g of dry solids. The solubility of MC was evaluated with the method described by Arrazola *et al.* [2014], in which 1 g of MC was poured in 100 mL of distilled water and stirred to dissolve. The sample was centrifuged for 10 min at 1409 × g, and 25 mL of the supernatant was placed in a glass capsule to evaporate the liquid in an oven at 105°C for 5 h. Solubility (%) was calculated by weight difference.

Scanning electron microscopy and particle size determination

The external morphology of MC was evaluated by laser microscopy (OLS4000 LEXT® 3D, Olympus, Tokyo, Japan) and scanning electron microscopy (ESEM EDAX®, GSE detector, Philips, Netherlands) coupled with energy dispersive spectrometry (spectrometer model 6110 XFlash®, Bruker corporation, Billerica, MA, USA) using an acceleration voltage of 15 kV. The samples were fixed to double-sided metal adhesive tape, and coated with a 10 to 15 nm graphite film *via* evaporation for one min. The Image Pro PLUS® version 7.0 (Media Cybernetics, Inc., Rockville, MD, USA) software was used to determine the diameter of the microcapsules *via* image processing.

Anthocyanin stability during storage

The stability of the anthocyanins in the MC was evaluated using the accelerated shelf life method proposed by Labuza & Schmidl [1985]. In brief, approximately 500 mg of MC of each treatment were put in Eppendorf tubes which were sealed with aluminum foil to protect them from light, and placed in a rack. The rack with the tubes was placed in an oven at 35°C. The TAC of the MC was monitored every seven days during a 70-day period, using the differential pH method [Giusti & Wrolstad, 2001]. The analysis was done in triplicate. The color of the MC was determined with a HunterLab MiniScan EZ 4500L spectrophotometer (Hunter Associates, Reston, VA, USA) in the CIE L*a*b* scale at day 0, and after 70 days of storage. The following

TABLE 2. Box-Behnken experimental design (different extraction conditions) and response values for the total anthocyanin content (TAC) of chagala-poli fruit.

Treatment	pH	Ethanol concentration (%)	Sonication time (min)	Experimental TAC (mg Mv3-Gal/100 g FW*)	Predicted TAC (mg Mv3Gal/100 g FW)
T1	2.0	75	30	1557±31	1466
T2	2.5	100	30	206±6	244
T3	3.0	50	20	652±25	598
T4	2.0	100	20	325±36	378
T5	3.0	75	30	822±36	887
T6	2.5	75	20	1166±43	1103
T7	2.0	75	10	1422±47	1357
T8	3.0	75	10	825±11	917
T9	3.0	100	20	190±8	89
T10	2.5	75	20	1044±43	1103
T11	2.5	100	10	218±10	228
T12	2.5	75	20	1100±21	1103
T13	2.0	50	20	1227±4	1328
T14	2.5	50	30	1008±14	998
T15	2.5	50	10	972±7	934

*FW – fresh weight.

parameters: luminosity (L^* , with 0 for black and 100 for white); a^* ($+a^*$, red color; $-a^*$, green color); and b^* ($+b^*$, yellow color; $-b^*$, blue color) were obtained with the equipment. The measurements were done in triplicate.

The degradation of the anthocyanins in the MC was studied with the first-order kinetic model. The value of the degradation constant (k) was determined according to Equation (3):

$$\ln(C_t) = \ln C_0 - k(t) \quad (3)$$

where: C_t is TAC of MC at time t ; C_0 is initial TAC of the MC; and t is storage time. The half-life of the MC was determined according to Equation (4), at the specific storage temperature.

$$t_{1/2} = -\ln(0.5) / kT \quad (4)$$

where: $t_{1/2}$ is the half-life time of anthocyanins in the MC; k is the kinetic degradation constant; and T is storage temperature [Idham *et al.*, 2012].

Anthocyanin retention (AR) was determined using the equation:

$$AR(\%) = 100 - AL(\%) \quad (5)$$

where: AL is the loss of anthocyanins at the time t and was calculated using the following equation:

$$AL(\%) = \left[1 - \frac{C_t}{C_0}\right] \times 100 \quad (6)$$

Statistical analysis

The statistical analysis of data from optimized anthocyanin extraction were performed using Statgraphics Centurion version 16.1 (Manugistics Inc., Statistical Graphics Corporation, Rockville, MD, USA) software. Data from efficiency of microencapsulation and MC characteristics and color changes during storage were analyzed by one-way analysis of variance (ANOVA) and comparison Tukey's tests ($p < 0.05$) were performed using the statistical package SAS version 9.1.

RESULTS AND DISCUSSION

Optimization of anthocyanins extraction

The TAC for all 15 treatments, and those calculated using the response surface model are shown in Table 2. The TAC ranged from 190 to 1557 mg Mv 3-Gal equivalents/100 g FW for T9 and T1 treatments, respectively. The differences in TAC between these two treatments show the importance of selecting the suitable levels of the factors involved in anthocyanin extraction. The experiments that resulted in the highest anthocyanin recovery included T1, T7, and T13, which utilized a pH value of 2 and ethanol percentage between 50 and 75%.

The ANOVA showed a coefficient of determination (R^2) of 0.9760, indicating that the quadratic model was consistent with the experimental data. In addition, the adjusted value of R^2 (0.9634) showed a high correlation between the experimental values and the predicted values for the recovery of anthocyanins (Table 3).

TABLE 3. Analysis of variance of the effect of the process variables, as linear and quadratic terms, and the interactions, on the optimization of anthocyanin extraction from chagalapoli fruit.

Source	Sum of squares	df	Mean square	F statistic	P-value
A: pH	1.04E+06	1	1.04E+06	148.58	<0.0001
B: Ethanol concentration (%)	2.13E+06	1	2.13E+06	304.41	<0.0001
C: Sonication time (min)	6184.64	1	6184.64	0.88	0.359
AB	97121.5	1	97121.5	13.88	0.0014
AC	9546.17	1	9546.17	1.36	0.2573
BC	1153.44	1	1153.44	0.16	0.6893
AA	4710.25	1	4710.25	0.67	0.4222
BB	2.07677E+06	1	2.0768E+06	296.7	<0.0001
CC	5734.1	1	5734.1	0.82	0.3767
Total error	132992	19	6999.56		
Total	5.56E+06	29			

R² = 0.9760 Adjusted R²=0.9634

df – degrees of freedom.

The adjusted model that predicts the response of TAC is shown in Equation 7, where y is TAC.

$$y = 638.96 + 1103.44A - 254.95B + 25.25BA - 34.54 \times B^2 \quad (7)$$

This model was validated with ANOVA before building the response surface graphs presented in Figure 1.

The ANOVA results show that the pH (A) and ethanol concentration (B) had a significant ($p < 0.05$) effect on the process of anthocyanin extraction (Table 3). The pH effect was linear ($p < 0.05$), indicating that the recovery of anthocyanins increased as the pH decreased (Figure 1A and B).

This remark is consistent with the results obtained by Rodrigues *et al.* [2015], who evaluated the effects of pH in a range of 0.5 to 6.5 on the optimization of the extraction of anthocyanins from jaborcaba (*Myrciaria* spp.) skins, and found that anthocyanin recovery was favored at a pH below 3.5 and above 4. A previous study [Brouillard, 1982] demonstrated that pH affected the stability of anthocyanins, since their structure can undergo a reversible transformation in aqueous media, in a pH-dependent manner. The flavylium cation structure predominated at pH of 1, while the quinoidal base predominated at pH between 2 and 4, but the most stable chemical structure of anthocyanins was the flavylium cation.

The concentration of ethanol, both in its linear and quadratic form, had a positive effect on the extraction process (Table 3 and Figure 1C). However, a decrease in the recovery of anthocyanins occurred at ethanol concentrations higher than 70%. The highest recovery of anthocyanins was achieved at ethanol concentration between 60% and 70%. This is in agreement with previous studies [Khazaei *et al.*, 2016], which showed that the recovery of anthocyanins was facilitated at ethanol levels of 60–70%. Sonication time

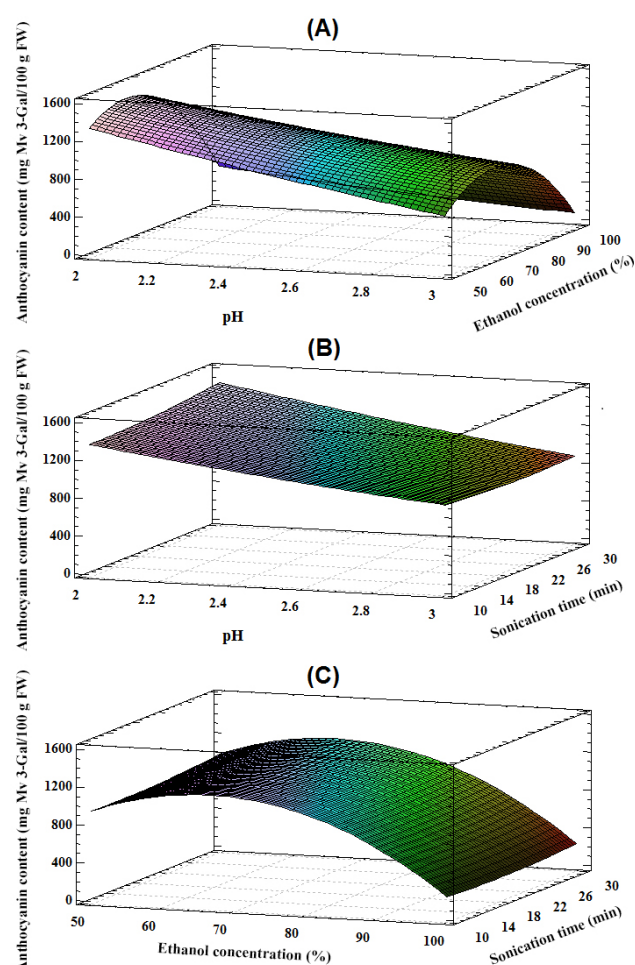


FIGURE 1. Response surface plots of the Box–Behnken design using polynomial equations of the effects of pH and ethanol concentration (A), pH and sonication time (B), and ethanol concentration and sonication time (C) on total anthocyanin content of chagalapoli fruit fresh weight (FW).

showed no significant effect on the recovery of anthocyanins (Figure 1B). The time (min) of sonication tested in the model may not have been sufficient to affect anthocyanin yield. However, sonication as a tool to improve recovery of phytochemicals from vegetal tissue has been highly valued [Rosello-Soto *et al.*, 2015]. The optimized conditions for the extraction of anthocyanins were: ethanol concentration of 63.5% (v/v), pH of 2.0, and sonication time of 30 min.

The optimal point was verified experimentally, resulting in an anthocyanin recovery of 1545 mg Mv 3-Gal equivalents/100 g FW. This value is higher than that reported by Joaquín-Cruz *et al.* [2015] for the same fruit (796 mg cyanidin-3-*O*-glucoside equivalents/100 g FW) who used acidified methanol as a solvent and no sonication treatment. The differences among the values reported by Joaquín-Cruz *et al.* [2015] and in the present study could be due to the type of anthocyanin used to express TAC. The protocol developed in this work could be applied to commercial anthocyanin extraction for food applications due to its single extraction step performed with substances that are safe for use in foods (GRAS classification).

HPLC analysis of chagalapoli fruit anthocyanins

The chromatogram presented in Figure 2 shows the profile of the anthocyanins extracted from CF at the optimized extraction conditions, which ensured the highest TAC. Twelve

anthocyanins were detected of which the most abundant was malvidin 3-*O*-galactoside (Mv 3-Gal), followed by petunidin 3-*O*-galactoside (Pt 3-Gal) and delphinidin 3-*O*-galactoside (Dp 3-Gal). These three anthocyanins accounted for approx. 78.4% of the relative percentage of peak area of the separated anthocyanins. Other anthocyanins detected in CF were malvidin di-*O*-hexoside (peak 2), cyanidin 3-*O*-galactoside (peak 3), delphinidin 3-*O*-arabinoside (peak 5), cyanidin 3-*O*-arabinoside (peak 7), peonidin 3-*O*-galactoside (peak 8), petunidin 3-*O*-arabinoside (peak 9), and malvidin 3-*O*-arabinoside (peak 12). The anthocyanin profile obtained is similar to that reported by Joaquín-Cruz *et al.* [2015] for CF anthocyanins extracted with acidified methanol and no sonication treatment, which probably means that the anthocyanin profile of CF is not altered by the extraction conditions, and the procedure defined could be used to enhance anthocyanin recovery from CF.

Microencapsulation process parameters and microcapsule characterization

Table 4 lists the results of determinations of the variables related to the microencapsulation process, *i.e.* EE and physicochemical characteristics of the MC. The EE is a variable that relates/describes the ability of wall materials to trap or hold the core material to be encapsulated. High values of EE are associated with low levels of core material on the surface

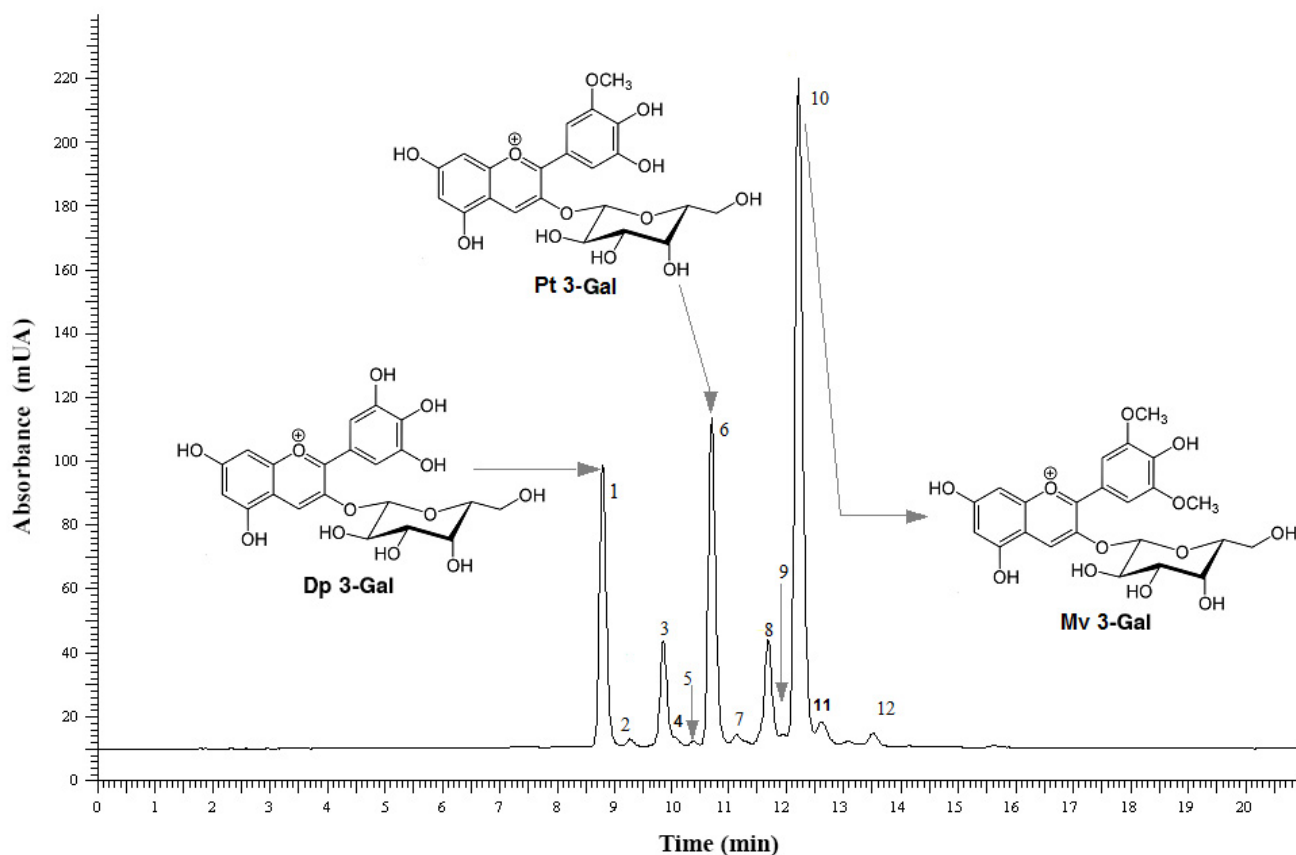


FIGURE 2. RP-HPLC chromatogram of the anthocyanins from chagalapoli fruit (*Ardisia compressa* Kush).

Anthocyanins were obtained under the optimized extraction process. Pt 3-Gal: petunidin 3-*O*-galactoside, Mv 3-Gal: malvidin 3-*O*-galactoside, Dp 3-Gal: delphinidin 3-*O*-galactoside, Gal: galactoside. Peaks 1–12 correspond to different anthocyanins present in the extract.

TABLE 4. Encapsulation productivity and efficiency and physicochemical characteristics of chagalapoli fruit anthocyanin microcapsules obtained with different combinations of maltodextrin (M) and Capsul® (C) as wall materials.

Treatments	EP (%)	EE (%)	MT (g/100 g)	a_w	H (g/100 g)	S (%)
100M	95.60±0.76 ^{b1}	99.40±0.00 ^b	1.83±0.12 ^c	0.15±0.01 ^a	13.81±0.07 ^a	97.06±0.08 ^b
75M25C	95.71±0.92 ^b	99.65±0.02 ^a	2.63±0.07 ^a	0.13±0.01 ^{ab}	13.15±0.11 ^b	97.42±0.04 ^a
50M50C	98.27±0.55 ^a	99.66±0.01 ^a	2.47±0.19 ^{ab}	0.13±0.01 ^{ab}	11.48±0.32 ^c	96.52±0.11 ^c
25M75C	99.25±0.85 ^a	99.65±0.01 ^a	2.74±0.40 ^a	0.11±0.00 ^b	11.42±0.11 ^c	97.10±0.11 ^b
100C	99.47±0.19 ^a	99.67±0.01 ^a	1.89±0.01 ^{bc}	0.13±0.00 ^{ab}	10.82±0.07 ^d	96.40±0.20 ^c
SMD (0.05)	1.934	0.0311	0.6285	0.0193	0.4889	0.3043

EP – encapsulation productivity; EE – encapsulation efficiency; MT – moisture content; a_w – water activity; H – hygroscopicity; S – solubility; SMD – significant minimum difference. M100: maltodextrin 100%; 75M25C: 75% maltodextrin 25% Capsul®; 50M50C: 50% maltodextrin 50% Capsul®; 25M75C: 25% maltodextrin 75% Capsul®; 100C: 100% Capsul®. ¹Mean of three repetitions ± standard deviation. Means with different letters within a given column indicate statistically significant difference ($p < 0.05$).

of the microcapsule and improved stability of the microencapsulated compound [Mahdavi *et al.*, 2016]. The values obtained for this variable were greater than 99 g/100 g for all treatments (Table 4).

Although significant differences ($p < 0.05$) were found among the treatments, differences may not be relevant from a practical point of view. Results of this study are similar to those of Norkaew *et al.* [2019] who reported 100 g/100 g of EE in the encapsulation of anthocyanins from black rice using maltodextrin and gelatin as wall material, on their own or in combination, but higher compared to the results reported by Righi da Rosa *et al.* [2019] who microencapsulated blueberry anthocyanins with maltodextrin DE20 and starch “hi-maize” as wall materials. The mentioned authors used similar drying conditions as in this study.

The variables MT, a_w , and H are important for microcapsule storage, because they are related to the water “status”

of the MC, and indeed, with the stability of polysaccharides forming the encapsulating wall. The MT of the microcapsules from the five treatments ranged from 1.83 to 2.74 g/100 g. The lower values were obtained in the treatments with single wall material (Table 4). MT is affected by the feed flow rate and the inlet and outlet temperatures during the spray drying process. It is desirable to have low MT values to enhance storability of the MC. The values obtained are lower than those reported by Silva *et al.* [2013] for MC of jaboticaba anthocyanins made with M (4.84 g/100 g), and a mixture of M:C in a 17.7:83.3 ratio (5.3 g/100 g), obtained under the same drying conditions. The a_w of microcapsules was between 0.11 and 0.15. The a_w values obtained are below the maximum limit of 0.3 required to guarantee the stability of the powders during storage [Tonon *et al.*, 2009]. García-Tejeda *et al.* [2015] reported a_w values of 0.19 and 0.26 for anthocyanin MC produced with modified starches derived from normal



FIGURE 3. Microcapsules of anthocyanins from chagalapoli fruit prepared with different proportions of maltodextrin (M) and Capsul® (C) as wall materials, at the initial day and after one week of storage in open plastic containers at room temperature.

and waxy maize, respectively. In the case of MC, the variables MT and a_w are dependent on the drying temperature (inlet and outlet temperatures), with high temperatures resulting in low values of these variables [Frascareli *et al.*, 2012].

The proportion of M:C significantly affected the hygroscopicity of the MC. Greater H values were observed for treatments with a high proportion of M (100M and 75M25C) in which the particles had an intense pink-red color due to hydration after seven days of storage in open plastic containers (Figure 3). Silva *et al.* [2013] reported similar results on hygroscopicity of microcapsules prepared using M and C mixtures during the encapsulation of jaboticaba anthocyanins.

It is recommended that the H value of MC be between 10 and 12 g/100 g to prevent absorbing moisture from the atmosphere during storage. Microcapsules with high H (>14 g/100 g), become soft and thereby lose their protective

properties against external agents, such as oxygen, light, and free radicals, which could degrade anthocyanins [Silva *et al.*, 2013].

The solubility (S) of the microcapsules varied from 96.4 to 97.4%, and no effect of M or C proportion in the wall material mixtures was observed. The solubility values of the microcapsules obtained were sufficient for the complete incorporation in hydrophilic food systems.

Microcapsule morphology

The MC were spherical in shape and had different sizes (Figure 4), which is typical of spray-drying generated powders. Mixtures of different wall materials result in different MC morphology. The 100M treatment produced smaller microspheres with a smoother surface than the treatments in the presence of C, in which spherical MC predominated,

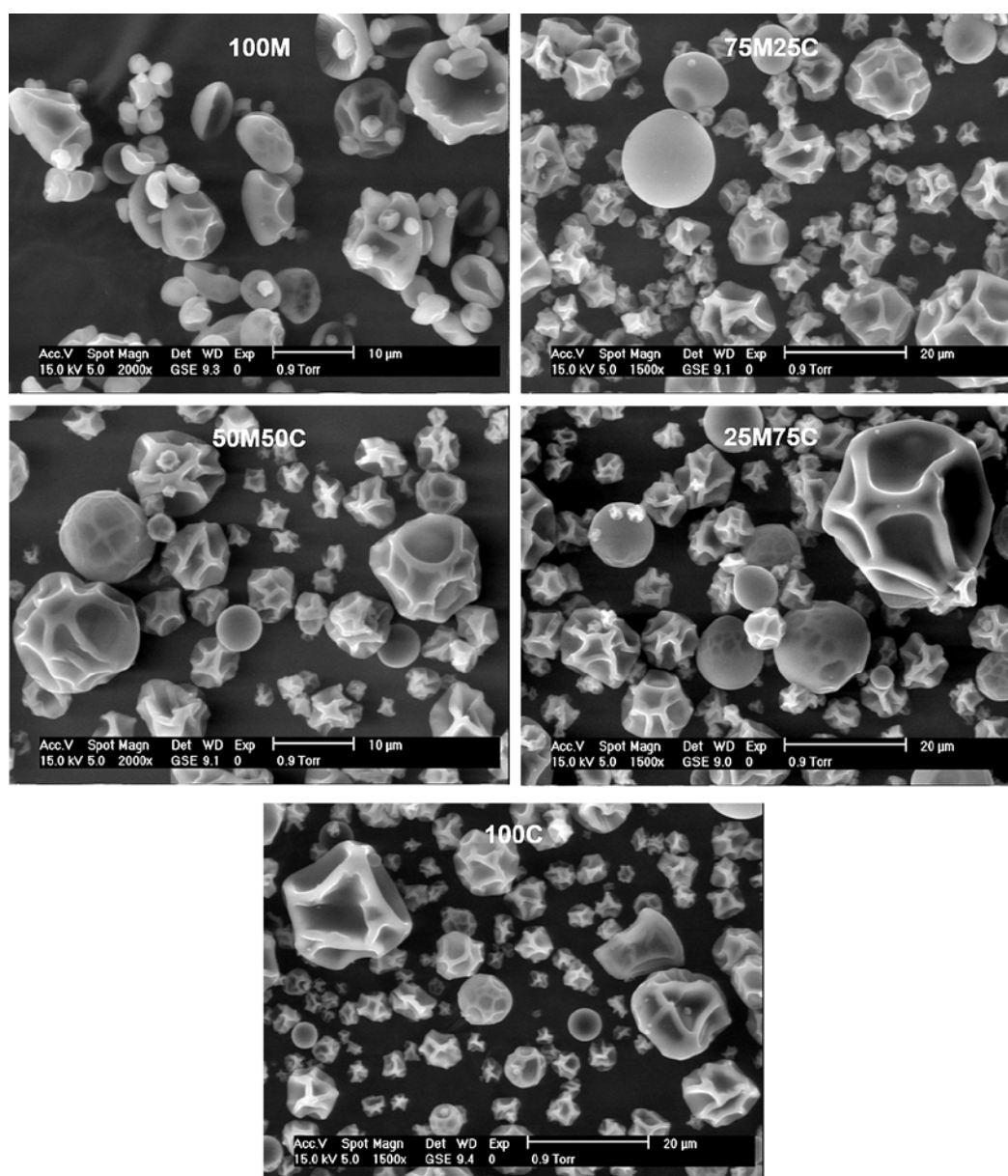


FIGURE 4. External structure of anthocyanin microcapsules of chagalapoli fruit produced using different combinations of wall materials. M100: maltodextrin 100%; 75M25C: 75% maltodextrin 25% Capsul®; 50M50C: 50% maltodextrin 50% Capsul®; 25M75C: 25% maltodextrin 75% Capsul®; 100C: 100% Capsul®.

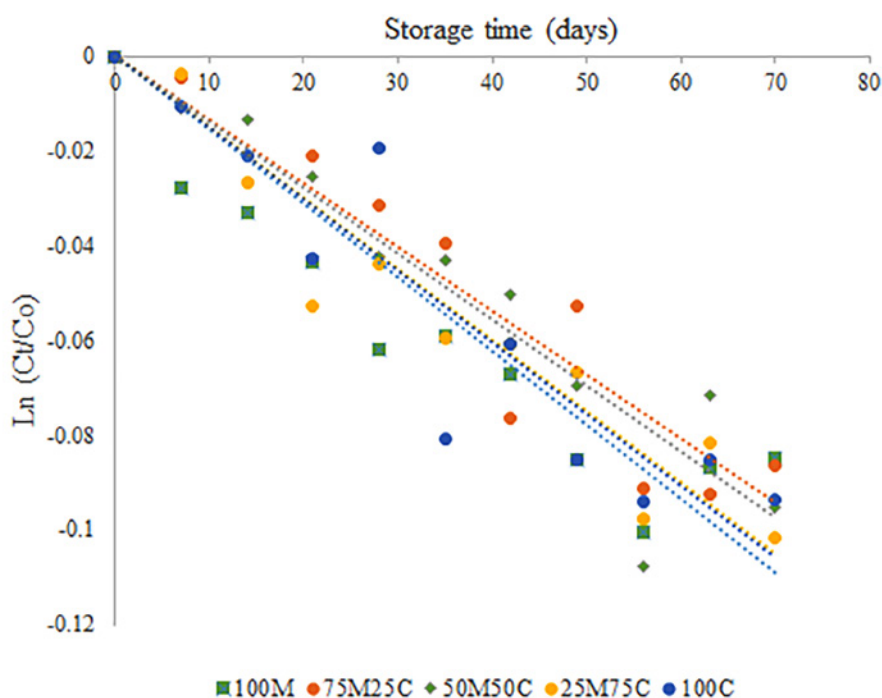


FIGURE 5. Degradation of anthocyanins in microcapsules stored at 35°C as a logarithm of the content ratio at storage time t (C_t) and initial (C_0).

Microcapsules produced using different combinations of wall materials; M100: maltodextrin 100%; 75M25C: 75% maltodextrin-25% Capsul®; 50M50C: 50% maltodextrin 50% Capsul®; 25M75C: 25% maltodextrin 75% Capsul®; 100C: 100% Capsul®.

but with a rough surface, that according to Tonon *et al.* [2009] is attributed to the shrinkage of the particles due to the loss of moisture and cooling. The morphological characteristics observed in the MC from the different treatments are similar to those described by Silva *et al.* [2013] for MC of jaboticaba anthocyanins with M and C as wall materials. The smooth spheroidal morphology of MC with M as the wall material is related to the content of low molecular weight sugars in this polysaccharide, which can act as a plasticizer and prevent shrinkage during surface drying. Lokuwan [2007] reached this conclusion after comparing the morphology characteristics of microcapsules prepared with wall materials with different dextrose equivalents (DE). As stated by Barros & Stringheta [2006], MC with intact and regular walls result in an improved microencapsulation process because those with rough surfaces have larger contact areas than those with smooth surfaces, which can render them more susceptible to degradation. The MC had average diameters of 5.1 μm (100M), 5.3 μm (75M25C), 6.7 μm (50M50C), 5.8 μm (25M75C), and 6.1 μm (100C). These values are lower than the average diameter of 10.9 μm reported for 10 DE maltodextrin microcapsules by Tonon *et al.* [2009].

Stability of anthocyanin microcapsules during storage

The degradation of anthocyanins in the MC fitted the first order kinetic model (Figure 5), as reported previously by Idham *et al.* [2012]. The R^2 for the anthocyanin stability data of the different wall materials were >0.8 (Table 5). The R^2 value is an indicator of how the data fit to the model used to explain the phenomenon. The wall material treatments that fitted better were 50M50C and 25M75C.

Righi da Rosa *et al.* [2019] evaluated the stability of blackberry microencapsulated anthocyanins with M and modified maize starch (hi-maize) over 20 days, reporting R^2 values of 0.9678 to 0.9809 for the data adjusted to the first order model.

The degradation constant of the microencapsulated CF anthocyanins ranged from 1.35×10^{-3} to $1.65 \times 10^{-3} \text{ day}^{-1}$, which resulted in a half-life time which ranged from 424 to 520 days (Table 5). The stability of the microencapsulated anthocyanins during storage is attributed to the favorable characteristics of the MC related to stability, such as moisture content (MT), water activity (a_w), and hygroscopicity (H). Moser *et al.* [2017] reported a half-life time of 545 days for grape anthocyanin microencapsulated with blends of soy

TABLE 5. Degradation kinetic variables of the anthocyanin microcapsules during storage at 35°C.

Wall material	R^2	$k \times 10^{-3}$ (1/days)	Half-life $t_{1/2}$ (days)	AR (%)
100M	0.8143	1.35	520±82	90.3±1.4
75M25C	0.8254	1.65	424±54	89.5±2.0
50M50C	0.9100	1.50	464±44	91.0±0.8
25M75C	0.9258	1.60	451±62	89.0±1.2
100C	0.8520	1.60	451±62	91.0±1.2

M – maltodextrin; C – Capsul®; AR – anthocyanin retention. M100: maltodextrin 100%; 75M25C: 75% maltodextrin 25% Capsul®; 50M50C: 50% maltodextrin 50% Capsul®; 25M75C: 25% maltodextrin 75% Capsul®; 100C: 100% Capsul®.

protein and maltodextrin, stored at 35°C. Stability of the core materials in the MC is affected by the EE during the microencapsulation process in a direct manner. The higher the EE, the longer the stability of the microencapsulated compounds [Li *et al.*, 2018]. Anthocyanin retention (AR) in the MC prepared with the different wall material mixtures after 70 days of storage at 35°C and protected from light, ranged from 89.0 to 91.0%.

The initial color parameters (L^* , a^* , and b^*) of the MC were of 37.9, 39.4, and -4.1 for 100M; 40.3, 39.2 and -4.6 for 75M25C; 44.3, 38.8 and -5.3 for 50M50C; 45.9, 39.7, and -5.5 for 25M75C; and 48.1, 39.9, and -5.8 for 100C (Figure 6A). The incorporation of C in the wall material blends resulted in the brightest MC which had the highest value of L^* in the treatment 100C. The values of a^* were less affected; however, MC from the 25M75C and 100C treatments had higher values of this variable, which means that their MC were of a light red color (Figure 6B), while b^* values decreased with increasing C proportion in the blends, which means that the color of the MC increased to blue tint (Figure 6C). The color of the MC is affected both, by the wall materials used, and the chemical structure of the anthocyanins microencapsulated [Norkaew *et al.*, 2019]. In some cases, color changes are marked, as in the study of Norkaew *et al.* [2019], who when incorporating whey protein in mixtures with M or gum Arabic obtained intense dark MC; while in others [Idham *et al.*, 2012], combinations of M with gum Arabic as wall materials caused slight changes in the color parameters.

Storage resulted in color change of the MC. The L^* values increased from 0.05 to 12.1%, meaning that the MCs became clearer and brighter at the end of storage. The smallest changes in L^* were presented in the MC with a higher proportion of C in the wall material mixture (Figure 6A). The variations on a^* were lower (0.7 to 2.9%), with no significant differences of a^* values between the 25M75C and 100C MC treatments (Figure 6B). The b^* values decreased in the 100M, 75M25C and 50M50C MC treatments, meaning that with storage the yellowness was reduced, while blueness increased. In the 25M75C and 100C MC variants, no differences of b^* values were observed between 0 and 70 days of storage (Figure 6C). According to these results, incorporation of C in the wall material blends to prepare the MC improved the color stability.

CONCLUSIONS

Among the variables examined to optimize the extraction of anthocyanins from CF, only the ethanol concentration and pH contributed significantly to the model that showed the best fit to the experimental data ($R^2=0.9760$). The optimized extracting conditions were 63.5% (v/v) ethanol as a solvent, pH of 2, sonication time of 30 min, and a ratio of fruit pulp to solvent of 1:5 (w/v). Anthocyanins from CF can be encapsulated with a mixture of maltodextrin: Capsul® in a 50:50 ratio, with a high product encapsulation efficiency and microcapsules characteristics favorable for storage. Under the conditions used to prepare the microcapsules of CF anthocyanins in this study, and the storage conditions applied; the half-life time of the microcapsules was longer than one year. The incorporation of Capsul® in the blends of wall

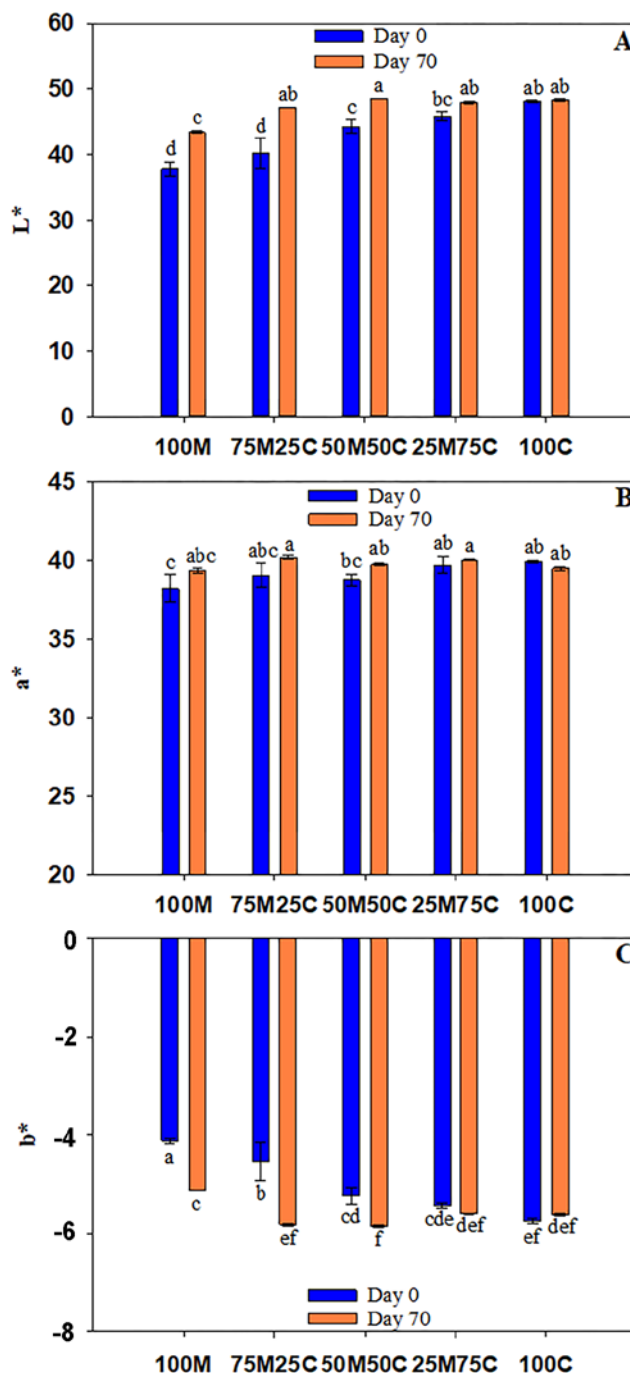


FIGURE 6. Color parameters of the microcapsules of chagalapoli fruit anthocyanins at 0 and 70 days of storage at 35°C; lightness – L^* (A), redness – a^* (B), and yellowness – b^* (C).

Microcapsules produced using different combinations of wall materials; M100: maltodextrin 100%; 75M25C: 75% maltodextrin 25% Capsul®; 50M50C: 50% maltodextrin 50% Capsul®; 25M75C: 25% maltodextrin 75% Capsul®; 100C: 100% Capsul®. Different letters above the bars indicate significant differences ($p < 0.05$).

materials improved color stability of the microcapsules during storage. Chagalapoli fruit is a suitable source of anthocyanins and due to its particular anthocyanin profile, dominated by malvidin derivatives, its anthocyanin microcapsules could be used in foods to get shades of color that are not possible to achieve with the common anthocyanin pigments based on cyanidin derivatives.

ACKNOWLEDGEMENTS

V.A.G acknowledges CONACYT, Mexico for a scholarship for her Master Science studies (Registration number: 554465).

CONFLICT OF INTERESTS

Authors declare they do not have any conflict of interests.

ORCID IDs

I. Andrade-González <http://orcid.org/0000-0002-4004-6308>
 F. Hernández-Rosas <https://orcid.org/0000-0003-3718-3245>
 J.A. Herrera-Corredor <https://orcid.org/0000-0002-2392-2521>
 F. Martínez-Bustos <https://orcid.org/0000-0002-2132-5598>
 Y. Salinas-Moreno <https://orcid.org/0000-0001-8145-2225>

REFERENCES

- AACC (1995). Approved Methods of the American Association of Cereal Chemists, 9th ed. International, St. Paul, MN, Method. 44–19.
- Arrazola, G., Herazo, I., Alvis, A. (2014). Anthocyanin microencapsulation of eggplant (*Solanum melongena* L.) and evaluation of color stability and antioxidant capacity. *Información Tecnológica*, 25(3), 31–42 (in Spanish; English abstract). <https://doi.org/10.4067/S0718-07642014000300006>
- Barros, F.A.R.D., Stringheta, P.C. (2006). Anthocyanin microencapsulation – an alternative to increase its applicability as a food ingredient. *Biotecnologia Ciência e Desenvolvimento*, 36, 18–24 (in Portuguese; English abstract).
- Bendokas, V., Skemiene, K., Trumbeckaite, S., Stanys, V., Passamonti, S., Borutaite, V., Liobikas, J. (2020). Anthocyanins: From plant pigments to health benefits at mitochondrial level. *Critical Reviews in Food Science and Nutrition*, 60(19), 3352–3365. <https://doi.org/10.1080/10408398.2019.1687421>
- Brouillard, R. (1982). Chemical structure of anthocyanins. In P. Markakis (Ed.), *Anthocyanins as Food Colors*, New York: Academic Press, pp. 1–40. <https://doi.org/10.1016/B978-0-12-472550-8.50005-6>
- de Brito, E.S., de Araujo, M.C.P., Alves, R.E., Carkeet, C., Clevidence, B.A. Novotny, J.A. (2007). Anthocyanins present in selected tropical fruits: Acerola, jambolão, jussara, and guajiru. *Journal of Agricultural and Food Chemistry*, 55(23), 9389–9394. <https://doi.org/10.1021/jf0715020>
- Escobar-Puentes, A.A., García-Gurrola, A., Rincón, S., Zepeda, A., Martínez-Bustos, F. (2020). Effect of amylose/amylopectin content and succinylation on properties of corn starch nanoparticles as encapsulants of anthocyanins. *Carbohydrate Polymers*, 250, art. no. 116972. <https://doi.org/10.1016/j.carbpol.2020.116972>
- Fossen, T., Slimestad, R., Andersen, O.M. (2001). Anthocyanins from maize (*Zea mays*) and reed canary grass (*Phalaris arundinacea*). *Journal of Agricultural and Food Chemistry*, 49(5), 2318–2321. <https://doi.org/10.1021/jf001399d>
- Frascareli, E.C., Silva, V.M., Tonon, R.V., Hubinger, M.D. (2012). Effect of process conditions on the microencapsulation of coffee oil by spray drying. *Food and Bioproducts Processing*, 90(3), 413–424. <https://doi.org/10.1016/j.fbp.2011.12.002>
- García-Tejeda, Y.V., Salinas-Moreno, Y., Martínez-Bustos, F. (2015). Acetylation of normal and waxy maize starches as encapsulating agents for maize anthocyanins microencapsulation. *Food and Bioproducts Processing*, 94, 717–726. <https://doi.org/10.1016/j.fbp.2014.10.003>
- Ghafoor, K., Hui, T., Choi, Y. H. (2011). Optimization of ultrasonic-assisted extraction of total anthocyanins from grape peel using response surface methodology. *Journal of Food Biochemistry*, 35(3), 735–746. <https://doi.org/10.1111/j.1745-4514.2010.00413.x>
- Giusti, M.M., Wrolstad, R.E. (2001). Anthocyanins. Characterization and measurement of anthocyanins by UV-visible spectroscopy. In R.E. Wrolstad (Ed.), *Current Protocols in Food Analytical Chemistry*. John Wiley & Sons, New York, USA; unit F1.2.1–1. <https://doi.org/10.1002/0471142913.faf0102s00>
- Giusti, M.M., Wrolstad, R.E. (2003). Acylated anthocyanins from edible sources and their applications in food systems. *Biochemical Engineering Journal*, 14(3), 217–225. [https://doi.org/10.1016/S1369-703X\(02\)00221-8](https://doi.org/10.1016/S1369-703X(02)00221-8)
- Idham, Z., Muhamad, I.I., Sarmidi, M.R. (2012). Degradation kinetics and color stability of spray-dried encapsulated anthocyanins from *Hibiscus sabdariffa* L. *Journal of Food Processing Engineering*, 35(4), 522–542. <https://doi.org/10.1111/j.1745-4530.2010.00605.x>
- Joaquín-Cruz, E., Dueñas, M., García-Cruz, L., Salinas-Moreno, Y., Santos-Buelga, C., García-Salinas, C. (2015). Anthocyanin and phenolic characterization, chemical composition and antioxidant activity of chagalapoli (*Ardisia compressa* K.) fruit: A tropical source of natural pigments. *Food Research International*, 70, 151–157. <https://doi.org/10.1016/j.foodres.2015.01.033>
- Khazaei, K.M., Jafari, S., Ghorbani, M., Kakhki, A.H., Sarfarazi, M. (2016). Optimization of anthocyanin extraction from saffron petals with response surface methodology. *Food Analytical Methods*, 9, 1993–2001. <https://doi.org/10.1007/s12161-015-0375-4>
- Labuza, T.P., Schmidl, M.K. (1985). Accelerated shelf-life testing of foods. *Food Technology*, 39(9), 57–62.
- Li, Y.B., Wu, L., Weng, M.J., Tang, B.S., Lai, P.F., Chen, J.C. (2018). Effect of different encapsulating agent combinations on physicochemical properties and stability of microcapsules loaded with phenolics of plum (*Prunus salicina* Lindl.). *Powder Technology*, 340, 459–464. <https://doi.org/10.1016/j.powtec.2018.09.049>
- Loksuwan, J. (2007). Characteristics of microencapsulated β -carotene formed by spray drying with modified tapioca starch, native tapioca starch and maltodextrin. *Food Hydrocolloids*, 21(5–6), 928–935. <https://doi.org/10.1016/j.foodhyd.2006.10.011>
- Luzardo-Ocampo, I., Ramírez-Jiménez, A.K., Yañez, J., Mojica, L., Luna-Vital, D.A. (2021). Technological applications of natural colorants in food systems: A review. *Foods*, 10(3), art. no. 634. <https://doi.org/10.3390/foods10030634>
- Mahdavi, S.A., Jafari, S.M., Assadpour, E., Ghorbani, M. (2016). Storage stability of encapsulated barberry's anthocyanin

- and its application in jelly formulation. *Journal of Food Engineering*, 181, 59–66.
<https://doi.org/10.1016/j.jfoodeng.2016.03.003>
22. Moreno, S.Y., Sánchez, G.S., Hernández, D.R., Lobato, N.R. (2005). Characterization of anthocyanin extracts from maize kernels. *Journal of Chromatography Science*, 43(9), 483–487.
<https://doi.org/10.1093/chromsci/43.9.483>
23. Moser, P., Nicoletti-Telis, V.R., de Andrade Neves, N., García-Romero, E., Gomez-Alonso, S., Hermosín-Gutiérrez, I. (2017). Storage stability of phenolic compounds in powdered BRS Violeta grape juice microencapsulated with protein and maltodextrin blends. *Food Chemistry*, 214, 308–318.
<https://doi.org/10.1016/j.foodchem.2016.07.081>
24. Najafabadi, N.S., Sahari, M.A., Barzegar, M., Esfahani, Z.H. (2020). Role of extraction conditions in the recovery of some phytochemical compounds of the jujube fruit. *Journal of Agricultural Science and Technology*, 22(2), 439–451.
25. Norkaew, O., Thitisut, P., Mahatheeranont, S., Pawin, B., Sookwong, P., Yodpitak, S., Lungkaphin, A. (2019). Effect of wall materials on some physicochemical properties and release characteristics of encapsulated black rice anthocyanin microcapsules. *Food Chemistry*, 294, 493–502.
<https://doi.org/10.1016/j.foodchem.2019.05.086>
26. Pedro, A.C., Granato, D., Rosso, N.D. (2016). Extraction of anthocyanins and polyphenols from black rice (*Oryza sativa* L.) by modeling and assessing their reversibility and stability. *Food Chemistry*, 191, 12–20.
<https://doi.org/10.1016/j.foodchem.2015.02.045>
27. Righi da Rosa, J., Nunes, G.L., Motta, M.H., Fortes, J.P., Cezimbra-Weis, G.C., Rychcki-Hecktheuer, L.H., Muller, E.I., de Menezes, C.R., Severo da Rosa, C. (2019). Microencapsulation of anthocyanin compounds extracted from blueberry (*Vaccinium* spp.) by spray drying: Characterization, stability and simulated gastrointestinal conditions. *Food Hydrocolloids*, 89, 742–748.
<https://doi.org/10.1016/j.foodhyd.2018.11.042>
28. Robert, P., Gorena, T., Romero, N., Sepulveda, E., Chavez, J., Saenz, C. (2010). Encapsulation of polyphenols and anthocyanins from pomegranate (*Punica granatum*) by spray drying. *International Journal of Food Science and Technology*, 45(7), 1386–1394.
<https://doi.org/10.1111/j.1365-2621.2010.02270.x>
29. Rocha, G.A., Fávoro-Trindade, C.S., Ferreira Grosso, C.R. (2012). Microencapsulation of lycopene by spray drying: Characterization, stability and application of microcapsules. *Food Bioproducts Processing*, 90(1), 37–42.
<https://doi.org/10.1016/j.fbp.2011.01.001>
30. Rodrigues, S., Fernandes, F.A.N., de Brito, E.S., Sousa, A.D., Narain, N. (2015). Ultrasound extraction of phenolics and anthocyanins from jaboticaba peel. *Industrial Crops and Products*, 69, 400–407.
<https://doi.org/10.1016/j.indcrop.2015.02.059>
31. Roselló-Soto, E., Galanakis, C.M., Brnčić, M., Orlien, V., Trujillo, F.J., Mawson, R., Barba, F.J. (2015). Clean recovery of antioxidant compounds from plant foods, by-products and algae assisted by ultrasounds processing. Modeling approaches to optimize processing conditions. *Trends in Food Science & Technology*, 42(2), 134–149.
<https://doi.org/10.1016/j.tifs.2015.01.002>
32. Silva, P.I., Stringheta, P.C., Teófilo, R.F., Nolasco de Oliveira, I.R. (2013). Parameter optimization for spray-drying microencapsulation of jaboticaba (*Myrciaria jaboticaba*) peel extracts using simultaneous analysis of responses. *Journal of Food Engineering*, 117(4), 538–544.
<https://doi.org/10.1016/j.jfoodeng.2012.08.039>
33. Swamy, G.J., Sangamithra, A., Chandrasekar, V. (2014). Response surface modeling and process optimization of aqueous extraction of natural pigments from *Beta vulgaris* using Box-Behnken design of experiments. *Dyes and Pigments*, 111, 64–74.
<https://doi.org/10.1016/j.dyepig.2014.05.028>
34. Tarone, A.G., Cazarin, C.B.B., Marostica Junior, M.R. (2020). Anthocyanins: New techniques and challenges in microencapsulation. *Food Research International*, 133, art. no. 109092.
<https://doi.org/10.1016/j.foodres.2020.109092>
35. Tonon, R.V., Brabet, C., Hubinger, M.D. (2010). Anthocyanin stability and antioxidant activity of spray-dried açai (*Euterpe oleracea* Mart.) juice produced with different carrier agents. *Food Research International*, 43(3), 907–914.
<https://doi.org/10.1016/j.foodres.2009.12.013>
36. Tonon, R.V., Brabet, C., Pallet, D., Brat, P., Hubinger, M.D. (2009). Physicochemical and morphological characterization of açai (*Euterpe oleracea* Mart.) powder produced with different carrier agents. *International Journal of Food Science & Technology*, 44(10), 1950–1958.
<https://doi.org/10.1111/j.1365-2621.2009.02012.x>
37. Turchiuli, C., Fuchs, M., Bohin, M., Cuvelier, M.E., Ordonnaud, C., Peyrat-Maillard, M.N., Dumoulin, E. (2005). Oil encapsulation by spray drying and fluidised bed agglomeration. *Innovative Food Science and Emerging Technologies*, 6(1), 29–35.
<https://doi.org/10.1016/j.ifset.2004.11.005>

Effect of Ultrasound, Steaming, and Dipping on Bioactive Compound Contents and Antioxidant Capacity of Basil and Parsley

Magdalena Dadan^{1*} , Urszula Tylewicz^{2,3} , Silvia Tappi^{2,3} , Katarzyna Rybak¹ ,
Dorota Witrowa-Rajchert¹ , Marco Dalla Rosa^{2,3} 

¹Department of Food Engineering and Process Management, Institute of Food Sciences, Warsaw University of Life Sciences, Nowoursynowska 159c, 02-776 Warsaw, Poland; katarzyna_rybak@sggw.edu.pl (K.R.), dorota_witrowa_rajchert@sggw.edu.pl (D.W.-R.)

²Department of Agricultural and Food Sciences, Alma Mater Studiorum-Università di Bologna, Piazza Goidanich 60, Cesena 47521, Italy;

urszula.tylewicz@unibo.it (U.T.), silvia.tappi2@unibo.it (S.T.), marco.dallarosa@unibo.it (M.D.R.)

³Interdepartmental Centre for Agri-Food Industrial Research, Alma Mater Studiorum-Università di Bologna, Via Quinto Bucci, Cesena 47521, Cesena, Italy;

urszula.tylewicz@unibo.it (U.T.), silvia.tappi2@unibo.it (S.T.), marco.dallarosa@unibo.it (M.D.R.)

Key words: basil, parsley leaves, ultrasound treatment, steaming, chlorophyll, lutein, total phenolic content

Fresh basil and parsley leaves are perishable and they are often processed by drying, which is an energy-consuming process and contributes to nutrient degradation. These downsides can, however, be mitigated by various pre-drying treatments. Thus, the objective of this study was to assess the impact of different treatments (ultrasound, steaming, dipping) and their duration (20, 30 min) on contents of chlorophylls and lutein (analyzed by UPLC-PDA), total phenolic content (TPC), as well as antioxidant capacity (determined as DPPH radical scavenging activity) in basil and parsley leaves. The changes in the chemical properties after treatments were more significant in the case of basil than parsley, probably due to a lower thickness of leaf epidermis layer and stiffness of the former. In comparison to fresh leaves, enhanced extractability of chlorophyll a after all treatments and TPC after dipping for 20 min, was observed in basil. In parsley, instead, the chlorophyll content remained unchanged after treatments, but TPC decreased. Lutein content remained stable in both herbs following different treatments. Irrespectively of the treatment type, the TPC and antioxidant capacity were higher after 20 min of basil treatments, while in the case of parsley, higher TPC was determined after longer treatments (30 min). The study demonstrated that the investigated treatments could preserve or even enhance the chemical properties of herbs.

INTRODUCTION

Basil and parsley are seasoning herbs widely cultivated and distributed in a dried form to nearly every part of the world. They feature high antioxidant activity linked to the content of vitamin C, carotenoids, phenolics, and other antioxidants [Boggia *et al.*, 2015; Pérez-Gálvez *et al.*, 2020; Śledź *et al.*, 2013]. Currently, there is a lot of interest in their potential use as ingredients in functional foods, which is due to the high content of natural antioxidants (including phenolics) and essential oils [Ahmed *et al.*, 2019; Liberal *et al.*, 2020]. Certain compounds present in basil, especially quercetin and ursolic acid, have been proved to inhibit the formation of nitric oxide II – an inflammatory factor mediating cancer development. Its anti-inflammatory properties have also been confirmed in the treatment of conjunctivitis and eyeball inflammation, skin diseases,

and asthma; it has also been proved to act as an antipyretic agent [Kurian, 2012]. Also parsley can exhibit anti-inflammatory properties by reducing the secretion of histamine, as well as a multitude of other activities, like antipyretic, stimulating digestion, relieving bloating and colic, diuretic, carminative, stimulating menstruation, cleansing the liver and preventing kidney stones and gout [Charles, 2012; Kurian, 2012; Peter, 2012]. Many studies have shown the ability of its leaf extracts to scavenge free radicals [Charles, 2012; Liberal *et al.*, 2020]. Moreover, studies have confirmed the antimutagenic effect of parsley apigenin and myristicin, which inhibited the activity of some enzymes responsible for pro-cancer transformations [Charles, 2012; Kurian, 2012]. Furthermore, such pigments as chlorophylls and carotenoids, apart from their role in photosynthesis and color perception, exhibit antimutagenic activity and antiseptic properties [Kopsell & Kopsell, 2006; Wang

* Corresponding Author:
Tel.: +48 22 593 75 60; Fax: +48 22 593 75 76;
E-mail: magdalena_dadan@sggw.edu.pl (M. Dadan)

Submitted: 12 March 2021
Accepted: 16 August 2021
Published on-line: 2 September 2021



et al., 2019]. It is worth emphasizing that many studies have proved the antioxidant activity of not only carotenoids but also chlorophylls, although they are not generally classified as antioxidants [Kopsell & Kopsell, 2006; Pérez-Gálvez *et al.*, 2020]. Furthermore, chlorophyll has also been found capable of either inhibiting or reversing multi-drug resistance in the case of cancer cells and bacteria [Wang *et al.*, 2019]. Among carotenoids, lutein is the main representative of xanthophylls, found in the leaves of higher plants [Murkovic *et al.*, 2000; Perry *et al.*, 2009]. The presence of carotenoids in leaf chloroplasts is associated with their function of transferring energy to chlorophylls. In addition, carotenoids neutralize free radicals formed under conditions of excessive exposure, thus protecting the entire photosynthetic apparatus of the plant. In an analogous way, lutein and zeaxanthin perform their functions also in the human body [Krinsky *et al.*, 2003]. In addition to antiradical activity, lutein also plays a key role in the visual process. Various studies have confirmed that lutein and zeaxanthin, present in high concentrations in the macula of the eye (even 1000 times higher than in blood plasma [Hammond, 2008]), prevent the age-related development of cataracts and macular degeneration (AMD) [Krinsky *et al.*, 2003]. Therefore, it is generally recommended to consume large amounts of lutein-containing products to prevent the development of cataracts and AMD. Based on the scientific literature [Rodriguez-Amaya, 2016], it can be stated that among the commercial leafy vegetables, the best sources of lutein include (in a descending order): basil, parsley, spinach, coriander, kale, rocket, and chicory.

Drying is the most common way of preserving herb leaves ensuring their microbial safety and long shelf-life [Boggia *et al.*, 2015; Chong *et al.*, 2021]. Pre-treatments applied prior to the drying of vegetables are generally aimed at reducing processing times and therefore decreasing the processing cost due to the lower energy consumption. Thermal treatments, such as blanching or steaming, can also reduce microbial load, inhibit enzymes, and enhance the extraction of components. However, even if they exert the aforementioned benefits, the use of high temperatures may decrease the nutritional value of herbs and cause undesirable color changes and degradation of heat-sensitive compounds. For this reason, the interest in non-thermal pre-processing of raw material before drying has increased in recent years, especially in relation to raw materials containing thermolabile compounds [Kaiser *et al.*, 2013; Xiao *et al.*, 2017].

Among different non-thermal technologies, ultrasound (US) treatment has gained particular attention, especially due to the uncomplicated construction of devices. From a physical point of view, US is a form of energy transmitted by a wave pressure, which causes vibrations of air that is inaudible to the human ear. The effects of US on biological cells depend on many factors, often related to each other. In fact, different effects are observed when US propagates in homogeneous liquids than in solid-liquid systems and two immiscible liquids [Mason *et al.*, 2011]. Cavitation, along with compression and decompression of solid material and turbulences, especially those occurring at the interface, are very important in intensifying the heat and mass exchange during the US treatment [Dadan *et al.*, 2021; Nowacka *et al.*, 2021; Witrowa-Rajchert *et al.*, 2014].

The effect of US on the content of bioactive compounds in leaves is not clear, and only a few related information can

be found in the literature. The implosion of cavitation bubbles and the associated sudden and vast, although limited to a small area, changes in pressure and temperature, as well as turbulence of the medium, can activate a series of chemical transformations [Kentish & Ashokkumar, 2011]. The generation of free radicals may lead to the degradation of antioxidants [Dadan *et al.*, 2018]. Moreover, the structural damages to the tissue may increase the leakage of water-soluble components [Dadan *et al.*, 2021; Gouda *et al.*, 2021; Witrowa-Rajchert *et al.*, 2014]. On the other hand, an increased content of some antioxidants, such as phenolics and carotenoids, and increased antioxidant capacity after US treatment were observed in various matrices, such as fresh and dried apple [Wiktor *et al.*, 2016], carrot [Dadan & Nowacka, 2021] as well as dried thyme [Rodriguez *et al.*, 2013], basil [Sledz *et al.*, 2017], parsley [Sledz *et al.*, 2016], and mulberry leaves [Tao *et al.*, 2016]. For this reason, US treatment is more often used to extract various compounds (*e.g.* phenolics, chlorophylls, essential oils, *etc.*) from herbal materials [Gouda *et al.*, 2021]. Moreover, it has also been observed to increase the retention of these compounds in the dried material due to reduced drying time [Rodriguez *et al.*, 2013].

In previous studies [Dadan *et al.*, 2017; 2018; Sledz *et al.*, 2017], the application of US pre-treatment has been confirmed to reduce the drying time of basil and parsley leaves and to preserve or even improve the bioactive compound content in the final products. However, chemical parameters were measured only after the drying process. The present study was therefore expected to explain the influence of a single treatment and not of both treatments (pre-treatment and drying) on herb quality. Thus, its objective was to assess the impact of different treatments (ultrasound, steaming, dipping) on the total phenolic content (TPC), antioxidant capacity, and contents of chlorophylls and lutein in basil and parsley leaves.

MATERIALS AND METHODS

Material

Basil and parsley seedlings were purchased in a garden market (Cesena, Italy). The seedlings of a similar degree of maturity were replanted and placed in a room with limited access to sunlight for 3 weeks in order to assure the homogeneity of the material. During this period, the air humidity and temperature were kept constant at the levels of 47.5 ÷ 50.0% and 18 ÷ 22°C, respectively. Afterward, healthy and mature leaves were picked directly before the treatments. All the experiments were concluded within 1 week.

Treatments: ultrasound (US), steaming (STEAM), and dipping (DIP)

The ultrasound treatment (US) was performed by the immersive method at the frequency of 35 kHz and the outlet power of 160 W using a water bath sonicator (TransSonic TP 690-A, Elma, Singen, Germany) for 20 and 30 min. It caused water temperature to increase to max. 8 and 11°C after 20 and 30 min, respectively. Steaming (STEAM) was carried out in a single layer above boiling water (99 ± 1°C) for 3 s. The temperature was assured by covering the material placed on a sieve with a lid. To ensure the same water/leaves contact time, after

3 s of the STEAM treatment, the leaves were kept in the water for 20 and 30 min. A metal net provided full immersion of the herbs. Dipping (DIP) in water for 20 and 30 min was used to assess the impact of immersion during the treatments. All the treatments were performed at the water temperature of $22.3 \pm 1.6^\circ\text{C}$. For each treatment, 5.02 ± 0.03 g of the herbal material on average were weighed and transferred into a beaker that was then filled with tap water. The material to water ratio was 1:40 (*w/w*). Immediately after the treatments, the leaves were placed on a filter paper to remove excess water and then left for 15 min to assure the same conditions. Afterward, to ensure sample homogeneity, the leaves were directly frozen, then freeze-dried, and ground into powder in a grinder. The powder was then used for all chemical assays. All the treatments were repeated 3 times.

Chlorophyll and lutein content

The contents of chlorophyll a and b, and lutein were determined according to the procedure described by Guzman *et al.* [2012] with modifications proposed by Sledz *et al.* [2016]. In brief, about 0.08 g (the accuracy of ± 0.0001 g) of freeze-dried material, which corresponded to approximately 0.6 g of fresh material, was weighed. Afterward, the pigments were extracted with acetone 80% (*v/v*, 10°C) with an addition of magnesium carbonate (0.1 g). The supernatant was filtered through $2\ \mu\text{m}$ PTFE filters. Five separate extractions were carried out for each sample.

The contents of chlorophylls and lutein in extracts were determined using a Waters ACQUITY UPLC system with a photodiode array (PDA) detector (Milford, MA, USA) and a Waters ACQUITY HSS T3 C18 column. Solvent A was a mixture of acetonitrile/methanol/chloroform (74/19/7, *v/v/v*), and solvent B was 0.05% (*w/v*) ammonium acetate. The gradient elution of mobile phase was used as follows: 0–8 min – 85% A, 15% B; 8–9 min – eluent A from 85 to 100%; 9–25 min – eluent A from 100 to 98%. The settings were as follows: injection volume – $10\ \mu\text{L}$, injection temperature – 15°C , flow rate – $0.4\ \text{mL}/\text{min}$; column temperature – 35°C , detector setting – $450\ \text{nm}$ (lutein) or $650\ \text{nm}$ (chlorophyll a and b). The compounds were identified based on the retention time of external standards of chlorophyll a, chlorophyll b, and lutein (Sigma-Aldrich, Burlington, MA, USA), while their contents were computed based on the peak area in comparison to the calibration curves of the standards.

Total phenolic content (TPC)

The extraction of phenolics from basil and parsley leaf powders was carried out in three separate repetitions as described by Śledź *et al.* [2013]. An ethanol solution at the concentration of 80% (*v/v*) was used as an extraction solvent. The mass of the powder approximated 0.21 g in the case of parsley and 0.06 g in the case of basil. Different masses of the material taken to prepare the extract resulted from different scavenging activities of the two species. The material to solvent ratio was 1:25 (*w/v*). The mixture was homogenized (1 min, 30,000 rpm), boiled (2 min), and filtered. The extracts were stored at -18°C for no longer than 24 h. After removing the extracts from frozen storage, they were equilibrated at room temperature (approx. 20°C), filtered again,

and subsequently used for both TPC and antioxidant capacity determinations.

The TPC was determined by the method with the Folin-Ciocalteu reagent [Singleton & Rossi, 1965] with modifications reported previously in detail [Dadan *et al.*, 2018]. For this purpose, water, extract, and Folin-Ciocalteu reagent (8.2, 0.3, and 0.5 mL, respectively) were mixed. After 3 min, sodium carbonate was added (1 mL, 1.7 M), and the solution was stirred again. A blank sample was prepared in an analogous way, but the extract was replaced with distilled water. After 1 h of storage in the dark at room temperature, the absorbance was measured at 750 nm against the blank sample using a Shimadzu UV-1601 spectrophotometer (Kyoto, Japan). The determination was conducted in 6 repetitions. Gallic acid (Sigma Aldrich) was used as a standard, and the calibration curve was plotted for the concentration range of 0.001– $-0.020\ \text{mg}/\text{mL}$. The results were expressed in mg of gallic acid equivalents per g of dry matter of plant material ($\text{mg}/\text{g d.m.}$).

Antioxidant capacity

Various concentrations of basil and parsley extracts (prepared as explained in *Total phenolic content (TPC)* section) in 80% (*v/v*) ethanol were used to evaluate their antiradical activity against 2,2-diphenyl-1-picrylhydrazyl (DPPH) radical (Sigma Aldrich) [Brand-Williams *et al.*, 1995]. A constant volume of $100\ \mu\text{M}$ DPPH \cdot solution was transferred into tubes containing the extract and ethanol, and the mixture was immediately stirred and then stored in the dark for 30 min [Dadan *et al.*, 2018]. The absorbance was measured at 515 nm against 80% (*v/v*) ethanol (Shimadzu UV-1601 spectrophotometer). Because the herbal extracts absorb radiation at 515 nm, the absorbance was measured for the extract (A_E) without DPPH \cdot . The percentage inhibition of the radical was calculated as follows [Dadan *et al.*, 2018]:

$$\%Inh = \frac{A_{DPPH} - A - A_E}{A_{DPPH}} \times 100 \quad (1)$$

where: %Inh – percentage inhibition of DPPH radical; A_{DPPH} – the absorbance of a control sample – a DPPH \cdot solution without extract; A – the absorbance of the extract with a DPPH \cdot solution; A_E – the absorbance of extract without DPPH \cdot .

The measurements were repeated 6 times. Afterward, the EC_{50} coefficient, characterizing an extract concentration required to scavenge 50% of DPPH radicals, was computed. The results were expressed in mg of dry matter of plant material per 100 mL of the extract ($\text{mg d.m.}/100\ \text{mL}$).

Statistical analysis

The significance of the differences between the analyzed results was assessed with the one-way ANOVA with Tukey's test (Statistica 12, StatSoft Polska, Cracow, Poland). The normality was checked with Shapiro-Wilk's test, whilst the homogeneity of variance with Levene's test. The significance of the influence of treatment type, time or their interactions was assessed with the two-way ANOVA with repetitions (Microsoft Excel 2013, Redmond, WA, USA). The significance level was set at 0.05 for all tests.

RESULTS AND DISCUSSION

Chlorophyll content

Figure 1 presents the contents of chlorophyll a (high bars) and b (low bars) in fresh and treated basil (Figure 1a) and parsley (Figure 1b). In fresh basil, chlorophyll a and b contents were 11.40 ± 0.66 and 3.62 ± 0.18 mg/g d.m., respectively. The total chlorophyll content reached 15.02 ± 0.84 mg/g d.m., similarly as that reported by Landi *et al.* [2013].

All treatments caused a significant ($p < 0.05$) increase in the chlorophyll a content in basil, in comparison to fresh leaves. In turn, in the case of chlorophyll b, its content was statistically unchanged ($p \geq 0.05$) following different treatments. The highest content of chlorophyll a was determined in basil treated with US for 30 min (US 30 min) and it was significantly ($p < 0.05$) higher than in STEAM 20 sample. Higher extractability of, *e.g.*, phenolics (including flavonoids), carotenoids, and essential oils, and/or better antioxidant capacity were reported in various herbal matrices as a consequence of US application [Gouda *et al.*, 2021; Rodriguez *et al.*, 2013; Sledz *et al.*, 2017; Tao *et al.*, 2016]. The authors explained that the increased extraction yield was due to the occurrence of cavitation and “sponge effect” causing cell disruption. In the present study, steaming caused no differences in the chlorophyll content in basil compared to dipping.

Kaiser *et al.* [2013] reported that steaming resulted in an increased release of components due to the thermal damage of cellular structure and subcellular membranes. Also, Di Cesare *et al.* [2003] demonstrated a higher content of chlorophyll in blanched basil after drying. It can be concluded that all treatments probably contributed to an impairment of the cells and/or membranes (*e.g.* thylakoid membranes of chloroplasts) in basil and then to a release of chlorophylls. In all basil samples, the contents of chlorophyll a and b were significantly affected by leaf dipping in water, which increased them irrespective of duration. Probably the dipping treatment contributed to loosening the structure and better extractability of the pigments from basil.

In the case of fresh parsley leaves (Figure 1b), lower chlorophyll contents were noted, *i.e.*: 6.21 ± 0.74 mg/g d.m. for chlorophyll a, 1.48 ± 0.21 mg/g d.m. for chlorophyll b, and 7.69 ± 0.94 mg/g d.m. (7.45 mg/g of fresh matter, f.m.) for total chlorophyll. In turn, Akbudak & Akbudak [2013] determined a total chlorophyll content in parsley at 2.33 mg/g (on f.m. basis). Presumably, the slight discrepancies in the obtained results were due to different varieties and growth conditions of plants or different maturation stages of leaves.

Differences in chlorophyll a and b content were not statistically significant ($p \geq 0.05$) in parsley. The observed results were opposite to those found for the treated basil, probably

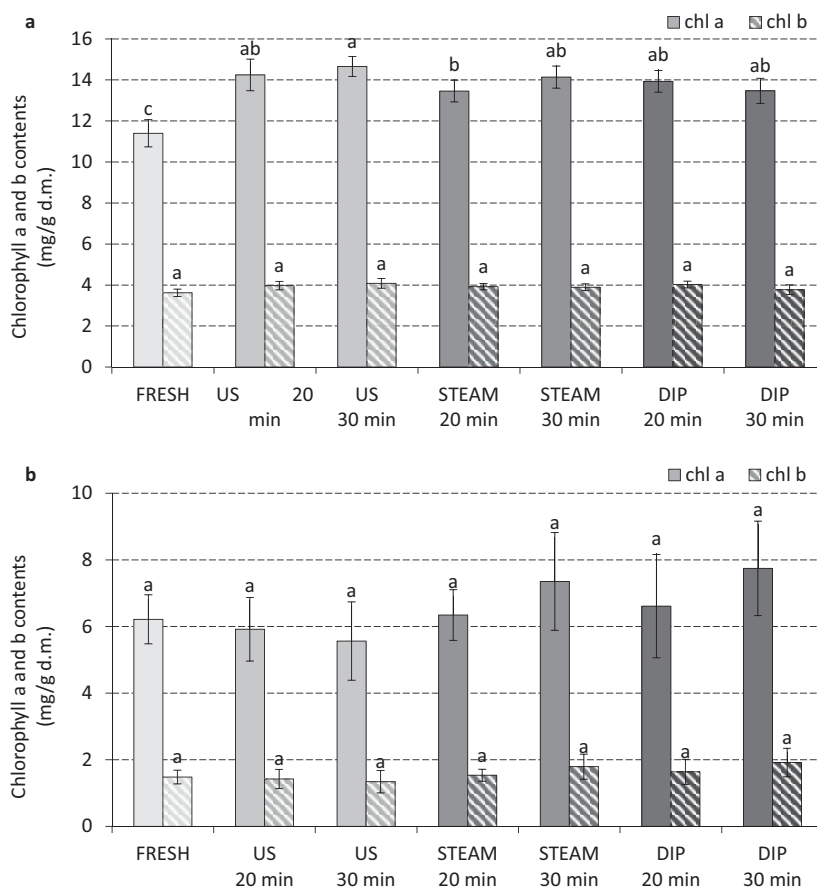


FIGURE 1. Chlorophyll a (high bars) and chlorophyll b (low bars with diagonal lines) contents of basil (a) and parsley (b) leaves: fresh and subjected to 20 or 30 min of the following treatments: US – ultrasound; STEAM – steaming followed by dipping; and DIP – dipping.

Different letters above the bars (separate for chlorophyll a and b) indicate significant differences ($p < 0.05$) between the values.

because of the different thickness of epidermis (the layer of cells on the leaves devoid of chlorophylls) between the two species. Parsley is characterized by a high turgor and stiffness of leaves and therefore presented a high stability of green pigments, while basil is more “sensitive” to soaking, which resulted in a higher “relaxation” of external structures after the applied treatments and possible impact on the internal structures containing chloroplasts.

Chlorophyll a imparts blue-green color, while chlorophyll b is more yellow-green. In higher plants, chlorophyll a is present in higher concentration than the b form. Because two types of chlorophyll can be degraded to a different extent during various processing treatments [Di Cesare *et al.*, 2003; Rodriguez-Amaya, 2019], maintaining the ratio of the contents of chlorophyll a and chlorophyll b (Chl a/Chl b) as close as possible to the level in fresh plant guarantees a stable, natural color of dried herbs. The Chl a/Chl b ratios in fresh and treated basil and parsley leaves are presented in Figure 2a and Figure 2b, respectively. The Chl a/Chl b ratio varied from 3.15 ± 0.04 (FRESH) to 3.64 ± 0.05 (STEAM 30 min) for basil, as well as from 4.04 ± 0.04 (DIP 20 min) to 4.21 ± 0.11 (FRESH) for parsley. These values were consistent with those shown in the literature; Di Cesare *et al.* [2003] found that chlorophyll a content in basil leaves was 2.5–3 times higher than that of chlorophyll b. In the current study, a higher

content of chlorophyll a following different treatments of basil samples resulted in a significant increase in the Chl a/Chl b ratio (by 9–16%) in comparison to the fresh material. The highest value of the ratio was observed when basil was subjected to STEAM 30 min; however, the values did not significantly ($p \geq 0.05$) differ compared to those obtained by other treatments for 30 min and US treatment for 20 min. The last sample showed the Chl a/Chl b ratio significantly ($p < 0.05$) higher in comparison to the samples obtained by other treatments for the same treatment time (20 min). It was proven that the duration of basil processing had a significant impact on the Chl a/Chl b ratio ($p = 0.0003$). Furthermore, also the interaction of treatment duration and type was statistically relevant ($p = 0.0057$), whereas the treatment type did not have a significant influence ($p \geq 0.05$). Concerning parsley leaves, the applied treatments did not affect the Chl a/Chl b ratio. The significance of treatment duration and type and the interaction of both these factors was not confirmed ($p \geq 0.05$).

The obtained results did not confirm literature data indicating degradation of chlorophylls as a consequence of blanching [Oliveira *et al.*, 2016], and of reactive oxygen species formed during sonication [Kentish & Ashokkumar, 2011]. Probably, a different mechanism of degradation (not thermal as the blanching was relatively short) as well as enhanced extraction of chlorophylls occurred. What is more, the study

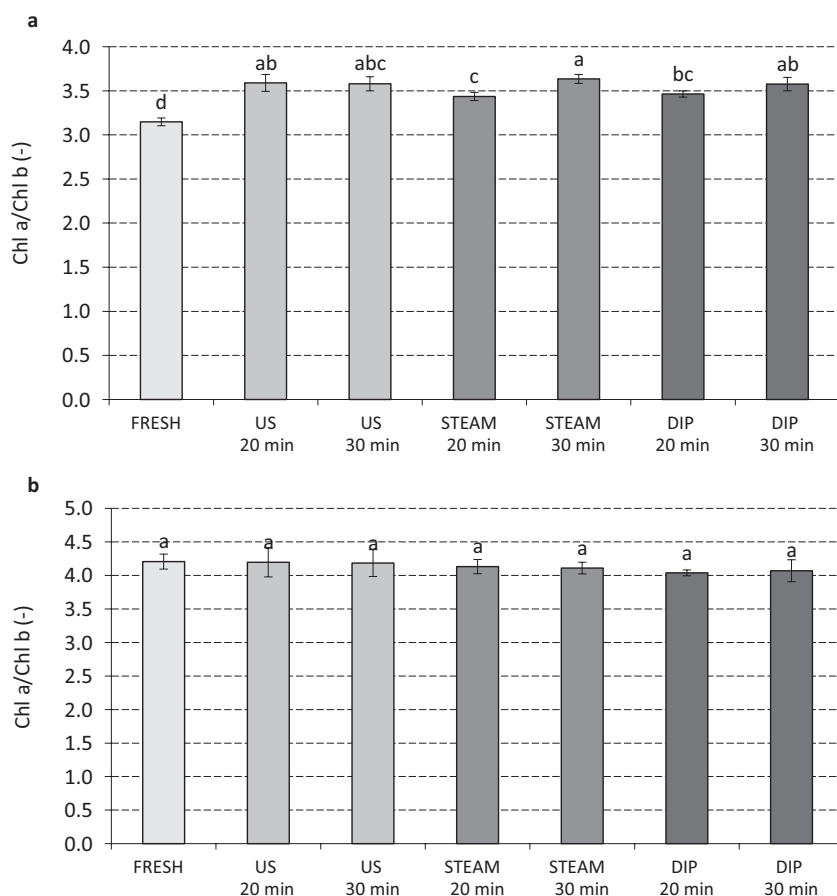


FIGURE 2. Chlorophyll a to chlorophyll b ratio (Chl a/Chl b) in basil (a) and parsley (b) leaves: fresh and subjected to 20 or 30 min of the following treatments: US – ultrasound; STEAM – steaming followed by dipping; and DIP – dipping.

Different letters above the bars indicate significant differences ($p < 0.05$) between the values.

proved the benefits of applying treatments in the case of basil and no contraindications of their use for parsley, giving therefore many reasons to promote the possibility of implementing additional treatments before, e.g., drying or freezing, which cause no adverse changes in the material.

Lutein content

The lutein content in fresh and treated basil and parsley leaves is presented in Figures 3a and 3b, respectively. Both species showed to be a good source of lutein, with contents of 92.3 ± 4.8 mg/100 g d.m. in fresh basil and 41.3 ± 5.3 mg/100 g d.m. in fresh parsley, which corresponded to a content of 6.73 ± 0.35 and 6.18 ± 0.79 mg/100 g f.m., respectively. Similar results were obtained by Murkovic *et al.* [2000], who reported that the sum of lutein and zeaxanthin amounted to 7.05 mg/100 g f.m. in basil and 6.4 mg/100 g f.m. in parsley. Also, Daly *et al.* [2010] determined a higher content of lutein and zeaxanthin in basil than in parsley. Moreover, Perry *et al.* [2009] have stated that green leafy vegetables are the best sources of lutein, in comparison to other vegetables and fruits. However, Dadan *et al.* [2018] found a higher content of lutein in dried parsley leaves (81.1 – 130.6 mg/100 g d.m.), which was probably due to using different varieties of parsley and/or plants growing under different climate and soil conditions.

The lutein content in the material subjected to the different treatments was stable and did not show any statistical

difference ($p \geq 0.05$) in both basil (Figure 3a) and parsley (Figure 3b). In fact, based on the analysis of the influence of treatment type and duration, it can be concluded that none of the factors significantly differentiated the content of lutein in both species ($p \geq 0.05$). Similar observations were reported in our previous studies in dried parsley [Dadan *et al.*, 2018; Sledz *et al.*, 2016], confirming the high stability of lutein during treatments. As reported by Perry *et al.* [2009], carotenoids in leaves are responsible for the protection of chlorophylls from external factors. Hence, the stability of lutein inhibited chlorophyll degradation. It is also possible that, as a result of structure softening, the susceptibility of lutein to the extraction increased, which “camouflaged” its degradation.

Total phenolic content (TPC)

Herbs are excellent sources of antioxidants, among which phenolics are the main represented group. The total phenolic content (TPC) in fresh and differently treated (US-treated, steamed or dipped) basil is shown in Figure 4a. A TPC of fresh basil was 37.7 ± 1.3 mg/g d.m. This value obtained for the basil cultivated in Italy (current study) was slightly higher than those obtained for basil cultivated in Israel [Hosain *et al.*, 2010] and Poland [Sledz *et al.*, 2013], amounting to 20 and 29.74 mg/g d.m., respectively. This could probably be due to the differences in the variety and climate conditions during plant growth. Figure 4a shows that both treatment type and duration influenced the TPC in basil. In general,

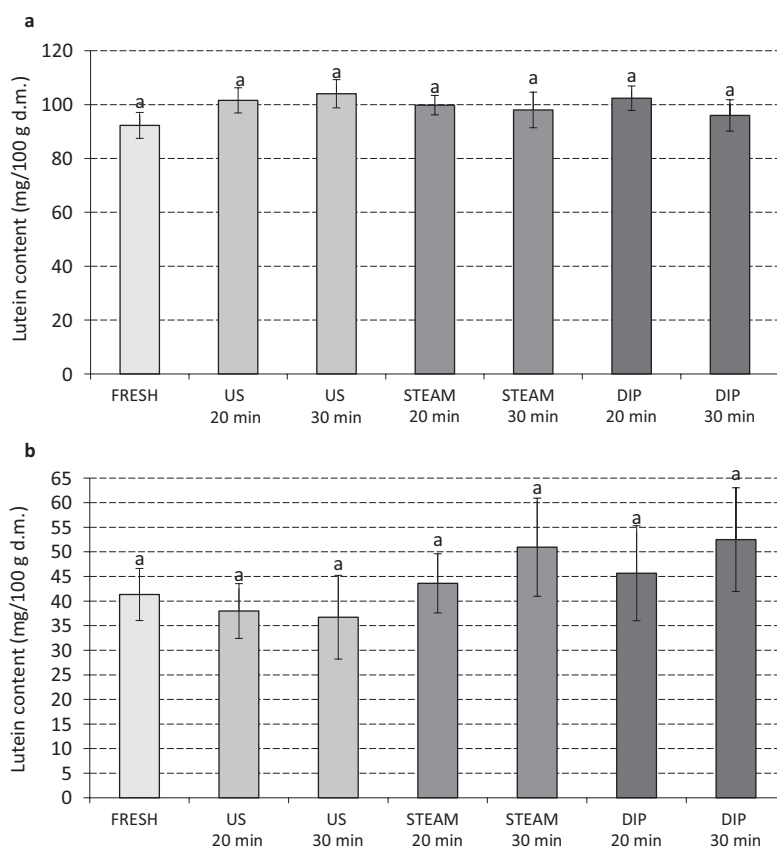


FIGURE 3. Lutein content of basil (a) and parsley (b) leaves: fresh and subjected to 20 or 30 min of the following treatments: US – ultrasound; STEAM – steaming followed by dipping; and DIP – dipping.

Letter a above the bars indicate no significant differences ($p \geq 0.05$) between the values.

with treatment time extension, a significantly ($p < 0.05$) lower TPC was determined in basil, regardless of treatment type.

The highest TPC was noted in DIP 20 min basil sample. This could be a result of water stress, which promotes the activation of basil defence mechanism, causing an additional synthesis of phenolics [Mazzeo *et al.*, 2011]. That kind of beneficial response to mild stress and degradation as a result of high stress is generally known as hormetic effect [Kouda & Iki, 2010]. A longer dipping time resulted in the leaching of these “released” substances into the liquid medium during treatment. However, the TPC of DIP 30 min sample was at the same level as in the fresh leaves. The samples treated by ultrasound and steam for 20 min showed statistically ($p \geq 0.05$) unchanged TPC in comparison to the fresh one. However, these values were lower than in the samples just dipped in water (DIP 20 min), as also observed by Chemat *et al.* [2011]. The total content of phenolics may stem from different opposite phenomena. An increased content might be observed due to water stress and increased extraction [Wiktor *et al.*, 2016]. In turn, a decrease can be caused by degradation due to free radicals generated during sonication [Kentish & Ashokkumar, 2011] or leakage of intracellular phenolic compounds and release of oxidative enzymes upon mechanical stress caused by US [Santacatalina *et al.*, 2014]. To better understand the observed differences, a complete characterization of the phenolic profile is probably necessary. Instead, steaming could promote damage to basil leaf layers

caused by fast delivery of the thermal power during the treatment and, therefore, the leakage of phenolics into the water. In fact, the lowest content of phenolics was determined in basil samples subjected to the soaking in water for 30 min after steaming (Figure 4a). Mazzeo *et al.* [2011] found an increase in the phenolic content in spinach steam-blanching for 20 min; however, they did not perform a dipping in water after blanching. It is worth noticing that in the current research, the material dipped in water for similar periods but not subjected to steaming was always characterized by a higher TPC than the samples subjected to steaming, concluding that the use of steam was not a beneficial treatment for basil.

A different effect of the applied treatments on the TPC was observed in parsley leaves (Figure 4b). In fresh parsley, the TPC was 25.4 ± 0.5 mg/g d.m., which was 33% lower than in basil (Figure 4a). All the treatments caused a significant ($p < 0.05$) decrease in TPC compared to the fresh parsley leaves. The lowest TPC was determined in the samples treated with US for 20 min and dipped. However, extending US treatment time from 20 to 30 min increased the TPC, probably due to the fact that 30 min was a threshold to observe a hormetic effect in parsley, as it was explained above. Ince *et al.* [2014] found that US treatment did not enhance phenolic extraction in nettle compared with the conventional extraction method. Therefore, a different response of basil and parsley leaves to the US treatment could probably be related to the differences in the tissue structure, such as thickness of the skin, the cell

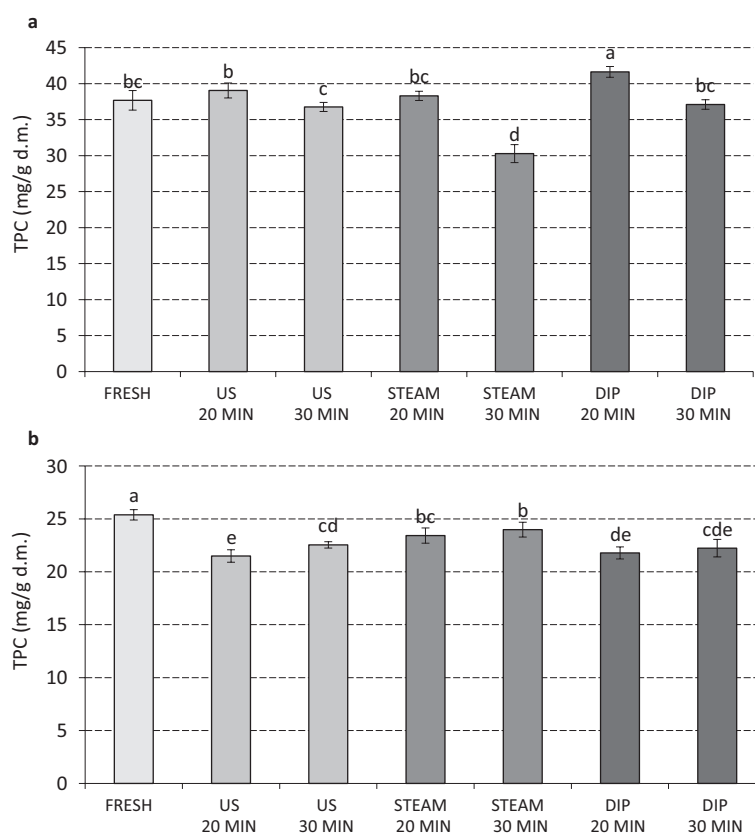


FIGURE 4. Total phenolic content (TPC) of basil (a) and parsley (b) leaves: fresh and subjected to 20 or 30 min of the following treatments: US – ultrasound; STEAM – steaming followed by dipping; and DIP – dipping.

Different letters above the bars indicate significant differences ($p < 0.05$) between the values.

turgor, and leaf “stiffness”. Furthermore, the different changes observed in the content of chlorophylls and TPC after the applied treatment could also be due to the different location of considered compounds inside the cells. Phenolics are located inside the vacuoles, while chlorophylls inside the chloroplast [Mannozi *et al.*, 2018]. In general, US can damage cell membranes and walls, contributing to a greater degree of phenolic extraction from the tissue [Wiktor *et al.*, 2016]. Perhaps this increased efficiency of extraction in parsley leaves was “camouflaged” by degradation of phenolics, as a result of the formation of reactive oxygen species or enhanced activity of enzymes, such as polyphenol oxidase, released from tissues [Kentish & Ashokkumar, 2011]. Among the treated parsley samples, the highest TPC was in those treated by steaming, even though it was significantly lower in comparison to the fresh leaves (Figure 4b). The highest retention of phenolics in a thermally-processed material may be related to the hormetic effect or removal of air from the cells [Oliveira *et al.*, 2016].

Antioxidant capacity

The EC_{50} value, which indicates the concentration of the extract necessary to scavenge half of the initial DPPH radicals, of fresh basil was 7.50 ± 0.24 mg d.m./100 mL (Figure 5a). For fresh parsley instead, a value of 67.0 ± 6.5 mg d.m./100 mL was determined (Figure 5b), which means that the antioxidant capacity of basil was 9 times higher than that of parsley.

It is worth noting that the TPC in parsley was also lower than in basil, but only 1.5 times (Figures 4a and 4b). It can be assumed that the differences in antioxidant capacity could be due to the different composition of phenolic compounds in both species, which requires further studies.

Concerning basil leaves, the results in Figure 5a indicate that antioxidant capacity of all samples treated for 20 min did not show any significant ($p \geq 0.05$) differences in comparison to the fresh leaves. However, an extension of the treatment time till 30 min resulted in a significant ($p < 0.05$) reduction of antioxidant capacity (an increase of the EC_{50}). In the case of fresh basil, the EC_{50} was higher in the samples following different treatments by 30% (US 30 min), 54% (STEAM 30 min), and 32% (DIP 30 min). These results do not match neither the data of lutein content nor TPC. However, as stated above, since various phenolics might exert different antioxidant activities, a complete characterization of the phenolic profile might give some insight to the observed differences. Based on the two-way ANOVA, it was noticed that the treatment duration had the greatest impact on basil antiradical activity against DPPH \cdot . The type of treatment and the interaction of both factors also significantly ($p < 0.05$) differentiated EC_{50} values, but to a lesser extent. Wiktor *et al.* [2016] showed that with an elongation of sonication (40 kHz) time, the content of polyphenols in apple significantly decreased, which was not translated into a statistically significant increase

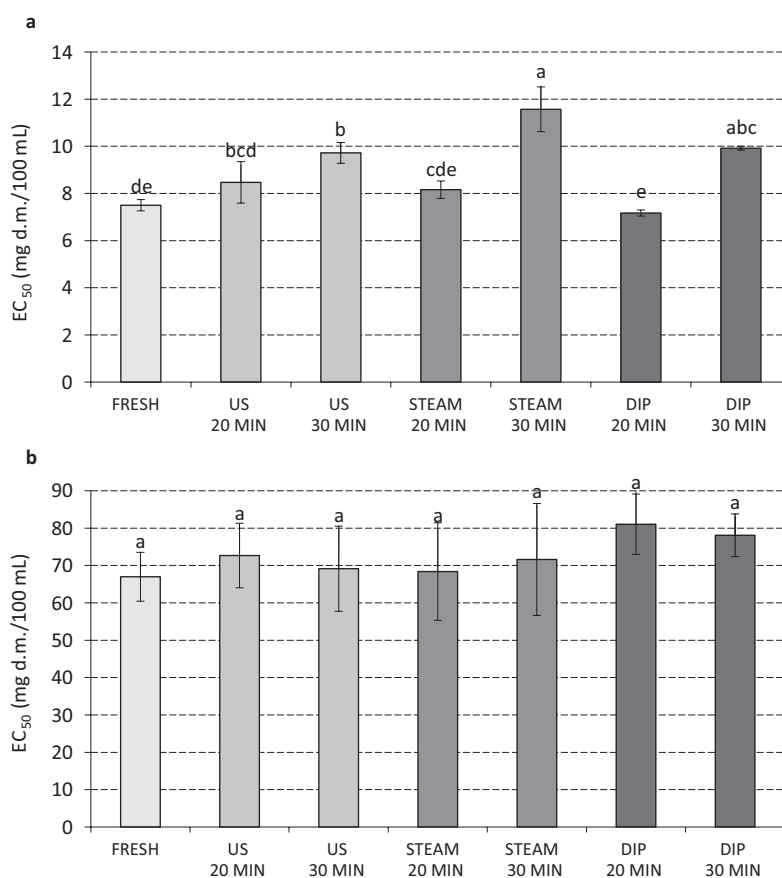


FIGURE 5. EC_{50} of DPPH \cdot scavenging activity of basil (a) and parsley (b) leaves: fresh and subjected to 20 or 30 min of the following treatments: US – ultrasound; STEAM – steaming followed by dipping; and DIP – dipping.

Different letters above the bars indicate significant differences ($p < 0.05$) between the values.

of the EC₅₀. On the other hand, antioxidant capacity and TPC did not differ significantly between the treatments carried out from 5 to 30 min at a frequency of 21 kHz.

Concerning the results of the antioxidant capacity of parsley, no significant ($p \geq 0.05$) differences in the EC₅₀ were observed in the fresh material and those subjected to the different treatments (Figure 5b). Moreover, the effects of treatment type and duration on the DPPH• scavenging activity of parsley extracts were not significant ($p \geq 0.05$). The various extent of changes observed in the scavenging ability against DPPH• in the case of basil and parsley could be due to the different anatomical and morphological structure of their leaves.

CONCLUSIONS

The study revealed that basil contained a higher amount of all the investigated bioactive compounds (chlorophylls, lutein, and total phenolics), and exhibited a higher antioxidant capacity, in comparison to parsley. It was also characterized by greater changes as a consequence of US treatment, steaming and dipping, presumably due to a different thickness of epidermis layer. In basil, all the treatments promoted an increase of the chlorophyll a content, while TPC increased only after 20 min of dipping and was reduced by steaming for 30 min. Parsley subjected to treatments was characterized by a stable content of chlorophylls but by a lower content of total phenolics. Lutein remained stable in both herbs regardless of treatment type. Finally, the antioxidant capacity was reduced after 30 min of all treatments in basil, while remained stable in parsley.

The obtained results demonstrated that the ultrasound, steaming or dipping treatments only slightly affected the quality of herbal leaves. Considering our previously reported data [Dadan et al., 2017; Sledz et al., 2017, 2016] showing that ultrasound and steaming reduced the drying time of basil and parsley, while US additionally reduced the total energy consumption [Dadan et al., 2017], the sonication is recommended as a pre-treatment before drying in the case of both species.

ACKNOWLEDGEMENTS

The authors wish to thank to Prof. Malgorzata Nowacka for proof-reading the manuscript.

RESEARCH FUNDING

This study was supported by a statutory activity subsidy from the Polish Ministry of Science and Higher Education for the Faculty of Food Sciences of Warsaw University of Life Sciences.

CONFLICT OF INTERESTS

The authors declare that they have no conflict of interest.

ORCID IDs

M. Dadan <https://orcid.org/0000-0001-7647-0592>
 M. Dalla Rosa <https://orcid.org/0000-0002-0405-7026>
 K. Rybak <https://orcid.org/0000-0003-3595-0818>

S. Tappi <https://orcid.org/0000-0003-0711-859X>
 U. Tylewicz <https://orcid.org/0000-0002-8192-6803>
 D. Witrowa-Rajchert <https://orcid.org/0000-0002-0937-3204>

REFERENCES

- Ahmed, A.F., Attia, F.A.K., Liu, Z., Li, C., Wei, J., Kang, W. (2019). Antioxidant activity and total phenolic content of essential oils and extracts of sweet basil (*Ocimum basilicum* L.) plants. *Food Science and Human Wellness*, 8(3), 299–305. <https://doi.org/10.1016/j.fshw.2019.07.004>
- Akbudak, N., Akbudak, B. (2013). Effect of vacuum, microwave, and convective drying on selected parsley quality. *International Journal of Food Properties*, 16(1), 205–215. <https://doi.org/10.1080/10942912.2010.535400>
- Boggia, R., Zunin, P., Hysenaj, V., Bottino, A., Comite, A. (2015). Dehydration of basil leaves and impact of processing composition. In V. Preedy (Ed.), *Processing and Impact on Active Components in Food*, Chapter 78, Elsevier Inc., London, pp. 645–653. <https://doi.org/10.1016/B978-0-12-404699-3.00078-0>
- Brand-Williams, W., Cuvelier, M.E., Berset, C. (1995). Use of a free radical method to evaluate antioxidant activity. *LWT – Food Science and Technology*, 28(1), 25–30. [https://doi.org/10.1016/S0023-6438\(95\)80008-5](https://doi.org/10.1016/S0023-6438(95)80008-5)
- Charles, D.J. (2012). Parsley. In K.V. Peter (Ed.), *Handbook of Herbs and Spices*, vol. 1, Se, Woodhead Publishing Limited, Cambridge, pp. 430–451. <https://doi.org/10.1533/9780857095671.430>
- Chemat, F., Zill-e-Huma, Khan, M.K. (2011). Applications of ultrasound in food technology: Processing, preservation and extraction. *Ultrasonics Sonochemistry*, 18(4), 813–835. <https://doi.org/10.1016/j.ultsonch.2010.11.023>
- Chong, C.H., Figiel, A., Szummy, A., Wojdyło, A., Chua, B.L., Khek, C.H., Yuan, M.C. (2021). Herbs drying. In Ch.M. Galankis (Ed.), *Aromatic herbs in food. Bioactive compounds, processing, and applications*, Chapter 5, Academic Press, pp. 167–200. <https://doi.org/10.1016/B978-0-12-822716-9.00005-6>
- Dadan, M., Nowacka, M. (2021). The assessment of the possibility of using ethanol and ultrasound to design the properties of dried carrot tissue. *Applied Sciences (Switzerland)*, 11(2), art. no. 689. <https://doi.org/10.3390/app11020689>
- Dadan, M., Nowacka, M., Rybak, K., Wiktor, A., Witrowa-Rajchert, D. (2017). An optimisation of microwave-convective drying of parsley leaves subjected to ultrasound and steaming treatments, carried out on the basis of the response surface methodology. *Zeszyty Problemowe Postępów Nauk Rolniczych*, 589, 15–25 (in Polish; English abstract). <https://doi.org/10.22630/ZPPNR.2017.589.17>
- Dadan, M., Nowacka, M., Wiktor, A., Sobczynska, A., Witrowa-Rajchert, D. (2021). Ultrasound to improve drying processes and prevent thermolabile nutrients degradation. In F.J. Barba, G. Cravotto, F. Chemat, J.M. Lorenzo Rodriguez, P.E.S. Munekata (Eds.), *Design and Optimization of Innovative Food Processing Techniques Assisted by Ultrasound*, Academic Press, London, pp. 55–110. <https://doi.org/10.1016/B978-0-12-818275-8.00010-6>
- Dadan, M., Rybak, K., Wiktor, A., Nowacka, M., Zubernik, J., Witrowa-Rajchert, D. (2018). Selected chemical composition

- changes in microwave-convective dried parsley leaves affected by ultrasound and steaming pre-treatments – An optimization approach. *Food Chemistry*, 239, 242–251.
<https://doi.org/10.1016/j.foodchem.2017.06.061>
12. Daly, T., Jiwan, M.A., O'Brien, N.M., Aherne, S.A. (2010). Carotenoid content of commonly consumed herbs and assessment of their bioaccessibility using an *in vitro* digestion model. *Plant Foods for Human Nutrition*, 65, 164–169.
<https://doi.org/10.1007/s11130-010-0167-3>
 13. Di Cesare, L.F., Forni, E., Viscardi, D., Nani, R.C. (2003). Changes in the chemical composition of basil caused by different drying procedures. *Journal of Agricultural and Food Chemistry*, 51(12), 3575–3581.
<https://doi.org/10.1021/jf021080o>
 14. Gouda, M., Bekhit, A.E., Tang, Y., Huang, Y., Huang, L., He, Y., Li, X. (2021). Recent innovations of ultrasound green technology in herbal phytochemistry: A review. *Ultrasonics Sonochemistry*, 73, art. no. 105538.
<https://doi.org/10.1016/j.ultsonch.2021.105538>
 15. Guzman, I., Yousef, G.G., Brown, A.F. (2012). Simultaneous extraction and quantitation of carotenoids, chlorophylls, and tocopherols in *Brassica* vegetables. *Journal of Agricultural and Food Chemistry*, 60(29), 7238–7244.
<https://doi.org/10.1021/jf302475d>
 16. Hammond, B.R. (2008). Possible role for dietary lutein and zeaxanthin in visual development. *Nutrition Reviews*, 66(12), 695–702.
<https://doi.org/10.1111/j.1753-4887.2008.00121.x>
 17. Hossain, M.B., Barry-Ryan, C., Martin-Diana, A.B., Brunton, N.P. (2010). Effect of drying method on the antioxidant capacity of six *Lamiaceae* herbs. *Food Chemistry*, 123(1), 85–91.
<https://doi.org/10.1016/j.foodchem.2010.04.003>
 18. Ince, A.E., Sahin, S., Sumnu, G. (2014). Comparison of microwave and ultrasound-assisted extraction techniques for leaching of phenolic compounds from nettle. *Journal of Food Science and Technology*, 51(10), 2776–2782.
<https://doi.org/10.1007/s13197-012-0828-3>
 19. Kaiser, A., Carle, R., Kammerer, D.R. (2013). Effects of blanching on polyphenol stability of innovative paste-like parsley (*Petroselinum crispum* (Mill.) Nym ex A. W. Hill) and marjoram (*Origanum majorana* L.) products. *Food Chemistry*, 138(2–3), 1648–1656.
<https://doi.org/10.1016/j.foodchem.2012.11.063>
 20. Kentish, S., Ashokkumar, M. (2011). The physical and chemical effect of ultrasound. In H. Feng, G.V. Barosa-Canovas, J. Weiss (Eds.), *Ultrasound Technologies for Food and Bioprocessing*, LLC, New York, pp. 1–12.
https://doi.org/10.1007/978-1-4419-7472-3_1
 21. Kopsell, D.A., Kopsell, D.E. (2006). Accumulation and bioavailability of dietary carotenoids in vegetable crops. *Trends in Plant Science*, 11(10), 499–507.
<https://doi.org/10.1016/j.tplants.2006.08.006>
 22. Kouda, K., Iki, M. (2010). Beneficial effects of mild stress (hormetic effects): dietary restriction and health. *Journal of Physiological Anthropology*, 29(4), 127–132.
<https://doi.org/10.2114/jpa2.29.127>
 23. Krinsky, N.I., Landrum, J.T., Bone, R.A. (2003). Biologic mechanisms of the protective role of lutein and zeaxanthin in the eye. *Annual Review of Nutrition*, 23(1), 171–201.
<https://doi.org/10.1146/annurev.nutr.23.011702.073307>
 24. Kurian, A. (2012). Health benefits of herbs and spices. In K.V. Peter (Ed.), *Handbook of Herbs and Spices*, vol. 2, Se, Woodhead Publishing Limited, Cambridge, pp. 72–88.
<https://doi.org/10.1533/9780857095688.72>
 25. Landi, M., Pardossi, A., Remorini, D., Guidi, L. (2013). Antioxidant and photosynthetic response of a purple-leaved and a green-leaved cultivar of sweet basil (*Ocimum basilicum*) to boron excess. *Environmental and Experimental Botany*, 85, 64–75.
<https://doi.org/10.1016/j.envexpbot.2012.08.008>
 26. Liberal, Á., Fernandes, Á., Polyzos, N., Petropoulos, S.A., Dias, M.I., Pinela, J., Petrović, J., Soković, M., Ferreira, I.C.F.R., Barros, L. (2020). Bioactive properties and phenolic compound profiles of turnip-rooted, plain-leaved and curly-leaved parsley cultivars. *Molecules*, 25(23), art no. 5606.
<https://doi.org/10.3390/molecules25235606>
 27. Mannozi, C., Fauster, T., Haas, K., Tylewicz, U., Romani, S., Dalla Rosa, M., Jaeger, H. (2018). Role of thermal and electric field effects during the pre-treatment of fruit and vegetable mash by pulsed electric fields (PEF) and ohmic heating (OH). *Innovative Food Science & Emerging Technologies*, 48, 131–137.
<https://doi.org/10.1016/j.ifset.2018.06.004>
 28. Mason, T.J., Paniwnyk, L., Chemat, F., Vian, M.A. (2011). Chapter 10. Ultrasonic Food Processing. In A. Proctor (Ed.), *Alternatives to Conventional Food Processing*, Royal Society of Chemistry, Cambridge, pp. 387–414.
<https://doi.org/10.1039/9781849730976-00387>
 29. Mazzeo, T., N'Dri, D., Chiavaro, E., Visconti, A., Fogliano, V., Pellegrini, N. (2011). Effect of two cooking procedures on phytochemical compounds, total antioxidant capacity and colour of selected frozen vegetables. *Food Chemistry*, 128(3), 627–633.
<https://doi.org/10.1016/j.foodchem.2011.03.070>
 30. Murkovic, M., Gams, K., Draxl, S., Pfannhauser, W. (2000). Development of an Austrian Carotenoid Database. *Journal of Food Composition and Analysis*, 13(4), 435–440.
<https://doi.org/10.1006/jfca.2000.0909>
 31. Nowacka, M., Dadan, M., Tylewicz, U. (2021). Current applications of ultrasound in fruit and vegetables osmotic dehydration processes. *Applied Sciences (Switzerland)*, 11(3), art. no. 1269.
<https://doi.org/10.3390/app11031269>
 32. Oliveira, S.M., Brandão, T.R.S., Silva, C.L.M. (2016). Influence of drying processes and pretreatments on nutritional and bioactive characteristics of dried vegetables: A review. *Food Engineering Reviews*, 8(2), 134–163.
<https://doi.org/10.1007/s12393-015-9124-0>
 33. Pérez-Gálvez, A., Viera, I., Roca, M. (2020). Carotenoids and chlorophylls as antioxidants. *Antioxidants*, 9(6), art. no. 505.
<https://doi.org/10.3390/antiox9060505>
 34. Perry, A., Rasmussen, H., Johnson, E.J. (2009). Xanthophyll (lutein, zeaxanthin) content in fruits, vegetables and corn and egg products. *Journal of Food Composition and Analysis*, 22(1), 9–15.
<https://doi.org/10.1016/j.jfca.2008.07.006>
 35. Peter, K.V. (2012). Introduction to herbs and spices: medicinal uses and sustainable production. In K.V. Peter (Ed.), *Handbook of Herbs and Spices*, vol. 2, Se, Woodhead Publishing Limited, Cambridge, pp. 1–16.
<https://doi.org/10.1533/9780857095688.1>
 36. Rodríguez-Amaya, D.B. (2016). Chapter 5. Composition and influencing factors. In *Food Carotenoids: Chemistry, Biology and Technology*, John Wiley & Sons Ltd., Oxford, pp. 96–131.
<https://doi.org/10.1002/9781118864364.ch5>

37. Rodríguez-Amaya, D.B. (2019). Natural food pigments and colorants. In J.-M. Mérillon, K.G. Ramawat (Eds.), *Bioactive Molecules in Food*, Springer, Cham., pp. 867–901.
https://doi.org/10.1007/978-3-319-78030-6_12
38. Rodríguez, J., Melo, E.C., Mulet, A., Bon, J. (2013). Optimization of the antioxidant capacity of thyme (*Thymus vulgaris* L.) extracts: Management of the convective drying process assisted by power ultrasound. *Journal of Food Engineering*, 119(4), 793–799.
<https://doi.org/10.1016/j.jfoodeng.2013.07.016>
39. Santacatalina, J.V., Rodríguez, O., Simal, S., Cárcel, J.A., Mulet, A., García-Pérez, J.V. (2014). Ultrasonically enhanced low-temperature drying of apple: Influence on drying kinetics and antioxidant potential. *Journal of Food Engineering*, 138, 35–44.
<https://doi.org/10.1016/j.jfoodeng.2014.04.00>
40. Singleton, V.L., Rossi, J.A. (1965). Colorimetry of total phenolic with phosphomolibdic-phosphotungstic acid reagents. *American Journal of Enology and Viticulture*, (16), 144–158.
41. Śledź, M., Nowacka, M., Wiktor, A., Witrowa-Rajchert, D. (2013). Selected chemical and physico-chemical properties of microwave-convective dried herbs. *Food and Bioprocess Processing*, 91(4), 421–428.
<https://doi.org/10.1016/j.fbp.2013.02.010>
42. Sledz, M., Wiktor, A., Nowacka, M., Witrowa-Rajchert, D. (2017). Drying kinetics, microstructure and antioxidant properties of basil treated by ultrasound. *Journal of Food Process Engineering*, 40(1), art. no. e12271.
<https://doi.org/10.1111/jfpe.12271>
43. Sledz, M., Wiktor, A., Rybak, K., Nowacka, M., Witrowa-Rajchert, D. (2016). The impact of ultrasound and steam blanching pre-treatments on the drying kinetics, energy consumption and selected properties of parsley leaves. *Applied Acoustics*, 103 Part B, 148–156.
<https://doi.org/10.1016/j.apacoust.2015.05.006>
44. Tao, Y., Wang, P., Wang, Y., Kadam, S.U., Han, Y., Wang, J., Zhou, J. (2016). Power ultrasound as a pretreatment to convective drying of mulberry (*Morus alba* L.) leaves: Impact on drying kinetics and selected quality properties. *Ultrasonics Sonochemistry*, 31, 310–318.
<https://doi.org/10.1016/j.ultsonch.2016.01.012>
45. Wang, E., Braun, M.S., Wink, M. (2019). Chlorophyll and chlorophyll derivatives interfere with multi-drug resistant cancer cells and bacteria. *Molecules*, 24(16), art. no. 2968.
<https://doi.org/10.3390/molecules24162968>
46. Wiktor, A., Sledz, M., Nowacka, M., Rybak, K., Witrowa-Rajchert, D. (2016). The influence of immersion and contact ultrasound treatment on selected properties of the apple tissue. *Applied Acoustics*, 103 Part B, 136–142.
<https://doi.org/10.1016/j.apacoust.2015.05.001>
47. Witrowa-Rajchert, D., Wiktor, A., Sledz, M., Nowacka, M. (2014). Selected emerging technologies to enhance the drying process: A review. *Drying Technology*, 32(11), 1386–1396.
<https://doi.org/10.1080/07373937.2014.903412>
48. Xiao, H.-W., Pan, Z., Deng, L.-Z., El-Mashad, H.M., Yang, X.-H., Mujumdar, A.S., Gao, Z.J., Zhang, Q. (2017). Recent developments and trends in thermal blanching – A comprehensive review. *Information Processing in Agriculture*, 4(2), 101–127.
<https://doi.org/10.1016/j.inpa.2017.02.001>

Hydrolyzed Collagen from Salmon Skin Increases the Migration and Filopodia Formation of Skin Keratinocytes by Activation of FAK/Src Pathway

Wanwipha Woonnoi¹, Lalita Chotphruethipong², Supita Tanasawet¹ , Soottawat Benjakul³ ,
Nuthathai Sutthiwong⁴, Wanida Sukketsiri^{1*} 

¹Division of Health and Applied Sciences, Faculty of Science, Prince of Songkla University, Hat Yai, Songkhla 90110, Thailand

²International Center of Excellence in Seafood Science and Innovation, Faculty of Agro-Industry, Prince of Songkla University, Hat Yai, Songkhla 90110, Thailand

³Department of Food Technology, Faculty of Agro-Industry, Prince of Songkla University, Hat Yai, Songkhla 90110, Thailand

⁴Expert Centre of Innovative Health Food (InnoFood),

Thailand Institute of Scientific and Technological Research (TISTR), Khlong Luang, Pathum Thani 12120, Thailand

Key words: cell culture, keratinocyte stem cells, marine collagen, re-epithelialization, skin barrier, wound healing

Previous studies reported hydrolyzed collagen increase cell proliferation and migration involved in the wound repair process. Nevertheless, the knowledge related with wound repair mechanism of hydrolyzed collagen from salmon skin (HCSS) has not been fully elucidated. Therefore, this study aimed to elucidate the effects of HCSS on the migration of keratinocyte HaCaT cells. Additionally, its molecular mechanism through cell division control protein 42 (Cdc42), Ras-related C3 botulinum toxin substrate 1 (Rac1), and Ras homolog family member A (RhoA) *via* focal adhesion kinase (FAK)-steroid receptor coactivator (Src) regulation and keratinocyte stem cells (KSCs) markers were also evaluated. After 24 h of incubation, keratinocyte proliferation was detected by 3-(4,5-dimethylthiazol-2-yl)-2,5-diphenyltetrazolium bromide (MTT) and double stranded DNA (dsDNA) assays, and by determining the total cellular protein content. Keratinocyte migration and filopodia formation were measured by wound healing assay and phalloidin-rhodamine staining, respectively. The migratory related proteins were evaluated by western blot analysis. HCSS had a high content of hydrophobic amino acids and imino acids. HaCaT cell proliferation and migration were significantly increased in response to HCSS at the concentration of 100–1000 $\mu\text{g}/\text{mL}$. The formation of filopodia was subsequently increased in response to HCSS at concentrations of 100–1000 $\mu\text{g}/\text{mL}$. Moreover, HCSS upregulated Cdc42, Rac1, and RhoA protein expression and activated the phosphorylation of FAK and Src pathway. HCSS at the concentration of 100–1000 $\mu\text{g}/\text{mL}$ could trigger stemness by increased KSC markers, including keratin 19 and β -catenin expression. This study has demonstrated that HCSS induces proliferation and migration of keratinocytes, subsequently promotes the second phase of wound healing process by FAK-Src activation and also increases the KSC properties.

INTRODUCTION

Human skin, especially the epidermis, is a major barrier against noxious pollutants which could be impaired by various factors including ultraviolet (UV), chemical and mechanical stimuli [Baroni *et al.*, 2012]. Furthermore, the renewal of skin in epidermis layer is important for human skin barrier function [Baroni *et al.*, 2012; Wickett & Visscher, 2006]. In response to skin damages, the renewal process and cell proliferation were observed in the UV, heat, and wound-induced skin injury [Wikramanayake *et al.*, 2014]. Keratinocyte stem cells (KSCs) regulate epidermal renewal and skin homeostasis. In addition, KSCs can produce extracellular matrix (ECM) components, cytokines, and growth factors in both normal function and response to skin injury [Fuchs, 2008; Pincelli

& Marconi, 2010; Sotiropoulou & Blanpain, 2012]. The decrease of KSCs numbers and activities leads to the epidermal barrier impairment [Yang *et al.*, 2019a]. Besides, keratinocyte proliferation and migration are accepted to play a major role in the re-epithelialization process of skin repair and healing [Abate *et al.*, 2021].

Fish skins are a by-product of the food industry and a rich source of collagen. Marine collagen has been noted to promote cell proliferation and migration of skin cells by augmenting various mediators in the stimulation of skin wound repair process [Chotphruethipong *et al.*, 2021a; Hu *et al.*, 2017; Yang *et al.*, 2019b] and KSCs function [Thaweekitphathanaphakdee *et al.*, 2019]. To date, bioactive peptides released from marine origin proteins, for example fish collagen have been reported to exhibit many biological effects including anti-inflammatory,

* Corresponding Author:

Email: wanida.su@psu.ac.th (W. Sukketsiri)

Submitted: 27 April 2021

Accepted: 19 August 2021

Published on-line: 3 September 2021



anti-oxidant, anti-aging, and wound repair activities [Chotphruethipong *et al.*, 2021a; Edgar *et al.*, 2018; Huang *et al.*, 2015]. Protein hydrolysates prepared by enzymatic processes from fish skin cause a reduction of aging and skin damage by photoaging [Chalamaiah *et al.*, 2019; Chen *et al.*, 2016; Edgar *et al.*, 2018]. However, the information on the mechanism of hydrolyzed collagen from salmon skin (HCSS) effect on the proliferation and migration of human keratinocytes HaCaT remains unclear. Therefore, the main purpose of this study was to examine the effects of HCSS on keratinocyte proliferation and migration. The properties of KSC markers were also elucidated in this study.

MATERIALS AND METHODS

Salmon skin preparation

Frozen salmon skins were obtained from King-fisher Holdings Co., Ltd., Songkhla, Thailand. The skins at $3 \times 3 \text{ cm}^2$ were applied with NaOH (100 mM) and subsequently washed until neutral pH was reached [Chotphruethipong *et al.*, 2019]. Alkali-treated skins were saturated in 10 volumes of 100 mM citric acid for 2 h, followed by washing with tap water until wash water became neutral [Chotphruethipong *et al.*, 2019]. The resulting swollen skins were utilized for hydrolyzed collagen preparation.

Preparation of hydrolyzed collagen from salmon skin (HCSS) and analysis of amino acid composition

HCSS was prepared using two-step enzymatic hydrolysis. Firstly, the swollen skins were treated with papain (3% of solid content of fish skin) as tailored by Benjakul *et al.* [2018a]. The reaction was performed at 40°C for 3 h and subsequently terminated by heating at 90°C for 15 min. Thereafter, Alcalase (2% of solid content of fish skin) was added into the mixture, followed by hydrolysis at 50°C for 2 h. After hydrolysis, the inactivation was done at 90°C for 15 min. The obtained hydrolyzed collagen was filtered, and the filtrate was concentrated with the solid content of 10% according to the method of Benjakul *et al.* [2018a]. The resulting concentrate was subjected to drying using a spray-dryer [Benjakul *et al.*, 2018a]. Salmon hydrolyzed collagen powder was packed in ziplock bag and stored at -40°C until used for analyses. The content of amino acids in HCSS was determined as detailed by Benjakul *et al.* [2018b]. Briefly, HCSS was hydrolyzed under reduced pressure in 4 M methanesulphonic acid containing 0.2% (v/v) 3-(2-aminoethyl)indole at 115°C for 24 h and neutralized with 3.5 M sodium hydroxide. Digest was diluted with 0.2 M citrate buffer (pH 2.2). An aliquot of 0.4 mL was analyzed using an amino acid analyzer (MLC-703; Atto Co., Tokyo, Japan).

Molecular weight (MW) distribution of HCSS

Size exclusion chromatography was applied to determine MW distribution of HCSS powder by using a $2.5 \times 50 \text{ cm}$ Sephadex G-25 gel filtration column (GE Healthcare Bio-Science AB, Uppsala, Sweden) [Chotphruethipong *et al.*, 2021c]. The absorbance was detected at 220 and 280 nm. Blue dextran (2,000,000 Da) was used for void volume measurement. The MW standards were insulin chain B (3495.89 Da),

vitamin B₁₂ (1355.4 Da), glycine-tyrosine (238.25 Da), and tyrosine (181.2 Da). MW of the fraction was estimated from the plot between available partition coefficient (K_{av}) and the logarithm of MW of the standards.

Keratinocyte culture and cell viability assays of HCSS

Human keratinocyte HaCaT cell line was purchased from the Cell Line Service, Heidelberg, Germany and cultured with 5% CO₂ atmosphere at 37°C in complete Dulbecco's Modified Eagle Medium (DMEM) supplemented with 10% heat-inactivated fetal bovine serum (FBS) (Gibco, Carlsbad, CA, USA), 2 mM L-glutamine (Gibco), 100 U/mL penicillin, and 100 $\mu\text{g}/\text{mL}$ streptomycin (Gibco). Keratinocyte HaCaT with a density of 1×10^4 cells/well were seeded in 96-well plate. Then, keratinocyte HaCaT were exposed to 0, 1, 5, 10, 25, 50, 75, 100, 250, 500, and 1000 $\mu\text{g}/\text{mL}$ of HCSS for 24, 48, and 72 h. After each time of incubation, 500 $\mu\text{g}/\text{mL}$ of 3-(4,5-dimethylthiazol-2-yl)-2,5-diphenyltetrazolium bromide (MTT) was applied into each well for 2 h, the insoluble purple formazan was solubilized in dimethyl sulfoxide (DMSO). The cell viability was assessed at 570 nm with a microplate reader (Synergy™ HT, Bio-tek Instruments, Winooski, VT, USA).

Detection of cell proliferation by MTT and double stranded DNA (dsDNA) assay

Keratinocyte HaCaT at 1×10^4 cells/well were cultured into 96-well plate. The cells were incubated with 0, 50, 100, 500, and 1000 $\mu\text{g}/\text{mL}$ of HCSS for 24 h. Cell proliferation was detected using a colorimetric MTT assay [Lü *et al.*, 2012]. Briefly, 500 $\mu\text{g}/\text{mL}$ of MTT was applied into each well for 2 h. The insoluble purple formazan was solubilized in DMSO. The cell viability was assessed at 570 nm with a microplate reader (Synergy™ HT). For dsDNA assay, cells were washed and incubated with 0.1% Triton X-100 for 10 min. Thereafter, the DNA content in keratinocyte HaCaT was measured using a dsDNA assay kit (Invitrogen, Carlsbad, California, USA). The intensity of fluorescence was measured at 485 nm (emission wavelength) and 535 nm (excitation wavelength) using a microplate reader (Synergy™ HT), and the percentage of HaCaT proliferation was calculated using the following formula:

$$\text{Cell proliferation (\%)} = \frac{\text{DNA concentration of cells treated with HCSS}}{\text{DNA concentration of untreated cells}} \times 100 \quad (1)$$

Detection of cell proliferation by total cellular protein content assay

Keratinocyte HaCaT at a density of 1×10^4 cells/well was grown in 96-well plates. Then, cells were incubated with 0, 50, 100, 500, and 1000 $\mu\text{g}/\text{mL}$ of HCSS for 24 h. After 24 h of incubation, the cells were mixed with cold trichloroacetic acid (TCA) solution (40%, w/v) and incubated for 1 h at 4°C as described by Thaweekitphathanaphakdee *et al.* [2019]. Sulforhodamine B (Sigma-Aldrich, St. Louis, MO, USA) solution (0.04%, w/v) was added to each well and incubated for 1 h at room temperature. Thereafter, the cells were washed quickly with acetic acid (1%, v/v), and then 0.01 M Tris base was applied to each culture well. The absorbance at 510 nm was measured by a microplate reader (Synergy™ HT)

and the percentage of HaCaT proliferation was calculated using the following formula:

$$\text{Cell proliferation (\%)} = \frac{\text{absorbance of mixture with HCSS}}{\text{absorbance of control}} \times 100 \quad (2)$$

Wound healing assays

The effect of HCSS on the migration of skin keratinocytes was evaluated using an *in vitro* scratch wound healing assay. The HaCaT keratinocytes (3.5×10^5 cells/well) were grown in 6-well plates with DMEM medium containing 0.1% FBS. Prior to HCSS treatment (0–1000 $\mu\text{g/mL}$), a sterile P200 micropipette tip was used to make a wound space. The wound areas were captured on the image field at 3 points per line at 0 and 24 h using a phase-contrast microscope (Olympus IX70 Inverted Microscope, Olympus Corporation, Tokyo, Japan). The percentage of wound area was calculated as described by Singkhorn *et al.* [2018].

Filopodia formation determination by phalloidin-rhodamine staining

After HCSS treatment at the concentrations of 0, 50, 100, 500, and 1000 $\mu\text{g/mL}$ for 24 h, filopodia formation was determined as described previously [Singkhorn *et al.*, 2018]. Briefly, the cells were fixed with paraformaldehyde (4%, *w/v*), and the Triton-X100 (0.1%) was added for cell permeabilization. After blocking with 2% bovine serum albumin (BSA) for 1 h, keratinocyte HaCaT was incubated with phalloidin-rhodamine (10 $\mu\text{g/mL}$) and Hoechst 33342 (10 $\mu\text{g/mL}$) for 30 min. The images were taken with a fluorescence microscope (Olympus IX70 with DP50), and the percentage of filopodia formation was determined using the following formula:

$$\text{Filopodia formation (\%)} = \frac{\text{number of filopodia}}{\text{number of cells}} \times 100 \quad (3)$$

Western blot analysis

Keratinocyte HaCaT were exposed to HCSS at the concentrations of 0, 50, 100, 500, and 1000 $\mu\text{g/mL}$ for 24 h. The treated cells were then lysed in the lysis buffer containing protease and phosphatase inhibitor for 30 min at 4°C. The lysed cells were collected and centrifuged at $14,024 \times g$ for 15 min. Protein of the samples (75 μg) was separated by 10% sodium dodecyl sulphate-polyacrylamide gel electrophoresis and moved onto nitrocellulose membranes. The non-specific protein of membranes was blocked using 5% non-fat dry milk or 3% BSA in Tris-buffered saline containing 0.1% Tween 20 for 2 h. The primary antibodies to FAK (Santa Cruz Biotechnology, Dallas, TX, USA; 1:1000), pFAK (Santa Cruz Biotechnology; 1:1000), Src (Abcam, Cambridge, UK; 1:1000), pSrc (Abcam; 1:1000), Akt (Santa Cruz Biotechnology; 1:1000), pAkt (Santa Cruz Biotechnology; 1:1000), RhoA (Abcam; 1:1000), Rac1 (Abcam; 1:1000), Cdc42 (Abcam; 1:1000), keratin 19 (Abcam; 1:1000), β -catenin (Abcam; 1:1000), and β -actin (Thermo Scientific, Waltham, MA, USA; 1:1,000) were incubated at 4°C overnight. The membranes were washed and incubated with secondary antibody conjugated to horseradish peroxidase at room temperature for 1 h. The protein bands were exposed using an enhanced chemiluminescence

(ECL) western blotting detection reagent (Merck Millipore, Burlington, MA, USA) and analyzed by ImageJ software (Image Processing and Analysis in Java, National Institutes of Health, <http://rsbweb.nih.gov/ij/>).

Statistical analysis

The data were described as a mean \pm standard error of the mean (SEM). Statistical comparisons were made using one-way analysis of variance and Tukey post hoc test. Differences were considered significant when *p* values were below 0.05 ($p < 0.05$).

RESULTS AND DISCUSSION

Amino acid composition of hydrolyzed collagen from salmon skin (HCSS)

As shown in Table 1, Gly was found as the dominant amino acid (19.66 g/100 g), followed by Pro (10.95 g/100 g), Gln/Glu (9.24 g/100 g), Ala (7.64 g/100 g), and Asn/Asp (7.49 g/100 g). Moreover, HCSS contained imino acids (Hyp and Pro) (16.20 g/100 g). Gly is located at every third position in the collagen polypeptide chains in the presence of imino acids (Pro

TABLE 1. Relative amino acid composition of hydrolyzed collagen from salmon skins (HCSS).

Amino acid	Content (g/100 g)
Alanine (Ala)	7.64
Arginine (Arg)	7.00
Asparagine/ Asparatic acid (Asn/Asp)	7.49
Cysteine (Cys)	0.04
Glutamine/Glutamic acid (Gln/Glu)	9.24
Glycine (Gly)	19.66
Histidine (His)	ND
Isoleucine (Ile)	1.63
Leucine (Leu)	4.22
Lysine (Lys)	5.25
Hydroxylysine (Hyl)	0.76
Methionine (Met)	2.74
Phenylalanine (Phe)	3.08
Hydroxyproline (Hyp)	5.25
Proline (Pro)	10.95
Serine (Ser)	5.13
Threonine (Thr)	3.42
Tyrosine (Tyr)	3.50
Valine (Val)	2.89
Tryptophan (Trp)	0.11
Total	100.00

ND: Not detected

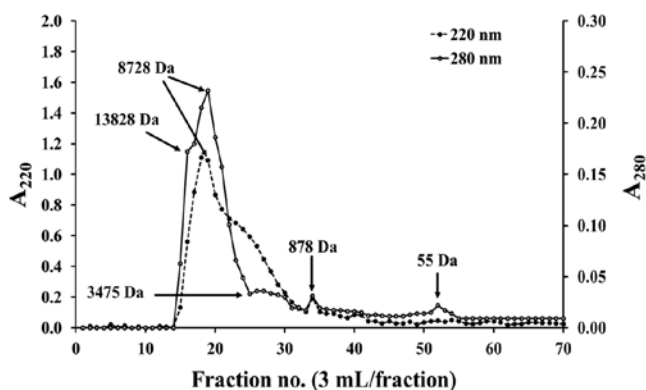


FIGURE 1. Elution profile by Sephadex G-25 size exclusion chromatography of hydrolyzed collagen powder from salmon skin.

and Hyp) as Gly-Pro-Hyp [Benjakul *et al.*, 2018b]. A high content of hydrophobic amino acids, constituting approximately 50.07 g/100 g of total amino acids, was also noted (Table 1). These amino acids played an essential role in the proliferation of skin cells [Chotphruethipong *et al.*, 2021a,b]. Additionally, bioactive peptides from fish skin rich in Pro, Hyp, and Gly promoted the wound healing process [Chotphruethipong *et al.*, 2021a]. Previous reports have shown that marine collagen from the skin of Nile tilapia has a high content of Gly-Pro-Hyp [Hu *et al.*, 2017; Yang *et al.*, 2019b].

Size distribution of HCSS

HCSS contained peptides with various molecular weights (MW) (Figure 1), with those having MWs of 8728, 878, and 55 Da being dominant. Peptides with high MW (>8 kDa) were also found (Figure 1). In general, the size of peptides is a vital factor affecting bioactivity of hydrolyzed collagen. The smaller size peptides exhibited higher bioactivities, especially cell proliferation activity [Chotphruethipong *et al.*, 2021c,d]. Also, short chain peptides could be rapidly digested and absorbed in the human body [Morgan & Breen, 2021].

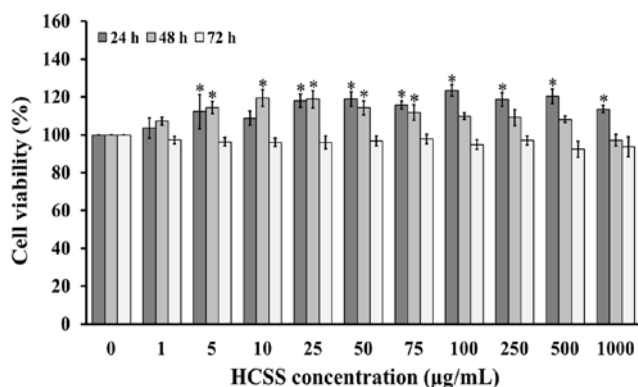


FIGURE 2. The viability of HaCaT keratinocytes after treatment with hydrolyzed collagen from salmon skin (HCSS) at concentrations of 0–1000 µg/mL for 24, 48, and 72 h.

Results are presented as mean \pm standard error of the mean of four independent experiments (n=4). The asterisk above bars indicates a significant difference between the HCSS treatment and the corresponding control without HCSS ($p < 0.05$).

Effect of HCSS on cell viability of keratinocyte HaCaT

Human keratinocyte cell lines are used as *in vitro* models to study the biological activities of molecules linked with dermatological conditions such as wound healing, contact dermatitis, psoriasis, or skin cancer. In our study, first, the effect of various concentrations of HCSS on keratinocyte HaCaT cell viability was assessed using the MTT assay to determine the cytotoxic effect and ensure the safe use of HCSS. As shown in Figure 2, exposure of the HaCaT cells to HCSS (5–1000 µg/mL) for 24 h, and HCSS (5–75 µg/mL) for 48 h caused a significant ($p < 0.05$) increase in cell viability. However, HCSS at concentrations of 1–1000 µg/mL had no effect on the cell viability of keratinocyte HaCaT after 72 h of treatment. These findings proved the safety of all concentrations of HCSS as they did not cause the loss of cell viability even at the highest concentrations. Altogether, we could explain that the increment of cell viability may result from the high content of hydrophobic amino acids in HCSS (Table 1). Our findings were similar to the previous studies reporting that the hydrolyzed collagen from seabass skin significantly enhanced fibroblast and keratinocyte viability [Chotphruethipong *et al.*, 2021a,b]. Research conducted by Yang *et al.* [2019b] also showed that peptides from *Nibeja japonica* skin collagen increased cell viability of NIH-3T3 fibroblasts. Additionally, abalone collagen was observed to increase keratinocyte viability [Thaweekitphathanaphakdee *et al.*, 2019]. Based on the results, we selected the HCSS concentrations of 50, 100, 500, and 1000 µg/mL for further experiments.

Proliferative effects of HCSS

Cell proliferation involves crucial events at a cellular level in the second phase of wound repair process and also important for epidermis renewal [Martin & Nunan, 2015; Yang *et al.*, 2019a]. Therefore, HCSS at 50, 100, 500, and 1000 µg/mL was further investigated for the proliferative activity in skin keratinocyte HaCaT cells. The cells were maintained in the growth medium (1% FBS) in the presence or absence of HCSS at 50, 100, 500, and 1000 µg/mL for 1 day. The MTT assay revealed that HCSS at 100, 500, and 1000 µg/mL significantly ($p < 0.05$) increased HaCaT proliferation after 1 day of cultivation in keratinocyte HaCaT (Figure 3A). Moreover, the proliferative activity of HCSS at 50, 100, 500, and 1000 µg/mL was confirmed using the dsDNA assay and total cellular protein content determination because the MTT assay has some limitations in cell proliferation measurement [Van Tonder *et al.*, 2015]. HCSS at 100, 500, and 1000 µg/mL induced a significant ($p < 0.05$) increase of cell proliferation in both assays (Figure 3B and Figure 3C), and the effect of HCSS on HaCaT cells was concentration dependent. Results from these three assays demonstrated that HCSS had a proliferative effect in keratinocytes. Our findings were in a good agreement with several previous studies in which fibroblast [Benjakul *et al.* 2018b; Chotphruethipong *et al.*, 2021a; Yang *et al.*, 2019b] and keratinocyte proliferation [Chotphruethipong *et al.*, 2021b; Thaweekitphathanaphakdee *et al.*, 2019] was promoted in response to peptides with hydrophobic amino acids (AAs) treatment. Sánchez & Vázquez [2017] reported that the size of peptides, their AAs composition and sequence affect their cell proliferation potential. In addition,

several studies reported that peptides of hydrolyzed collagen rich in Gly, Pro, and Ala affected the proliferation of fibroblast L929, MRC5, and bone marrow-mesenchymal stem (BMMS) cells [Benjakul *et al.* 2018b; Chotphruethipong *et al.*, 2021a; Elango *et al.*, 2019]. After 24 h of oral prolyl-hydroxyproline (a collagen-derived bioactive peptide) administration in rats, the radioactive (^{14}C) dipeptides of prolyl-hydroxyproline were observed in rats' osteoblasts, osteoclasts, dermal fibroblasts, epidermal cells, synovial cells, and chondrocytes [Kawaguchi *et al.*, 2012]. Previous studies demonstrated also that Pro-Hyp affected the fibroblasts [Shigemura *et al.*, 2009] and osteoblast

[Kimira *et al.*, 2017] proliferation. In this study, we found higher levels of Gly, Pro, and Ala in HCSS consistent with the proliferation of skin keratinocyte HaCaT cells. Therefore, it can be assumed that Pro and Hyp of HCSS peptides may regulate keratinocyte proliferation.

HCSS increases the migration and filopodia formation in keratinocytes HaCaT

Besides cell proliferation, an appropriate keratinocyte migration is required for minor, superficial, and basic skin lesions for the second phase of wound healing. Keratinocytes are also involved in more complex pathological states, for example ulcers or pressure sores [Horikoshi *et al.*, 2018]. Therefore, a wounded area was further determined to assess the potential effect of HCSS at 50, 100, 500, and 1000 $\mu\text{g}/\text{mL}$ on the migratory activity of HaCaT cells. Based on the wound-healing assay, HCSS at 50, 100, 500, and 1000 $\mu\text{g}/\text{mL}$ significantly decreased the wound area in a concentration dependent manner with 20.57 ± 5.58 , 8.31 ± 2.79 , 0.00 ± 0.00 , and $0.00 \pm 0.00\%$, respectively (Figure 4A and Figure 4B). A low concentration of HCSS supported the efficiency in wound closure by 70–80% as compared to the control. The wound area was completely closed after 24 h when HCSS was used at concentrations of 500 and 1000 $\mu\text{g}/\text{mL}$. This result implied that HCSS could stimulate keratinocyte migration, especially at the high concentration. In general, collagen had a crucial role in wound repair by promoting the endothelial cells mobility to develop new blood vessels [Martin & Nunan, 2015]. Thus, the granulation tissue development was increased, and wound area was declined [Chotphruethipong *et al.*, 2021a]. Hyp, a specific component of collagen, is an important indicator to determine collagen deposition during wound healing process [Huang *et al.*, 2015]. Chen *et al.* [2019] documented that fish collagen rich in Hyp could accelerate wound healing process of Sprague Dawley rats. Similarly, an earlier report claimed that collagen hydrolysates rich in Gly, Pro, and Ala had a potential activity in wound closure [Chotphruethipong *et al.*, 2021a]. Thus, amino acids, especially Gly and Pro, found in HCSS might promote keratinocyte migration as ascertained by the decreased wound gap. Thus, it can be postulated that an increase in the rate of keratinocytes proliferation and migration undoubtedly leads to fast wound healing.

The cytoskeleton is one of essential constituents in wound healing requiring the shrinkage of actomyosin, cell migration and enlistment of repair systems [Abreu-Blanco *et al.*, 2012]. The migration of cell involves the formation of cell protrusion, for example lamellipodia and filopodia [Singhorn *et al.*, 2018]. This is the first study to elucidate the protrusion of cell that facilitated cell migration in response to HCSS treatment in keratinocytes. Keratinocyte HaCaT cells were exposed to HCSS (50–1000 $\mu\text{g}/\text{mL}$) for 24 h. Our results showed that 100, 500, and 1000 $\mu\text{g}/\text{mL}$ HCSS treatment significantly enhanced the number of filopodia per cells as compared with the control (Figure 4C and Figure 4D). The highest activity was presented in cells treated with HCSS at 1000 $\mu\text{g}/\text{mL}$. Taken together, our results revealed the migratory activities of HCSS in keratinocytes. This result was consistent with wound area (Figure 4A and Figure 4B) as evidenced by the increased formation of filopodia, particularly at the HCSS concentrations

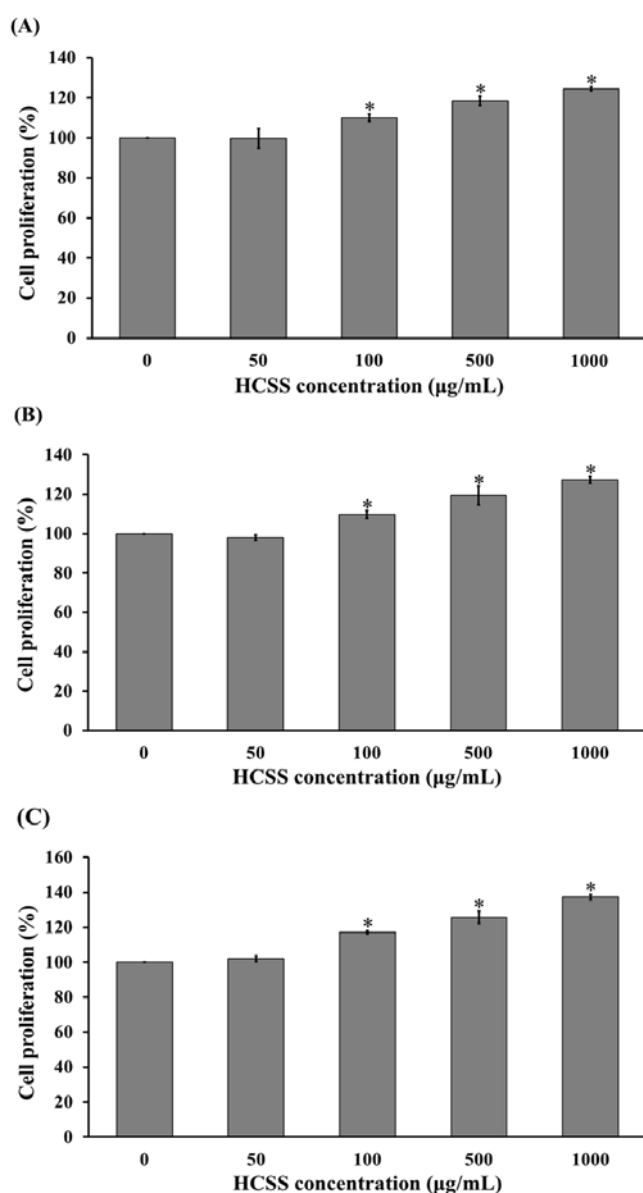


FIGURE 3. The proliferation of skin HaCaT keratinocytes after treatment with hydrolyzed collagen from salmon skin (HCSS) at concentrations of 0, 50, 100, 500 and 1000 $\mu\text{g}/\text{mL}$ for 24 h. (A) 3-(4,5-dimethylthiazol-2-yl)-2,5-diphenyltetrazolium bromide (MTT) assay, (B) double stranded DNA (dsDNA) assay and (C) total cellular protein assay.

Results are presented as mean \pm standard error of the mean of four independent experiments ($n=4$). The asterisk above bars indicates a significant difference between the HCSS treatment and the corresponding control without HCSS ($p < 0.05$).

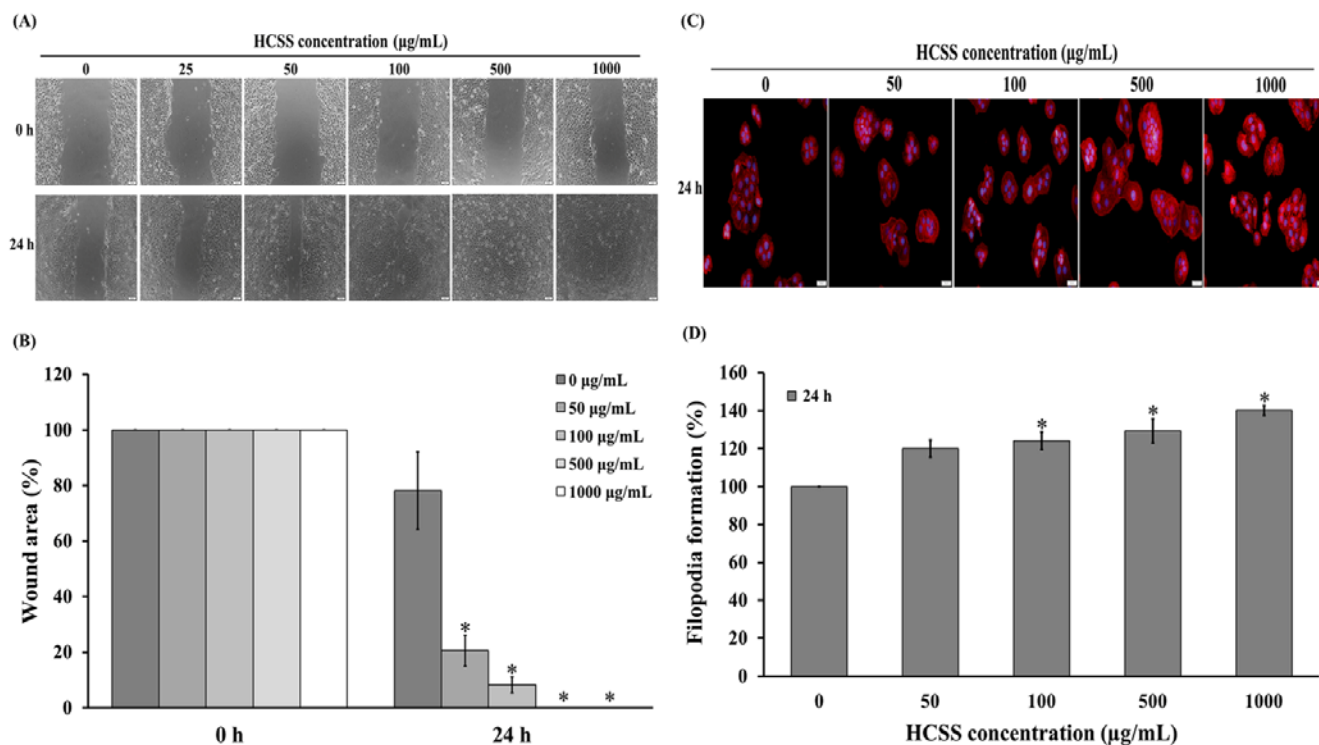


FIGURE 4. The migration activities and filopodia formation of skin HaCaT keratinocytes after treatment with hydrolyzed collagen from salmon skin (HCSS) at concentrations of 0, 50, 100, 500 and 1000 $\mu\text{g/mL}$ for 24 h. (A) wound healing assay, (B) the percentage of wound area, (C) phalloidin-rhodamine stained for filopodia (scale bar = 50 μm), and (D) percentage of filopodia formation.

Results are presented as mean \pm standard error of the mean of four independent experiments ($n=4$). The asterisk above bars indicates a significant difference between the HCSS treatment and the corresponding control without HCSS ($p < 0.05$).

of 100, 500, and 1000 $\mu\text{g/mL}$. Our findings agree with results of previous studies which have shown that hydrolyzed collagen from fish skin increased the formation of lamellipodia in fibroblasts [Chotphruethipong *et al.*, 2021a]. Altogether, we could explain that the upregulation of filopodia formation in this study may be due to the AAs content in hydrolyzed collagen and may subsequently contribute to the increased keratinocyte migration in the wound healing process.

HCSS increases cell migration and filopodia formation via focal adhesion kinase (FAK)/steroid receptor coactivator (Src) activation

In the present study, the migratory activity of skin keratinocytes was induced by HCSS administration. Several signaling molecules have been identified and found to be necessary in the control of cell migration, extension, and cytoskeleton contraction, for example, FAK, Src, protein kinase B (Akt), Ras-related C3 botulinum toxin substrate 1 (Rac1), Ras homolog family member A (RhoA), and cell division control protein 42 (Cdc42) [Masraks *et al.*, 2020; Ritto *et al.*, 2017; Singkhorn *et al.*, 2018]. The upstream regulatory cell signals of cell migration controllers, such as FAK, Src, and Akt, were further analyzed. The results revealed that HCSS administration increased the expression of pFAK (phosphorylated at Tyr397) and pSrc (phosphorylated at Tyr418), in keratinocyte HaCaT at 100, 500, and 1000 $\mu\text{g/mL}$ (Figure 5A and Figure 5B). However, the pAkt (phosphorylated at Ser473) was not affected by the HCSS treatment. FAK and Src are

important for reepithelialization during the wound repair process [Seo *et al.*, 2018; Singkhorn *et al.*, 2018]. In addition, stimulation of FAK and Src complex activates keratinocytes migration in epidermal wound healing [Petpiroon *et al.*, 2015; Seo *et al.*, 2018; Singkhorn *et al.*, 2018]. Nevertheless, this is the first study to examine the mechanism of HCSS induced keratinocyte migration through the FAK-Src complex pathway activation. Few studies reported that the amino acid domain containing Asn, Gly, Gln, and Ala in collagen can interact with $\alpha_2\beta_1$ integrin on the cell membrane that is involved in the activation of the FAK-c-Jun N-terminal kinase (JNK) pathway [Chiu *et al.*, 2014]. Thus, we could explain that the activation of FAK-Src by HCSS may result from the presence of Asn, Gly, Gln, and Ala in hydrolyzed collagen which was found in the high level in our study.

Our previous reports demonstrated that Cdc42, Rac1, and RhoA proteins were involved in the filopodia formation and migration of skin keratinocytes [Ritto *et al.*, 2017; Singkhorn *et al.*, 2018]. In order to authenticate the mechanism of HCSS effect on the migration stimulation in keratinocyte, we used western blot to examine the important downstream Cdc42, Rac1, and RhoA proteins expression involved in the migration process. In this study, Cdc42, Rac1, and RhoA proteins expression was established to be raised in response to HCSS treatment at the concentrations 100, 500, and 1000 $\mu\text{g/mL}$ (Figure 5C and Figure 5D). To our knowledge, this is the first study that described the downstream Cdc42, Rac1 and RhoA proteins activation by HCSS. Thus, we suggest that HCSS

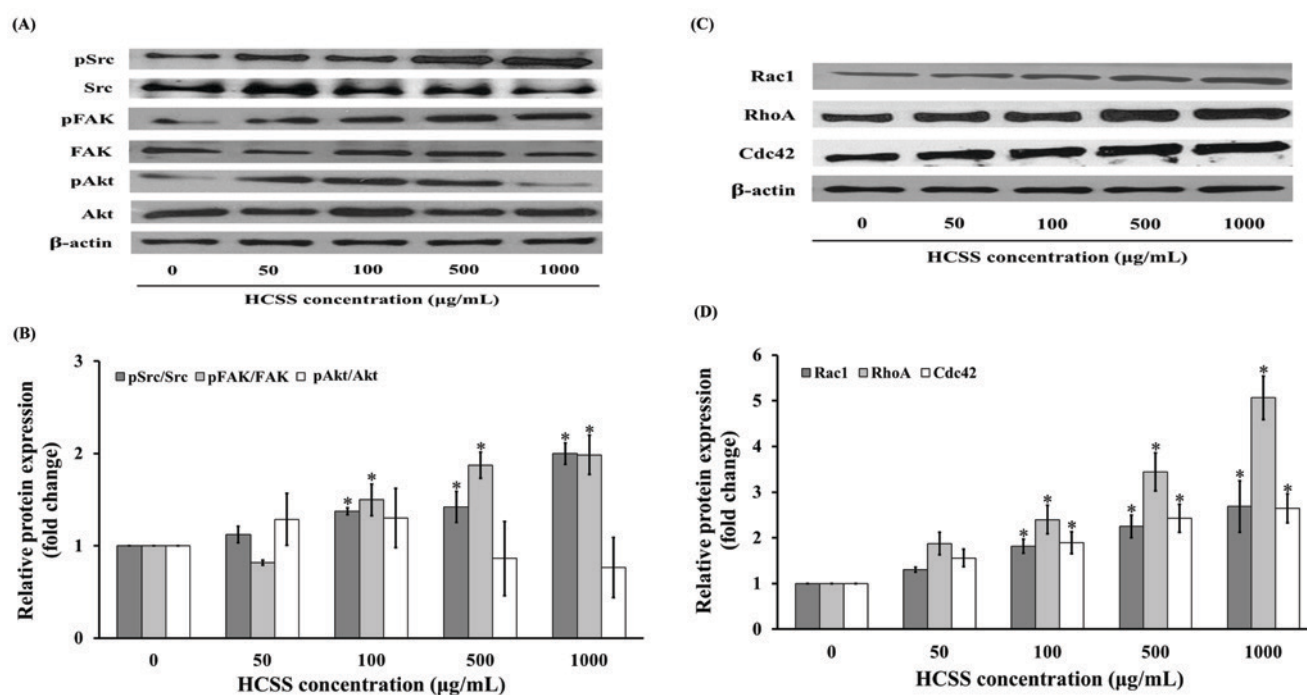


FIGURE 5. The migration protein expression of skin HaCaT keratinocytes after treatment with hydrolyzed collagen from salmon skin (HCSS) at concentrations of 0, 50, 100, 500 and 1000 $\mu\text{g}/\text{mL}$ for 24 h. (A) western blotting indicating the expression of pSrc, Src, pFAK, FAK, pAkt, and Akt, (B) the relative expression of pSrc/Src, pFAK/FAK, and pAkt/Akt, (C) western blotting indicating the expression of Rac1, RhoA, and Cdc42, and (D) the relative expression of Rac1, Cdc42, and RhoA.

Results are presented as mean \pm standard error of the mean of four independent experiments ($n=4$). The asterisk above bars indicates a significant difference between the HCSS treatment and the corresponding control without HCSS ($p < 0.05$).

regulated cell migration and cytoplasmic protrusions formation of skin by activating FAK/Src upstream pathways, and Rac1, Cdc42, and RhoA downstream pathway.

HCSS increases the expression of stem cell markers

Keratinocyte stem cells (KSCs) are accountable for sustaining epidermal homeostasis and healing the tissue damages [Fuchs, 2008; Pincelli & Marconi, 2010; Sotiropoulou & Blanpain, 2012]. Several evidence indicate that KSCs contain various proteins which demonstrated the powerful function in maintaining stem cell-like phenotypes, for example keratin 19, β -catenin, and others [Abbas *et al.*, 2011; Leng *et al.*, 2020]. The present study showed that HCSS treatment at the concentrations 100, 500, and 1000 $\mu\text{g}/\text{mL}$ significantly enhanced keratin 19 and β -catenin protein expression in keratinocyte HaCaT cells when compared to the untreated control (Figure 6A and Figure 6B). Our results were similar to those from the previous studies reporting that the collagen extract from abalone caused an increase in KSCs marker expression, such as ALDH1A1, keratin 19, and β -catenin in keratinocyte HaCaT cells [Thaweekitphathanaphakdee *et al.*, 2019]. In addition, collagen type I enhanced the properties of stem cell-like phenotype by the $\alpha_2\beta_1$ -integrin activation [Kirkland, 2009]. Integrin is a cell surface receptor that plays a crucial role in maintaining several signaling cascades such as Akt [Desgrosellier & Cheresch, 2010] and Wnt/ β -catenin [Crampton *et al.*, 2009; Leng *et al.*, 2020]; thereby mediates cell survival and proliferation, and stimulates stemness of cells [Leng *et al.*, 2020]. It is possible that HCSS may activate stemness

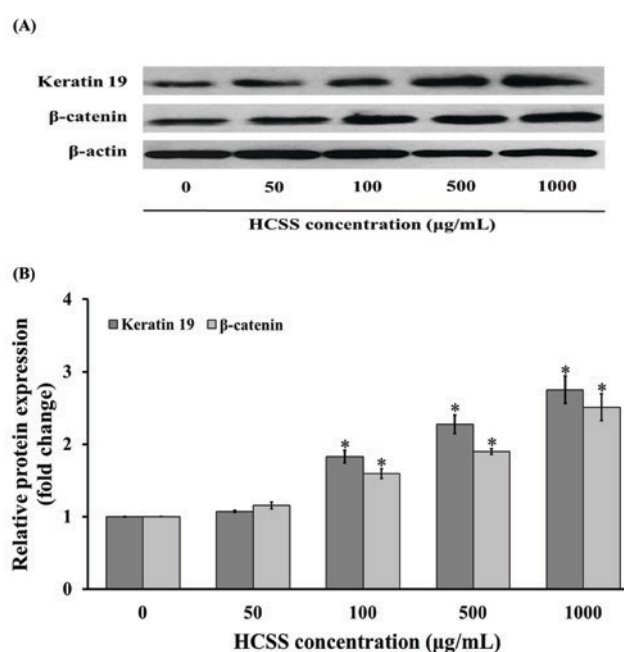


FIGURE 6. The expression of stem cell markers in skin HaCaT keratinocytes after treatment with hydrolyzed collagen from salmon skin (HCSS) at concentrations of 0, 50, 100, 500 and 1000 $\mu\text{g}/\text{mL}$ for 24 h. (A) western blotting indicating the expression of keratin 19 and β -catenin, and (B) the relative expression of keratin 19 and β -catenin.

Results are presented as mean \pm standard error of the mean of four independent experiments ($n=4$). The asterisk above bars indicates a significant difference between the HCSS treatment and the corresponding control without HCSS ($p < 0.05$).

of keratinocytes by β -catenin-dependent mechanism. Our results add to the existing knowledge that HCSS improves the keratinocytes stemness properties, which are essential for epidermal homeostasis and skin barrier function [Fuchs, 2008; Pincelli & Marconi, 2010; Sotiropoulou & Blanpain, 2012].

CONCLUSIONS

Fish skins, being by-products of the food industry, represent a viable material for producing collagen hydrolysates. A hydrolyzed collagen from salmon skins (HCSS) significantly activated the migration of keratinocytes, a predominant cell type in the epidermis, by the activation FAK-Src upstream pathway and Rac1, RhoA, and Cdc42 downstream pathway. In addition, HCSS significantly increased the expression levels of stem cell markers, which are crucial factors for keratinocyte stem cell's function. Taken together, HCSS has been highlighted to elicit the beneficial effect which may have a promising utilization for wound healing, skin repair, and skin barrier function.

ACKNOWLEDGEMENTS

We thank Publication clinic, Prince of Songkla University for the assistance in manuscript language editing.

RESEARCH FUNDING

This research was funded by Participation in the Partnership Program in Production of Graduates in Master's Degree between the Thailand Institute of Scientific and Technological Research (TISTR) and Educational Institutions (6110220098).

CONFLICT OF INTERESTS

The authors declare no conflict of interest.

ORCID IDs

S. Tanasawet <https://orcid.org/0000-0002-6877-9298>
 S. Benjakul <https://orcid.org/0000-0001-9433-3671>
 W. Sukketsiri <https://orcid.org/0000-0003-0836-1487>

REFERENCES

- Abate, M., Citro, M., Pisanti, S., Caputo, M., Martinelli, R. (2021). Keratinocytes migration promotion, proliferation induction, and free radical injury prevention by 3-hydroxytyrosol. *International Journal of Molecular Sciences*, 22(5), art. no. 2438. <https://doi.org/10.3390/ijms22052438>
- Abbas, O., Richards, J.E., Yaar, R., Mahalingam, M. (2011). Stem cell markers (cytokeratin 15, cytokeratin 19 and p63) in *in situ* and invasive cutaneous epithelial lesions. *Modern Pathology*, 24, 90–97. <https://doi.org/10.1038/modpathol.2010.180>
- Abreu-Blanco, M.T., Watts, J.J., Verboon, J.M., Parkhurst, S.M. (2012). Cytoskeleton responses in wound repair. *Cellular and Molecular Life Sciences*, 69, 2469–2483. <https://doi.org/10.1007/s00018-012-0928-2>
- Baroni, A., Buommino, E., De Gregorio, V., Ruocco, E., Ruocco, V., Wolf, R. (2012). Structure and function of the epidermis related to barrier properties. *Clinics in Dermatology*, 30(3), 257–262. <https://doi.org/10.1016/j.clinidermatol.2011.08.007>
- Benjakul, S., Karnjanapratum, S., Visessanguan, W. (2018a). Production and characterization of odorless antioxidative hydrolyzed collagen from seabass (*Lates calcarifer*) skin without descaling. *Waste and Biomass Valorization*, 9, 549–559. <https://doi.org/10.1007/s12649-017-0008-9>
- Benjakul, S., Karnjanapratum, S., Visessanguan, W. (2018b). Hydrolysed collagen from *Lates calcarifer* skin: its acute toxicity and impact on cell proliferation and collagen production of fibroblasts. *International Journal of Food Science & Technology*, 53(8), 1871–1879. <https://doi.org/10.1111/ijfs.13772>
- Chalamaiah, M., Ulug, S.K., Hong, H., Wu, J.P. (2019). Regulatory requirements of bioactive peptides (protein hydrolysates) from food proteins. *Journal of Functional Foods*, 58, 123–129. <https://doi.org/10.1016/j.jff.2019.04.050>
- Chen, T., Hu, H., Fan, Y., Wang, S., Chen, Q., Si, L., Li, B. (2016). Protective effect of gelatin peptides from pacific cod skin against photoaging by inhibiting the expression of MMPs via MAPK signaling pathway. *Journal of Photochemistry and Photobiology B: Biology*, 165, 34–41. <https://doi.org/10.1016/j.jphotobiol.2016.10.015>
- Chen, J., Gao, K., Liu, S., Wang, S., Elango, J., Bao, B., Dong, J., Liu, N., Wu, W. (2019). Fish collagen surgical compress repairing characteristics on wound healing process *in vivo*. *Marine Drugs*, 17(1), art. no. 33. <https://doi.org/10.3390/md17010033>
- Chiu, L.H., Lai, W.F., Chang, S.F., Wong, C.C., Fan, C.Y., Fang, C.L., Tsai, Y.H. (2014). The effect of type II collagen on MSC osteogenic differentiation and bone defect repair. *Biomaterials*, 35(9), 2680–2691. <https://doi.org/10.1016/j.biomaterials.2013.12.005>
- Chotphruethipong, L., Aluko, R.E., Benjakul, S. (2019). Hydrolyzed collagen from porcine lipase-defatted seabass skin: antioxidant, fibroblast cell proliferation, and collagen production activities. *Journal of Food Biochemistry*, 43(5), art. no. e12825. <https://doi.org/10.1111/jfbc.12825>
- Chotphruethipong, L., Sukketsiri, W., Aluko, R.E., Sae-leaw, T., Benjakul, S. (2021a). Effect of hydrolyzed collagen from defatted Asian sea bass (*Lates calcarifer*) skin on fibroblast proliferation, migration and antioxidant activities. *Journal of Food Science and Technology*, 58, 541–551. <https://doi.org/10.1007/s13197-020-04566-4>
- Chotphruethipong, L., Sukketsiri, W., Battino, M., Benjakul, S. (2021b). Conjugate between hydrolyzed collagen from defatted seabass skin and epigallocatechin gallate (EGCG): characteristics, antioxidant activity and *in vitro* cellular bioactivity. *RSC Advances*, 11, 2175–2184. <https://doi.org/10.1039/D0RA07135H>
- Chotphruethipong, L., Binlath, T., Hutamekalin, P., Sukketsiri, W., Aluko, R.E., Benjakul, S. (2021c). *In vitro* antioxidant and wound-healing activities of hydrolyzed collagen from defatted Asian sea bass skin as influenced by different enzyme types and hydrolysis processes. *RSC Advances*, 11, 18144–18151. <https://doi.org/10.1039/D1RA03131G>

15. Chotphruethipong, L., Binlath, T., Hutamekalin, P., Aluko, R.E., Tapaamorndech, S., Zhang, B., Benjakul, S. (2021d). Impact of hydrolyzed collagen from defatted sea bass skin on proliferation and differentiation of preosteoblast MC3T3-E1 cells. *Foods*, 10(7), art. no. 1476.
<https://doi.org/10.3390/foods10071476>
16. Crampton, S.P., Wu, B., Park, E.J., Kim, J.H., Solomon, C., Watterman, M.L., Hughes, C.C. (2009). Integration of the β -catenin-dependent Wnt pathway with integrin signaling through the adaptor molecule Grb2. *PLoS One*, 4, art. no. e7841.
<https://doi.org/10.1371/journal.pone.0007841>
17. Desgrosellier, J.S., Cheresch, D.A. (2010). Integrins in cancer: biological implications and therapeutic opportunities. *Nature Reviews Cancer*, 10, 9–22.
<https://doi.org/10.1038/nrc2748>
18. Edgar, S., Hopley, B., Genovese, L., Sibilla, S., Laight, D., Shute, J. (2018). Effects of collagen-derived bioactive peptides and natural antioxidant compounds on proliferation and matrix protein synthesis by cultured normal human dermal fibroblasts. *Scientific Reports*, 8, art. no. 10474.
<https://doi.org/10.1038/s41598-018-28492-w>
19. Elango, J., Robinson, J., Zhang, J., Bao, B., Ma, N., de Val, J.E.M.S., Wu, W. (2019). Collagen peptide upregulates osteoblastogenesis from bone marrow mesenchymal stem cells through MAPK- Runx2. *Cells*, 8(5), art. no. 446.
<https://doi.org/10.3390/cells8050446>
20. Fuchs, E. (2008). Skin stem cells: rising to the surface. *Journal of Cell Biology*, 180(2), 273–284.
<https://doi.org/10.1083/jcb.200708185>
21. Horikoshi, Y., Kamizaki, K., Hanaki, T., Morimoto, M., Kitagawa, Y., Nakaso, K., Kusumoto, C., Matura, T. (2018). α -Tocopherol promotes HaCaT keratinocyte wound repair through the regulation of polarity proteins leading to the polarized cell migration. *BioFactors*, 44(2), 180–191.
<https://doi.org/10.1002/biof.1414>
22. Hu, Z., Yang, P., Zhou, C., Li, S., Hong, P. (2017). Marine collagen peptides from the skin of Nile tilapia (*Oreochromis niloticus*): characterization and wound healing evaluation. *Marine Drugs*, 15(4), art. no. 102.
<https://doi.org/10.3390/md15040102>
23. Huang, R., Li, W., Lv, X., Lei, Z., Bian, Y., Deng, H., Wang, H., Li, J., Li, X. (2015). Biomimetic LBL structured nanofibrous matrices assembled by chitosan/collagen for promoting wound healing. *Biomaterials*, 53, 58–75.
<https://doi.org/10.1016/j.biomaterials.2015.02.076>
24. Kawaguchi, T., Nanbu, P.N., Kurokawa, M. (2012). Distribution of prolylhydroxyproline and its metabolites after oral administration in rats. *Biological and Pharmaceutical Bulletin*, 35(3), 422–427.
<https://doi.org/10.1248/bpb.35.422>
25. Kimira, Y., Odaira, H., Nomura, K., Taniuchi, Y., Inoue, N., Nakatani, S., Shimizu, J., Wada, M., Mano, H. (2017). Collagen-derived dipeptide prolylhydroxyproline promotes osteogenic differentiation through Foxg1. *Cellular & Molecular Biology Letters*, 22, art. no. 27.
<https://doi.org/10.1186/s11658-017-0060-2>
26. Kirkland, S.C. (2009). Type I collagen inhibits differentiation and promotes a stem cell-like phenotype in human colorectal carcinoma cells. *British Journal of Cancer*, 101, 320–326.
<https://doi.org/10.1038/sj.bjc.6605143>
27. Leng, L., Ma, J., Lv, L., Wang, W., Gao, D., Zhu, Y., Wu, Z. (2020). Both Wnt signaling and epidermal stem cell-derived extracellular vesicles are involved in epidermal cell growth. *Stem Cell Research & Therapy*, 11, art. no. 415.
<https://doi.org/10.1186/s13287-020-01933-y>
28. Lü, L., Zhang, L., Wai, M.S.M., Yew, D.T.W., Xu, J. (2012). Exocytosis of MTT formazan could exacerbate cell injury. *Toxicology in Vitro*, 26(4), 636–644.
<https://doi.org/10.1016/j.tiv.2012.02.006>
29. Martin, P., Nunan, R. (2015). Cellular and molecular mechanisms of repair in acute and chronic wound healing. *British Journal of Dermatology*, 173(2), 370–378.
<https://doi.org/10.1111/bjd.13954>
30. Masraka, W., Tanasawet, S., Hutamekalin, P., Wongtawatchai, T., Sukketsiri, W. (2020). Luteolin attenuates migration and invasion of lung cancer cells via suppressing focal adhesion kinase and non-receptor tyrosine kinase signaling pathway. *Nutrition Research and Practice*, 14(2), 127–133.
<https://doi.org/10.4162/nrp.2020.14.2.127>
31. Morgan, P.T., Breen, L. (2021). The role of protein hydrolysates for exercise-induced skeletal muscle recovery and adaptation: a current perspective. *Nutrition & Metabolism*, 18, art. no. 44.
<https://doi.org/10.1186/s12986-021-00574-z>
32. Petpiroon, N., Suktap, C., Pongsamart, S., Chanvorachote, P., Sukrong, S. (2015). Kaempferol-3-O-rutinoside from *Afgekia mahidoliae* promotes keratinocyte migration through FAK and Rac 1 activation. *Journal of Natural Medicines*, 69, 340–348.
<https://doi.org/10.1007/s11418-015-0899-3>
33. Pincelli, C., Marconi, A. (2010). Keratinocyte stem cells: friends and foes. *Journal of Cellular Physiology*, 225(2), 310–315.
<https://doi.org/10.1002/jcp.22275>
34. Ritto, D., Tanasawet, S., Singkhorn, S., Klaypradit, W., Hutamekalin, P., Tipmanee, V., Sukketsiri, W. (2017). Astaxanthin induces migration in human skin keratinocytes via Rac1 activation and RhoA inhibition. *Nutrition Research and Practice*, 11(4), 275–280.
<https://doi.org/10.4162/nrp.2017.11.4.275>
35. Sánchez, A., Vázquez, A. (2017). Bioactive peptides: A review. *Food Quality and Safety*, 1, 29–46.
<https://doi.org/10.1093/fqsafe/fyx006>
36. Shigemura, Y., Iwai, K., Morimatsu, F., Iwamoto, T., Mori, T., Oda, C., Taira, T., Park, E.Y., Nakamura, Y., Sato, K. (2009). Effect of prolyl-hydroxyproline (Pro-Hyp), a food-derived collagen peptide in human blood, on growth of fibroblasts from mouse skin. *Journal Agricultural and Food Chemistry*, 57(2), 444–449.
<https://doi.org/10.1021/jf802785h>
37. Singkhorn, S., Tantisira, M.H., Tanasawet, S., Hutamekalin, P., Wongtawatchai, T., Sukketsiri, W. (2018). Induction of keratinocyte migration by ECa 233 is mediated through FAK/Akt, ERK, and p38 MAPK signaling. *Phytotherapy Research*, 32(7), 1397–1403.
<https://doi.org/10.1002/ptr.6075>
38. Seo, G.Y., Hyun, C., Koh, D., Park, S., Lim, Y., Kim, Y.M., Cho, M. (2018). A novel synthetic material, BMM, accelerates wound repair by stimulating re-epithelialization and fibroblast activation. *International Journal of Molecular Sciences*, 19(4), art. no. 1164.
<https://doi.org/10.3390/ijms19041164>

39. Sotiropoulou, P.A., Blanpain, C. (2012). Development and homeostasis of the skin epidermis. *Cold Spring Harbor Perspectives in Biology*, 4, art. no. a008383.
<https://doi.org/10.1101/cshperspect.a008383>
40. Thaweekitphathanaphakdee, S., Chanvorachote, P., Prateepchinda, S., Khongkow, M., Sucontphunt, A. (2019). Abalone collagen extracts potentiate stem cell properties of human epidermal keratinocytes. *Marine Drugs*, 17(7), art. no. 424.
<https://doi.org/10.3390/md17070424>
41. Van Tonder, A., Joubert, A.M., Cromarty, A.D. (2015). Limitations of the 3-(4,5-dimethylthiazol-2-yl)-2,5-diphenyl-2H-tetrazolium bromide (MTT) assay when compared to three commonly used cell enumeration assays. *BMC Research Notes*, 8, art. no. 47.
<https://doi.org/10.1186/s13104-015-1000-8>
42. Wickett, R.R., Visscher, M.O. (2006). Structure and function of the epidermal barrier. *American Journal of Infection Control*, 34(10), Suppl., S98-S110.
<https://doi.org/10.1016/j.ajic.2006.05.295>
43. Wikramanayake, T.C., Stojadinovic, O., Tomic-Canic, M. (2014). Epidermal differentiation in barrier maintenance and wound healing. *Advances in Wound Care*, 3(3), 272–280.
<https://doi.org/10.1089/wound.2013.0503>
44. Yang, R., Liu, F., Wang, J., Chen, X., Xie, J., Xiong, K. (2019a). Epidermal stem cells in wound healing and their clinical applications. *Stem Cell Research & Therapy*, 10, art. no. 229.
<https://doi.org/10.1186/s13287-019-1312-z>
45. Yang, F., Jin, S., Tang, Y. (2019b). Marine collagen peptides promote cell proliferation of NIH-3T3 fibroblasts via NF-κB signaling pathway. *Molecules*, 24(22), art. no. 4201.
<https://doi.org/10.3390/molecules24224201>

Protective Effect of the Ethanol Extract from *Hericium erinaceus* Against Ethanol-Induced Gastric Ulcers

Guoying Lv¹ , Xiaoya Song², Zuofa Zhang^{1*} 

¹Institute of Horticulture, Zhejiang Academy of Agricultural Science, Hangzhou, Zhejiang 310021, China

²Institute of Fungi, Lishui Academy of Agricultural and Forestry Sciences, Lishui, Zhejiang 323000, China

Key words: mushroom ethanol extract, gastroprotective activity, *Hericium erinaceus*, bioinformatics analysis

The fruiting bodies of *Hericium erinaceus* have been widely used for the treatment of dyspepsia, chronic gastric ulcers, and enervation. There remains a lack of data on the role of an ethanol extract from *H. erinaceus* (EEH) on ethanol-induced gastric ulcers. The ethanol-induced experimental gastric injury model was used to evaluate the gastroprotective activity of extracts. Ultra-high performance liquid chromatography-triple quadrupole-time of flight tandem mass spectrometry (UPLC-Triple-TOF-MS) analysis was used to identify the possible compounds present in EEH. Transcriptome sequencing (RNA-seq) and bioinformatics analyses were conducted to reveal the characteristics and molecular mechanism underlying EEH's protective effect of on gastric tissue injury. Administration of EEH at doses of 0.625, 1.25, and 2.5 g/kg body weight prior to ethanol ingestion dose-dependently inhibited gastric ulcers. EEH also significantly increased superoxide dismutase (SOD) activity and decreased malondialdehyde (MDA) content in the gastric tissue. Twelve compounds from EEH were identified including three diterpene compounds, two heteroterpene compounds, three isoindolinone compounds, one aromatic compound, *N*-(1-deoxy-D-fructos-1-yl)-L-valine, adenosine, and lumichrome. These compounds promote the inhibition of pathways involved in gastric ulcer formation. The RNA-seq results suggest that EEH indirectly protects the gastric tissue from injury by regulating the cell cycle and biological functions, up-regulating several signal molecules, or activating several proteasome functions. It was concluded that EEH represents a potential therapeutic option to reduce the risk of gastric ulceration.

INTRODUCTION

Gastric ulcers are a serious problem that affect more than 10% of individuals worldwide [O' Malley, 2003]. The process underlying their development is complex and multifactorial, and includes gastric mucosa ischemia, stress, smoking, *Helicobacter pylori* infection, alcohol, and poor dietary habits [Liu *et al.*, 2018]. In terms of conventional therapy, the drugs currently available for the treatment of gastric ulcers produce severe side effects [Chanda *et al.*, 2011]. Thus, many scientists are currently evaluating natural products to identify an effective ulcer treatment with fewer side effects than the current conventional treatment. Of note, various edible plants are used in folk medicine to treat gastric ulcers with promising results [Sathish *et al.*, 2011].

Hericium erinaceus, belonging to the Aphyllophorales, Hydnaeaceae and *Hericium* families [Friedman, 2015], is a precious medicinal and edible fungus in China. It serves a magnitude of physiological and health-promoting functions including immunity enhancement, antitumor, and antibacterial properties; it can also improve lipid metabolism and prevent gastrointestinal diseases [Kim *et al.*, 2011]. It has many active ingredients including phenolic compounds, erinacines,

steroids, terpenoids, peptides, and polysaccharides, which are responsible for its bioactivity [Lee *et al.*, 2016; Wu *et al.*, 2018]. *H. erinaceus* is considered to have an outstanding value as a potential therapeutic option for gastrointestinal problems. Currently, its fruiting bodies are widely used for the treatment of dyspepsia, chronic gastric ulcers and enervation. A previous study has reported that the ethanol extract from *H. erinaceus* elicits anti-inflammatory effects against ulcerative colitis [Qin *et al.*, 2016]. Furthermore, an aqueous extract and polysaccharides from *H. erinaceus* have been reported to eliminate ethanol-induced gastric damage [Wang *et al.*, 2018a]. However, to date, there is no published data on the role of the ethanol extract from *H. erinaceus* (EEH) on ethanol-induced gastric ulcers.

Combined biological and analytical studies have the potential to increase our understanding of the use of *H. erinaceus* and its possible bioactive effects. Therefore, the aim of the present study was to investigate the chemical composition and gastroprotective effect of EEH. Furthermore, transcriptome sequencing (RNA-seq) and bioinformatics analyses were conducted to reveal the characteristics and molecular mechanism underlying the protective effect of EEH on gastric tissue injury.

* Corresponding Author:

E-mail: zzf2050@163.com (Z. Zhang)

Submitted: 28 April 2021

Accepted: 24 August 2021

Published on-line: 3 September 2021



MATERIALS AND METHODS

Materials and preparation of extracts

Fruiting body of *H. erinaceus* was obtained from the Zhejiang Academy of Agricultural Science farm (Hangzhou, China). The samples were dried in a hot air oven at 60°C, ground, and then passed through a 120-mesh screen. The pretreated samples (100 g) were extracted with 3000 mL of ethanol at 25°C for 2 h. After sonication for 20 min, the extract was filtered through Whatman No. 4 paper. The residue was extracted again with 3000 mL of ethanol. The combined extracts were dried at 40°C under reduced pressure. A brown yellow paste-like extract was obtained.

Analysis of chemical compounds

The compounds in EEH were analyzed by ultra-high performance liquid chromatography-triple quadrupole-time of flight tandem mass spectrometry (UPLC-Triple-TOF-MS). An ACQUITY UPLC system (Waters Co., Milford, MA, USA) equipped with a ZORBAX SB C₁₈ column (100×4.6 mm, Agilent, Santa Clara, CA, USA) and a Triple TOF 5600+ time-of-flight mass spectrometer, equipped with an electrospray ionization source (AB SCIEX, Framingham, MA, USA), were applied for these analyses. The eluents and MS conditions were consistent with the method provided by Wang *et al.* [2018b] with some modifications.

The eluents were: A, 0.1% (v/v) methanoic acid in water; B, 0.1% (v/v) methanoic acid in acetonitrile. The elution conditions were: 0–22 min, linear gradient from 5% to 40% B; 22–33 min, linear gradient from 40% to 95% B; 33–36 min, 95% B; and 36–38 min, linear gradient from 95% to 5% B. The flow rate was 0.3 mL/min, and injection volume was 5 µL. The detection wavelength was 254 nm, and column temperature was 50°C. The MS conditions were listed as follows: positive ion scanning mode, scanning mass range: *m/z* 50–2000; pressure of gas 1 and gas 2: 55 psi; curtain gas pressure: 35 psi; temperature of the ion source: 550°C; voltage of the ion source: 4500 V; first order scanning: declustering potential: 100 V; collision energy: 40 V; second order scanning: TOF MS-Product Ion-IDA mode was used to collect MS data. CID energy was 20, 40, and 60 V.

Animals

The Institute of Cancer Research (ICR) male mice were obtained from the Experimental Animal Center of Zhejiang Province (certification No. SCXK (zhe) 2019–0002; Hangzhou, China). They were raised in cages in a room controlled at constant temperature of 23±2°C, relative humidity of 50–70%, and 12/12 h of light-dark periods. All experimental procedures were conducted in accordance with China legislation under No. 2019ZAASLA08 on the use and care of laboratory animals and within the guidelines established by the Institute for Experimental Animals of Zhejiang Academy of Agricultural Sciences.

Effect of EEH against ethanol-induced gastric ulcers in mice

Mice were randomized into six groups, each consisting of 10 animals. Groups 1 (normal group) and 2 (model

group) received saline (0.9% NaCl) at a dose of 10 mL/kg body weight; and group 6 received ranitidine (0.108 g/kg) as the positive group. Other three groups (3–5, administration group) received EEH at doses of 0.625, 1.25, and 2.5 g/kg body weight, respectively. The corresponding saline, extracts, and ranitidine were administered once daily for eight days. On the last day of treatment, 2 h after administration, absolute ethanol (0.1 mL/animal) was administered orally to mice of groups 2–6. Then, 1.5 h later, acute gastric mucosal injury model was established successfully, and the mice were sacrificed. The stomachs were removed and opened along the greater curvature; they were then washed several times with phosphate buffered saline (PBS, pH 7.4, 0.01 M) to remove dirt inside. The mice gastric mucosa was observed using a stereo microscope (Leica Micro Systems Imaging Solutions Ltd, Cambridge, UK). The ulcer inhibition was expressed in percent (%) as: ulcer inhibition (%) = [(ulcer index of model group – ulcer index of administration group) / ulcer index of model group] × 100%.

Histopathological analysis

For histopathological analysis, gastric tissues were cut into 5-mm sections, then they were immersed in 4% paraformaldehyde for 24 h to fix the specimens. The most serious parts of the ulcer region obtained from stomach were chosen to produce paraffin wax tissue sections (4 µm). The tissue sections were then prepared for hematoxylin and eosin (H & E) staining.

Measurement of superoxide dismutase (SOD) activity and malondialdehyde (MDA) content

Gastric tissues were homogenized in ice-cold saline (1:9, v/w), and supernatant of the gastric tissues was harvested. SOD activity and MDA content of the supernatant were evaluated using commercially available kits from Nanjing Jiancheng Bioengineering Institute (Nanjing, China).

RNA-seq analysis of mice stomachs

Ten ICR mice, weighing 18–22 g, were randomly divided into a blank control group (0.9% saline at a dose of 10 mL/kg body weight) and an experimental group (EEH at 2.5 g/kg body weight), with five mice in each group. The corresponding saline and EEH were given by gavage once per day for eight consecutive days. Two hours after the last administration, three mice in each group were randomly selected for transcriptome experiments. The animals were sacrificed, and the stomachs were removed and opened along the greater curvature; they were then rinsed with RNase free water, dried with filter paper, put into a cryopreservation tube, and quickly placed into liquid nitrogen.

Trizol Regent (Invitrogen, Waltham, MA, USA) was used to extract total RNA. A total amount of 2 µg RNA per sample was used as the input material for RNA sample preparation. Briefly, mRNA was purified from total RNA using poly-T oligo-attached magnetic beads. In the first chain synthesis, divalent cations in NEBNext buffer (5X) were used for pyrolysis. Random hexamer primers and RNase H were used to synthesize the first strand cDNA. Then, the second strand cDNA was synthesized with buffer, triphosphate acid base deoxynucleotide (dNTPs), DNA polymerase I, and ribonuclease H

TABLE 1. Effect of the ethanol extract from *Hericium erinaceus* (EEH) on the ulcer index and oxidative markers in mice with ethanol-induced gastric ulcers.

Group	Ulcer Index	Ulcer inhibition (%)	SOD activity (U/ μ g protein)	MDA content (nmol/mg protein)
Normal group	–	–	3.57 \pm 0.35**	12.35 \pm 2.58**
Model group +ethanol	33.40 \pm 4.20	–	1.19 \pm 0.41	34.57 \pm 3.47
0.625 g/kg EEH +ethanol	22.50 \pm 2.87*	32.63	1.35 \pm 0.28	29.61 \pm 1.96
1.25 g/kg EEH +ethanol	21.64 \pm 3.21*	35.20	1.67 \pm 0.29	21.35 \pm 2.85*
2.5 g/kg EEH +ethanol	11.00 \pm 3.57**	67.07	2.14 \pm 0.31*	18.66 \pm 3.11*
0.108 g/kg ranitidine+ethanol	25.63 \pm 4.18*	23.26	2.25 \pm 0.45*	20.58 \pm 4.05*

Each value represents mean \pm standard deviation (n=10). SOD: superoxide dismutase; MDA: malondialdehyde. *significantly different from the model group (p<0.05). **significantly different from the model group (p<0.01).

(RNase H) (Sangon Biotech, Shanghai, China). The library fragments were purified by rapid polymerase chain reaction (PCR) kits and eluted with ethidium bromide (EB) buffer (Sangon Biotech, Shanghai, China). The library was constructed by PCR amplification. After clustering, the library was sequenced on Illumina platform, and 150 bp paired end reading was generated.

Statistical analysis

Results were expressed as mean \pm standard deviation. Statistical analysis was performed using SPSS 19.0 software (SPSS Inc., Chicago, IL, USA) with ANOVA and Student's t-test. Differences between values were considered to be significant at p<0.05 or p<0.01.

The reference genomes and the annotation file were downloaded from the ENSEMBL database (<http://www.ensembl.org/index.html>). Bowtie2 v2.2.3 was used to build the genome index, and Clean Data was then aligned to the reference genome using HISAT2 v2.1.0. Genes with $q \leq 0.05$ and $|\log_2 \text{ratio}| \geq 1$ were identified as differentially expressed genes (DEGs).

RESULTS AND DISCUSSION

Effect of EEH on ethanol-induced gastric lesions

The gastric mucosa is a thin, fragile mucosal tissue, and it has a dynamic balance mechanism for self-repairs. The present study investigated the effects of EEH on ethanol-induced gastric lesions in mice. The ulcer index and ulceration inhibition rate were used to verify the gastroprotective effects of EEH (Table 1). The ulcer index of the ethanol-administered group was 33.40; however, the ulcer indices of the mice pre-treated with 0.625, 1.25 and 2.5 g/kg EEH were 22.50, 21.64 and 11.00, respectively, which were lower than the ulcer index of the ranitidine group (25.63), where the ulceration inhibition rates of the mice pre-treated with 0.625, 1.25 and 2.5 g/kg EEH were 32.63%, 35.20% and 67.07%, respectively (Table 1). The results indicate that the mice pre-treated with EEH and ranitidine had considerably reduced areas of gastric ulcer formation compared with the gastric ulcer model group.

The ethanol-induced experimental gastric injury model is a popular method to evaluate the gastroprotective activity of compounds or extracts [Sahin et al., 2019]. Previous studies have shown that ethanol directly damages gastric mucosa

within 60 min [Ma & Liu, 2014]. It is generally accepted that ethanol disturbs the gastric secretory activity, alters cell permeability, and depletes the gastric mucus [Salim, 1990]. Changes in pro-inflammatory cytokines and gastric mucosal defensive factors are the pathogenic factors involved in ethanol-induced gastric ulcers. In this study, the EEH pre-treatment in mice with gastric ulcers significantly reduced the area of gastric ulcer formation and the ulcer index, suggesting that EEH is able to ameliorate the gastric ulcers.

Histopathological studies

Ethanol is an ulcerogenic agent that produces erosions, ulcerative lesions. Histological evaluations of the gastric walls of ethanol-induced ulcerated mice are depicted in Figure 1. Compared with the normal group, ethanol administration induced gastric mucosa edema, leucocyte infiltration of the submucosal layer, hemorrhage damage, and epithelial cell loss.

Histopathological studies were used to verify the gastric protective effects of EEH. Pre-treatment with EEH and ranitidine for eight days provided a protective effect on the gastric mucosa, reducing the ulcerated area, submucosal edema, and leucocyte infiltration.

Effects of EEH on oxidative markers

As shown in Table 1, the ethanol-treated mice exhibited an obvious reduction in gastric SOD activities as compared with the normal group, which was significantly reversed by ranitidine and EEH (2.5 g/kg). EEH at doses of 0.625 g/kg and 1.25 g/kg also increased the SOD activity when compared with the model group, though these differences were not statistically significant. As for lipid peroxidation, MDA content was significantly increased in the ethanol-stimulated gastric tissue as compared to the normal group. However, this was markedly reversed by 1.25 and 2.5 mg/kg EEH treatments when compared with the model group.

Reactive oxygen species (ROS) play a key role in gastric lesions induced by ethanol [Mei et al., 2012]. They suppress antioxidant enzyme activities and initiate lipid peroxidation, which is an important event in the toxicity mechanism of ethanol [Pan et al., 2008]. Lipid peroxidation destroys the integrity of the membrane structure, which is represented by an apparent increase in MDA content [El-Maraghy et al., 2015]. Therefore, controlling the formation of ROS is essential for

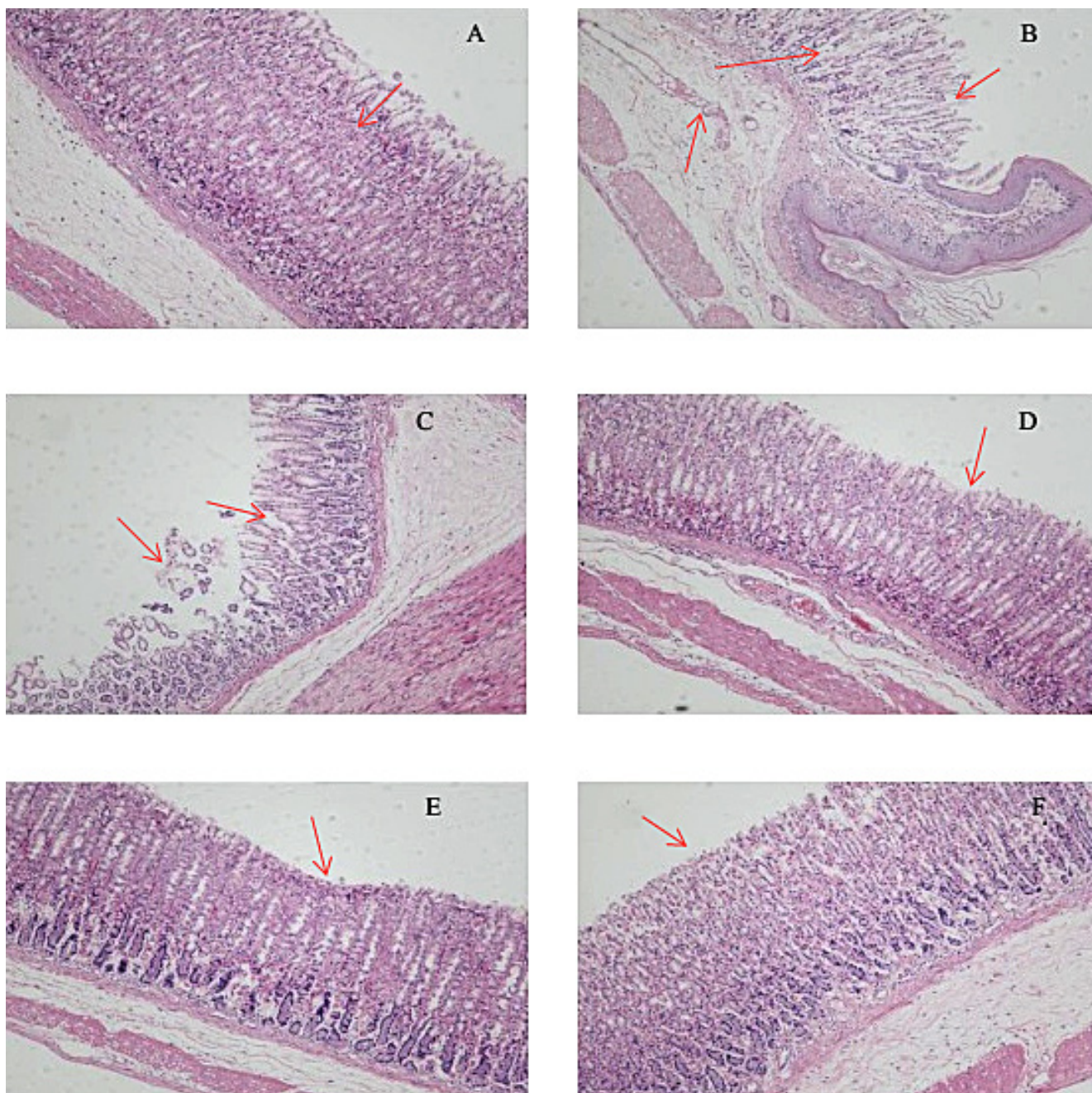


FIGURE 1. Photomicrograph of stomach of the mice from the normal group (A); the model group treated with ethanol (B); groups treated with *Hericium erinaceus* extract (EEH) and ethanol: 0.625 g/kg EEH+ethanol (C), 1.25 g/kg EEH+ethanol (D); 2.5 g/kg EEH+ethanol (E); and the group receiving ranitidine at dose of 0.108 g/kg and ethanol (F). Original magnification 100 \times .

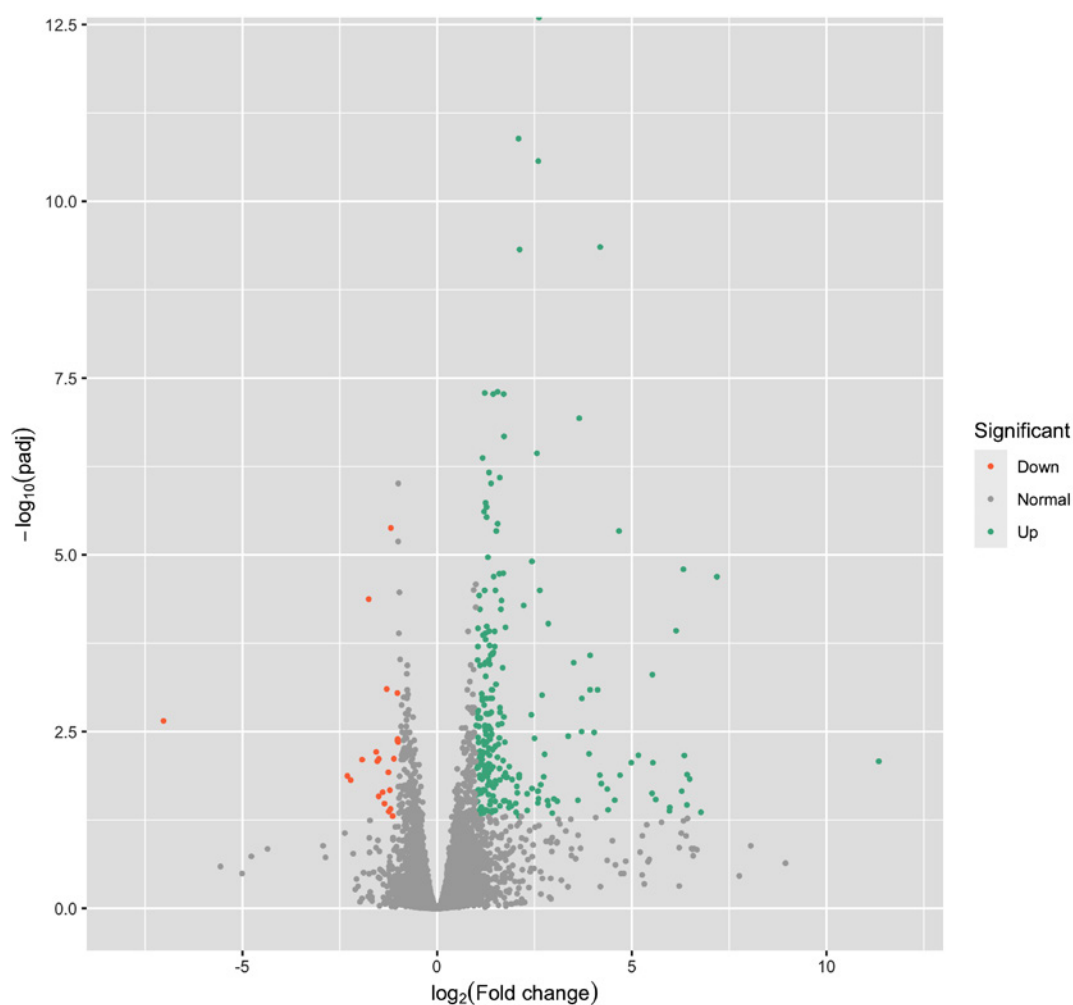
the treatment of gastric lesions. The function of SOD is to remove the harmful superoxide anion radicals, and SOD forms the first line of defense in protection against the destructive action of ROS. The important role of SOD in protecting the stomach against mucosa damage has previously been described by Pan *et al.* [2008]. In the present study, pre-treatment with EEH produced a significant reduction in MDA content and an improvement in SOD activity as compared with the model group, indicating that EEH exerted potent gastric protection by alleviating oxidative stress.

The consumption of antioxidant-rich foods may also help to protect the stomach. The anti-ulcer drug – lansoprazole – has

been reported to prevent the production of MDA [Agnihotri *et al.*, 2007]. Likewise, lycopene (antioxidant compound) has been shown to exhibit protective effects in indomethacin-induced ulcers and the antioxidative extract from *Sphenodesme involucrate* to effectively decrease the ulcer index [Sreeja *et al.*, 2018]. The antioxidant fraction of *Zingiber officinale* has been reported to confer protective actions against diclofenac sodium-induced gastric damage [Saiah *et al.*, 2018]. In turn, Chen *et al.* [2019] reported that the ethanol extract from *H. erinaceus* produced antioxidant activity. The mentioned authors identified hericenone C, hericine B, ergosterol, and ergosterol peroxide in this extract. These results were supported

TABLE 2. Chemical composition of the ethanol extract from *Hericum ernaceus* determined using the UPLC-Triple-TOF-MS analysis.

Peak No.	Proposed compounds	Retention time (min)	[M+H] ⁺ (m/z)	MS/MS fragment ions (m/z)	References
1	<i>N</i> -(1-Deoxy-D-fructos-1-yl)-L-valine	1.34	280	130, 198, 216, 262	
2	Adenosine	1.83	268	119, 136	Hui <i>et al.</i> [2012]
3	Herierin IV	2.83	171	53, 101, 153	Miyazawa <i>et al.</i> [2012]
4	Lumichrome	12.83	243	103, 172, 198	Tsukamoto <i>et al.</i> [1999]
5	Erinaceolactam E	22.25	415	232, 370, 398	Wang <i>et al.</i> [2016]
6	Erinaceolactam A	23.00	330	83, 192, 248	Wang <i>et al.</i> [2016]
7	Erinacerin N	24.04	415	232, 260, 316, 370, 398	Tang <i>et al.</i> [2015]
8	Erinacerin M	24.35	344	83, 206, 262	Tang <i>et al.</i> [2015]
9	Hericenone I	26.24	331	83, 177, 233	Yaoita <i>et al.</i> [2005]
10	Erinacerin B	27.11	333	83, 177, 233, 315	Tang <i>et al.</i> [2015]
11	Hericenone A	27.68	331	85, 145, 193, 247	Kawagishi <i>et al.</i> [1990]
12	<i>N</i> -De(phenylethyl)isohericerin	27.82	316	164, 192, 232	Li <i>et al.</i> [2015]

FIGURE 2. Comparison of operational taxonomic units (OTUs) of differentially expressed genes (DEGs) between blank control group and experimental group treated with the *Hericum ernaceus* extract (EEH).

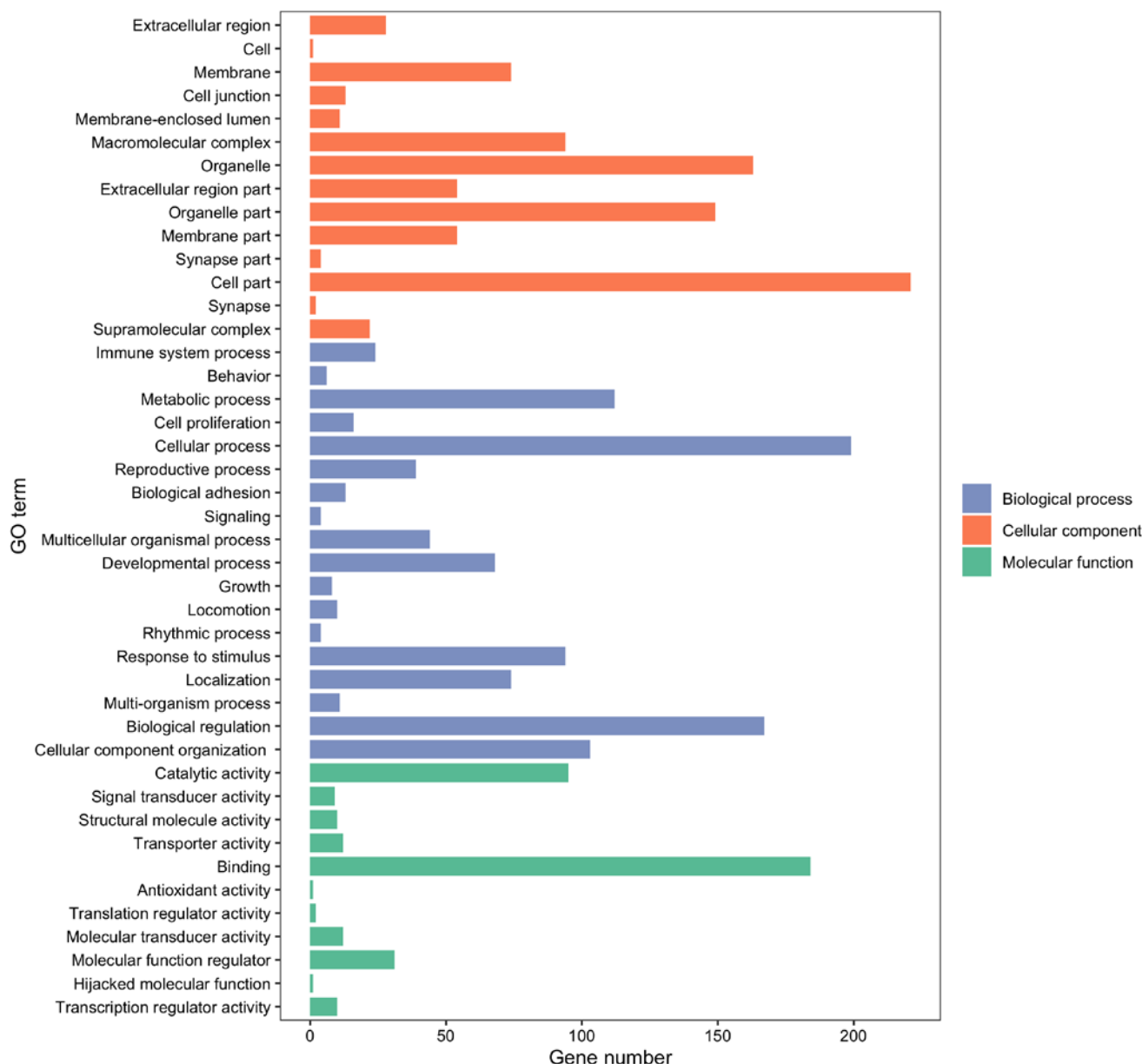


FIGURE 3. Gene Ontology (GO) function analysis of differentially expressed genes (DEGs) between the blank control group and the experimental group treated with the *Hericium erinaceus* extract (EEH).

by the research of Huang *et al.* [2017]. In addition, ethanol extracts from *H. erinaceus* have been found to exhibit the anti-*Helicobacter pylori* (an important factor in gastric disease) activity [Liu *et al.*, 2016]. The mechanisms underlying the gastroprotective activity of EEH are complex, and the factors play leading roles in EEH effects require further investigation.

Identification of the EEH compounds

The UPLC-Triple-TOF-MS analysis was performed to identify the possible compounds present in EEH by considering data from the literature and MS databases. Table 2 shows the proposed chemical composition of EEH; the MS chromatograms of the identified compounds are presented in Supplementary file (S1). A total of 12 compounds were tentatively identified, including three diterpene compounds (erinacerin N, erinacerin M, and erinacerin B), two heteroterpene

compounds (hericenone I and hericenone A), three isoindolinone compounds (erinaceolactam E, erinaceolactam A, and *N*-de(phenylethyl)isohericerin), one aromatic compound (hericerin IV), *N*-(1-deoxy-D-fructos-1-yl)-L-valine, adenosine, and lumichrome.

Previous research has demonstrated that adenosine can activate antioxidant enzymes *via* cell surface receptors [Ramkumar *et al.*, 1995]. Lumichrome is a photodegradation product of riboflavin and riboflavin possesses distinct antioxidant activity [Masek *et al.*, 2012]. Extensive studies have confirmed the anti-inflammation effects of erinacines and hericenones [Lee *et al.*, 2016]. Taken together, it appears that gastroprotective activity of EEH may be related to the synergistic effects of these compounds. The precise mechanism underlying the preventive effect of EEH on gastric ulcer and the active compounds responsible for this beneficial property need require further study.

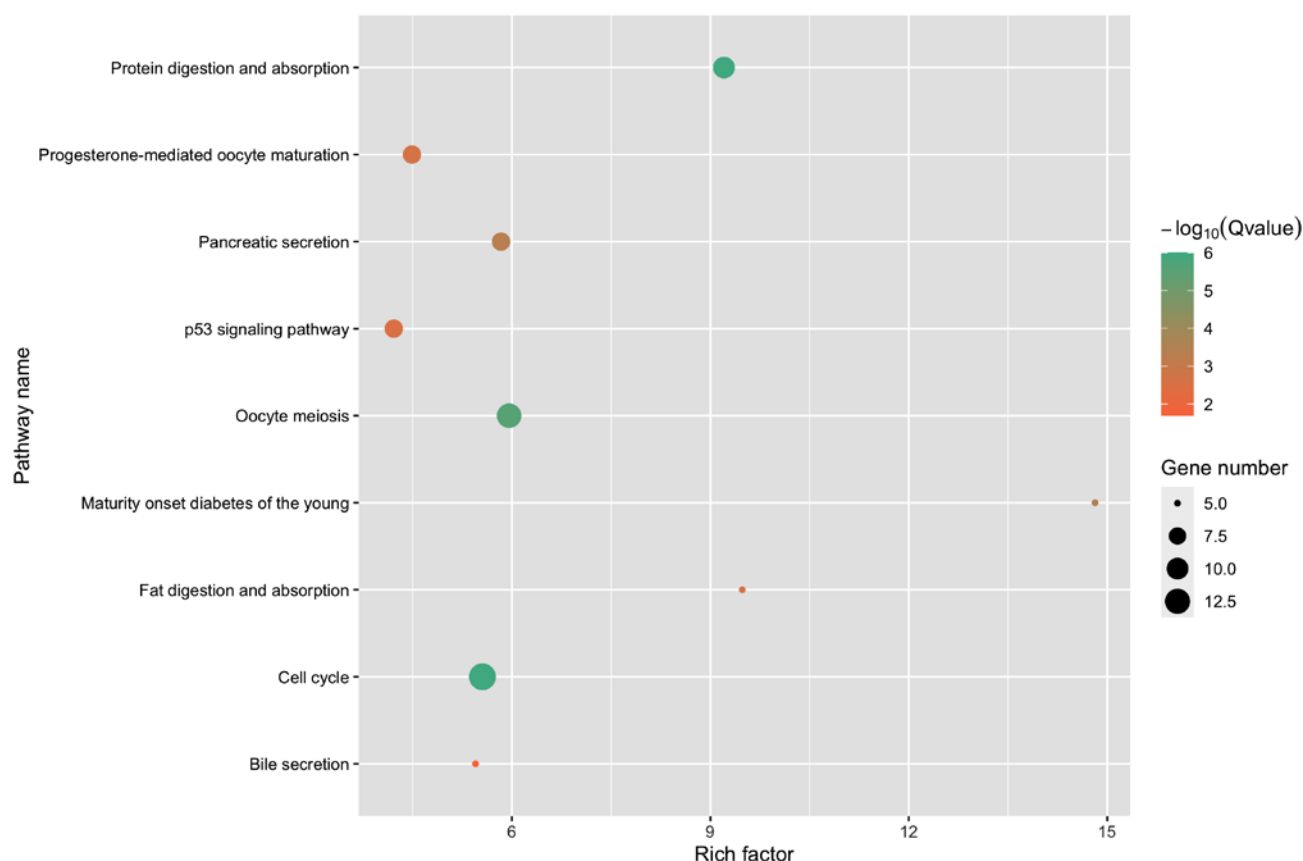


FIGURE 4. Kyoto Encyclopedia of Genes and Genomes (KEGG) pathway enrichment analysis of differentially expressed genes (DEGs) between the blank control group and the experimental group treated with the *Hericium erinaceus* extract (EEH).

RNA-seq analysis

The gastric tissues of blank control group and experimental group were analyzed by RNA-seq. Taking $|\log_2 \text{Fold change}| \geq 1$ and $q \leq 0.05$ as the thresholds, 278 DEGs were obtained, accounting for 1.0% of the total DEGs (Figure 2). The most differentially expressed genes were up- and down-regulated 11.3 and 7.03 times, respectively. The most significantly up-regulated genes were *Ins2*, *reg1*, *serpini2*, *cel*, and *erp27*, and the most significantly down-regulated genes were *duoxa2*, *serpina7*, *Xlr3b*, and *Col4a3*.

Reg1 is one of the genes that was significantly up-regulated. *Reg* and its related genes form a family belonging to the calcium-dependent lectin gene superfamily. This family expresses a group of small molecule secretory proteins. Asahara *et al.* [1996] performed *in situ* hybridization and immunohistochemical analyses and found that the expression of the *reg1* protein in enterochromaffin-like (ECL) cells in mouse gastric mucosa was increased after stress stimulation by water immersion. In addition, the *reg1* protein is expressed in the main cells and ECL cells of the human gastric fundus gland [Higham *et al.*, 1999]. *Reg* protein is expressed in many organs and tissues, especially in digestive system [Zhao *et al.*, 2013]. It promotes the proliferation and anti-apoptosis of gastric mucosal cells, while its overexpression can also reduce the chemosensitivity of gastric cancer patients.

The DEGs were counted and annotated using the NCBI, UniProt, Gene Ontology (GO), and Kyoto Encyclopedia of Genes and Genomes (KEGG) databases to obtain detailed

descriptive information. Figure 3 shows the most significant entries in the three functional annotation categories (cellular component, biological process, and molecular function). In biological process, the most significantly enriched DEGs were cellular process, biological regulation, and response to stimulus. In cellular components, the most significantly enriched DEGs were cell part, organelle part, and membrane. In molecular function, the most significantly enriched DEGs were binding and catalytic activity. A large number of DEGs existed in the above GO functions, suggesting that these functions play important roles in EEH effects on gastric tissue.

The pathways with significant differences and a large number of genes are shown in Figure 4: cell cycle, protein digestion and absorption, pancreatic secretion and the p53 signalling pathway

CONCLUSIONS

Ethanol-induced model is widely used for the reproduction of gastric injury or ulcer. Twelve compounds from EEH were identified in this work. The results have demonstrated that EEH has gastroprotective activity and is a valuable source of compounds for the prevention of gastric mucosal injury induced by ethanol. This preventive effect may be related to the synergistic action of these compounds. This study results provide scientific support for the use of EEH in the treatment of gastric ulcers. The RNA-seq results suggest that EEH indirectly protects against gastric tissue injury by regulating cell

cycle and biological function, up-regulating several signal molecules, or activating several proteasome functions. This study clearly highlights the viability of using EEH in adjuvant therapy of gastric ulcers. Further clinical assays should be performed to verify these findings, and the main compounds should be investigated in relation to their gastroprotective activity in EEH.

SUPPLEMENTARY MATERIALS

The following are available online at <http://journal.pan.olsztyn.pl/Protective-Effect-of-the-Ethanol-Extract-from-Hericium-erinaceus-Against-Ethanol,141560,0,2.html>; MS and MS/MS spectra and structures of compounds 1 to 12.

RESEARCH FUNDING

This research was funded by the New Variety Breeding Project of Science Technology Department of Zhejiang Province (Grant number: 2021C02073).

CONFLICT OF INTERESTS

There is no conflict of interest to declare.

ORCID IDs

G. Lv <https://orcid.org/0000-0002-9532-4838>
Z. Zhang <https://orcid.org/0000-0002-7228-0705>

REFERENCES

1. Agnihotri, N., Kaur, H., Kaur, N., Sarotra, P. (2007). Role of oxidative stress in lansoprazole-mediated gastric and hepatic protection in Wistar rats. *Indian Journal of Gastroenterology*, 26(3), 118–121.
2. Asahara, M., Mushiake, S., Shimada, S., Fukui, H., Kinoshita, Y., Kawanami, C., Watanabe, T., Tanaka, S., Ichikawa, A., Uchiyama, Y., Narushima, Y., Takasawa, S., Okamoto, H., Tohyama, M., Chiba, T. (1996). Reg gene expression is increased in rat gastric enterochromaffin-like cells following water immersion stress. *Gastroenterology*, 111(1), 45–55. <https://doi.org/10.1053/gast.1996.v111.pm8698224>
3. Chanda, S., Baravalia, Y., Kaneria, M. (2011). Protective effect of *Polyalthia longifolia* var. *pendula* leaves on ethanol and ethanol/HCl induced ulcer in rats and its antimicrobial potency. *Asian Pacific Journal of Tropical Medicine*, 4(9), 673–679. [https://doi.org/10.1016/S1995-7645\(11\)60172-7](https://doi.org/10.1016/S1995-7645(11)60172-7)
4. Chen, Z.G., Bishop, K.S., Tanambell, H., Buchanan, P., Smith, C., Quek, S.Y. (2019). Characterization of the bioactivities of an ethanol extract and some of its constituents from the New Zealand native mushroom *Hericium novae-zealandiae*. *Food & Function*, 10, 6633–6643. <https://doi.org/10.1039/C9FO01672D>
5. El-Maraghy, S.A., Rizk, S.M., Shanin, N.N. (2015). Gastric protective effect of crocin in ethanol-induced gastric injury in rats. *Chemical-Biological Interactions*, 229, 26–35. <https://doi.org/10.1016/j.cbi.2015.01.015>
6. Friedman, M. (2015). Chemistry, nutrition and health-promoting properties of *Hericium erinaceus* (Lion's Mane) mushroom fruiting bodies and mycelia and their bioactive compounds. *Journal of Agricultural and Food Chemistry*, 63(32), 7108–7123. <https://doi.org/10.1021/acs.jafc.5b02914>
7. Higham, A.D., Bishop, L.A., Dimaline, R., Blackmore C.G., Dobbins, A.C., Varro, A., Thompson, D.G., Dockray, G.J. (1999). Mutations of *RegIa* are associated with enterochromaffin-like cell tumor development in patients with hypergastrinemia. *Gastroenterology*, 116(6), 1310–1318. [https://doi.org/10.1016/S0016-5085\(99\)70495-6](https://doi.org/10.1016/S0016-5085(99)70495-6)
8. Huang, Y., Zhou, C.H., Dai, H.J., Huang, H.H. (2017). *In vitro* antioxidant activity of ethanol extract from *Hericium erinaceus* and its different polar fractions. *Science and Technology of Food Industry*, 21, 16–20.
9. Hui, Y., Zhao, S.S., Love, J.A., Ansley, D.M., Chen, D.D.Y. (2012). Development and application of a LC-MS/MS method to quantify basal adenosine concentration in human plasma from patients undergoing on-pump CABG surgery. *Journal of Chromatography B*, 885–886, 30–36. <https://doi.org/10.1016/j.jchromb.2011.12.006>
10. Kawagishi, H., Ando, M., Mizuno, T. (1990). Hericenone A and B as cytotoxic principles from the mushroom *Hericium erinaceum*. *Tetrahedron Letter*, 31(3), 373–376. [https://doi.org/10.1016/S0040-4039\(00\)94558-1](https://doi.org/10.1016/S0040-4039(00)94558-1)
11. Kim, S.P., Kang, M.Y., Kim, J.H., Nam, S.H., Friedman, M. (2011). Composition and mechanism of antitumor effects of *Hericium erinaceus* mushroom extracts in tumor-bearing mice. *Journal of Agricultural and Food Chemistry*, 59(18), 9861–9869. <https://doi.org/10.1021/jf201944n>
12. Lee, D.G., Kang, H.W., Park, C.G., Ahn, Y.S., Shin, Y. (2016). Isolation and identification of phytochemicals and biological activities of *Hericium ernaceus* and their contents in *Hericium* strains using HPLC/UV analysis. *Journal of Ethnopharmacology*, 184, 219–225. <https://doi.org/10.1016/j.jep.2016.02.038>
13. Li, W., Zhou, W., Kim, E.J., Shim, S.H., Kang, H.K., Kim, Y.H. (2015). Isolation and identification of aromatic compounds in Lion's Mane mushroom and their anticancer activities. *Food Chemistry*, 170, 336–342. <https://doi.org/10.1016/j.foodchem.2014.08.078>
14. Liu, B., Yili, A., Asia, H.A., Aikemu, M. (2018). Gastroprotective effect of the protease-rich extract from sheep abomasum against stress-induced gastric ulcers in rats. *Journal of Food Biochemistry*, 42(5), art. no. e12558. <https://doi.org/10.1111/jfbc.12558>
15. Liu, J.H., Li, L., Shang, X.D., Zhang, J.L., Tan, Q. (2016). Anti-*Helicobacter pylori* activity of bioactive components isolated from *Hericium erinaceus*. *Journal of Ethnopharmacology*, 183, 54–58. <https://doi.org/10.1016/j.jep.2015.09.004>
16. Ma, L., Liu, J.G. (2014). The protective activity of *Gonyza blinii* saponin against acute gastric ulcer induced by ethanol. *Journal of Ethnopharmacology*, 158, Part A, 358–363. <https://doi.org/10.1016/j.jep.2014.10.052>
17. Masek, A., Chrzescijanska, E., Zaborski, M., Maciejewska, M. (2012). Characterisation of the antioxidant activity of riboflavin in an elastomeric composite. *Comptes Rendus Chimie*, 15(6), 524–529. <https://doi.org/10.1016/j.crci.2012.01.012>
18. Mei, X., Xu, D., Xu, S., Zheng, Y., Xu, S. (2012). Novel role of Zn (II)-curcumin in enhancing cell proliferation and adjusting proinflammatory cytokine-mediated oxidative damage of etha-

- nol-induced acute gastric ulcers. *Chemico-Biological Interactions*, 197(1), 31–39.
<https://doi.org/10.1016/j.cbi.2012.03.006>
19. Miyazawa, M., Takahashi, T., Horibe, I., Ishikawa, R. (2012). Two new aromatic compounds and a new D-arabinitol ester from the mushroom *Hericium erinaceum*. *Tetrahedron*, 68(7), 2007–2010.
<https://doi.org/10.1016/j.tet.2011.11.068>
 20. O'Malley, P. (2003). Gastric ulcers and CERD: the new “plagues” of the 21st century update for the Clinical Nurse Specialist. *Clinical Nurse Specialist*, 17(6), 286–289.
<https://doi.org/10.1097/00002800-200311000-00008>
 21. Pan, J.S., He, S.Z., Xu, H.Z., Zhan, X.J., Yang, X.N., Xiao, H.M., Shi, H.X., Ren, J.L. (2008). Oxidative stress disturbs energy metabolism of mitochondria in ethanol-induced gastric mucosa injury. *World Journal of Gastroenterology*, 14(38), 5857–5867.
<https://doi.org/10.3748/wjg.14.5857>
 22. Qin, M., Geng, Y., Lu, Z., Xu, H., Shi, J., Xu, X., Xu, Z. (2016). Anti-inflammatory effects of ethanol extract of Lion's Mane medicinal mushroom, *Hericium erinaceus* (Agaricomycetes), in mice with ulcerative colitis. *International Journal of Medicinal Mushrooms*, 18(3), 227–234.
<https://doi.org/10.1615/IntJMedMushrooms.v18.i3.50>
 23. Ramkumar, V., Nie, Z., Rybak, L.P., Maggirwar, S.B. (1995). Adenosine, antioxidant enzymes and cytoprotection. *Trends in Pharmacological Sciences*, 16(9), 283–285.
[https://doi.org/10.1016/S0165-6147\(00\)89051-3](https://doi.org/10.1016/S0165-6147(00)89051-3)
 24. Sahin, H., Kaltalioglu, K., Erisgin, Z., Coskun-Cevher, S., Koyayli, S. (2019). Protective effects of aqueous extracts of some honeys against HCl/ethanol-induced gastric ulceration in rats. *Journal of Food Biochemistry*, 43(12), art. no. e 13054.
<https://doi.org/10.1111/jfbc.13054>
 25. Saiah, W., Halzoune, H., Djaziri, R., Tabani, K., Koceir, E.A., Omari, N. (2018). Antioxidant and gastroprotective actions of butanol fraction of *Zingiber officinale* against diclofenac sodium-induced gastric damage in rats. *Journal of Food Biochemistry*, 42(1), art. no. e12456.
<https://doi.org/10.1111/jfbc.12456>
 26. Salim, A.S. (1990). Removing oxygen-derived free radicals stimulates healing of ethanol-induced erosive gastritis in the rat. *Digestion*, 47(1), 24–28.
<https://doi.org/10.1159/000200472>
 27. Sathish, R., Vyawahare, B., Natarajan, K. (2011). Antiulcerogenic activity of *Lantana camara* leaves on gastric and duodenal ulcers in experimental rats. *Journal of Ethnopharmacology*, 134(1), 195–197.
<https://doi.org/10.1016/j.jep.2010.11.049>
 28. Sreeja, P.S., Arunachalam, K., Saikumar, S., Kasipandi, M., Dhivya, S., Murugan, R., Parimelazhagan, T. (2018). Gastroprotective effect and mode of action of methanol extract of *Sphenodesme involucrate* var. paniculate (C.B. Clarke) Munir (Lamiaceae) leaves on experimental gastric ulcer models. *Biomedicine & Pharmacotherapy*, 97, 1109–1118.
<https://doi.org/10.1016/j.biopha.2017.11.030>
 29. Tang, H.Y., Yin, X., Zhang, C.C., Jia, Q., Gao, J.M. (2015). Structure diversity, synthesis, and biological activity of cyathane diterpenoids in higher fungi. *Current Medicinal Chemistry*, 22(19), 2375–2391.
<https://doi.org/10.2174/0929867322666150521091333>
 30. Tsukamoto, S., Kato, H., Hirota, H., Fusetani, N. (1999). Lumichrome, a larval metamorphosis-inducing substance in the ascidian *Halocynthia roretzi*. *European Journal of Biochemistry*, 264(3), 785–789.
<https://doi.org/10.1046/j.1432-1327.1999.00642.x>
 31. Wang, X.L., Xu, K.P., Long, H.P., Zou, H., Cao, X.Z., Zhang, K., Hu, J.Z., He, S.J., Zhu, G.Z., He, X.A., Xu, P.S., Tan, G.S. (2016). New isoindolinones from the fruiting bodies of *Hericium erinaceum*. *Fitoterapia*, 111, 58–65.
<https://doi.org/10.1016/j.fitote.2016.04.010>
 32. Wang, X.Y., Yin, J.Y., Zhao, M.M., Liu, S.Y., Nie, S.P., Xie, M.Y. (2018a). Gastroprotective activity of polysaccharide from *Hericium erinaceus* against ethanol-induced gastric mucosal lesion and pylorus ligation-induced gastric ulcer, and its antioxidant activities. *Carbohydrate Polymers*, 186, 100–109.
<https://doi.org/10.1016/j.carbpol.2018.01.004>
 33. Wang, Y., Luan, G., Zhou, W., Meng, J., Wang, H., Hu, N., Suo, Y. (2018b). Subcritical water extraction, UPLC-Triple-TOF/MS analysis and antioxidant activity of anthocyanins from *Lucium ruhtenicum* Murr. *Food Chemistry*, 249, 119–126.
<https://doi.org/10.1016/j.foodchem.2017.12.078>
 34. Wu, F., Zhou, C., Zhou, D., Ou, S., Zhang, X., Huang, H. (2018). Structure characterization of a novel polysaccharide from *Hericium erinaceus* fruiting bodies and its immunomodulatory activities. *Food & Function*, 9(1), 294–306.
<https://doi.org/10.1039/C7FO01389B>
 35. Yaoita, Y., Danbara, K., Kikuchi, M. (2005). Two new aromatic compounds from *Hericium erinaceum* (Bull.:Fr.) Pers. *Chemical & Pharmaceutical Bulletin*, 53(9), 1202–1203.
<https://doi.org/10.1248/cpb.53.1202>
 36. Zhao, J., Wang, J., Wang, H., Lai, M. (2013). Chapter Five – Reg proteins and their roles in inflammation and cancer of the human digestive system. *Advances in Clinical Chemistry*, 61, 153–173.
<https://doi.org/10.1016/B978-0-12-407680-8.00006-3>

INSTRUCTIONS FOR AUTHORS

SUBMISSION. Original contributions relevant to food and nutrition sciences are accepted on the understanding that the material has not been, nor is being, considered for publication elsewhere. **All papers should be submitted and will be processed electronically via Editorial Manager system (available from PJFNS web site: <http://journal.pan.olsztyn.pl>).** On submission, a corresponding author will be asked to provide: **Cover letter; Files with Manuscripts, Tables, Figures/Photos; and Names of two potential reviewers (one from the author's homeland – but outside author's Institution, and the other from abroad).** All papers which have been qualified as relevant with the scope of our Journal are reviewed. All contributions, except the invited reviews are charged. Proofs will be sent to the corresponding author or to the first author and should be returned within one week since receipt. No new material may be inserted in the text at proof stage. It is the author's duty to proofread proofs for errors.

Authors should very carefully consider the preparation of papers to ensure that they communicate efficiently, because it permits the reader to gain the greatest return for the time invested in reading. Thus, we are more likely to accept those that are carefully designed and conform the instruction. Otherwise, papers will be rejected and removed from the on-line submission system.

SCOPE. The Polish Journal of Food and Nutrition Sciences publishes original, basic and applied papers, and reviews on fundamental and applied food research, preferably these based on a research hypothesis, in the following Sections:

Food Technology:

- Innovative technology of food development including biotechnological and microbiological aspects
- Effects of processing on food composition and nutritional value

Food Chemistry:

- Bioactive constituents of foods
- Chemistry relating to major and minor components of food
- Analytical methods

Food Quality and Functionality:

- Sensory methodologies
- Functional properties of food
- Food physics
- Quality, storage and safety of food

Nutritional Research Section:

- Nutritional studies relating to major and minor components of food (excluding works related to questionnaire surveys)

“News” section:

- Announcements of congresses
- Miscellanea

OUT OF THE SCOPE OF THE JOURNAL ARE:

- Works which do not have a substantial impact on food and nutrition sciences
- Works which are of only local significance i.e. concern indigenous foods, without wider applicability or exceptional nutritional or health related properties
- Works which comprise merely data collections, based on the use of routine analytical or bacteriological methods (i.e. standard methods, determination of mineral content or proximate analysis)
- Works concerning biological activities of foods but do not provide the chemical characteristics of compounds responsible for these properties
- Nutritional questionnaire surveys
- Works related to the characteristics of foods purchased at local markets
- Works related to food law
- Works emphasizing effects of farming / agricultural conditions / weather conditions on the quality of food constituents
- Works which address plants for non-food uses (i.e. plants exhibiting therapeutic and/or medicinal effects)

TYPES OF CONTRIBUTIONS. *Reviews:* (at least: 30 pages and 70 references) these are critical and conclusive accounts on trends in food and nutrition sciences; *Original papers:* (maximally: 30 pages and 40 references) these are reports of substantial research; *Reports on post and forthcoming scientific events, and letters to the Editor* (all up to three pages) are also invited (free of charge).

REVIEW PROCESS. All scientific contributions will be peer-reviewed on the criteria of originality and quality. Submitted manuscripts will be pre-evaluated by Editor-in-Chief and Statistical Editor (except for review articles), and when meeting PJFNS' scope and formal requirements, they will be sent to a section Editor who upon positive pre-evaluation will assign at least two reviewers from Advisory Board Members, reviewers suggested by the author or other experts in the field. Based on the reviews achieved, Section Editor and Editor-in-Chief will make a decision on whether a manuscript will be accepted for publication, sent back to the corresponding author for revision, or rejected. Once a manuscript is sent back to the corresponding author for revision, all points of the reviews should be answered or rebuttal should be provided in the Explanation letter. The revised manuscripts will be checked by Section Editor and by the original reviewers (if necessary), and a final decision will be made on acceptance or rejection by both Section Editor and Editor-in-Chief.

Polish Journal of Food and Nutrition Sciences uses CrossCheck's iThenticate software to detect instances of similarity in submitted manuscripts. In publishing only original research, PJFNS is committed to deterring plagiarism, including self-plagiarism. Your manuscript may be screened for similarity to published materials.

COPYRIGHT LICENSE AGREEMENT referring to Authorship Responsibility and Acknowledgement, Conflict of Interest and Financial Disclosure, Copyright Transfer, are required for all authors, i.e. *Authorship Responsibility and Acknowledgement*: Everyone who has made substantial intellectual contributions to the study on which the article is based (for example, to the research question, design, analysis, interpretation, and written description) should be an author. It is dishonest to omit mention of someone who has participated in writing the manuscript ("ghost authorship") and unfair to omit investigator who have had important engagement with other aspects of the work. All contributors who do not meet the criteria for authorship should be listed in an Acknowledgments section. Examples of those who might be acknowledged include a person who provided purely technical help, writing assistance, or a department chairperson who provided only general support. Any financial and material support should also be acknowledged. *Conflict of Interest and Financial Disclosure*: Authors are responsible for disclosing financial support from the industry or other conflicts of interest that might bias the interpretation of results. *Copyright License Agreement*: Authors agree that papers accepted become the copyright of the Institute of Animal Reproduction and Food Research of the Polish Academy of Sciences in Olsztyn, Poland, and may not be published elsewhere without the Editor's permission in writing.

A manuscript will not be published once the signed form has not been submitted to the Editor with the manuscript revised after positive reviews.

ETHICAL APPROVAL OF STUDIES AND INFORMED CONSENT. For all manuscripts reporting data from studies involving human participants or animals, formal approval by an appropriate institutional review board or ethics committee is required and should be described in the Methods section. For those investigators who do not have formal ethics review committees, the principles outlined in the Declaration of Helsinki should be followed. For investigations of humans, state in the Methods section the manner in which informed consent was obtained from the study participants (i.e., oral or written). Editors may request that authors provide documentation of the formal review and recommendation from the institutional review board or ethics committee responsible for oversight of the study.

UNAUTHORIZED USE AND COPYRIGHT AGREEMENT. Published manuscripts become the property of the Institute of Animal Reproduction and Food Research of the Polish Academy of Sciences (IAR&FR PAS) and may not be published elsewhere without written permission. Unauthorized use of the PJFNS name, logo, or any content for commercial purposes or to promote commercial goods and services (in any format, including print, video, audio, and digital) is not permitted by IAR&FR PAS.

MANUSCRIPTS. A manuscript in English must be single-sided, preferably in Times New Roman (12) with 1.5-point spacing, without numbers of lines. The Editor reserves the right to make literary corrections and to make suggestions to improve brevity. English is the official language. The English version of the paper will be checked by Language Editor. Unclear and unintelligible version will be sent to the author(s) for correction.

Every paper should be divided under the following headings in this order: a **Title** (possibly below 150 spaces), **Running title** (up to 50 spaces, submitted under the Title); the Names(s) of the author(s) in full. In paper with more than one author, the asterisk indicates the name of the author to whom correspondence and inquiries should be addressed, otherwise the first author is considered for the correspondence. Current full postal address of the indicated corresponding author or the first author must be given in a footnote on the title page; the Place(s) where the work was done including the institution name, city, country if not Poland. In papers originated from several institutions the names of the authors should be marked with respective superscripts; the **Key words** (up to 6 words or phrases) for the main topics of the paper; an **Abstract** (up to 250 words for regular papers and reviews and 100 words for Short Reports) summarizing briefly main results of the paper, no literature references; an **Introduction** giving essential background by saying why the research is important, how it relates to previous works and stating clearly the objectives at the end; **Materials and Methods** with sufficient experimental details permitting to repeat or extend the experiments. Literature references to the methods, sources of material, company names and location (city, country) for specific instruments must be given. Describe how the data were evaluated, including selection criteria used; **Results and Discussion** presented together (in one chapter). Results should be presented concisely and organized to supplement, but not repeat, data in tables and figures. Do not display the data in both tabular and graphic form. Use narrative form to present the data for which tables or figures are unnecessary. Discussion should cover the implications and consequences, not merely recapitulating the results, and it must be accomplished with concise **Conclusions**; **Acknowledgements** should be made to persons who do not fill the authorship criteria (see: Authorship forms); **Research funding** should include financial and material support; and **References** as shown below.

REFERENCES each must be listed alphabetically at the end of the paper (each should have an Arabic number in the list) in the form as follows: **Periodicals** – names and initials of all the authors, year of publication, title of the paper, journal title as in Chemical Abstracts, year of publication, volume, issue, inclusive page numbers; **Books** – names and initials of all the authors, names of editors, chapter title, year of publication, publishing company, place of publication, inclusive page numbers; **Patents** – the name of the application, the title, the country, patent number or application number, the year of publication.

For papers published in language other than English, manuscript title should be provided in English, whereas a note on the original language and English abstract should be given in parentheses at the end.

The reference list should only include peer-reviewed full-text works that have been published or accepted for publication. Citations of MSc/PhD theses and works unavailable to international Editors, Reviewers, and Readers should be limited as much as possible.

References in the text must be cited by name and year in square parentheses (e.g.: one author – [Tokarz, 1994]; two authors – [Słomimski & Campbell, 1987]; more than two authors – [Amarowicz *et al.*, 1994]). If more than one paper is published in the same year by the same author or group of authors use [Tokarz, 1994a, b]. Unpublished work must only be cited where necessary and only in the text by giving the person's name.

Examples:*Article in a journal:*

Slonimski, B.A., Campbell, L.D., Batista, E., Howard B. (2008). Gas chromatographic determination of indole glucosinolates. *Journal of Science and Food Agriculture*, 40(5), 131–143.

Book:

Weber, W., Ashton, L., Milton, C. (2012). *Antioxidants – Friends or Foes?* 2nd edition. PBD Publishing, Birmingham, UK. pp. 218–223.

Chapter in a book:

Uden, C., Gambino, A., Lamar, K. (2016). Gas chromatography. In M. Queresi, W. Bolton (Eds.), *CRC Handbook of Chromatography*, CRC Press Inc., Boca Raton, Florida, USA, pp. 44–46.

ABBREVIATIONS AND UNITS. Abbreviations should only be used when long or unwieldy names occur frequently, and never in the title; they should be given at the first mention of the name. Metric SI units should be used. The capital letter L should be used for liters. Avoid the use of percentages (% g/g, % w/w; Mol-%; vol-%), ppm, ppb. Instead, the expression such as g/kg, g/L, mg/kg, mg/mL should be used. A space must be left between a number and a symbol (e.g. 50 mL not 50mL). A small x must be used as multiplication sign between numeric values (e.g. 5×10^3 g/mL). Statistics and measurements should be given in figures, except when the number begins a sentence. Chemical formulae and solutions must specify the form used. Chemical abbreviations, unless they are internationally known, Greek symbols and unusual symbols for the first time should be defined by name. Common species names should be followed by the Latin at the first mention, with contracting it to a single letter or word for subsequent use.

FIGURES should be submitted in separate files. Each must have an Arabic number and a caption. Captions of all Figures should be provided on a separate page “Figure Captions”. Figures should be comprehensible without reference to the text. Self-explanatory legend to all figures should be provided under the heading “Legends to figures”; all abbreviations appearing on figures should be explained in figure footnotes. Three-dimensional graphs should only be used to illustrate real 3-D relationships. Start the scale of axes and bars or columns at zero, do not interrupt them or omit missing data on them. Figures must be cited in Arabic numbers in the text.

TABLES should be submitted in separate files. They should be as few in number and as simple as possible (like figures, they are expensive and space consuming), and include only essential data with appropriate statistical values. Each must have an Arabic number and a caption. Captions of all Tables should be provided on a separate page “Table Captions”. Tables should be self-explanatory; all abbreviations appearing in tables should be explained in table footnotes. Tables must be cited in Arabic numbers in the text.

PAGE CHARGES. A standard publication fee has been established at the rate of 450 EUR + tax (if applicable) irrespective of the number of pages and tables/figures. For Polish Authors an equivalent fee was set at 1950 PLN + VAT. Payment instructions will be sent to Authors via e-mail with acceptance letter.

Information on publishing and subscription is available from:

Ms. Joanna Molga
Editorial Office of Pol. J. Food Nutr. Sci.
Institute of Animal Reproduction and Food Research
Tuwima 10 Str., 10–748 Olsztyn 5, Poland
phone (48 89) 523–46–70, fax (48 89) 523–46–70;
e-mail: pjfns@pan.olsztyn.pl; <http://journal.pan.olsztyn.pl>

Nutrition

